

BULLETIN

OF THE AMERICAN PHYSICAL SOCIETY

OHIO
STATE

The 59th Annual Gaseous



Electronics Conference

October 10-13,

OHIO
STATE

2006

October 2006

Volume 51, No. 5

APS
physics

BULLETIN

OF THE AMERICAN PHYSICAL SOCIETY

Coden BAPSA6

Series II, Vol. 51, No. 5

Copyright 2006 by the American Physical Society

ISSN: 0003-0503

October 2006

APS COUNCIL 2006

President

John J. Hopfield,* *Princeton University*

President-Elect

Leo P. Kadanoff,* *University of Chicago*

Vice President

Arthur Bienenstock,* *Stanford University*

Executive Officer

Judy R. Franz,* *University of Alabama, Huntsville (on leave)*

Treasurer

Joseph Serene,* *Georgetown University (emeritus)*

Editor-in-Chief

Martin Blume,* *Brookhaven National Laboratory (emeritus)*

Past-President

Marvin L. Cohen,* *University of California, Berkeley*

General Councillors

Christina Back, Janet Conrad, Wendell Hill, Evelyn Hu,* Ann Orel, Arthur Ramirez, Richart Slusher, Laura Smoliar*

Division, Forum and Section Councillors

Charles Dermer (*Astrophysics*), Kate Kirby* (*Atomic, Molecular & Optical Physics*), Robert Eisenberg (*Biological*), Charles S. Parmenter (*Chemical*), Moses H. Chan (*Condensed Matter Physics*), Richard M. Martin (*Computational*), Harry Swinney* (*Fluid Dynamics*), Peter Zimmerman (*Forum on Education*), Roger Stuewer (*Forum on History of Physics*), Patricia Mooney* (*Forum on Industrial and Applied Physics*), David Ernst (*Forum on International Physics*), Philip "Bo" Hammer* (*Forum on Physics and Society*), J. H. Eberly (*Laser Science*), Leonard Feldman (*Materials*), Akif Balantekin (*Nuclear*), John Jaros* (*Particles & Fields*), Ron Ruth (*Physics of Beams*), James Drake* (*Plasma*), Scott Milner (*Polymer Physics*), Gianfranco Vidali (*New York Section*), Paul Wolf (*Ohio Section*)

**Members of the APS Executive Board*

Meetings Abstracts Coordinator:

Vinaya Sathyasheelappa

APS MEETINGS DEPARTMENT

One Physics Ellipse

College Park, MD 20740-3844

Telephone: (301) 209-3286

FAX: (301) 209-0866

Donna Baudrau, *Director of Meetings & Conventions*

Terri Gaier, *Senior Meeting Planner*

Don Wise, *Registrar*

Christine Parvez, *Meetings Program Coordinator*

International Councillor

Albrecht Wagner

Chair, Nominating Committee

Thomas Rosenbaum

Chair, Panel on Public Affairs

Ernest Moniz

ADVISORS

Representatives from other Societies

Kenneth Heller, *AAPT*; Marc Brodsky, *AIP*

International Advisors

Maria Ester Ortiz, *Mexican Physical Society*;

Louis Marchildon, *Canadian Association of Physicists*

Staff Representatives

Alan Chodos, *Associate Executive Officer*; Amy Flatten, *Director of International Affairs*; Ted Hodapp, *Director of Education and Outreach*; Michael Lubell, *Director, Public Affairs*; Stanley Brown, *Editorial Director*; Charles Muller, *Director, Journal Operations*; Michael Stephens, *Controller and Assistant Treasurer*

Administrator for Governing Committees

Ken Cole

The *Bulletin of the American Physical Society* is published 9X in 2006—March, April, May, July, October (3X), November, and December—by the American Physical Society through the American Institute of Physics. It contains information about meetings of the Society, including abstracts of papers to be presented, as well as transactions of past meetings. Reprints of papers can be obtained only by writing directly to the authors.

BULLETIN

OF THE AMERICAN PHYSICAL SOCIETY

Vol. 51, No. 5, October 2006

GEC Meeting 2006

TABLE OF CONTENTS

General Information	3
Special Sessions and Events	3
<i>Sessions</i>	3
Presentation Formats	3
GEC Student Award for Excellence	4
Registration	4
Banquet and Reception	4
E-mail and Other Business Services	4
Audio-Visual Equipment	4
Dining Options	4
Guest Program	4
Call for Nominations for GEC General and Executive Committees	5
<i>GEC Executive Committee</i>	5
<i>Conference Secretary</i>	6
Please Note	6
Epitome	7
Main Text	9
<i>Monday, October 9</i>	9

<i>Tuesday, October 10</i>	10
<i>Wednesday, October 11</i>	37
<i>Thursday, October 12</i>	47
<i>Friday October 13</i>	69
Author Index	75
Floor Plans	At End of Issue

59th Annual Gaseous Electronics Conference

October 9–13, 2006

Columbus, Ohio

GENERAL INFORMATION

Welcome to Columbus for the 59th Annual Gaseous Electronics Conference (GEC) of the American Physical Society. The GEC 2006 will address a broad range of topics at the forefront of Gaseous Electronics. The program includes The Allis Prize Lecture, The GEC Student Award for Excellence Talks, 27 invited talks and over 250 contributed papers presented in oral and poster sessions. The conference will be located at The Holiday Inn on The Lane, Columbus, OH.

SPECIAL SESSIONS AND EVENTS

The GEC Executive Committee is pleased to announce that the Allis Prize Lecture for 2006 will be presented by Mike Lieberman. His talk is entitled "Nanoelectronics and Plasma Processing—The Next 15 Years and Beyond," and will be presented on Wednesday morning at 10 AM in Salon CD. The Allis Prize Lecture, alternating each year with the GEC Foundation talk, commemorates the outstanding contributions of Will Allis to the field of ionized gases.

SESSIONS

- Session AS Opening Reception
- Session BT1 Plasma Sources I
- Session BT2 Plasma Boundaries: Sheaths and Boundary Layers
- Session CT1 Plasma Aerodynamics and Propulsion I
- Session CT2 Collision Processes with Biological and Environmental Applications
- Session DT1 Plasma Chemistry
- Session DT2 Electron Impact Ionization and Excitation I
- Session ET1 Plasma Sources II
- Session ET2 Oxygen-Iodine Lasers
- Session FPT Poster Session I
- Session GW1 Diagnostics I: Electrical

- Session GW2 High Pressure Discharges I
- Session HW Allis Prize Lecture
- Session LW1 Plasma Aerodynamics and Propulsion II
- Session LW2 Electron Impact Ionization and Excitation II
- Session MW1 Diagnostics II: Optical
- Session MW2 Thermal Plasmas, Arcs, and Breakdown
- Session PR1 Plasma Applications for Nanotechnology
- Session PR2 Computational Methods and Modeling for Plasmas
- Session QR1 High Pressure Discharges II
- Session QR2 Electron and Positron Collisions
- Session RR1 Material Processing in Low Pressure Plasmas
- Session RR2 Lighting Plasmas
- Session SRP Poster Session II
- Session UR Reception and Banquet
- Session VF1 Plasma-Surface Interactions
- Session VF2 Transport Theory and Electron Distribution Functions
- Session WF1 Capacitively Coupled Plasmas
- Session WF2 Heavy Particle Collisions, Attachment, and Recombination

PRESENTATION FORMATS

Papers that have been accepted for presentation are listed in the technical program. Invited papers are allotted 25 minutes, with 5 additional minutes for questions and discussion. Oral contributed presentations are allotted 12 minutes, with 3 additional minutes for questions. Poster sessions will be provided with 48 in. by 96 in. posterboards. Presenters may mount their posters anytime in the day upon which their presentation is scheduled. Poster materials must be removed at the close of the poster session.

GEC STUDENT AWARD FOR EXCELLENCE BANQUET AND RECEPTION

In order to recognize the outstanding contribution students make to the GEC and to encourage further student participation, the GEC will continue to award a prize for the best paper presentation by a student. A subcommittee of the GEC Executive Committee will choose the award winner. Students competing for the \$500 award, in the order of their appearance in the program, are:

Violaine Vizcaino, Australian National University, "Electron collisions with formic acid and tetrahydrofuran," Tuesday, October 10, 11:30 AM.

Scott Baalrud, University of Wisconsin, "Electron sheaths and non-ambipolar diffusion in laboratory plasmas," Tuesday, October 10, 8:00 AM.

Sampad Laha, Rice University, "Gaussian expansion and annular analysis of ultracold Sr plasma," Wednesday, October 11, 4:00 PM.

Erik Wagenaars, Eindhoven University, "Electric field measurements in moving ionization fronts during plasma breakdown," Wednesday, October 11, 5:00 PM.

Maria Herd, University of Wisconsin, "Infrared continuum radiation from metal halide hid lamps," Thursday, October 12, 2:00 PM.

Kuma Ohnishi, Tokyo Institute of Technology, "Deposition of vertically oriented single-walled carbon nanotubes...," Thursday, October 12, 8:30 AM.

Olivier Guaitella, Ecole Polytechnique, "Dynamic of the plasma current amplitude in a barrier discharge...," Thursday, October 12, 11:30 AM.

Jason Young, University of California – San Diego, "Resonances in positron-molecule annihilation," Thursday, October 12, 11:00 AM.

REGISTRATION

The registration desk will be located in the Holiday Inn Hotel, in the vicinity of the lobby. Registration will be available Monday afternoon from 4:00 – 6:00 PM and throughout most of the week, starting at 7:00 AM. The on-site conference registration fee is \$310 for regular registrations and \$190 for students and retirees.

An opening reception will be held on the evening of Monday, October 9, 2006, in The Ohio State University Department of Mechanical Engineering's Scott Laboratory, starting at 6:00 pm. Scott Laboratory is located on the main Ohio State University campus, a short walk from the conference hotel. The reception will be held in the Scott Laboratory Multi-Purpose room. Printed directions will be available on Monday afternoon in the GEC registration area.

The conference banquet will be held in Salon CD of the Holiday Inn Hotel on Thursday evening, October 12, starting with a reception in the lobby at 6:00 pm. Banquet tickets are \$40 and are available upon registration. Conference participants are encouraged to attend the reception and the banquet.

E-MAIL AND OTHER BUSINESS SERVICES

Wireless internet access will be available throughout the conference hotel, including all guest rooms and public areas. Other business services (fax, photocopy services, etc.) will be available from the hotel business center.

AUDIO-VISUAL EQUIPMENT

Each conference room will be equipped with an LCD projector. If additional equipment is required, please contact the conference secretary.

DINING OPTIONS

A list with dining options in the vicinity of the Holiday Inn Hotel is included in the registration packet provided to each conference participant.

GUEST PROGRAM

Welcome to Columbus, the capital city of Ohio. It is the largest city in Ohio, and the 15th largest in the nation, with a population of 750,000. Columbus is a friendly city and offers a wide variety of attractions for guests. There is everything from visual and performing

arts, professional and collegiate sports, excellent shopping and fine dining to a world renowned zoo.

The Holiday Inn on the Lane is located near the campus of The Ohio State University. This provides visitors with convenient access to many sites of interest, both at the University and in the Columbus area.

Cultural highlights include: The Wexner Center for the Arts, the Columbus Museum of Art, the King Arts Complex, the Franklin Park Conservatory, and the Center for Science and Industry (COSI). Of historic interest are: the Ohio Statehouse, German Village and the Santa Maria replica.

For shopping, dining, and entertainment, Columbus provides the Arena District, the Short North Market, Easton Town Center, Polaris Fashion Place, City Center Mall and much, much more! For those interested in wildlife, a visit to the Columbus Zoo and Aquarium is a must. It is the third largest municipally-owned zoo in North America and serves as animal sanctuary, scientific research center and family-fun spot.

For more information on the wide variety of activities and places of interest in Columbus, please visit www.ExperienceColumbus.com.

We hope that you enjoy your visit to Columbus!

CALL FOR NOMINATIONS FOR GEC GENERAL AND EXECUTIVE COMMITTEES

The GEC Executive Committee (ExComm) is the governing body of the GEC. It is the responsibility of the ExComm to oversee all aspects of the conference. This includes selection of meeting sites, budgetary decisions, selection of special topics and invited speakers, accepting and rejecting abstracts, and arranging of the program. The General Committee and the ExComm meet during the GEC, and the ExComm meets again during the summer to plan the program of the next GEC. There are numerous communications between members of the ExComm (usually via e-mail) during the year to ensure the successful completion of their duties. We have been fortunate over the years to have a dedicated group of volunteers who have been willing to take on these very necessary roles.

The by-laws of the Gaseous Electronics Conference describe the process whereby members of the ExComm are elected. At the GEC Business Meeting (to be held on Wednesday, October 11, at 11:00 in Salon CD of the

Holiday Inn Hotel), nominations are accepted for members of the GEC General Committee (GenComm).

The GenComm consists of the ExComm and 6 at-large members elected at the Business Meeting. The eligible voting membership of the GEC (defined as those attending the Business Meeting) elects 6 at-large members. The GenComm then meets to fulfill its only duty: to elect new members of the ExComm.

The ExComm membership consists of the Chair, Treasurer, Past-Secretary, Secretary, Secretary-elect, past or incoming Chair, and 4 at-large members. The Chair is a 4 year term (1 year incoming, 2 years Chair, and 1 year past-Chair), the Secretary is a 3 year term (1 year incoming, 1 year Secretary, 1 year past-Secretary), and all other ExComm members serve 2 years. The Secretary is the person who manages the local arrangements for the meeting and is usually recruited and appointed to the ExComm.

The ExComm welcomes nominations, including self-nomination, for both the GenComm and the ExComm. Becoming a GenComm and/or ExComm member provides a unique opportunity to see both how the GEC is run and to influence its future direction by helping to define the programs and choosing future sites.

Please submit your nominations to the GEC Chair or any member of the ExComm. The ExComm also welcomes inquiries on hosting future GECs.

GEC 2005 EXECUTIVE COMMITTEE

- Greg Hebner, Chair, Sandia National Laboratory
- Peter Ventzek, Chair-Elect, Tokyo Electron
- Walter Lempert, Secretary, Ohio State University
- William Rich, co-Secretary, Ohio State University
- Jong Shon, Past Secretary, JuSung Engineering Corporation
- Darrin Leonhardt, Secretary-Elect, Naval Research Laboratory
- Don Madison, Treasurer, University of Missouri-Rolla
- Stephen Buckman, Australia National University
- Uwe Czarnetzki, Ruhr Universitat Bochum
- Rainer Johnson, University of Pittsburgh
- Murtadha Khakoo, California State University Fullerton
- Kouichi Ono, Kyoto University

CONFERENCE SECRETARY

Walter Lempert, Secretary

Departments of Mechanical Engineering and Chemistry

The Ohio State University

650 Ackerman Rd - Room 130 F

Phone: 614/292-2736

Fax: 614/292-3163

E-mail: lempert.1@osu.edu

PLEASE NOTE

The APS has made every effort to provide accurate and complete information in this *Bulletin*. However, changes or corrections may occasionally be necessary and may be made without notice after the date of publication. To ensure that you receive the most up-to-date information, please check the meeting Corrigenda distributed with this *Bulletin*.

CALL FOR NOMINATIONS FOR THE APS COMMITTEE ON PROFESSIONAL STANDARDS

The APS Committee on Professional Standards (CPS) is a permanent body of the APS that is responsible for the development and maintenance of the APS Code of Professional Standards. The CPS is currently seeking nominations for its members. The committee is composed of representatives from the APS member societies and the APS itself. The committee's primary responsibility is to ensure that the APS maintains the highest standards of professional conduct. The committee will also be responsible for reviewing and recommending changes to the Code of Professional Standards. The committee will meet on a regular basis to discuss and act on matters related to the Code of Professional Standards. The committee will also be responsible for reviewing and recommending changes to the Code of Professional Standards. The committee will meet on a regular basis to discuss and act on matters related to the Code of Professional Standards. The committee will also be responsible for reviewing and recommending changes to the Code of Professional Standards. The committee will meet on a regular basis to discuss and act on matters related to the Code of Professional Standards.

Epitome of the 59th Annual Gaseous Electronics Conference of the American Physical Society

**18:00 MONDAY EVENING
9 OCTOBER 2006**

AS **Reception**
Ohio State - Department of
Mechanical Engineering, Multi
Purpose

**8:00 TUESDAY MORNING
10 OCTOBER 2006**

BT1 **Plasma Sources I**
Salon CD, Holiday Inn

BT2 **Plasma Boundaries: Sheaths and
Boundary Layers**
Salon B, Holiday Inn

**10:00 TUESDAY MORNING
10 OCTOBER 2006**

CT1 **Plasma Aerodynamics and
Propulsion I**
Adamovich, Popovic
Salon CD, Holiday Inn

CT2 **Collision Processes with
Biological and Environmental
Applications**
Brunger, Illenberger, Laroussi
Salon B, Holiday Inn

**13:30 TUESDAY AFTERNOON
10 OCTOBER 2006**

DT1 **Plasma Chemistry**
von Keudell
Salon CD, Holiday Inn

DT2 **Electron Impact Ionization and
Excitation I**
Foster, Schappe, Rescigno
Salon B, Holiday Inn

**16:00 TUESDAY AFTERNOON
10 OCTOBER 2006**

ET1 **Plasma Sources II**
Salon CD, Holiday Inn

ET2 **Oxygen-Iodine Lasers**
Salon B, Holiday Inn

**19:15 TUESDAY EVENING
10 OCTOBER 2006**

FPT1 **Poster Session IA**
Salon A, Holiday Inn

FPT2 **Poster Session IB**
Buckeye, Holiday Inn

**8:00 WEDNESDAY MORNING
11 OCTOBER 2006**

GW1 **Diagnostics I: Electrical**
Salon CD, Holiday Inn

GW2 **High Pressure Discharges I**
Heberlein, Tachibana
Salon B, Holiday Inn

**10:00 WEDNESDAY MORNING
11 OCTOBER 2006**

HW **Allis Prize Lecture**
Lieberman
Salon CD, Holiday Inn

**11:00 WEDNESDAY MORNING
11 OCTOBER 2006**

JW **Business Meeting**
Salon CD, Holiday Inn

**12:00 WEDNESDAY NOON
11 OCTOBER 2006**

KW **General Committee Meeting**
Salon CD, Holiday Inn

**13:30 WEDNESDAY AFTERNOON
11 OCTOBER 2006**

LW1 **Plasma Aerodynamics and
Propulsion II**
Shneider
Salon CD, Holiday Inn

LW2 **Electron Impact Ionization and Excitation II**
Schulz, Lower
Salon B, Holiday Inn

Salon CD, Holiday Inn

RR2 **Lighting Plasmas**
Sommerer, Bowden
Salon B, Holiday Inn

16:00 WEDNESDAY AFTERNOON
11 OCTOBER 2006

MW1 **Diagnostics II: Optical**
Salon CD, Holiday Inn

16:00 THURSDAY AFTERNOON
12 OCTOBER 2006

SRP1 **Poster Session IIA**
Salon A, Holiday Inn

MW2 **Thermal Plasmas, Arcs, and Breakdown**
Salon B, Holiday Inn

SRP2 **Poster Session IIB**
Buckeye, Holiday Inn

8:00 THURSDAY MORNING
12 OCTOBER 2006

18:00 THURSDAY EVENING
12 OCTOBER 2006

PR1 **Plasma Applications for Nanotechnology**
Samukawa
Salon CD, Holiday Inn

UR **Banquet**
Salon BCD, Holiday Inn

PR2 **Computational Methods and Modeling for Plasmas**
Salon B, Holiday Inn

8:00 FRIDAY MORNING
13 OCTOBER 2006

VF1 **Plasma-Surface Interactions**
Donnelly
Salon CD, Holiday Inn

10:00 THURSDAY MORNING
12 OCTOBER 2006

VF2 **Transport Theory and Electron Distribution Functions**
Viehland
Salon B, Holiday Inn

QR1 **High Pressure Discharges II**
Terashima
Salon CD, Holiday Inn

10:00 FRIDAY MORNING
13 OCTOBER 2006

QR2 **Electron and Positron Collisions**
McKoy, Johnson, Bray
Salon B, Holiday Inn Chair

WF1 **Capacitively Coupled Plasmas**
Booth
Salon CD, Holiday Inn

13:30 THURSDAY AFTERNOON
12 OCTOBER 2006

RR1 **Material Processing in Low Pressure Plasmas**
Barnes

WF2 **Heavy Particle Collisions, Attachment, and Recombination**
Gerlich
Salon B, Holiday Inn

SESSION AS: RECEPTION
Monday evening, 9 October 2006
Multi Purpose, Ohio State - Department of Mechanical Engineering at 18:00
Walter R. Lempert, Ohio State University, presiding

18:00
AS 1 Reception

The reception will be held in the Multi Purpose room of the Department of Mechanical Engineering at Ohio State University. The reception is open to all attendees of the GEC 2006 conference. The reception will provide an opportunity for attendees to meet and greet each other, as well as to enjoy refreshments. The reception will be held from 18:00 to 19:00 hours.

The reception will be held in the Multi Purpose room of the Department of Mechanical Engineering at Ohio State University. The reception is open to all attendees of the GEC 2006 conference. The reception will provide an opportunity for attendees to meet and greet each other, as well as to enjoy refreshments. The reception will be held from 18:00 to 19:00 hours.

The reception will be held in the Multi Purpose room of the Department of Mechanical Engineering at Ohio State University. The reception is open to all attendees of the GEC 2006 conference. The reception will provide an opportunity for attendees to meet and greet each other, as well as to enjoy refreshments. The reception will be held from 18:00 to 19:00 hours.

The reception will be held in the Multi Purpose room of the Department of Mechanical Engineering at Ohio State University. The reception is open to all attendees of the GEC 2006 conference. The reception will provide an opportunity for attendees to meet and greet each other, as well as to enjoy refreshments. The reception will be held from 18:00 to 19:00 hours.

The reception will be held in the Multi Purpose room of the Department of Mechanical Engineering at Ohio State University. The reception is open to all attendees of the GEC 2006 conference. The reception will provide an opportunity for attendees to meet and greet each other, as well as to enjoy refreshments. The reception will be held from 18:00 to 19:00 hours.

SESSION BT1: PLASMA SOURCES I

Tuesday morning, 10 October 2006

Salon CD Holiday Inn at 8:00

A.R. Ellingboe, Dublin City University, Ireland, presiding

Contributed Papers

8:00

BT1 1 Electron beam-generated ion-ion plasmas: Etching and diagnostics* S.G. WALTON, D. LEONHARDT, R.F. FERNSLER, *US Naval Research Laboratory* Positive ion-negative ion (ion-ion) plasmas are those where negative ions are the primary negative charge carrier and in the absence of any significant electron density, these negative ions are not confined to the bulk plasma. Thus, a nearly equal and anisotropic flux of positive and negative ions can be delivered to surfaces located adjacent to the plasma and eliminate electron-induced damage to substrates in etching applications. A requirement for the formation of ion-ion plasmas in low pressure, halogen-based gas backgrounds is a low electron energy so that the attachment rate is comparable to the ionization rate and the plasma electrons can be rapidly converted to negative ions. Electron beam-generated plasmas provide an opportunity to investigate ion-ion plasmas and their potential applications because of their uniquely low electron temperature compared to conventional discharges. In this presentation, we discuss recent investigations of ion-ion plasmas formed in pulsed, electron beam-generated plasmas produced in mixtures of SF₆ and their use in silicon etching. In this system, positive and negative ions were extracted using a low frequency (10-50 kHz), low voltage (0-300 V) bias. The results of Si etching experiments and plasma diagnostics will be presented with the goal of understanding the optimum system configuration and operating conditions.

*This work supported by the Office of Naval Research

8:15

BT1 2 Automated method for creating arbitrary substrate voltage wave forms for manipulating energy distribution of bombarding ions during plasma processing* AMY WENDT, *UW Madison* MARLANN PATTERSON, *UW Platteville* HSUAN-YIH CHU, *UW Madison* Accurate and reproducible control of ion bombardment energy during plasma processing is a means to better understand the nature of plasma-surface interaction and to control process outcomes. Ion energy distribution (IED) control can be achieved by tailoring the wave form shape of an rf bias applied to the substrate during processing, through the use of a programmable wave form generator in combination with a power amplifier. Due to the frequency dependence of the amplifier gain and the impedance of the plasma in contact with the substrate, however, it is not practical to predict the shape of wave form needed at the generator to produce a desired result at the substrate. Introduced here is a systematic approach using feedback control in the frequency domain to produce arbitrary wave form shapes at the substrate. Specifically, a fast Fourier Transform (FFT) of the substrate wave form is compared, one frequency at a time, with the FFT of a desired target wave form, to determine adjustments needed at the generator. This iterative procedure, which is fully automated and tested for several target wave form shapes, is repeated until the substrate wave form converges to the targeted shape, providing a quick systematic method for producing an arbitrary IED at the substrate.

*Support from NSF (ECS-0078522) and the UW Grad School.

8:30

BT1 3 Scaling laws in dc micro discharges* MARIJA RADMILOVIC-RADJENOVIC, *Associate Research Professor* ZORAN PETROVIC, *Research Professor* BRANISLAV RADJENOVIC, *Associate Research Professor* PAULE MAGUIRE, *Research Professor* CHARLES MAHONY, *Research Professor* INSTITUTE OF PHYSICS TEAM, VINCA INSTITUTE OF NUCLEAR SCIENCES TEAM, NANOTECHNOLOGY RESEARCH INSTITUTE, UNIVERSITY OF ULSTER TEAM In order to establish the operation regime of micro discharges we should start from the low pressure discharges and employ the standard scaling laws. Discharges should scale according to the reduced electric field E/N and pd - product proportional to the number of collisions. Finally, the scaling should be made in accordance with the jd^2 - describing the space charge effects [1]. We have calculated the Paschen curves and Volt- Ampere characteristic by using a PIC code and appropriate data for argon in order to establish whether the standard micro discharges operate in Townsend regime or in Glow Regime. [1] A.V. Phelps, Z.Lj. Petrović and B.M. Jelenković, *Phys. Rev. E* **47** 2825 (1993).

*141025 MNSTR

8:45

BT1 4 Hydrodynamic models for the positive column with neutral gas depletion. JEAN-LUC RAIMBAULT, LAURENT LIARD, PASCAL CHABERT, *LPTP CNRS Ecole Polytechnique* In the classical low-temperature plasma equilibrium, the ionization degree is sufficiently small that neutral density is considered constant. However, in many contemporary plasma reactors, such as helicons, the ionized fraction can be significant. This fraction may even reach 100% in plasma thrusters. In such circumstances, neutral dynamics has to be included in order to solve the plasma equilibrium. We have revisited the plasma equilibrium models, from low-pressure (Tonks-Langmuir) to high pressure (ambipolar diffusion) regime, including the neutral dynamics. The results show that neutrals are pushed towards the wall by the electronic pressure, creating a neutral depletion at the center of the discharge. The effect is significant when the electronic pressure becomes comparable to the neutral pressure. The electron temperature becomes a function of the electron density, so that particle and power balance are not decoupled. Finally, we derived a new expression for the edge-to-center electron density ratio which accounts for neutral density depletion.

9:00

BT1 5 Numerical Simulation of the DC Discharge Using CFD-ACE+ NING ZHOU, PENG ZHANG, *ESI-CFD, 6767 Old Madison Pike NW, Suite 600, Huntsville, AL 35806* ESI R&D TEAM A low pressure DC discharge is simulated using the CFD-ACE+. The electron kinetics is obtained from the kinetic module. The local and non-local approaches are used separately for solving the kinetic equation. The results are compared at different locations in the discharge. It is shown that although the local approximation gives a good description of the electron energy distribution function (EEDF) in the bulk plasma, it fails to give accurate information of the EEDF near the wall, which is highly non-Maxwellian. As a result, the non-local approach is more appropriate for the kinetic treatment of plasma electrons in a low pressure DC discharge. The ion number density and momentum are obtained from a fluid model. For comparison, the electron continuity equations are also included. Based on the simulation model, the species'

density profile, the power balance and the influence of the electron-electron coulomb collisions on the EEDF and discharge physics are investigated. The simulation results are also compared with results from pure fluid model without kinetic description.

9:15

BT1 6 Simulation of moving striations in rare gas plasmas VLADIMIR KOLOBOV, ROBERT ARSLANBEKOV, *CFD Research Corporation, Huntsville, AL, USA* Ionization waves (moving striations) have been observed in classical DC discharges of rare gases in a wide range of gas pressures and discharge currents. Recently, striations have been also observed in plasma display cells and other micro-discharges. We have obtained moving striations in computer experiments using self-consistent discharge model. The model includes Boltzmann solver for electron kinetics, fluid model for ion transport, Poisson equation for the electric field and (optionally) an external circuit model. Simulations are performed from cathode to anode in 1d or 2d settings. Striations appear initially near the cathode and propagate towards the anode as observed in experiments. The model allows studies of nonlinear waves and effects of external circuit on the wave properties. We will discuss the mechanism of striations for different operating conditions and present results of simulations for a DC discharge in Argon gas for a typical pressure of 1 Torr, tube radius $R=1$ cm, for different discharge currents. High sensitivity of striations to the state of electron gas and ionization kinetics makes them an ideal tool for testing discharge models and advanced plasma diagnostics.

SESSION BT2: PLASMA BOUNDARIES: SHEATHS AND BOUNDARY LAYERS

Tuesday morning, 10 October 2006

Salon B Holiday Inn at 8:00

M.A. Lieberman, University of California, Berkeley, presiding

Contributed Papers

8:00

BT2 1 Electron Sheaths and Non-ambipolar Diffusion in Laboratory Plasma* SCOTT BAALRUD, NOAH HERSHKOWITZ, *Engineering Physics Department, University of Wisconsin-Madison* Electron sheaths were first predicted by Langmuir in 1929 when he stated that, "with a large area, A , an anode sheath is a positive ion sheath, but that as A decreases, a point is reached where the positive ion sheath disappears and it is replaced by an electron sheath."¹ We show that electron sheath formation near a positive anode depends on the anode area, A_a , as well as the area available for ion loss, A_i . When $A_a/A_i < (m_e/m_i)^{1/2}$, the electron sheath potential monotonically decreases from the anode to the bulk plasma. When the anode is larger than this, a potential dip forms in the electron sheath to reduce the electron current lost to the anode. This potential dip is necessary to preserve global current balance and when it is present, total non-ambipolar diffusion can occur where all electrons are lost from the plasma through

an electron sheath and all positive ions are lost elsewhere. Additional measurements were carried out to identify the transition from positive (ion) to negative (electron) sheaths. Data were taken in low-pressure argon plasma generated by hot filaments and confined in a multidipole chamber.

*Work supported by US DOE grant FG02-97ER 54437.

¹I. Langmuir, *Physical Review* **33**, 954 (1929).

8:15

BT2 2 Total Non-Ambipolar RF Electron Source – Better than a Hollow Cathode* NOAH HERSHKOWITZ, BEN LONGMIER, SCOTT BAALRUD, *Engineering Physics Department, University of Wisconsin-Madison* A Radio Frequency (RF) plasma based electron source has been developed based on results of our electron sheath studies in weakly collisional DC plasmas. In total non-ambipolar flow, all of the electrons leaving the plasma are lost through an electron sheath at the aperture. This occurs if the ratio of the ion loss area to the extraction aperture area is approximately equal to the square root of the ratio of the ion mass to the electron mass, and the ion sheath potential drop at the chamber walls is much larger than T_e/e . Gridless extraction of electrons is achieved by using an axial expanding magnetic field of (maximum value of 100 Gauss) that makes it possible to achieve a uniform plasma potential across the exit aperture. An electron current of 15 A was achieved with 15 sccm Ar and 1200 W.

*Work supported by US DOE grant FG02-97ER 54437.

8:30

BT2 3 Arc cathode spots and normal spots on glow cathodes: self-organization phenomena* MIKHAIL BENOLOV, *Departamento de Fisica, Universidade da Madeira, Largo do Municipio, 9000 Funchal, Portugal* Current transfer from high-pressure DC arc plasmas to thermionic cathodes may occur in the diffuse mode, where the current is distributed over the front surface of the cathode in a more or less uniform way, or in a spot mode, where most of the current is localized in one or more small areas. The diffuse mode occurs at high values of the discharge current, spot modes occur at low currents. A similar phenomenon is observed on cold cathodes of DC glow discharges: current transfer can occur in the abnormal mode, where the current is more or less uniformly distributed over the cathode, or in the normal mode, where only part of the cathode is active; the abnormal mode occurs at high discharge currents and the normal mode occurs at low currents. Although physical mechanisms are very different, the overall patterns of the two phenomena are similar: the mode with a uniform current distribution operates on the falling branch of the current-voltage characteristic and is unstable due to a positive feedback; the spot mode operates on the growing section and is stable. In fact, both phenomena represent examples of self-organization. Mathematical descriptions also have important features in common. This allows one to develop a unified treatment of both phenomena, which is a subject of the present work.

*Work supported by the project POCI/FIS/60526/2004 of FCT, POCI 2010 and FEDER.

8:45

BT2 4 Revisiting the capacitive sheath IGOR KAGANOVICH, *Princeton Plasma Physics Laboratory* Traditional theory of the capacitive sheath assumes that the large negative charge at the electrode is screened by the ion space charge and the transition to the small rf electric field in the plasma occurs abruptly within the

narrow transition region of the Debye length. However, careful self-consistent kinetic treatment of the problem reveals existence of additional transition layer of length V_T/ω , where V_T is the electron thermal velocity and ω is the discharge frequency [1,2,3]. Electrons interacting with the capacitive sheath acquire velocity modulations. As a result, the electron density bunches appear in the region adjacent to the sheath. These electron density perturbations decay due to phase mixing over a length of order V_T/ω . The electron density perturbations polarize the plasma and produce an electric field in the plasma bulk. This electric field, in turn, changes the velocity modulations and total power deposition. Recent particle-in-cell simulations [4,5] confirm the prediction of analytic theory. [1] L. D. Landau, *J. Phys. (USSR)* **10**, 25 (1946). [2] Igor D. Kaganovich, *Phys. Rev. Lett.* **89**, 265006 (2002). [3] I. D. Kaganovich, O. V. Polomarov, and C. E. Theodosiou, "Revisiting the anomalous rf field penetration into a warm plasma," to be published in *IEEE Trans. Plasma Sci.* (2006). [4] H. C. Kim, G. Y. Park, and J. K. Lee, **13**, 023501 (2006). [5] E. Kawamura, M. A. Lieberman, and A. J. Lichtenberg, *Phys. of Plasmas* **13**, 053506 (2006).

9:00

BT2 5 Influence of a micro-scale wafer structure upon sheath profile in 2f-CCP in SF₆/O₂ FUKUTARO HAMAOKA, TAKASHI YAGISAWA, TOSHIAKI MAKABE, *Keio University*
MEMS-dry processes have been developed on the basis of plasma technologies in microelectronic device fabrications. Deep Si etching for MEMS requires a high speed, selective and anisotropic process having several tens or hundreds μm in width and depth as compared with that of ULSI elements. During the MEMS process

at hundreds mTorr, the sheath thickness in front of the surface to be etched will be comparable to or smaller than the trench/hole width, and a distorted sheath field will have a strong influence on the incident ion flux and velocity distribution (i.e., plasma molding). In the present study, we will estimate the local characteristics of the plasma molding, i.e., the ion velocity distribution incident on a micro scale patterned wafer by using a series of repetitive calculation of the structure from cm to μm in 2f-CCP in SF₆/O₂ at 300 mTorr. Further investigation will be given for the feature profile of a Si-MEMS by plasma etching in the 2f-CCP system.

9:15

BT2 6 Ion Energy Distribution Measured in Pulsed Boron Trifluoride Glow Discharge LUDOVIC GODET, SVETLANA RADOVANOV, JAY SCHEUER, *Varian Semiconductor Equipment Associates* CHRISTOPHE CARDINAUD, GILLES CARTRY, *University of Nantes, France* VSEA TEAM
Pulsed plasma doping has emerged as an efficient technology for low energy implantation. The cathode sheath in the pulsed glow discharge plays a key role in defining the ion energy distribution of ions reaching the wafer. Understanding the structure, dynamics and collisional properties of the sheath is critical for successful application of these discharges to low energy plasma implantation. In this study, the ion energy distributions in the cathode sheath of a boron trifluoride discharge are discussed. Measured ion energy distributions are analyzed in the collisionless and collisional sheath regime. Based on the experimental ion energy distributions, the dopant depth profile is calculated. The optimal shallow dopant depth distribution in silicon can therefore be obtained by proper tuning of the plasma parameters.

SESSION CT1: PLASMA AERODYNAMICS AND PROPULSION I

Tuesday morning, 10 October 2006; Salon CD Holiday Inn at 10:00; J. William Rich, Ohio State University, presiding

Invited Papers

10:00

CT1 1 Repetitively Pulsed Nonequilibrium Plasmas for Plasma-Assisted Combustion, Flow Control, and Molecular Lasers.

IGOR ADAMOVICH, *Ohio State University*

The paper presents results of three experiments using high voltage, short pulse duration, high repetition rate discharge plasmas. High electric field during the pulse ($E/N \sim 500\text{-}1000$ Td) allows efficient ionization and molecular dissociation. Between the pulses, additional energy can be coupled to the decaying plasma using a DC field set below the breakdown threshold. While the DC sustainer discharge adds 90-95% of all the power to the flow, it does not produce any additional ionization. The pulser and the sustainer discharges are fully overlapped in space. Low duty cycle of the pulsed ionizer, $\sim 1/1000$, allows sustaining diffuse and uniform pulser-sustainer plasmas at high pressures and power loadings. The first experiment using the pulsed discharge is ignition of premixed hydrocarbon-air flows, which occurs at low pulsed discharge powers, ~ 100 W, and very low plasma temperatures, 100-200^o C. The second experiment is Lorentz force acceleration of low-temperature supersonic flows. The pulsed discharge was used to generate electrical conductivity in $M=3$ nitrogen and air flows, while the sustainer discharge produced transverse current in the presence of magnetic field of $B=1.5$ T. Retarding Lorentz force applied to the flow produced a static pressure increase of up to 15-20%, while accelerating force of the same magnitude resulted in static pressure rise of up to 7-8%, i.e. a factor of two smaller. The third experiment is singlet delta oxygen (SDO) generation in a high-pressure pulser-sustainer discharge. SDO yield was inferred from the integrated intensity of SDO infrared emission spectra calibrated using a blackbody source. The measured yield exceeds the laser threshold yield by about a factor of three, which makes possible achieving positive gain in the laser cavity. The highest gain measured so far is 0.03%/cm.

10:30

CT1 2 Aerodynamic Effects in Weakly Ionized Gas: Phenomenology and Applications.*SVETOZAR POPOVIC, *Old Dominion University, Physics Department*

Successful application of gas discharges in aerodynamics requires their efficient generation, sustaining and control at supersonic or hypersonic flow conditions. Wall-free plasma formations that meet the requirements may then act as time-controlled and space-localized actuators to modify the flow. Potential candidates for this challenging task are plasmas contained in open or linear-cavity microwave field structures. We present and discuss direct observations of aerodynamic effects activated or modified by wall-free discharges. Further, we compare two generic types of wall-free discharges. First group, applicable for inlet-type structures, consists of a periodic series of microwave-induced plasmoids generated in a linear cavity, using the outgoing wave from a microwave antenna and the reflected wave from a nearby on-axis concave reflector. The plasmoids are spaced at half-wavelength separations according to the standing-wave pattern. The plasmoids are enhanced by an "effective focusing" in the near field of the antenna (Fresnel region) as a result of diffraction effects and mode structure. Second group, applicable to supersonic and hypersonic boundary layers, are the surface microwave discharges enhanced by a structure of Hertz dipoles. Standard microwave discharge phenomenology, such as microwave breakdown, mode structure and plasma parameters, is revisited to present a quantitative interpretation of the observed effects. Special attention is given to complex phenomena specific to flow-plasma interaction (double electric layers, ionization waves, instabilities), which provide the physical basis for localized heating in the aerodynamic flow.

*Supported by NASA Langley Research Center

Contributed Papers

11:00

CT1 3 Modeling of Asymmetric Dielectric Barrier Discharge Plasma Actuators for Flow Control

SERGEY MACHERET, ALEXANDER LIKHANSKII, MIKHAIL SHNEIDER, RICHARD MILES, *Princeton University* Asymmetric dielectric barrier discharge (DBD) plasma actuators have been demonstrated to be effective in low-speed flow control. However, understanding of their physics is currently insufficient. We have developed a comprehensive kinetic model for asymmetric DBD actuators in air. Modeling showed that charging of the dielectric during the avalanche ionization lasts a small fraction of the cycle but plays crucial role. The tangential force on the gas is shown to be directed downstream in both cathode and anode half-cycles, with critical role of negative ions in the cathode half-cycle and of positive ions in the anode half-cycle. The motion of positive ions toward the exposed electrode in the cathode half-cycle considerably decreases the integrated downstream force. Based on the detailed understanding of DBD actuator operation, an optimal voltage waveform is proposed, consisting in high repetition rate nanosecond pulses of negative voltage in combination with positive dc bias applied to the exposed electrode. Computations show that repetitive-pulse waveform can induce gas velocities similar to those in conventional sine-voltage DBD actuators at considerably lower voltages and smaller plasma sizes. Application of repetitive-pulse waveform with several kilovolt peak voltages is predicted to generate wall jet velocities at least an order of magnitude higher than those in conventional DBD actuators.

11:15

CT1 4 Modeling of plasma-assisted combustion in premixed air-fuel supersonic flows

ANATOLY NAPARTOVICH, IGOR KOCHETOV, *Troitsk Institute for Innovation and Fusion Research* SERGEY LEONOV, *Institute of High Temperature RAS TRINITY TEAM, IHT RAS COLLABORATION* Numerical model was developed combining traditional approach of thermal combustion chemistry with advanced description of the plasma kinetics based on solution of electron Boltzmann equation. This approach allows us to describe self-consistently strongly non-equilibrium electric discharge in chemically unstable gas. A com-

parison is made between plasma-assisted and thermal ignitions for the hydrogen/air and ethylene/air mixtures. A pseudo-one-dimensional plug flow model was developed to calculate gas flow evolution in plane duct. Numerical simulations predicted a notable reduction of the ignition length and the energy input in the discharge required for the ignition of the pre-mixed fuel. In particular, for the hydrogen/air mixture in the duct of length 80 cm, the inlet static gas temperature 700 K and static gas pressure 1 bar the minimum reduced energy input in the dc glow discharge is 150 J/g, while for the thermal ignition it is as twice as high. The numerical simulation of dc discharge-initiated combustion of a hydrogen-air mixture in a supersonic duct has shown that the effects of acceleration is not very sensitive to the fuel/oxidant ratio and gradually decreases with fuel dilution. It is shown that the ethylene/air mixture can be ignited by the glow discharge at the reduced energy input 1.6 times greater than the hydrogen/air mixture.

11:30

CT1 5 MHD Flow Control and Power Generation in Low-Temperature Supersonic Flows

IGOR ADAMOVICH, MUNETAKE NISHIHARA, *Ohio State University* The paper presents results of cold MHD flow deceleration and MHD power generation experiments using repetitively pulsed, short pulse duration, high voltage discharge to produce ionization in $M=3$ nitrogen and air flows. MHD effect on the flow is detected from the flow static pressure measurements. Retarding Lorentz force applied to the flow produces a static pressure increase of up to 17-20%, while accelerating force of the same magnitude results in static pressure increase of up to 5-7%. No discharge polarity effect on the static pressure was detected in the absence of the magnetic field. The fraction of the discharge input power going into Joule heat in nitrogen and dry air, inferred from the present experiments, is low, $\alpha=0.1$, primarily because energy remains frozen in the vibrational energy mode of nitrogen. Comparison of the experimental results with the modeling calculations shows that the retarding Lorentz force increases the static pressure rise produced by Joule heating of the flow, while the accelerating Lorentz force reduces the pressure rise. This result provides first direct evidence of cold supersonic flow deceleration by Lorentz force.

11:45

CT1 6 Ignition of Gaseous and Liquid Hydrocarbon Fuels by Repetitively Pulsed, Nanosecond Pulse Duration Plasma IGOR ADAMOVICH, AINAN BAO, YURII UTKIN, SAURABH KESHAV, *Ohio State University* The paper presents results of plasma assisted combustion experiments in premixed hydrocarbon-air flows excited by a low-temperature, transverse, repetitively pulsed discharge plasma. The experiments have been conducted with methane, ethylene, methanol, and ethanol fuels in a wide range of equivalence ratios and flow velocities. The plasma was generated by high-voltage (16-18 kV), short pulse duration (20-30 nsec), high repetition rate (up to 50 kHz) pulses. The high reduced electric field during the pulse allows efficient electronic excitation and

molecular dissociation. The low duty cycle of the discharge, $\sim 1/1000$, greatly improves its stability and helps sustaining diffuse and volume-filling plasma. In a wide range of conditions, generating the plasma in premixed air-fuel flows resulted in flow ignition and flameholding. Plasma assisted ignition occurred at a low discharge powers, ~ 100 W ($\sim 1\%$ of heat of reaction), and very low flow temperatures, 100-200^o C. The reacted fuel fraction, measured by the FTIR absorption spectroscopy, is up to 85-95%. Plasma temperature was inferred from nitrogen second positive band system emission spectra and calibrated using thermocouple measurements in flows preheated by an in-line flow heater (without plasma).

SESSION CT2: COLLISION PROCESSES WITH BIOLOGICAL AND ENVIRONMENTAL APPLICATIONS

Tuesday morning, 10 October 2006; Salon B Holiday Inn at 10:00; Birgit Lohmann, Griffith University, Australia, presiding

Invited Papers

10:00

CT2 1 Nanoscale Interactions Driving Macroscopic Phenomena: New Insights into the role of Electron-Driven Processes in Atmospheric Behaviour.*

MICHAEL BRUNGER, *ARC Centre for Antimatter-Matter Studies, Flinders University*

Electrons with energies over a wide range (eV to keV) drive a variety of atomic processes, such as ionisation and excitation of atoms and molecules. The products then play a role in the chemical reactions that occur in the atmosphere, and so influence macroscopic parameters, such as the density of minor constituents and the electron density. This talk describes new insights into the role of these electron-driven processes in atmospheric behaviour.

*In collaboration with Laurence Campbell and Peter Teubner, ARC Centre for Antimatter-Matter Studies, Flinders University; David Cartwright, formerly of Los Alamos National Labs.

10:30

CT2 2 Electron processing at low energies: from basics to environmental and biological applications.*

EUGEN ILLENBERGER, *FU Berlin*

Electron initiated reactions play a key role in nearly any field of pure and applied sciences, in the gas phase as well as in condensed phases or at interfaces. This include substrate induced photochemistry, radiation damage of biological material (and, accordingly, the molecular mechanisms, how radio sensitizers used in tumour therapy operate), reactions induced by electrons in surface tunnelling microscopy (STM), or any kind of plasma used in industrial plasma processing. In each of these fields the electron-molecule interaction represents a key step within an eventually complex reaction sequence. A particularly interesting field is the interaction of electrons with molecules at energies below the level of electronic excitation. In this range many molecules exhibit large cross sections for resonant electron capture, often followed by the decomposition of the transient negative compound (M^{-*}) according to $e^{-} + M \rightarrow M^{-*} \rightarrow R + X^{-}$. We report on such dissociative electron attachment (DEA) processes studied at different stages of aggregation, namely in single molecules under collision free conditions, in clusters formed by supersonic gas expansion, and on the surface of solids or in molecular nano films. In the meantime it has also been recognised that in the damage of living cells by high energy radiation the attachment to flow energy secondary electrons to DNA is a key initial process leading to strand breaks. These secondary electrons are created along the ionisation track of the primary high-energy quantum. Apart from that, biomolecular systems exhibit unique features in DEA, likebond and site selective decompositions.

*Work supported by the Deutsche Forschungsgemeinschaft and the European Union.

11:00

CT2 3 Interaction of cold plasmas with biological cells: What we have learned so far.MOUNIR LAROUSSE, *Old Dominion University*

In the last two decades, non-equilibrium, low temperature, atmospheric pressure plasmas have gained acceptance as an attractive technological solution in industrial applications such as the surface modification of polymers and the cleaning of flue gases. As more reliable "cold" plasma sources are developed, new and interesting applications continue to emerge. Amongst the more recent applications, the use of atmospheric pressure cold plasmas in the biomedical field is presently experiencing a heightened interest from the plasma science research community. This is due to promising possibilities to use these plasmas in medical research such as wound healing, tissue engineering, surface modification of biocompatible materials, and the sterilization of reusable heat-sensitive medical instruments. However, before any of these exciting possibilities become reality, an in-depth understanding of the effects of plasma on the cellular and sub-cellular levels has to be achieved. In this paper, a review of the knowledge that has been gained during the last few years will be presented. First an overview of research efforts on the inactivation of bacterial cells will be presented. This includes the evaluation of the inactivation kinetics and the roles played by the various plasma agents (such as UV photons and free radicals) in the inactivation process. In the second part of this talk, plasma sub-lethal effects on both prokaryotic and eukaryotic cells will be discussed. Finally, the prospects of the use of "cold" plasmas in the biomedical field are outlined.

Contributed Papers

11:30

CT2 4 Electron Collisions with Formic Acid and Tetrahydrofuran

V. VIZCAINO, J.P. SULLIVAN, S.J. BUCKMAN, *CAMS, Australian National University* C. COLYER, *CAMS, Flinders University, Australia* We have measured absolute elastic electron scattering cross sections for the biologically relevant molecules CHOOH (formic acid) and C₄H₈O (tetrahydrofuran - THF). The formate group is an important constituent of a number of amino acids and THF forms part of the DNA backbone. The experiments cover the energy range from 1 to 50 eV and include both angular and energy dependent measurements. We make comparisons with a number of theoretical approaches, including the Kohn variational, and R-matrix techniques and a calculation based on a density functional technique.

11:45

CT2 5 Non-thermal atmospheric plasmas in dentistry*RAYMOND SLADEK, EVA STOFFELS, *Eindhoven University of Technology*

Non-thermal atmospheric plasmas are very efficient in the deactivation of bacteria. A relatively new area is the use of these plasmas in biomedical and dental applications. In this work, application of a novel device in dentistry is investigated, the plasma needle. The plasma needle is used to generate a non-thermal atmospheric micro-plasma. A promising application of this micro-plasma is the treatment of dental cavities, to stop caries without causing pain and removing too much healthy tissue. Various bacterial model systems are used to test the bactericidal efficiency of the plasma needle: bacteria in droplets, thin films and (multi-species) biofilms. The effects of plasma needle treatment on bacterial viability, growth and composition are discussed. The results indicate that plasma can become a useful tool for dental treatment.

*This research was sponsored by the Netherlands Organization for Scientific Research (NWO).

SESSION DT1: PLASMA CHEMISTRY

Tuesday afternoon, 10 October 2006; Salon CD Holiday Inn at 13:30; Pascal Chabert, Ecole Polytechnic, presiding

Invited Papers

13:30

DT1 1 Controlled Particle Generation in an Inductively Coupled Plasma.ACHIM VON KEUDELL, *Ruhr-University Bochum*

Carbon clusters with diameters in the range of 10 to 50 nm are produced by injecting pulses of acetylene into an inductively coupled plasma (ICP) from argon and helium. The injection causes an instability of the inductively coupled plasma, which becomes visible as an oscillation of the emission intensity. The frequency of this oscillation can be uniquely correlated to the particle diameter. Consequently, the measurement of the oscillation frequency represents a method to determine particle diameters in-situ. This particle driven instability of an inductive plasma is characterized by space and time resolved Langmuir probe measurements as well as by optical emission spectroscopy. These data indicate that the oscillation corresponds to the rotation of a localized plasmoid and a particle cloud around the symmetry axis of the reactor. The rotation is driven by the ion wind crossing the interface between the plasmoid and the particle cloud. The interplay of the particles with the performance of the inductive plasma is modelled using a hydrodynamic code.

Contributed Papers

14:00

DT1 2 Optimization of H₂ Production in Ar/NH₃ Micro-discharges* RAMESH ARAKONI, ANANTH N. BHOJ, *University of Illinois* MARK J. KUSHNER, *Iowa State University*

Hydrogen powered vehicles and portable fuel cells may require real-time generation of H₂ to provide fuel safely and with rapid response. One such method is to produce H₂ from feedstock gases that can be more safely stored, such as NH₃. Microdischarge plasmas are being investigated as a means of H₂ production from NH₃ and other gases. The high power densities (10s kW/cm³) that can be obtained in microdischarges provide an intense source of electron impact as well as thermal decomposition of the feedstock gases. By operating at high pressures (> 100s Torr), reformation of the dissociated products leads to efficient production of H₂. In this work, results from a computational investigation of production of H₂ in high pressure microdischarges sustained in Ar/NH₃ mixtures will be discussed. Plug-flow and 2-dimensional plasma hydrodynamics models were used to develop scaling laws to optimize the energy efficiency of the process (e.g., eV/H₂ molecule produced). The 2-d model resolves non-equilibrium electron, ion and neutral transport using fluid equations. The microdischarge geometry of interest is a sandwich flow-through reactor with a central hole a few hundred microns in diameter, power of a few W and residence times of a few microseconds.

*Work supported by the National Science Foundation

14:15

DT1 3 Low-temperature upgrading of low-calorific biogas for CO₂ mitigation using DBD-catalyst hybrid reactor TOMOHIRO NOZAKI, HIROYUKI TSUKIJHARA, WATARU FUKUI, KEN OKAZAKI, *Dept of Mechanical & Control Engineering, Tokyo Institute of Technology*

Although huge amounts of biogas, which consists of 20-60% of CH₄ in CO₂/N₂, can be obtained from landfills, coal mines, and agricultural residues, most of them are simply flared and wasted: because global warming potential of biogas is 5-15 times as potent as CO₂. Poor combustibility of such biogas makes it difficult to utilize in conventional energy system. The purpose of this project is to promote the profitable recovery of methane from poor biogas via non-thermal plasma technology. We propose low-temperature steam reforming of biogas using DBD generated in catalyst beds. Methane is partially converted into hydrogen, and then fed into internal combustion engines for improved ignition stability as well as efficient operation. Low-temperature steam reforming is beneficial because exhaust gas from an engine can be used to activate catalyst beds. Space velocity (3600-15000 hr⁻¹), reaction temperature (300-650 °C), and energy cost (30-150 kJ per mol CH₄) have been investigated with simulated biogas (20-60% CH₄ in mixtures of CO₂/N₂). The DBD enhances reaction rate of CH₄ by a factor of ten at given catalyst temperatures, which is a rate-determining step of methane steam reforming, while species concentration of upgraded biogas was governed by thermodynamic equilibrium in the presence of catalyst.

14:30

DT1 4 Mechanism of Ethane Destruction in Dielectric Barrier Discharge in Air: Detailed Elementary Reaction Model and Experiment LEV KRASNOPEROV, CAMILA MODENESE, LARISA KRISHTOPA, *New Jersey Institute of Technology*

Free radical destruction mechanism was extended by inclusion of reactions of excited and ionic species. The mechanism consists of 935

reactions of 85 neutral species, 9 excited states and 38 ions. The reactions include 9 initiation processes in streamers, 66 processes involving excited states and 83 reactions involving ions. The reactant, the final products as well as the major intermediates of the destruction of ethane in air in corona discharge were identified and quantified Carbon dioxide (CO₂), water (H₂O), formaldehyde (H₂CO), acetaldehyde (CH₃CHO), methanol (CH₃OH), ethanol (C₂H₅OH), formic acid (HCOOH), acetic acid (CH₃COOH), methyl nitrate (CH₃ONO₂) and ethyl nitrate (C₂H₅ONO₂) were identified among the major destruction products. The destruction efficiency predicted by the mechanism is in good agreement with the experiment, the major contribution is being due to the ionization transfer reactions. Reactions of excited species play but only a minor role. The product spectrum is consistent with the subsequent low temperature free radical reactions complicated by the presence of ozone and nitrogen oxides. The generic reaction mechanism for other organic as well as inorganic compounds is discussed.

14:45

DT1 5 Gas phase Boudouard disproportionation reaction between highly vibrationally excited CO molecules KATHERINE ESSENHIGH, YURII UTKIN, CHAD BERNARD, IGOR ADAMOVICH, WILLIAM RICH, *Ohio State University* NONEQUILIBRIUM THERMODYNAMICS LABORATORIES TEAM

The gas-phase Boudouard disproportionation reaction (1) between highly vibrationally excited CO molecules in nonequilibrium optically excited plasma has been studied in this work. CO(v) + CO(w) → CO₂ + C The experiments were conducted in a mixture of Ar and CO at different CO partial pressures. The cw CO laser beam (14 Watt) was used to create an optically pumped plasma in a small glass reactor. The vibrational distribution function (VDF) of CO was measured in the plasma region using the fourier transform infrared emission spectroscopy. Carbon dioxide production rate was determined from the absorption of CO₂ asymmetric stretch. Small amounts of helium was added to the mixture to alter the VDFs and change the of CO₂ production rate. The activation energy E_a ~ 11eV was inferred by using the transition state theory to fit the experimental data. This activation energy is very close to the CO dissociation energy of 11.09eV. Such a high activation energy suggests that both colliding particles have to be in very highly excited vibrational states for the reaction (1) to occur. The total rate constant K_B for the reaction (1) was found to be 6 · 10⁻¹⁷ cm³/sec.

15:00

DT1 6 Chlorine atom concentration determination via gas phase titration SREERUPA BASU, *Ohio University*

Chlorine oxidizes elemental mercury in coal flue gas. Addition of chlorine gas into an electrostatic precipitator, used to clean the flue gas, will thus increase the mercury removal efficiency in the precipitator. Determination of the chlorine atom concentration, formed inside the chamber, is a key to evaluate this efficiency. A series of experiments are performed to dissociate the chlorine gas in a corona-discharge field formed inside a 15X3 cm flow pyrex tube at P=1atm, and the chlorine atoms formed are measured by reacting them with butane. The reaction products are quantified using a GC-FID. The quantification of the chlorine atoms formed under varying parametric conditions like the voltage supplied, amount of chlorine gas injected into the reaction chamber and the distance between the electrodes will thus help in optimizing the amount of chlorine reagent gas needed to be added to a precipitator to obtain enhanced mercury removal efficiency.

SESSION DT2: ELECTRON IMPACT IONIZATION AND EXCITATION I

Tuesday afternoon, 10 October 2006; Salon B Holiday Inn at 13:30; Jim Colgan, Los Alamos National Laboratory, presiding

Invited Papers

13:30

DT2 1 Latest Developments in the Theoretical Calculation of Atomic Ionization by Charged Particle Impact.MATT FOSTER, *Theoretical Division, T-4 Los Alamos National Laboratory*

The ionization of atoms by electron or ion impact for highly differential scattering has primarily concentrated on the traditional ($e, 2e$) scattering plane. The initial and final momentum vectors of the projectile define the scattering plane. The assumption has been that all the important physical effects would be observed in the scattering plane due to symmetry. Previous work on ion impact ionization of helium showed that experiment and theory are in good agreement in the scattering plane and in poor agreement out-of-the-scattering plane for $C6^+$ projectile ions. In this presentation, we will show that the same out-of-plane effects can be observed for electron-impact ionization of magnesium. Proper quantum mechanical distorted wave treatment of electron-impact ionization involves fewer approximations than heavy ion ionization. These electron-impact ionization results can be used to determine the physical effects causing the unexplained out-of-the-plane structure for heavy particle collisions. This process revealed that the out-of-plane structure was caused by very close collisions between the projectile and nucleus.

14:00

DT2 2 Electron Excitation and Ionization of the Chlorine Molecule.SCOTT SCHAPPE, *Lake Forest College*

Despite its technological importance, many of the emission systems in molecular chlorine have received surprisingly little study. I will present our experimental measurements of absolute emission cross sections for 10 to 700 eV electrons incident on chlorine molecules. The emission systems include the dominant $Cl_2^+ A^2\Pi - X^2\Pi$ and the Cl_2 systems at 256 nm and 306 nm. The $A - X$ system possesses a very dense band spectrum and I will discuss our efforts to extract individual vibrational cross sections and discuss this system's contribution to the total chlorine ionization cross section.

14:30

DT2 3 Dynamics of resonant excitation and attachment processes in electron-molecule collisions.*T.N. RESCIGNO, *Lawrence Berkeley National Laboratory*

Vibrational excitation and dissociation of small molecules by low-energy electron impact are dominated by resonant processes. In the collision of electrons with molecules and molecular ions, are dominated by resonant processes, Our theoretical understanding of these basic processes comes principally from resonance scattering theory and simple one-dimensional models of the reaction dynamics. This talk will focus on dramatic effects in low-energy dissociative electron attachment (DEA) that are purely polyatomic in origin and that can only be studied with a multi-dimensional treatment of the dissociation dynamics. These effects will be illustrated by our studies of DEA in water, hydrogen disulfide and formic acid.

*Work performed under auspices of USDOE by LBNL and supported by DOE OBES Division of Chemical Sciences.

Contributed Papers

15:00

DT2 4 Near-threshold absolute angle-differential cross sections for electron-impact excitation of argon and xenon.*

MICHAEL ALLAN, *University of Fribourg, Switzerland* OLEG ZATSARINNY, KLAUS BARTSCHAT, *Drake University* Following up on our recent work on $e - Ne$ collisions [1], absolute angle-differential cross sections for electron-impact excitation of argon and xenon atoms to the lowest four $np^5(n+1)s$ levels, and the $5p^55d[7/2]_3$ level in xenon, have been measured and calculated as a function of electron energy up to a few eV above threshold. For argon, excellent agreement is observed between the experimental data and predictions from a Breit-Pauli B -spline R -matrix (BSR) method, in which non-orthogonal orbital sets are used to optimize the target description [2,3]. The agreement is still satisfactory for the more complex xenon target, suggesting that

predictions from the BSR model should already be sufficiently accurate for many modelling applications. Nevertheless, the remaining discrepancies indicate the need for further refinement of the theoretical model. [1] M. Allan, K. Franz, H. Hotop, O. Zatsarinny and K. Bartschat, *J. Phys. B* **39** L139, 2006. [2] O. Zatsarinny and K. Bartschat, *J. Phys. B* **37** (2004) 4693. [3] O. Zatsarinny, *Comp. Phys. Commun.* **174** (2006) 274.

*This work was supported by the Swiss National Science Foundation (MA) and by the United States National Science Foundation (OZ and KB).

15:15

DT2 5 Fluorescence Polarization of Helium Negative Ion Resonances Excited by Polarized Electron Impact*

T.J. GAY, J.W. MASEBERG, *University of Nebraska* The helium triply-excited negative ion $2s^22p^2P$ and $2s2p^2^2D$ resonance states can autoionize to populate the singly excited 3^3D level. Optical obser-

vation of interference from these resonant channels in the $3^3D \rightarrow 2^3P$ 587.5 nm transition is possible and measurements of the intensity and linear polarization fraction of this line are available [1-4]. In contrast to previous work, we utilize spin-polarized electrons and report the integrated Stokes parameters P_1 , P_2 , and P_3 in the 55-60 eV region. Our null result for P_2 indicates that even though these resonances are long lived (~ 200 ps), magnetic forces acting on the temporarily-captured electron are negligible. Values of P_3 show no statistically-significant variation from their asymptotic non-resonant levels. [1] A. Defrance, *J. Phys. B* **13**, 1229 (1980). [2] D. Cvejanović et al., *J. Phys. B* **33**, 2265 (2000). [3] H. Batelaan et al., *J. Phys. B* **24**, 5151 (1991). [4] P. J. M. van der Burgt et al., *J. Phys. B* **19**, 2015 (1986).

*Supported by NSF Grant PHY-0354946.

SESSION ET1: PLASMA SOURCES II

Tuesday afternoon, 10 October 2006

Salon CD Holiday Inn at 16:00

S.G. Walton, Naval Research Laboratory, presiding

Contributed Papers

16:00

ET1 1 Multilevel non-empirical approach to calculation of light emission properties of chemically active non-equilibrium plasma B. POTAPKIN, S. ADAMSON, V. ASTAPENKO, I. CHERNYSHEVA, M. DEMINSKY, A. DEMURA, N. DYATKO, A. ELETSKII, A. KNIZHNIK, I. KOCHETOV, A. NAPARTOVICH, E. RYKOVA, S. UMANSKII, A. ZAITSEVSKII, *Kintech* G. COTZAS, D. MIKHAEL, V. MIDHA, D. SMITH, T. SOMMERER, *GE Global Research* A multi-level approach for calculation of the properties of non-equilibrium plasmas using first principles and theories of elementary processes is described in the paper. In the framework of this approach, unknown properties of molecules, ions and atoms (structure, energy curves, and transition dipole moments) are calculated using quantum-chemical methods. The calculation results are then used to determine emission probabilities, Frank-Condon factors of electronic-vibration transitions, cross sections for electron impact excitation, dissociation, dissociative recombination and attachment. Ion-molecular reactions are treated in terms of the statistical theory. The energy transfer processes involving electronically species are described through the asymptotic approach. The electron impact excitation cross sections for atoms and molecules are calculated using the modified Born approximation. The resulting kinetic state-to-state scheme is then used to compute the dependencies of the electron energy balance and the radiative emission efficiency as a function of the plasma parameters. As an example of this multilevel approach, the radiative emission properties of an Ar-InI DC glow discharge were calculated using the Chemical Workbench computational environment.

16:15

ET1 2 Computational modeling of HC discharges in the presence of an applied magnetic field* SETH VEITZER, PETER STOLTZ, *Tech-X Corporation* We present work on the numerical modeling of hollow cathode discharges using the multi-dimensional, massively parallel, hybrid PIC simulation code VORPAL. We simulate the formation of a plasma in the hollow cathode by modeling the production of ion- and electron-induced secondary electrons from the cathode walls, and electron impact ionization of background Helium gas. We simulate discharge of built-up current through the application of an external magnetic field, effectively shorting out the production of plasma due to secondary electrons, and we compare our results here to published experimental findings. We also discuss the numerical methods that we use to develop the simulations, including the physical models we implement and simulation parameters needed for accurate modeling.

*Supported by DOE grant #DE-FG02-03ER83797 and DOD grant #FA8650-04-C-2511.

16:30

ET1 3 Radially localized helicon mode in helicon plasma sources. GUANGYE CHEN, CHARLES LEE, ALEXEY AREFIEV, BORIS BREIZMAN, RAJA LAXMINARAYAN, ROGER BENGTON, *The University of Texas at Austin* It has been widely believed that helicon waves are excited in helicon discharges. However, an important but often underappreciated feature of helicon plasma sources is that the plasma density is typically strongly nonuniform across the confining magnetic field with a peak at the axis. This nonuniformity can create a radial potential well for non-axisymmetric helicons, allowing radially localized helicon (RLH) waves [1]. This work presents theoretical and experimental evidence that the RLH waves play a significant role in a helicon plasma source. The measurements of a plasma response to a secondary low-power rf generator with variable frequency indicate the existence of an eigenmode close to the driving frequency of the main generator. The 2D plasma density profile was measured and then used to calculate the rf field structure for the experimental setup. The calculations confirm that an RLH wave is the eigenmode excited in the experiment. The calculations were performed using a 2D field solver for a single resonant azimuthal harmonic ($m=1$) under the assumption that the density profile is axisymmetric. 1D field calculations for the measured radial density profile were used to identify the RLH wave by its dispersion relation and to distinguish it from the conventional helicon and Trivelepiece-Gould waves. [1]B. N. Breizman and A. V. Arefiev, *Phys. Rev. Lett.* **84**, 3863 (2000).

16:45

ET1 4 Ionization processes in the high power impulse magnetron sputtering discharge (HIPIMS) JON T. GUDMUNDSSON, *University of Iceland* JOHAN BOHLMARK, *Chemfilt Ion-sputtering AB* ARUTIUN P. EHIASARIAN, *Sheffield Hallam University* ULF HELMERSSON, *Linkoping University* High power impulse magnetron sputtering (HIPIMS) is a technique that utilizes ionized physical vapor deposition (IPVD). High density plasma is created by applying a high power pulse to a planar magnetron discharge. The plasma parameters in the HIPIMS discharge will be reviewed and discussed as well as some applications of the HIPIMS technique. Measurements of the temporal and spatial behavior of the plasma parameters indicate peak electron density of the order of 10^{19} m^{-3} , that expands from the target with a fixed speed that depends on the gas pressure and the gas type.

The high electron density results in a high degree of ionization of the deposition material. Furthermore, the ionization processes and the fractional ionization of the sputtered material is explored using a time dependent global (volume averaged) model. The model calculations give integrated ionized flux fraction in the range of 80 - 90% for Al, Cu and C targets and average power 300 W at 10 mTorr argon pressure.

17:00

ET1 5 Transition from weakly to strongly magnetized gas discharge plasma VALERY GODYAK, *Osrav Sylvania* NATALIA STERNBERG, *Clark University* A study of the fluid model for cylindrical weakly ionized quasi-neutral plasmas in an axial magnetic field is presented. The model takes into account ionization, ion and electron inertia, as well as frictional forces for ions and electrons. The behavior of the plasma parameters for arbitrary magnitudes of the magnetic field, arbitrary gas pressure and plasma size is presented, making the model applicable for a wide range of discharge conditions. A magnetic field parameter is introduced, which specifies a parameter range for the magnetic field, gas pressure and plasma size where the Boltzmann equilibrium with the ambipolar field for the electron distribution is satisfied. In addition, a parametric relation for the magnetic field, gas pressure and plasma size is obtained, which separates the region of weak magnetic field effects from the region of strong magnetic field effects. For strongly magnetized plasmas, an asymptotic solution with non-zero plasma density at the plasma boundary is presented. Analytical approximations for the ionization frequency and the plasma density at the plasma boundary are found for arbitrary external discharge parameters. The theoretical results are supported by numerical computations.

17:15

ET1 6 Ion Source Development at the SNS* ROBERT WELTON, MARTIN STOCKLI, SYD MURRAY, *ORNL-SNS* RICK GOULDING, *ORNL-FED* JERRY CARR, *ORNL-GIT* JUSTINE CARMICHAEL, *ORNL-WPI* The US Spallation Neutron Source* (SNS) has recently begun producing neutrons and is currently on track to becoming a world-leading facility for material science based on neutron scattering. The facility is comprised of an H^- ion source, a linear accelerator, an accumulator ring and a liquid-Hg target. Over the next several years the average H^- current from the ion source will be increased in order to meet the baseline facility requirement of 1.4 MW of beam-on-target power and the SNS power upgrade power requirement of 2+ MW. Meeting these goals will require H^- currents of 40-80 mA with an RMS emittance of 0.25-0.35 π mm mrad and a $\sim 7\%$ duty-factor. To date, the RF-driven multicusp SNS ion source has only been able to demonstrate sustained operation at 33 mA of beam current at a $\sim 7\%$ duty-factor. This report details our efforts to develop variations of the current ion source which can meet these requirements: designs and experimental results are presented for source variations featuring helicon plasma generators, high-power external antennas employing Cs, glow-discharge plasma guns supplying supplemental electrons and advanced Cs collars.

*SNS is managed by UT-Battelle, LLC, under contract DE-AC05-00OR22725 for the U.S. Department of Energy.

SESSION ET2: OXYGEN-IODINE LASERS

Tuesday afternoon, 10 October 2006

Salon B Holiday Inn at 16:00

Yurii Utkin, Ohio State University, presiding

Contributed Papers

16:00

ET2 1 Electric discharge oxygen-iodine laser: three decades from the idea to the laser development. ANDREY IONIN, *Lebedev Physics Institute* The overview of experimental research aimed at the research and development of an electric discharge oxygen-iodine laser (DOIL) since the first negative attempt of launching a DOIL in the 1970's is presented. The problem is tightly connected with the development of singlet delta oxygen (SDO) electric generator, which could substitute in future for SDO chemical one used for a high-power COIL resulting in the development of a high-power DOIL. The main experimental and theoretical efforts focused onto studying and understanding of physical processes, which could help in or prevent from achieving and exceeding the threshold SDO yield at partial oxygen pressure adequate for modern oxygen-iodine laser technology, are discussed. Quite recently obtained results on gain and output characteristics of DOIL, and some projects aimed at the development of high-power DOIL are discussed.

16:15

ET2 2 Singlet delta oxygen production in low-temperature plasma. ANDREY IONIN, *Lebedev Physics Institute* The overview of experimental research in the field of physics and engineering of singlet delta oxygen (SDO) production in low-temperature plasma of various electric discharges is presented. The main attention is paid to the SDO production with SDO yield adequate for the development of an electric discharge oxygen-iodine laser (DOIL). Experimental procedures of SDO production in self-sustained and non-self-sustained discharges, and analysis of different plasma-chemical processes occurring in oxygen low-temperature plasma which brings limitation to the maximum SDO yield and to the life-time of the SDO in an electric discharge and its afterglow are discussed.

16:30

ET2 3 Pulse discharge production of iodine atoms for COIL. ANATOLY NAPARTOVICH, IGOR KOCHETOV, *Troitsk Institute for Innovation and Fusion Research* NIKOLAY VAGIN, NIKOLAY YURYSHEV, *Lebedev Physics Institute RAS* TRINITY TEAM, *LEBEDEV PHYSICS INSTITUTE COLLABORATION* The pulse mode of operation of the chemical oxygen iodine laser (COIL) is attractive for a large body of new applications. Pulsed electric discharge is most effective to turn COIL operation into pulse mode by instant production of iodine atoms. Numerical model is developed for simulations of the pulsed COIL initiated by electric discharge. The model comprises a system of kinetic equations for neutral and charged species, electric circuit equation, gas thermal balance equation, and the photon balance equation. Reaction rate coefficients for processes involving electrons are found by solving the electron Boltzmann equation, which is re-calculated in a course of computations when plasma parameters changed. The processes accounted for in the Boltzmann equation include excitation and ionization of atoms and molecules, electron-ion recombination, electron-electron collisions, second-kind collisions, and

stepwise excitation of molecules. The last processes are particularly important because of a high singlet oxygen concentration in gas flow from the singlet oxygen chemical generator. Results of numerical simulations for conditions of the experiments are compared with results of measurements. Data will be presented for various conditions: gas pressure and composition, electrode geometry, electric circuit parameters.

16:45

ET2 4 O₂(¹Δ) Production and Oxygen-Iodine Kinetics in Flowing Afterglows for Electrically Excited Chemical-Oxygen-Iodine Lasers* RAMESH ARAKONI, *University of Illinois* NATALIE Y. BABAEVA, MARK J. KUSHNER, *Iowa State University* Chemical oxygen-iodine lasers (COILs) achieve oscillation on the ²P_{1/2} → ²P_{3/2} transition of atomic iodine at 1.315 μm by a series of excitation transfers from O₂(¹Δ). In electrically excited COILs, (eCOILs) the O₂(¹Δ) is produced in a flowing plasma, typically He/O₂, at a few to tens of Torr. eCOILs additionally differ from conventional systems in the large amount of O atoms produced due to electron impact dissociation. O atoms are advantageous in that they react with and dissociate I₂, but O atoms also quench I(²P_{1/2}). To some degree, the O atom density in the afterglow can be controlled by injecting NO or NO₂ which consumes O atoms. This also impacts O₃ production, particularly at higher pressures where quenching of O₂(¹Δ) by O₃ is problematic. In this paper, results from computational investigations using plug-flow and 2-dimensional plasma hydrodynamics models will be discussed for scaling laws in eCOIL systems for O₂(¹Δ) production. We will discuss O-atom management with NO/NO₂ additives and I(²P_{1/2}) production with I₂ injection. Scaling to higher pressures will be discussed where gas heating and O₃ quenching of O₂(¹Δ) become important.

*Work supported by Air Force Office of Scientific Research and National Science Foundation.

17:00

ET2 5 Gain Measurements in a Non-Self-Sustained Electric Discharge Pumped Oxygen-Iodine Laser Cavity IGOR ADAMOVICH, ADAM HICKS, YURII UTKIN, WALTER LEMPERT, J. WILLIAM RICH, *Ohio State University* The paper presents results of singlet delta oxygen (SDO) yield measurements in a high-pressure, non-self-sustained crossed discharge and small signal gain measurement on the iodine atom transition in the M=3 supersonic cavity downstream of the discharge. The results demonstrate operation of a stable and diffuse crossed discharge in O₂ - He mixtures at pressures of up to P₀=120 torr and discharge powers of up to 2.2 kW. The reduced electric field in the sustainer discharge in O₂-He flows ranges from 6 to 12 Td. Singlet delta oxygen yield in the discharge, up to 5.0-5.7% at the discharge temperatures of 400-420 K, was inferred from the integrated intensity of the (0,0) band of the SDO infrared emission spectra calibrated using a blackbody source. These results suggest that the measured singlet delta oxygen yield would exceed the threshold yield at the flow temperature achieved in the supersonic cavity, T=120 K, by about a factor of three. Gain measurements clearly confirmed this prediction. Preliminary measurements demonstrate gains of up to 0.03%/cm measured in the supersonic cavity at these conditions.

17:15

ET2 6 Collisional broadening coefficients of singlet (¹Δ_g) oxygen with helium SKIP WILLIAMS, *Air Force Research Laboratory* JEFFREY GALLAGHER, GLEN PERRAM, *Air Force Institute of Technology* A novel laser-based technique applicable to metastable species detection is discussed. Off-axis integrated-cavity-output spectroscopy (ICOS) has been applied to the study of singlet (¹Δ_g) oxygen. Singlet oxygen was generated in a microwave plasma, and the afterglow passed through an off-axis ICOS measurement system consisting of an 82-cm long, high-finesse optical cavity bounded by two highly reflective mirrors. The mirror reflectivity was determined by performing cavity-ringing-down measurements and observing ringdown times of 220-250 μs in a range from 1494 nm to 1512 nm. A diode laser was current tuned, and light exiting the cavity was focused onto an InGaAs detector. The cavity transmission was recorded as a function of laser frequency. Details of the method will be presented as well as the spectroscopic characterization of selected transitions of the (1,0) band of the *b*¹Σ_g⁺ - *a*¹Δ_g Noxon system of oxygen (radiative lifetime 160 minutes). Pressure broadening coefficients with helium as the collision partner for selected transitions will also be presented.

SESSION FPT1: POSTER SESSION IA

Tuesday evening, 10 October 2006

Salon A, 7:15pm - 9:15pm Holiday Inn at 19:15

FPT1 1 MATERIAL PROCESSING

FPT1 2 Passivation of the SiC gate-oxide interface using remote microwave plasmas* S.F. ADAMS, J.D. SCOFIELD, C.A. DEJOSEPH, JR., *Air Force Research Laboratory, Wright-Patterson AFB, OH* J.M. WILLIAMSON, *Innovative Scientific Solutions, Inc., Dayton, OH* J.D. UMBEL, *UES, Inc., Dayton, OH* A well-known challenge in fabricating a SiC MOSFET switch is attaining a low density of defects on the gate oxide/SiC interface. The typical high temperature thermal oxide process leaves carbon impurities at the SiC/SiO₂ interface which cause high densities of defect states. The result is a decrease in channel conductivity, thus decreasing device efficiency. We have investigated two approaches to this problem involving treatment with atomic species generated by remote microwave plasma. First, a plasma passivation technique was analyzed employing atomic nitrogen to extract the carbon impurities from the interface. Second, an O₂ plasma was used to grow an initial highly-structured SiO₂ layer on the SiC surface using a low temperature slow-growth process. Results will be presented including the effects of these plasma processes on SiC MOSFET optimization along with the role that atomic nitrogen and oxygen plays in each plasma process.

*This work supported by the Air Force Office of Scientific Research.

FPT1 3 Plasma Treatment of Bulk Niobium Surfaces* M. RASKOVIC, S. POPOVIC, L. VUSKOVIC, *Dominion University, Norfolk, VA* S.B. RADOVANOV, L. GODET, *Varian Semiconductor Equipment Associates, Gloucester, MA* In-situ plasma treatment is one of possible methods for preparation of Nb surface in superconducting radio-frequency (SRF) cavities used in linear

particle accelerators. The aim is to remove Nb oxides and other poor superconductors from the bulk niobium surface and to eliminate surface roughness. The choice of the plasma technique is limited by the requirement for the discharge to fit into the relatively complex geometry of SRF cavities, which are to serve as vessels for pulsed or barrel-type reactors. For the surface treatment we used the microwave cavity discharge system with Ar/Cl₂ [1] and the repetitively pulsed d.c. diode system with Ar/BF₃ [2]. The preliminary studies on planar samples with both systems show results with positive influence on the surface smoothness comparing to buffered chemical polishing method, currently in use. In addition, images obtained with several surface characterization techniques show substantial reduction of feature size on the surface. The gas-phase kinetics of both discharges has been performed. Results are compared with the process diagnostics data in order to develop better understanding of the processes, the optimization strategy, and the in-situ reactor design. [1] M. Raskovic, et al., EPAC 06, Edingburgh, Scotland, June 26-30, 2006. [2] S. Radovanov, et al., J. Appl. Phys. 98, 113307 (2005).

*Supported by DOE.

FPT1 4 Hafnium Oxide Film Synthesis via Laser Ablation Plasma Ion Deposition* N.M. JORDAN, R.M. GILGENBACH, L.M. WANG, S. ZHU, M. ATZMON, Y.Y. LAU, *Plasma, Pulsed-Power, and Microwave Lab, Nuclear Engineering and Radiological Sciences Dept., University of Michigan* M.C. JONES, *Sandia National Labs* This research investigates the feasibility of synthesizing thin films of hafnium oxide via laser ablation plasma ion deposition (LAPID). HfO₂ is of great interest as a high dielectric constant material in the semiconductor fabrication industry. Experiments are underway to deposit and implant films of hafnium and hafnium-oxide on silicon substrates. A KrF laser (400 mJ @ 248 nm) ablates solid Hf foils in an oxygen environment or sintered pellets of hafnium-oxide in vacuum. Silicon substrates can be biased (+ or -, either pulsed or DC) by voltages up to 10 kV for ion implantation and deposition. Experiments study correlations among parameters such as laser energy, film thickness, background gas pressure, film composition, and ion energy. Ablation plasma plumes are characterized by optical emission spectroscopy. Composition and morphology of deposited films are analyzed by SEM, TEM, X-ray Energy Dispersive Spectroscopy, X-ray Photoelectron Spectroscopy, X-ray diffraction and Atomic Force Microscopy. Film deposition rates are estimated to be on the order of 0.055 nm/pulse at a laser repetition rate of 15 pulses/s, equating to 8 nm/s.

*Supported by the AFOSR MURI on Cathodes and RF Windows. NMJ is partially supported by an Applied Materials Graduate Fellowship.

FPT1 5 Direct injection of liquids into low pressure plasmas* MATTHEW GOECKNER, DAISUKE OGAWA, *UT Dallas* RICHARD TIMMONS, *UT Arlington* LAWRENCE OVERZET, *UT Dallas* SAM SANCHEZ, *UT Arlington* Being forced to use only gaseous precursors in plasma processing reactors is a significant and irrational limitation. Only a small minority of the molecules that could prove useful can be put into the vapor phase. On the other hand, a much greater fraction can be put into solution. We have found that by using a simple fuel injector directly coupled to a heated reactor, one can inject a variety of liquids directly into the plasma environment. A temperature controlled capillary tube can be used to accomplish the same thing. The liquids can also have a

variety of solids dispersed in them: metals, dielectrics, aromatics, proteins, viruses, etc. While we have not had time yet to do detailed studies on a very wide range of liquids and dispersed solids, we do have the proof of principle. We have made films from injecting 1] ethanol, 2] hexane 3] iron nanoparticles dispersed in hexane and 4] ferrocene dissolved in benzene into capacitively coupled plasmas at approximately 50 mTorr. The details of the reactor and the films produced to date will be explained in the poster. Briefly: we use capacitively coupled plasma sources. Typical pressures are well below 1 Torr and powers below 10 Watts. The hexane films have growth rates around 10 nm/min.

*Support by: AFOSR/SPRING under grant #FA9550-05-1-0393 is gratefully acknowledged.

FPT1 6 CAPACITIVELY COUPLED PLASMAS I

FPT1 7 High Efficiency Singlet Oxygen Generator (SOG) Based on RF Discharge OLGA PROSHINA, OLEG BRAGINSKY, ALEXANDER KOVALEV, DMITRY LOPAEV, YURY MANKELEVICH, TATYANA RAKHIMOVA, ANNA VASILIEVA, *Institute of Nuclear Physics, Moscow State University, Russia* One of the main problems in a laser power increasing is the pressure scaling of SOG. It was shown in our previous studies that the SO concentration in RF discharge plasma saturates with the increase of both pressure and specific energy deposition. The new three-body mechanism of fast SO quenching by oxygen atoms has been revealed. The HgO coating of a discharge tube wall allowed us to reduce atom oxygen density in the discharge region and so to depress the role of the three-body quenching. In the present report the experimental and theoretical study of the power supply frequency and NO admixture influence on the discharge structure and the SO yield was carried out in RF discharge with HgO coating. The increase of the power frequency from 13.56 to 80 and 160 MHz allows to get the uniform spatial discharge structure at an oxygen pressures up to 30 Torr and the high singlet oxygen yields up to 15%. It was shown that the simultaneous using of the NO admixture, the HgO wall coating and the high power frequency gives the effective conditions for SO excitation. The record values both the SO yield (21% at p_{O2}=10 Torr; 17% at p_{O2}=20 Torr) with the high energy efficiency (~ 18%) were obtained at first. A 2D self-consistent model was used to study RF discharges in gas flow. Results of the simulation agree with the experimental data.

FPT1 8 Behavior of ion sheath adjacent to a planar capacitive discharge operated in pulsed mode C. GAMAN, S.K. KARKARI, A.R. ELLINGBOE, *Dublin City University, Ireland* The dynamics of a radio-frequency sheath is important in understanding the ion-energy distribution at the substrate during a plasma process. The ion-energy depends on the mean ion-transit time through the sheath with respect to the rf-angular frequency, the rf-amplitude and the position in the sheath where the ions are created. When the radio-frequency discharge is operated in pulsed mode, the capacitive rf-fields rapidly penetrate in to bulk plasma which results in sheath expansion by exclusion of electrons from the sheath boundary. The spatial and phase-resolve behaviour of electron density has been experimentally investigated using a floating hairpin resonance probe in a hydrogen discharge, which is created in a confined symmetric parallel plate capacitively coupled radiofrequency discharge. The results show time-variation in spatial electron density as a function of rf phase during the beginning of the on-phase of the pulsed rf and relaxation of electron density in the sheath during the off-phase of the rf cycle.

FPT1 9 Investigation of a radio-frequency capacitive sheath and the effect of DC bias control on the power absorption at low pressures D. GAHAN, F. SOBERON, M.B. HOPKINS, *Dublin City University, Ireland* Many of today's processing plasma tools are operated at low pressures to achieve high etch directivity and reduce side erosion on the wafer. At these pressures electron-neutral collisions are rare and the electrons cannot gain energy through the Ohmic heating process. Instead the heating mechanism is attributed to a stochastic process between the electrons and the sheath electric field. Theoretical models of this stochastic process include the hard wall approximation and the pressure heating effect. The former is inconsistent with electron current conservation in the sheath whilst the latter shows a difference in power absorption when the electron loss to the electrodes is considered. This paper examines the effects of electron current of a capacitive sheath by controlling this current with an additional DC bias. Experimental and particle-in-cell model results for a low pressure argon plasma are compared and presented. Results show that the electron power absorption is more effective when the electron conduction current is removed. The model also shows a high harmonic content on the sheath voltage which is attenuated by removing the electron current. These high frequency harmonics are measured in the experiment with a floating probe and their correlation with the electron current is in agreement with the model results.

FPT1 10 Neutral gas flow effect in a large area CCP plasma source TAESANG LEE, SEUNG-HOON PARK, HOYUL BAEK, YONGSEOK JHO, CHOONG-SEOCK CHANG, *Korea Advanced Institute of Science and Technology / New York University* We modified XPDP2 code to include neutral gas flow effect on CCP discharge for argon gas. Parallelized multi-grid method is used for efficient field calculation. Particle simulation is used for gas flow calculation and spatially non uniform gas distribution is obtained. Ionization, charge exchange and neutral-neutral collision effect are considered for realistic neutral gas simulation. Multi-time scale simulation is used to get steady state discharge including gas depletion by ionization. Preliminary results are obtained and compared with the results from uniform background neutral gas distribution.

FPT1 11 Analytic Model for Self-Excited Plasma Series Resonances* UWE CZARNETZKI, *Institute for Plasma and Atomic Physics, Ruhr University Bochum* THOMAS MUSSEN-BROCK, RALF-PETER BRINKMANN, *Institute for Theoretical Electrical Engineering, Ruhr University Bochum* Self-excited Plasma Series Resonances (PSR) are observed in capacitive discharges as high frequency oscillations superimposed on the normal RF current. This high-frequency contribution to the current is generated by a series resonance between the capacitive sheath and the inductive and ohmic bulk of the plasma. The non-linearity of the sheath leads to a complex dynamic. The effect is applied e.g. as a diagnostic technique in commercial etch reactors where analysis is performed by a numerical model. Here a simple analytical investigation is introduced. In order to solve the non-linear equations analytically, a series of approximation is necessary. Nevertheless, the basic physics is conserved and excellent agreement with numerical solutions is found. The model provides explicit

and simple formula for the current waveform and the spectral range of the oscillations. In particular, the dependence on the discharge parameters is shown. Further, the model gives insight into an additional dissipation channel opened by the high frequency oscillations. With decreasing pressure the ohmic resistance of the bulk is decreasing too, while the amplitude of the PSR oscillations is growing. This results in substantially higher power dissipation.

*This project is funded by SFB 591.

FPT1 12 THEORY AND MODELING

FPT1 13 PIC simulation of capacitive plasma with non-homogeneous boundary conditions T.A. ABU SHAMALEH, M.M. TURNER, *Dublin City University, Ireland* In earlier work, we have studied the effect of boundary non-homogeneity in a capacitive system using a lumped element circuit model. That study concentrated on what is known as the triple junction boundary configuration in the vicinity of capacitive plasma sheath. In this case, metal structures behind a dielectric wall produce disturbances in an adjacent plasma, which are suspected to cause damage to the plasma reactor wall. The investigation showed that the implementation of sheath dynamics - as opposed to a static sheath - have significant effects on the surface voltage distribution along the dielectric surface. Furthermore, quantitative differences have been observed depending on what sheath model is being implemented within the model. In the current investigation, we will be tackling the same system using the particle in cell method. The aim is to be able to investigate the detailed behaviour of a capacitive plasma in the presence of a potential disturbance at the boundary. By comparing the results of our previous and current study, we can judge which sheath theory is more representative of the plasma sheath's behaviour under such conditions, and to what extent the deviation from the expected behaviour occurs.

FPT1 14 Analytical solution of sheaths for cylindrical and spherical objects. NOAH HERSHKOWITZ, *University of Wisconsin - Madison* LUTFI OKSUZ, *Suleyman Demirel Universitesi - Isparta, Turkey* A novel exact analytical solution method is given in order to solve the space charge limited current for Poisson equation for cylindrical and spherical geometries. Using this method Poisson equation is solved for different Cartesian, cylindrical and spherical sheaths for Child Langmuir sheath problem. The ion collections, developed for cylindrical, spherical and planar geometries showed spherical probe can collect much more current than the other geometries. The solutions are examined for collisional and collisionless cases. Analytical solutions are compared with the experimental results.

FPT1 15 Kinetic properties of particle-in-cell simulations compromised by Monte Carlo collisions M.M. TURNER, *Dublin City University, Ireland* The particle-in-cell method with Monte Carlo collisions is frequently employed when a detailed kinetic simulation of a weakly collisional plasma is required. In such cases, one usually desires, *inter alia*, an accurate calculation of the particle distribution functions in velocity space. However, velocity space diffusion affects most, perhaps all, kinetic simulations to some degree, leading to numerical thermalization, and consequently distortion of the velocity distribution functions, among other undesirable effects. The rate of such thermalization can be

considered a figure of merit for kinetic simulations. In this paper, we show that, contrary to previous assumption, the addition of Monte Carlo collisions to a particle-in-cell simulation seriously degrades certain properties of the simulation. In particular, the thermalization time can be reduced by as much as three orders of magnitude. We show that this effect makes obtaining a strictly converged simulation results difficult in many cases of practical interest.

FPT1 16 Using Modern C++ Idiom for the Discretisation of Sets of Coupled Transport Equations in Numerical Plasma Physics* JAN VAN DIJK, BART HARTGERS, JOOST VAN DER MULLEN, *Eindhoven University of Technology* Self-consistent modelling of plasma sources requires a simultaneous treatment of multiple physical phenomena. As a result plasma codes have a high degree of complexity. And with the growing interest in time-dependent modelling of non-equilibrium plasma in three dimensions, codes tend to become increasingly hard to explain-and-maintain. As a result of these trends there has been an increased interest in the software-engineering and implementation aspects of plasma modelling in our group at Eindhoven University of Technology. In this contribution we will present modern object-oriented techniques in C++ to solve an old problem: that of the discretisation of coupled linear(ized) equations involving multiple field variables on ortho-curved meshes. The 'LinSys' code has been tailored to the transport equations that occur in transport physics. The implementation has been made both efficient and user-friendly by using modern idiom like expression templates and template meta-programming. Live demonstrations will be given. The code is available to interested parties; please visit www.dischargemodelling.org.

*This research is sponsored by the Dutch Science Foundation STW.

FPT1 17 Modeling and experimental study of dielectric barrier discharges for mercury free flat lamps BEAUDETTE TRISTAN, GUILLOT PHILIPPE, BELENGUER PHILIPPE, CALEGARI THIERRY, THERESE LAURENT, *CPAT* AUDAY GUILLAUME, *Saint Gobain Recherche* CPAT COLLABORATION, SAINT GOBAIN RECHERCHE COLLABORATION, In this paper, a simple dielectric barrier discharge flat lamp developed by Saint-Gobain Glass is characterized. The lamp is consisting of two glass plates separated by a constant gas gap. The glass thickness is 4 mm and the gap 2 mm. The surface is 30cm x 30cm. A transparent conducting material (electrode) has been deposited on both external sides and phosphors (white emitting powders) on both internal sides of the dielectric. The lamp can be filled with rare gas mixture and can operate in a pressure range of 100-400 torr. A sinusoidal excitation voltage can be used up to 3000V in a frequency range of 10-50 kHz. In this work, we will present some results concerning a Ne-Xe 50% mixture at a pressure of 188 torr and we will discuss the influence of the applied voltage (amplitude and frequency) on the consuming power, the light emission and mostly on the non-homogeneity of the discharge. Using a 2 dimensional model developed in our laboratory, the effects of the applied voltage (amplitude and frequency) and the pressure will be studied. Particularly on the distance between the streamers when the discharge is not homogeneous. Finally experimental and theoretical results will be compared.

FPT1 18 Numerical study on characteristics of neutral beam in plasma-grid-reflector system for material processing SEUNG-HOON PARK, YONG-SEOK JHO, TAESANG LEE, *Korea Advanced Institute of Science and Technology* CHOONG-SEOCK CHANG, *Korea Advanced Institute of Science and Technology and Courant Institute-NYU* Low energy neutral beam source has been proposed as one of candidates reducing charging damage in the nano-scale etching process. The neutral beam is generated by interaction between accelerated ion from a grid which is applied hundreds voltage with a metal reflector. Whole simulation is composed of two parts, ion beam simulation and ion-reflector interaction simulation. Ion beam simulation describes ion trajectory, such as ion trajectory deflection and variation of ion energy caused by ion-ion interaction, in a grid and a reflector. Fast Multipole Method (FMM) is used for calculation of long-range interaction of ions. Ion-reflector interaction simulation is performed using molecular-dynamics for calculation ion reflection characteristics. The neutral distribution is obtained by ion-reflector simulation from ion distribution onto a reflector surface.

FPT1 19 Charging potential fluctuation induced by point particle effect in a sub-10 nm trench TAESANG LEE, YONG-SEOK JHO, *Korea Advanced Institute of Science and Technology* SEONGSIK KIM, *National Fusion Research Center / Korea Advanced Institute of Science and Technology* CHOONGSEOCK CHANG, *Korea Advanced Institute of Science and Technology / New York University* Monte Carlo simulation of charging process in a sub 10nm trench shows that charging potential fluctuation increases up to the level of incident ion energy. Size dependence of charging fluctuation is observed. Trench systems with different width are selected as reference systems to see the characteristics for this phenomena. Summation formula is derived for coulomb interaction in a 2D periodic system instead of solving Poisson equation with conventional FEM or FDM method. It is observed that charging fluctuation increases as the trench size decreases. The relation between these fluctuations and ion energy distribution on the trench bottom is finally shown which may affect on etching process.

FPT1 20 2D electromagnetic modeling of a microwave plasma torch R. ALVAREZ, L.L. ALVES, *CFP, IST* This work models the 2D electromagnetic field distribution, produced within a metallic reactor by a microwave driven Axial Injection Plasma Torch. The coaxial torch imposes a TEM mode to excite the device, which leads to the development of a symmetric TM mode inside the cylindrical reactor. Maxwell's equations were discretized on a variable grid, featuring smaller cells near the torch tip (around which the plasma density is higher) and at the reactor walls. Special attention was given to boundary conditions. At the reactor axis, symmetry considerations impose a zero value for the azimuthal component of the magnetic field. The reactor walls were assumed to be perfect conductors, thus leading to zero tangential electric fields. Finally, at the excitation boundary, the incident field was set equal to the theoretical solution inside a coaxial waveguide, with a first-order Absorbing Boundary Condition imposed to the reflected field component. The resulting linear system was solved using a Gauss-Seidel algorithm combined with a Successive Over-Relaxation iterative method. Solutions were obtained by imposing a spatial distribution of the plasma permittivity, obtained from the experimental observations of the electron density profile within the device. In the future, the electromagnetic code is to be coupled with a transport model for charged particles, in view of the self-consistent description of this microwave plasma torch.

FPT1 21 OODR-LIF experiments on $N_2(A^3\Sigma_u^+)$ in volume and in surface atmospheric pressure DBDs* SANTOLO DE BENEDETTIS, PAOLO F. AMBRICO, GIORGIO DILECCE, CNR, IMIP-Bari, Italy MILAN SIMEK, Academy of Sciences, Prague, Cz rep CNR COLLABORATION, AVCR COLLABORATION A calibrated optical double resonance laser induced fluorescence, OODR-LIF, has been used to measure $N_2(A^3\Sigma_u^+)$ metastable density at high pressure in the voltage cycle of volume and surface atmospheric DBDs. OODR_LIF excitation-detection scheme is: $N_2(A^3\Sigma_u^+, v) + h\nu_{L1} \rightarrow N_2(B^3\Pi_g, v') + h\nu_{L2} \rightarrow N_2(C^3\Pi_g, v'') \rightarrow N_2(C^3\Pi_g, v'') + h\nu_E$. The two exciting photons (itred- ν_{L1} and UV- ν_{L2}) are generated by two independently tunable and synchronized lasers. In volume DBD, $N_2(A)$ is measured in the discharge gap ($d=1.5$ mm, voltage 10 kV_{pp} at 1.8 kHz) pulsed at $T_{ON}=5$ ms and $T_{OFF}=10$ ms. In surface DBD, $N_2(A)$ is measured in the gas layer over a comb electrode deposited over a ceramic plate back covered by a metallic large background electrode. The current and the applied voltage are monitored by a digitizing oscilloscope. The measured time-resolved emissions of N_2 SPS and NO- γ bands allows exploring the correlations between emissions, LIF and discharge current and implementing a calibration of OODR-LIF. The measured density is about 10^{13} cm⁻³ in volume DBD while lower in a surface DBD.

*Project FIRB-MIAO

FPT1 22 ELECTRON AND PHOTON COLLISIONS

FPT1 23 Electron Impact Excitation of the Electronic States of Water PENNY THORN, N. DIAKOMICHALIS, M.J. BRUNGER, L. CAMPBELL, P.J.O. TEUBNER, ARC Centre for Antimatter-Matter Studies, SoCPES, Flinders University, GPO Box 2100, Adelaide, 5001 Australia H. KATO, C. MAKOCHEKANWA, M. HOSHINO, H. TANAKA, Physics Dept., Sophia University, Chiyoda-ku, Tokyo 102-855, Japan We report differential and integral cross sections for excitation of the lowest lying 3B_1 , 1B_1 , 3A_1 and 1A_1 electronic states of water. The energy range of these measurements is 15-50eV and the angular range of the DCS measurements is 10-90°. From these DCS the corresponding ICS is calculated using a molecular phase shift analysis technique. Where possible, comparison is made to the results of available theory. One of the main objectives of this study is to perform statistical equilibrium calculations to determine if the origin of the OH Meinel bands in our atmosphere are due to electron driven processes.

FPT1 24 Photoionization Angular Distributions for the Hydrogen Molecular Ion.* OLA AL-HAGAN, J.L. PEACHER, D.H. MADISON, University of Missouri-Rolla Walter and Briggs [J. Phys. B: At. Mol. Opt. Phys. **32**, 2487 (1999)] used a perturbation method to calculate the single photoionization of the molecular hydrogen ion. They used an ansatz "2C" wave function and they presented results for the angular distribution of the photoionized electron. More recently Rescigno et al. [Phys. Rev. A **72**, 052709 (2005)] have carried out a non-perturbative calculation for the same process. They used a numerical grid-based method combined with exterior complex scaling. Their results show that the photoelectron distribution follows the direction of photon polarization, while the simpler perturbative "2C" model of Walter and Briggs predicts alignment along the molecular axis. We will present our perturbative results for this process in order to determine the source of the difference between the angular distributions obtained by the other two calculations.

*Work supported by the NSF PHY-0456528

FPT1 25 Electron Excitation out of the Metastable Levels of Ar into Levels of the $3p^55p$ * R.O. JUNG, JOHN B. BOFFARD, L.W. ANDERSON, CHUN C. LIN, University of Wisconsin-Madison We have measured electron-impact excitation cross sections out of the two metastable levels of the $3p^54s$ configuration into the levels of the $3p^55p$ configuration of Ar by observing fluorescence from the decay of these levels (390-470 nm). Metastable atoms are produced in a hollow cathode discharge. After exiting the discharge, the atoms are excited by a variable energy electron beam and the resulting fluorescence from the decay of excited levels is detected by a PMT. To determine cross sections out of each metastable level (3P_0 and 3P_2) separately, a Ti:Sapphire laser (pumped by an Ar⁺ laser) is used to depopulate the target atoms in the $J = 2$ metastable level. We find that the cross sections have peak magnitudes between 10^{-17} and 10^{-16} cm². These cross sections are one to two orders of magnitude smaller than the corresponding metastable excitation cross sections into $3p^54p$ levels¹, but are still two orders of magnitude larger than the $3p^55p$ excitation cross sections from the ground state.²

*Supported by the National Science Foundation.

¹G. A. Piech *et al*, Phys. Rev. Lett. **81**, 309 (1998).

²T. Weber *et al*, Phys. Rev. A **68**, 032719 (2003).

FPT1 26 Cross sections for simultaneous ionization/excitation of argon* JOHN B. BOFFARD, CHUN C. LIN, University of Wisconsin-Madison Optical emissions from $3p^44p$ argon ion levels (420-490 nm) are widely used in plasma diagnostics. Cross sections for electron-impact from the ground state have been studied extensively since the 1960's for levels involved in argon-ion laser emissions. Much less work, however, has been performed on measuring cross sections for other excited levels. We present measurements for simultaneous ionization/excitation cross sections into virtually all of the levels of the $3p^44p$, $3p^44d$, and $3p^45s$ configurations, and a number of additional higher levels. Emission cross sections from 300-900 nm were measured using a monochromator/PMT combination, whereas near-IR transitions in the range 850-1500 nm were measured using a FTS/Ge detector combination.

*Supported by the National Science Foundation.

FPT1 27 Monte Carlo simulation of 337.1 nm and 391.4 nm emission due to the electron thermalization in Nitrogen.* ZORAN PETROVIC, VLADIMIR STOJANOVIC, Institute of Physics, Belgrade Electron thermalization in nitrogen is studied by Monte Carlo simulations for electron energies from 20 eV to 10 keV. The purpose of this work is to clarify the origin of electron excitation of Second Positive System (2P) corresponding to $C^3\Pi_u-B^3\Pi_g$ transition at energies much higher than ionization the threshold. Such emission occurs when cosmic ray induced particles are thermalized in the atmosphere and may be used to detect very high energy elementary particles. Spatially resolved emission profiles are calculated at pressures of 1 Torr and 760 Torr. Relaxation of the electron energy is followed. At the same time anisotropic scattering for elastic and inelastic collisions, and energy partitioning in ionization events are included in the model. We proved that secondary electrons significantly affect the emission of 2⁺ emission band while their effect on 1⁻ emission band is minimal. For 337.1 nm emission, we find that below 30 eV, single

collisions of secondary electrons with gas are main the source of excitation while number of multiple electron collisions with gas significantly increase with energy. For electron energies up to 10 keV, single collisions of secondary electrons dominate in excitation of 391.4 nm emission.

*Work at the Institute of Physics is supported by the MNZS, under grant 141025.

FPT1 28 Photodetachment Spectroscopy of Ce^{-*} N.D. GIBSON, *Denison University* C.W. WALTER, K.A. STARR, C.M. JANCZAK, P. ANDERSSON, *Gothenburg University* Tunable infrared and visible laser photodetachment spectroscopy has been performed on Ce^{-} using a crossed laser-ion beam apparatus. The relative photodetachment cross section for neutral production was measured over the photon energy range 0.5 eV – 2.6 eV. The spectrum shows several continuum threshold features and reveals five narrow peaks associated with negative ion resonances. The present measurements will be compared to recent theoretical [1] and experimental [2] results which are in significant disagreement on fundamental physical quantities such as the electron affinity of Ce and the ground state configuration of Ce^{-} . [1] S.M. O'Malley and D.R. Beck, *Phys. Rev. A* **61**, 034501 (2000); X. Cao and M. Dolg, *Phys. Rev. A* **69**, 042508 (2004). [2] V.T. Davis and J.S. Thompson, *Phys. Rev. Lett.* **88**, 073003 (2002).

*This material is based on work supported by the National Science Foundation under Grant Nos. 0140233 and 0456916.

FPT1 29 Electron Scattering by Deoxyribose and Related Molecules* CARL WINSTEAD, VINCENT MCKOY, *California Institute of Technology* Interactions between slow electrons and DNA are now known to be a cause of genetic damage, but the mechanisms that lead to DNA strand breaks remain a subject of investigation. Studies of electron collisions with DNA subunits in the gas phase may help to elucidate those mechanisms. In the present work, we apply the Schwinger multichannel method, an *ab initio* computational procedure, to compute elastic electron scattering cross sections for 2-deoxyribose, the sugar found in the DNA backbone, and for some related molecules. For deoxyribose, the calculations indicate the presence of shape resonances in two distinct energy ranges. When a phosphate group is added, these ranges merge into a single broad maximum.

*Supported by DOE Office of Basic Energy Sciences.

FPT1 30 Electron Impact Excitation Collision Strengths For Ni XI. NUPUR VERMA, *Deen Dayal Upadhyaya College, Delhi University, India.* ALOK JHA, MAN MOHAN, *Department of Physics and Astrophysics, Delhi University, India.* In recent years, there has been considerable interest in the study of interaction of electrons and photons with ionized atoms, particularly with the iron group elements. Nickel is an important impurity in modern fusion research devices, especially in those where the vessel walls are constructed largely of high-nickel-content alloys (e.g. The Joint European Torus). We have used the R-matrix method to calculate electron impact collision strengths from the ground state to the first 16 fine-structure levels of argon-like Ni XI. The relativistic effects are incorporated in the Breit Pauli approximation by including one body mass correction, Darwin, and spin-orbit interaction terms in the scattering equations. Configuration interaction wave functions are used to represent the lowest 9 LS-coupled target states. The low energy region is dominated by closed chan-

nel (or Feshbach) resonances which perturb the otherwise smoothly varying background collision strength. The effective collision strengths are determined by integrating the collision strengths over a Maxwellian distribution of electron energies. Results are presented for the effective collision strengths for a wide temperature range. Our results are the only collision strengths and rate coefficients available for this ion. We believe that the data calculated in this work will be useful in solar, astrophysical and laser applications.

FPT1 31 High-precision calculations for electron collisions with krypton and xenon.* OLEG ZATSARINNY, KLAUS BARTSCHAT, *Drake University* We extended our earlier work on electron collisions with Ne [1] and Ar [2] to the heavier noble gas targets Kr and Xe. In our B-Spline R-matrix method [3,4], relativistic effects are accounted for through the most important terms of the Breit-Pauli hamiltonian in the inner region of the R-matrix box. Several sets of non-orthogonal valence orbitals were employed to account for the strong term dependence in the one-electron orbitals. Using non-orthogonal basis sets avoids the need for pseudo-orbitals to improve upon the target description and reduces pseudo-resonance problems. The agreement between our predictions and experiment [5] is much better than that obtained in previous calculations based on the standard R-matrix approach with strictly orthogonal orbitals, particularly in details such as resonance positions and widths. Our new results for excitation from both the ground and the metastable states are believed to represent a significant improvement of the current database for electron collisions with heavy noble gases. [1] O. Zatsarinny and K. Bartschat, *J. Phys. B* **37** (2004) 2173. [2] O. Zatsarinny and K. Bartschat, *J. Phys. B* **37** (2004) 4693. [3] O. Zatsarinny and C. Froese Fischer, *J. Phys. B* **33** (2000) 313. [4] O. Zatsarinny, *Comp. Phys. Commun.* **174** (2006) 274. [5] S.J. Buckman and C.W. Clark, *Rev. Mod. Phys.* **66** (1994) 539.

*Work supported by the NSF under PHY-0244470, PHY-0311161 and PHY-0555226.

FPT1 32 Elastic scattering of electrons from the heavy noble gases A.D. STAUFFER, *York University* R.P. MCEACHRAN, *Australian National University* Since the cross sections for elastic scattering of electrons from the noble gases are much larger than the excitation cross section, elastic scattering plays a dominant role in the diffusion of electrons through these gases. In order to study the spread of an electron cloud in a gas, differential cross sections are required. For the heavier noble gases such as krypton and xenon, the relativistic j-j coupling formulation provides a more accurate description of these atoms than the usual LS coupling scheme. We have developed an optical potential approach to elastic scattering within this formulation which takes account of the open inelastic channels within a single channel potential scattering approximation. This yields more accurate cross sections, particularly for large angle scattering which play a large role in the spread of electrons within a gas. We will present detailed results for differential cross sections in comparison with recent experiments which have measured differential scattering cross sections over the whole angular range. Our ultimate goal is to produce sufficient data to provide an accurate basis for modeling studies.

FPT1 33 Excitation of atmospheric species by electron impact.* CHARLES P. MALONE, PAUL V. JOHNSON, *Jet Propulsion Laboratory* J. WILLIAM MCCONKEY, *University of Windsor and Jet Propulsion Laboratory* MURTADHA A. KHAKOO, *California State University Fullerton* JOSEPH M. AJELLO, ISIK KANIK, *Jet Propulsion Laboratory* Electron collisions with neutral atomic and molecular targets, such as O, H₂, and N₂, have been investigated. Resulting fluorescence was probed using various monochromator-detector combinations. Line and band intensities were investigated as a function of wavelength and incident electron energy. In addition, electron energy-loss spectroscopy (EELS) was utilized such that differential cross sections (DCSs) and integral cross sections (ICSs) were obtained. The emission cross sections, DCSs, and ICSs, for these atmospheric species will be presented.

*This work was performed at the Jet Propulsion Laboratory, California Institute of Technology, under a contract with the NASA. Financial support through NASA's PATM and OPR programs is gratefully acknowledged.

FPT1 34 Electron Impact Excitation of Molecular Nitrogen* MURTADHA A. KHAKOO, SHIYANG WANG, *Cal State University Fullerton*, CA 92834 CHARLES P. MALONE, PAUL V. JOHNSON, ISIK KANIK, *Jet Propulsion Laboratory, California Institute of Technology, Pasadena, CA 91109* We present differential cross-sections for electron impact excitation of the N₂ b,c,o ¹Π_u and b',c' ¹Σ_g⁺ from the X¹Σ_g⁺ ground state at 17.5eV, 20eV, 30eV, 50eV and 100eV for scattering angles from 5° to 130°. The DCSs were obtained by unfolding the energy loss spectrum of N₂ taking into account Rydberg-valence mixing between these levels. These DCSs constitute the first systematic study of the high-lying states of N₂ of importance in plasma and astrophysics applications.

*Funded by NSF-AMOP Division and by NASA Outer Planets Research Program.

FPT1 35 Excitation of the Resonance Lines of Copper and Silver by Electron Impact* BERNHARD STUMPF, *University of Idaho* We present a summary of our experimental investigations of the copper resonance lines 4P-4S (324.8, 327.4 nm) and silver resonance lines 5P-5S (328.1, 338.3 nm) excited by electrons with energies from threshold (3.8 eV) to 1000 eV. Linear polarizations and excitation cross sections have been measured for the unresolved copper resonance lines and for the resolved silver resonance lines. Systematic experimental errors like instrumental polarization, finite solid angle of observation, and radiation trapping have been carefully studied and corrected. Relative experimental cross sections are normalized at an energy of 1000 eV with respect to first Born theory. We compare our experimental data with theoretical calculations using the close-coupling method and the relativistic distorted-wave approximation.

*Supported by NSF/Idaho-EPCoR and by the State Board of Education of the State of Idaho

FPT1 36 Benchmark Measurements and Theory for Electronic Excitation of He by Electron Impact M. LANGE, J. MATSUMOTO, J.C. LOWER, S.J. BUCKMAN, *CAMS, Australian National University* K. BARTSCHAT, O. ZATSARINNY, *Drake University, USA* I. BRAY, D. FURSA, *CAMS, Murdoch University, Australia* We present measurements and calculations of near-threshold electron impact excitation of the n=2 and n=3 levels of the He atom. The measurements have been performed

using a new differential, position sensitive, time-of-flight technique. The theoretical calculations include the R-matrix with pseudostates, B-Spline R-Matrix and convergent close coupling approaches. The agreement between experiment and theory is very good and leads us to propose some benchmark cross sections for several energies and angles for these excited states.

FPT1 37 Accelerate the transition of radioisotopes or unwanted weapons-grade ²³⁹Pu into stable nuclei with a system of high frequency modulation for a net energy gain EUGENE PAMFILOFF, *Dept. of Physics and Astronomy, University of Georgia, UGA, USA, Optigon Research and Development, Division of Vivitar, VPDM, CA, retired* A process of high frequency stimulation of nucleons can be utilized for the accelerated fission, decay or controlled transition of unstable isotopes. For example ²³⁸U could be persuaded to transition promptly into ²⁰⁶Pb, where portions of the total mass difference of 29873.802 MeV per nucleus becomes available energy. The proposals of this paper describe an effective system for nuclei stimulation configured to accelerate such a series of 14 transitions over several milliseconds, instead of 4.47 x 10⁹ years. Positive ions or ionized capsules of fuel suspended by magnetic fields and subjected to the system of correlated frequency modulation of multiple beam lines, tailored to the specific target, will emit sufficient energy to stimulate subsequent targets. The system can be applied to all radioisotopes, including ²³²Th, nuclear waste product isotopes such as ²³⁹Pu, and a variety of other suitable unstable or stable nuclei. Through the proposed confinement system and application of high frequency stimulation in the 10²² to 10²⁴ Hz regime, the change in rest mass can be applied to both the fragmentation of subsequent, periodically injected targets, and the production of heat, making a continuous supply of energy possible. The system allows the particle fragmentation process to be brought into the laboratory and provides potential solutions to the safe disposal of fissile material.

FPT1 38 POST-DEADLINE

FPT1 39 Flow Velocity Measurement with Mach Probe and Laser-Induced Fluorescence in the Un-magnetized Ar Plasma HYUN-JONG WOO, KYU-SUN CHUNG, *Hanyang University* TAIHYEOP LHO, *National Fusion Research Center* The Mach probe (MP), composed of two opposite-directional electric probes, is generally used for the measurement of plasma flow velocity in edge of magnetic fusion devices, space propulsion systems, processing plasmas, sheath and pre-sheath regions. Although several un-magnetized MP theories are available, they have not been completely calibrated and should be checked by comparative (or simultaneous) measurement with another diagnostic tools such as laser-induced fluorescence or optical emission spectroscopy. Most of the previous calibrations have been done in the low Mach number (say, less than 0.5), where the existing theories predict the very similar numbers, so that the validity of the calibration is still in doubt. In this work, the plasma flow velocity is measured via MP and LIF in un-magnetized Ar plasma generated by LaB₆ cathode, one of two sources of Diversified Plasma Simulator (DiPS). For meaningful comparison of MP and LIF, we increase the plasma flow velocity over the 0.5C_s, where C_s is the ion sound velocity, by generating a steep density gradient from diverging magnetic field and measure the flow velocity flat magnetic field near the diverging magnetic field. Although magnetic field are applied in plasma, the ion gyro-radius is still less than the probe radius. Hence, the MP results is analyzed by un-magnetized probe theories and these are compared to LIF results.

FPT1 40 Why is the Mach probe formula expressed as $R = J_{up}/J_{dn} = \exp[KM_\infty]$? KYU-SUN CHUNG, *Hanyang University* Normalized drift velocity of the flowing plasmas can be deduced by a Mach probe, which has two directional probes at opposite sides. The relation between the ratio (R) of the upstream ion saturation current density (J_{up}) to the downstream (J_{dn}) and the normalized drift velocity ($M_\infty = V_d/\sqrt{T_e/m_i}$) of plasma has generally been fitted into an exponential form as $R = J_{up}/J_{dn} = \exp[KM_\infty]$, where K is a calibration factor depending upon the magnetic flux density, collisionality, viscosity, and ion temperature of plasmas. Without going into detailed theories for various conditions of plasmas and probes, a simple explanation is given in terms of decaying current density in the downstream region. Existing theories and experiments of Mach probes in magnetized and unmagnetized flowing plasmas are summarized along with key physics and comments.

FPT1 41 Measurements of the density of metastable helium atoms in dielectric barrier discharges ALI EL-ASTAL, *Department of Physics, Al-Aqsa University, Gaza P.O. Box 4051, Gaza Strip, The Palestinian Authority* GAGIK NERSISYAN, TOM MORROW, WILLIAM GRAHAM, *Physics and Astronomy, Queens University Belfast, BT7 INN, Northern Ireland* Measurements of the density of metastable helium atoms in dielectric barrier discharges operating in glow discharge mode are reported. The measurements were made in two systems using three different approaches. One DBD was created in air with helium flowing in the inter-electrode gap, in the other the DBD was in a vacuum chamber in static pure helium with some impurities present. In the first system a multi-pass absorption technique at 388.865 nm was used, the lack of any absorption signal over a path length of 25 cm indicated an upper limit of the metastable density in this system of $2 \times 10^{10} \text{ cm}^{-3}$ [1]. In the second system the time dependence of the helium metastable density using laser collisional-induced fluorescence established that the maximum density in this system was in the range 0.5 to $2.5 \times 10^{10} \text{ cm}^{-3}$ and from the time dependence the metastable density at the next breakdown was estimated to be about 10^4 . When the glass plates in the latter system were replaced by optical quality quartz, helium metastable absorption can be seen as an optogalvanic effect on the measured discharge current, indicating a higher metastable density in this case. [1] G. Nersisyan, T. Morrow, W.G. Graham, *Appl. Phys. Lett.* **85**, 1487 (2004).

FPT1 42 Study of the non-local electron kinetics in rare gas and reactive plasmas GORDON K. GRUBERT, DETLEF LOFFHAGEN, *INP Greifswald, F.-L.-Jahn-Str. 19, 17489 Greifswald, Germany* The development of a time- and space-dependent hybrid model for the analysis and self-consistent modelling of capacitively coupled rf discharges between plane electrodes is in progress. This model includes the coupled solution of hydrodynamic equations for the charge carriers and neutral species in the plasma, an equation system for the external electrical circuit, the Poisson equation determining the internal electric field, and the time-dependent, spatially inhomogeneous Boltzmann equation providing transport and rate coefficients of the electrons. In the current presentation the kinetic behaviour of the electrons in axially inhomogeneous discharges in rare and molecular gases is discussed on the basis of the space-dependent electron Boltzmann equation. The analysis is performed by using the multi-term approximation of an expansion of the electron velocity distribution function in Legendre polynomials. Main details of an improved

technique for solving the partial differential equation system resulting from the substitution of this expansion into the kinetic equation are represented. Results of the velocity distribution and relevant macroscopic properties of the electrons are reported and the impact of the spatial variation of the electric field is discussed. The work is supported by DFG Sonderforschungsbereich/Transregio 24.

FPT1 43 Electron Impact Ionization of Atoms and Ions B.C. SAHA, *Department of Physics, Florida A&M University* A.K. BASAK, *Department of Physics, University of Rajshahi, Rajshahi, Bangladesh* Electron impact ionization cross sections are at the heart of many active fields ranging from astro- to medical-physics. These applications require cross sections for a wide range of species as a function of projectile energies. This demand, however, is very hard to fulfill neither by experiments nor initial calculations. Various analytical and semi-classical models are commonly used to generate such a vast ionization cross sections. We recently applied a modified version [1] of the Bell et al. equations [2] including both the ionic and relativistic corrections. We will show in this presentation how to generalize the much-needed MBELL parameters for treating the orbital quantum numbers in dependency; comparing our results with experimental findings tests the accuracy of this procedure; very good agreements are obtained even in relativistic energies. Details will be presented at the meeting. [1] A. K. F. Haque, M. A. Uddin, A. K. Basak, K. R. Karim and B. C. Saha, *Phys. Rev. A* **73**, 052703 (2006). [2] K. L. Bell, H. B. Gilbody, J. G. Hughes, A. E. Kingston, and F. J. Smith, *J. Phys. Chem. Ref. Data* **12**, 891 (1983).

FPT1 44 Optical and electrical characteristics of hollow-needle to plate atmospheric-pressure discharge in nitrogen* MILAN SIMEK, JIRI SCHMIDT, *Institute of Plasma Physics, Academy of Sciences of the Czech Republic, Za Slovankou 3, 18221 Prague 8, Czech Republic* STANISLAV PEKAREK, JOSEF KHUN, *Czech Technical University, FEE, Technicka 2, 16627 Prague 6, Czech Republic* We have studied basic optical and electrical characteristics of the DC hollow needle to plate electrical discharge enhanced by the gas flow through the needle. Substantial advantage of this arrangement is that all gas supplied to the discharge passes through the discharge zone and therefore it is affected by plasma chemical processes. Depending on the energy dissipated between electrodes, we previously observed two basic discharge regimes: a) DC corona and b) DC corona superimposed with pulsed filamentary streamers [1]. In this work, we have analyzed radiation induced by filamentary streamers. In addition to nitrogen emissions driven by electron impact processes we have detected emission induced by specific energy transfer processes [2]. We have also determined mean repetition frequency of filamentary streamers (0.1-15 kHz) for the needle-to-plane gap and for the nitrogen flow through the needle ranging between 2-6 mm and 1-10 slm, respectively. [1] M. Simek and S. Pekarek, *GEC 2005, Bull. Am. Phys. Soc.* **50**, 29 (2005); [2] M. Simek et al., *Pure Appl. Chem.* **78**, 1213 (2006).

*Supported by the GA AV, contract number IAA1043403.

FPT1 45 A Tunable, High Energy, Fourier Transform Limited Laser Source for Spectroscopy Applications PATRICK DUPRE, TERRY MILLER, *The Ohio State University (OH)* We have constructed a Ti:Sa pulsed amplifier and used its beam for mainly infra-red radiation generation either by Scattering Raman Stimu-

lated (SRS) or by Difference Frequency Mixing (DFM). The IR radiation is used to probe cold-jet radical plasmas by CRDS (see the paper devoted to the radical generation). The master (seed) source is a CW high resolution tunable ring Ti:Sa laser injected inside the amplifier which consists of an unstable resonator (slave cavity) including a GRM profile output coupler. The tuning of the slave cavity is accomplished by using the Ramp-Lock-and-Fire (RLF) technique consisting of matching (usually) on resonance the cavity length through the end mirror mounted on an actuator before firing the frequency doubled 20 Hz Nd:YAG pump laser. The implementation of the RLF technique is under the full control of a Digital Signal Processor (DSP). Energy up to 100 mJ and spectral linewidths in the range of 10–30 MHz (FWHM) have been obtained. The detailed functioning of the system will be shown as well as the features of the generated radiation showing the near Fourier transform limited pulse behavior. A model for the amplifier will also be discussed.

FPT1 46 Surface modification of substrates for bacteria and cell culture. TOM BAEDE, RAYMOND SLADEK, EVA STOFFELS, DEPARTMENT OF BIOMEDICAL ENGINEERING - EINDHOVEN UNIVERSITY OF TECHNOLOGY TEAM, The plasma needle is a medical device that consists of a tungsten wire placed in a tube through which helium flows. A RF voltage frequency of 13.05 MHz is applied to the wire to produce the plasma. The device has a non-thermal effect and is therefore suited for both organic and inorganic surfaces. It was designed to manipulate tissues, but can also be used to modify the bacterial adhesion properties of material surfaces. The surface modification has a number of applications, most notably cell culture and the preventive treatment of caries. The research consists of two sets of experiments. In the first experiments the effect of the plasma treatment on the wettability was studied by means of contact angle measurements. The wettability quantifies the hydrophilic behavior of a surface. Plasma treatment with the plasma needle significantly increased the wettability of the studied materials. The persistence of the wettability change was also examined. For some materials the effect was only temporary. Bacteria are very particular about the surfaces they adhere to and the wettability of the surface plays an important role in their preference. The next set of experiments dealt with the effect of plasma treatment on bacterial adhesion. This effect was measured by comparing the growth rates of *E. coli* and *S. mutans* bacteria that were cultured on both plasma and non-treated surfaces. The effect appears to be species specific.

FPT1 47 The effect of microwave and pulse corona discharges on hydrocarbons partial oxidation, combustion and detonation initiation ALEXANDER BABARITSKII, MAXIM DEMINSKY, VIKTOR JIVOTOV, DMITRII MEDVEDEV, SERGEY KOROBTSEV, ROMAN SMIRNOV, GRIGORY KONOVALOV, MIKHAIL KROTOV, MARINA STRELKOVA, BORIS POTAPKIN, RRC "Kurchatov Institute" We present experimental and theoretical results on application of microwave plasmas for stimulation of partial oxidation processes for hydrogen rich gas production from gas and liquid hydrocarbons. Said results ranging from investigation of plasma catalysis mechanism, kinetics and energy balance to plasma reactor design and heat management issues. It is appeared that relatively small plasma energy deposition (0.1eV per outcome H₂, or CO molecule) under certain range of plasma

parameters leads to the significant acceleration of partial oxidation processes and this effect can be used for compact on board plasma reformer development. The paper includes test results of 10 st.m³/h plasma reformer. Experimental and theoretical results devoted to MW plasma and pulse corona discharge application for combustion and detonation initiation are discussed as well.

FPT1 48 Addressable Silicon Microplasma Arrays: Discharge Properties for Pixelized Microcavities having a Multi-Electrode Geometry P. TCHERTICHIAN, S.-H. SUNG, T.L. KIM, S.-J. PARK, J.G. EDEN, *Laboratory for Optical Physics and Engineering, Dept. of Elect. and Computer Engr., University of Illinois* The demonstration of a large array of microcavity plasma devices in Si has provided a new platform for the efficient light sources and high resolution displays. Device structures with vertically stacked multilayers allow opportunities to modify the device geometry to meet specific requirements of addressability or to obtain microplasma array with high spatial resolution. In this paper, we report the performance of addressable Si microplasma arrays having multiple electrodes with various geometric configurations. Each microcavity is driven by two or three thin layer electrodes which are individually patterned and embedded in the multilayer structure. We have fabricated 20×20 and 50×50 arrays of inverted pyramidal Si microcavities having (50 μm)² and (100 μm)² emitting apertures and all of the microplasma operate at atmospheric pressure with various molecular ultraviolet emitters. Stable glow discharges are observed in mixtures of atomic or molecular gases, such as Xe in Ne and D₂, H₂O in Ar, excited by AC (sinusoidal) or bipolar voltage waveform. Discharge characteristics and the spatial profiles of microplasma emission are dependent on the discharge electrode configurations and the power addressing function. The (100 μm)² microcavity device exhibits a higher UV emission intensity and efficiency than the (50 μm)² device under identical operating conditions.

FPT1 49 Confinement of Plasmas in Microcavities with Diamond or Circular Cross Sections and Driven by Al₂O₃ Encapsulated Electrodes K.S. KIM, J.D. READLE, T.M.SPINKA, L.Z. HUA, S.-J. PARK, J.G. EDEN, *Laboratory for Optical Physics and Engineering, Dept. of Elec. and Computer Engr., University of Illinois* Arrays of Al/Al₂O₃/glass microplasma devices with microcavities having diamond or circular cross-sectional geometries have been fabricated and operated in atomic and molecular gas mixtures at atmospheric pressure. Microcavities of the device are fabricated in only one of two electrodes, and the thickness of the completed device is less than 200 μm. Spatially-resolved emission from the microcavity is investigated in the microcavity devices having diameters between 50 μm and 500 μm by optical microscopy. Optical micrographs show the operation of the microplasma in two well-defined modes. One of these is evident at higher current densities at which we observe microplasmas centered in microcavities, each having a near-cylindrical cross-sectional geometry regardless of the shape of the microcavity. Also the diameter of the microplasma decreased with rising rare gas pressure to ~20% of the characteristics microcavity dimension. Details of discharge performance and its relation to microcavity shape, dimensions and electric field distribution will be discussed.

SESSION FPT2: POSTER SESSION IB
 Tuesday evening, 10 October 2006
 Buckeye, 7:15pm - 9:15pm Holiday Inn at 19:15

FPT2 1 PLASMA CHEMISTRY AND DIAGNOSTICS

FPT2 2 Performance Model of the Hairpin Microwave Resonator and Experimental Results L.K. WARNE, W.A. JOHNSON, R.S. COATS, R.E. JORGENSEN, G.A. HEBNER, Sandia National Laboratories A.M. PATERSON, J.P. HOLLAND, Applied Materials Microwave hairpin resonator structures are finding increased applications in a range of plasma systems. This poster presents circuit models for a hairpin resonator probe used for measuring electron density. A transmission line model is used along the resonator length and lumped loads are used to capture the parasitic capacitance at the open end and the parasitic inductance at the drive or shorted end along with a lumped radiation resistance. The impact of a plasma sheath surrounding the resonator wires as well as the finite conductivity of the wires are addressed. Electromagnetic simulations using a frequency domain method of moments code are also included as comparisons to the circuit model results. Finally, the impact of the external cavity formed by the electrodes is ascertained. The model calculations will be compared with experimental measurements to demonstrate these effects. This work was supported by the Division of Material Sciences, BES, Office of Science, U. S. Department of Energy, Applied Materials, and Sandia National Laboratories, a multiprogram laboratory operated by Sandia Corporation, a Lockheed Martin Company for the United States Department of Energy's National Nuclear Security Administration under contract DE-AC04-94AL85000.

FPT2 3 Sheath and collisional corrections in microwave hairpin resonators NICHOLAS SIEFERT, Air Force Research Laboratory BRIAN SANDS, UES, Inc. BISWA GANGULY, Air Force Research Laboratory We report the effect of electron-neutral collisions on the quality factor Q of hairpin resonators operating near 1 Torr. From the changes in Q , it is possible to determine change in the product of the electron-neutral collision frequency and the electron number density. The electron number density can be determined from the shift of the resonant frequency, so it may be possible to determine changes in the electron-neutral collision frequency. We also discuss effects of hairpin geometry and the sheath on electron number density measurements when considering a truncated transmission line model of the hairpin. Here, the location along the hairpin and the diameter of the wire are important for hairpin sensitivity and in determining the appropriate correction factor for the sheath. Additionally, we consider the collisionless sheath assumed by previous groups (e.g. Piejak et al. [J. Appl. Phys., **95**, 3785 (2004)]) and its viability at higher pressures. We also report measurements of the steady state electron number density using four different hairpins, with resonant frequencies between 2 GHz and 4 GHz, in order to demonstrate the reproducibility of the density measurements and we compare these measurements with numerical calculations.

FPT2 4 Looking for information in the Q of the hairpin probe NICHOLAS BRAITHWAITE, EVA VASEKOVA, JAFAR AL-KUZEE, The Open University THE OPEN UNIVERSITY TEAM A microwave resonator hairpin probe is used to measure the electron density of low pressure low temperature plasma. The probe acts as a quarter wave transmission line that is resonant at a fre-

quency determined by the dielectric properties of the surrounding medium. The quality factor Q of the hairpin resonance has been studied as a function of the pressure of the discharge gas and the power coupled to the discharge, for a number of gasses. The Q values were inferred from the Gaussian fitting of the recorded resonant curves of the probe. The theoretical values of the Q were calculated as a ratio of the energy stored in the cavity and the energy dissipated per one period. Since the dissipated energy depends on the collisions between electrons and the background gas, the quality factor tends to decrease with the gas number density, hence the pressure, as well as the electron number density. The measured values of Q were compared with the theoretical values and found to be in good agreement.

FPT2 5 Charged Particle Dynamics in a Dual-Frequency Capacitively Coupled Fluorocarbon Plasma* DRAGANA MARIC, GARRETT CURLEY, JEAN-PAUL BOOTH, PASCAL CHABERT, JEAN GUILLON, LPTP, Ecole Polytechnique, Palaiseau, France We are studying a customized 2 + 27.12 MHz industrial etch reactor, running in Ar/O₂ with c-C₄F₈ or CF₄ gas mixtures at pressures in the region of 50 mTorr. Independent control of ion flux and ion energy is an advantage of DFC plasmas, but little experimental data exists regarding the charged particle dynamics in complex industrial gas mixtures. Negative ions could play an important role in this type of plasma. The presence of negative ions will modify the positive ion flux arriving at a surface, and may even reach the surface and participate in etching. We measure the electron density using a microwave hairpin resonator and the positive ion flux with an ion flux probe: the ratio of these two quantities varies strongly with gas chemistry and gives evidence for the presence of negative ions. We have measured high electronegativity for high c-C₄F₈ flowrates. We have also examined the effect of varying the 2 MHz and 27.12 MHz powers on both the electron density and positive ion flux. This allows us to estimate the effect of varying power on the negative ion density. In addition CRDS was used to measure the F⁻ density [1]. This optical measurement will be compared to the probe technique. [1] Booth et al, Appl. Phys. Lett. 88 (2006) 151502.

*We acknowledge financial assistance from Lam Research Corporation.

FPT2 6 Characteristics of Spatial Electron Density Variation in a Pulsed-Rf and Bi-polar Pulsed-DC Magnetron Discharge S.K. KARKARI, A.R. ELLINGBOE, C. GAMAN, Dublin City University, Ireland I. SWINDELLS, J.W. BRADLEY, University of Liverpool, United Kingdom Magnetron discharges are highly popular in reactive sputtering of metals and insulators for depositing value-added coatings onto a wide variety of substrates. A large problem associated with DC sputtering is due to deposition of insulating films on to the target itself; resulting in frequent arcing and de-stabilization of the plasma process. Arcing is elevated by modulating the magnetron target voltage at pulse frequencies between 20 kHz to 350 kHz in the range of 50% to 90% duty cycle. Time-modulation can be achieved either by Bi-polar Pulsed DC or by Pulsed rf voltages applied to the sputtering target. We apply a time-resolved floating hairpin resonance probe, to characterize the spatial electron density as the discharge progresses during the pulsed cycle. With the Bi-polar pulsed biasing, we observe an expanding pre-sheath during the rise of the on-phase (negative voltage) and anomalous growth in density during the reverse phase (positive voltage) at specific positions in the discharge. This is contrasting to the pulsed-rf case, where we ob-

serve the electron density in the off-phase decays uniformly at all positions, with faster decay rates closer to the target. The electron density perturbations in the case of Bi-polar pulsed DC are explained using the expanding sheath theory and the state of the plasma potential modulation in the discharge.

FPT2 7 Effect of microwave field on the Langmuir probe characteristics AKIHIRO KONO, MITSUTOSHI ARAMAKI, *Nagoya University* In measurements of electron energy distribution near the dielectric plate of surface-wave excited plasma, a discrepancy has been found between Thomson-scattering results and Langmuir-probe results. The reason might be due to possible distortion of the probe characteristics caused by the microwave field, but the phenomenon is not well understood yet. In this study, the effect of microwave field on the probe characteristics is investigated computationally using a fluid model. The effect of oscillating microwave field was modeled as an oscillating probe bias potential $V_0 + V_1 \sin \omega t$ against field-free plasma. Electron and ion continuity, electron and ion momentum balance, and Poisson's equations are solved to obtain the current to a cylindrical probe as a function of the DC probe bias potential V_0 . The results indicate that the probe V-I characteristic is distorted and the second derivative d^2I/dV^2 shows a hump as if the population of electrons having energies around the hump is increased. The obtained d^2I/dV^2 curves resemble some of measured probe characteristics.

FPT2 8 Electrical and Optical Characterization of a pulsed plasma of N_2-H_2 * HORACIO MARTINEZ, *Centro de Ciencias Fisicas, Universidad Nacional Autonoma de Mexico* FAROOK BASHIR YOUSIF, *Facultad de Ciencias, Universidad Autonoma del Estado de Morelos* This paper considers the electrical and optical characterization of glow discharge pulsed plasma in N_2/H_2 mixture at pressures of 0.5-4.0 Torr and discharge current between 0.2 and 0.6 A. The discharge current and the applied voltage are measured using conventional techniques. The emission from the pulsed plasma of a steady-state electric discharge in a N_2/H_2 mixture in the wavelength range 200-600 nm is investigated. It is shown that, at a range pressure of 0.5 to 4.0 Torr, the discharge mainly emits within the wavelength range 280-500 nm. The emission consists of $N_2(C-X)$ 316 nm, 336 nm, 358 nm narrow peaks and a broad band with a maximum at $\lambda_{max} = 427$ nm. Also bands of $N_2N_2^+$ and NH excited states were observed. All bands have their maximum intensity at the discharge current of 0.4 A. The intensities of the main bands are determined as functions of the pressure and discharge current.

*This research was partially sponsored by DGAPA IN-109103 and CONACyT 41072-F.

FPT2 9 Measurement of ion density and electron temperature in Hanbit magnetic mirror device by using RF compensation triple probe IKJIN CHOI, KIHU HWANG, CHINWOOK CHUNG, *Department of Electrical Engineering Hanyang Univ.* SANGGON LEE, *National Fusion Research Center PLASMA RESEARCH LAB. COLLABORATION, NATIONAL FUSION RESEARCH CENTER COLLABORATION* There are several operating diagnostic tools placed at Hanbit magnetic mirror plasma, such as Langmuir probe, magnetic probe, diamagnetic loop etc. Because of Langmuir probes are relatively easy to make and probe tips can be formed with many designs, it is used at Hanbit plasma device to measure electron temperature, density, and distribution of electron at Hanbit plasma in a ways of axiality

and azimuth. The RF compensation triple probe was invented with an idea which is RF compensation technique used in single Langmuir probe. In case of DC, non-compensated triple probe is floated outside with high impedance, but in case of RF, it is connected with low impedance, non-floating. However, RF compensation triple probe is floated with high impedance which can measure plasma parameters with less distortion in case of RF. During checking plasma variables using RF compensation triple probe at Hanbit magnetic mirror plasma in axial way, many characteristics were observed which cannot observe with existing probes.

FPT2 10 Micro particles of different sizes as electrostatic probes in rf-plasma* RALF BASNER, GABRIELE THIEME, FLORIAN SIGENEGGER, *INP Greifswald, Germany* HOLGER KERSTEN, *University Kiel, Germany* GERALD SCHUBERT, HOLGER FEHSKE, *University Greifswald, Germany* The plasma is bounded to the surrounding surfaces by the self-organizing structure of a sheath. In plasma diagnostics a relatively large uncertainty exists for the determination of the structure of these plasma sheaths. When a dust particle is immersed in plasma, it is charged by collecting electrons and ions. Negatively charged micro-particles can be confined in a horizontal plasma sheath. The equilibrium position is defined by the balance of the forces acting on the particles. Commonly, the electrostatic and the gravitational force are important in laboratory complex plasmas. Then the equilibrium position above a lower electrode depends mainly on the particle charge, the electric field, and the particle mass. The levitated particles react sensitively with their position to changes in the plasma sheath thus they may serve as electrostatic probes for the electric field. This approach has been successfully demonstrated in front of the powered electrode. In contrast, we present preliminary measurements on the behaviour of charged dust grains in front of the grounded or biased but not powered electrode. These situations are of interest in plasma technology for treatment of substrate surfaces.

*Work supported by DFG, SFB/TR24.

FPT2 11 Real-time, Noninvasive Monitoring of Ion Energy at Insulating Electrodes MARK SOBOLEWSKI, *NIST* The dc self biasing voltage is often monitored during plasma processing to provide a rough estimate of ion bombardment energies. However, many plasma reactors use electrostatic chucks, which have a large dc impedance that makes dc bias measurements impossible. A chuck may also have a large rf impedance that produces a significant rf voltage drop across the chuck. In this study chuck impedance effects were investigated in an inductively coupled plasma reactor by incorporating insulating structures into the rf-biased lower electrode. Measurements were made to characterize the capacitive impedance of the insulating electrode itself and the combined impedance of the electrode plus the wafer. This impedance was included in a numerical model of the plasma and its sheaths and the combined model was used to analyze measured rf bias current and voltage waveforms. This approach allows a real-time, noninvasive monitoring technique developed for bare metallic electrodes to be extended to insulating electrodes, including electrostatic chucks. The technique not only determines the dc self bias voltage but also the total ion current and ion energy distributions at the wafer or chuck surface.

FPT2 12 Real time multi-dimensional control in a two-frequency, confined plasma etcher VLADIMIR MILOSAVLJEVIC, ANDREY M. ISLYAIKIN, CEZAR GAMAN, ALBERT R. ELLINGBOE, *Plasma Research Laboratory, NCPST, Dublin City University, Dublin 9, Ireland* Multi-dimensional control of plasma processes is of interest for reducing excursions in semiconductor manufacturing. Key parameters for plasma etching of dielectric films include ion-flux and gas-density of oxygen containing species in the plasma. The ion-flux is measured by with an isolated collection area built into the electrode surface, biased to -18Volts. Density of chemical species are measured using Mass-spectrometry or OES/Actinometry. The response-surface of the sensors in the process-space was collected over the process space. Sensor signals are not orthogonal, and do not directly map onto the input control parameters. The sensor data is compared to external setpoints for ion flux and chemical density. The functional dependencies of the response-surface, in conjunction with simple physical models, are used to deconvolute the sensor signals onto the control parameters. In this paper we demonstrate real-time control of ion-electrode-flux independent of plasma chemistry (O, O₂, CO, or CO₂) in a modified Exelan chamber (Lam Research). The control is stable to external perturbations to the operating point of the chamber.

FPT2 13 O atoms loss coefficient on porous SiO₂ and TiO₂ measured by plasma induced fluorescence KATIA ALLEGRAUD, LINA GATILOVA, OLIVIER GUAITELLA, JEAN GUILLON, ANTOINE ROUSSEAU, *LPTP, Ecole Polytechnique, Palaiseau, FRANCE* The time evolution of O atoms density in the gas phase during the post-discharge of a pulsed plasma is studied using a plasma induced fluorescence technique (PIF): a main long pulse creates the plasma and a shorter one re-excites atoms in the time post-discharge was used. The gas pressure is 133 Pa in N₂/O₂ mixture and the plasma is a pulsed DC discharge. The surface loss coefficient of O atoms on pyrex, porous silica, porous TiO₂ is measured, this latter being a photocatalytic material. It is shown that the presence of porous silica or TiO₂ leads to a strong increase of the O atom surface loss coefficient. When nano cluster of TiO₂ are deposited on porous silica, the loss coefficient is first high and comparable to the case of the porous silica, but decreases after few milliseconds. Such a decrease of the surface loss coefficient has recently been reported in a pulsed microwave discharge [1]. The effect of the pre-irradiation of the porous materials by external ultraviolet is also studied. [1] G. Cartry, X. Duten and A. Rousseau, *Plasma Sources Sci. Technol.* 15 (2006) 479–488.

FPT2 14 Production of carbonaceous particulates by interaction between a graphite plate and high-density hydrogen plasmas K. SASAKI, T. MAEDA, N. TAKADA, M. ARAMAKI, *Nagoya University, Japan* K. SHIBAGAKI, *Suzuka National College of Technology, Japan* This work is a simulation experiment for the divertor region of a nuclear fusion reactor. A graphite plate was irradiated by high-density hydrogen plasmas produced by helicon-wave discharges. The helicon source was a linear machine with uniform magnetic field, by which the high-density plasma column was confined radially. It was observed by the naked eye that the surface of the graphite plate was changed by the irradiation of the plasma column. The close observation using a secondary electron microscope indicated the formation of many particulates with diameters less than 10 μm. The diameter and the density of particulates were dependent on the radial position. The sources for the formation of particulates may be hydrocarbon and carbonic

radicals produced by the interaction between the high-density H₂ plasma and the graphite plate. By considering the setting of the helicon source, it is speculated that the growth of particulates occurs on the surface of the graphite plate. We adopted laser-desorption time-of-flight mass spectrometry for analyzing carbonaceous particulates. As a result, we found that H atoms were included in carbonaceous particulates, which is a critical problem from the viewpoint of safety hazards such as tritium inventory in D-T nuclear fusion reactors.

FPT2 15 Effect of electron detachment on the wall potential in the afterglow of an oxygen discharge E.A. BOGDANOV, A.A. KUDRYAVTSEV, *St. Petersburg State University, St. Petersburg, Russia* V.I. DEMIDOV, *UES, INC., Dayton, OH* C.A. DE- JOSEPH, JR., *Air Force Research Laboratory, Wright-Patterson AFB, OH* Using a detailed, self-consistent model of a low pressure O₂ discharge, it is shown that detachment of electrons in the afterglow can lead to a significant increase in the negative wall potential with respect to the plasma potential. This effect can be used to modify the near-wall sheath electric field and thickness, which may be important for some plasma processing applications. In addition, the effect can lead to an increase in electron density with time, and a reduction in diffusion cooling of electrons and can thus be used to modify the electron temperature. The simulation was performed on a 100% modulated rf discharge operating at 13.56 MHz, using a commercial software package (www.cfdrc.com) with modifications. The density and mean energy of the electron component is obtained by solving either the fluid balance equations or the kinetic equations for the EEDF. The self-consistent electric field is found from Poisson's equation. Heavy particles are described using the fluid model and includes 160 plasmachemical reactions.

FPT2 16 Plasma-photocatalysis combination for air pollutant removal: identification of the synergy mechanisms O. GUAITELLA, F. THEVENET, A. ROUSSEAU, *LPTP, Ecole Polytechnique, CNRS, Palaiseau, France* C. GUILLARD, *LACE, UCBL, CNRS, Lyon, France* G. STANCU, J. ROEPCKE, *INP, Greifswald, Germany* The coupling of a photocatalyst with a non thermal plasma (DBD) is studied; based on experimental results we discuss separately the contributions of (i) the chemistry involved as a function of the porosity of the material, and (ii) the influence of the photocatalytic activity on the chemistry of C₂H₂ oxidation. C₂H₂ removal is strongly increased by the presence of a porous material (SiO₂ or TiO₂): the destruction of C₂H₂ is driven by species created by the plasma and concentrated by a porous [1]. Our experiments confirm that C₂H₂ removal rate increases with the porosity of the material, whereas the selectivity also depends on the chemical composition of the surface. In parallel, the temporal evolution of C₂H₂ concentration was measured by Tuneable Diode Laser Absorption Spectroscopy (TDLAS) in the mid infrared region in a low pressure discharge during a single plasma pulse (one shot). The contribution of external ultraviolet radiation and plasma exposure were quantified, both with and without photocatalyst. The synergetic effect was clearly demonstrated [2]. [1] U. Roland, F. Holzer, F.-D. Kopinke, 2002, *Catalysis Today* 73, 315–323. [2] A. Rousseau, O. Guaitella, L.V. Gatilova, F. Thevenet, C. Guillard, J. Roepcke, G. D. Stancu, *Appl. Phys. Lett.* 87, 221501 (2005).

FPT2 17 Kinetic Modeling of Electron Loss Kinetics in high pressure O_2/N_2 Electron Beam Sustained Plasmas KRAIG FREDERICKSON, WALTER LEMPERT, *Ohio State University* Previous work has demonstrated that the effective rate of electron loss by three-body attachment in O_2 containing plasmas is significantly decreased in vibrationally excited nonequilibrium environments, an effect which has been attributed to an increased rate for the electron detachment pathway. Specifically it is postulated that the rate of detachment is greatly enhanced by the presence of vibrationally excited "rapid detacher" species, since in a collision between O_2^- and a molecule possessing two or more quanta of vibrational energy the low electron affinity of O_2 ($\sim 0.43\text{eV}$) is exceeded. Assuming that the detachment cross section for such collisions is approximately gas kinetic, modeling indicates that the calculated effective electron detachment rate is nearly equal to or in excess of the experimentally determined net electron attachment rate. Analysis of the vibrational level populations indicates that in the nonequilibrium environment created in this study there is sufficient population in the vibrational levels responsible for detachment to account for the observed 5-6 order of magnitude increase in the effective detachment rate.

FPT2 18 *in-situ* FTIR characterization of the plasma chemistry as functions of the plasma duty cycle and peak power in a 1,3-butadiene discharge in an inductively coupled Gaseous Electronics Conference (GEC) Cell. MATTHEW GOECKNER, ASHISH JINDAL, LAWRENCE OVERZET, *University of Texas at Dallas* Time averaged *in-situ* Fourier Transform Infrared Spectroscopy is used to characterize the plasma chemistry of pulsed 1,3 Butadiene ($H_2C=CHCH=CH_2$) discharges as functions of both the plasma duty cycle and on phase power in a GEC Cell. Various ratios of plasma on to off times for equivalent duty cycles are investigated at peak powers of 40, 50, 60, and 70 W. Variations in densities associated with the major observed spectral bands are examined and the possible dissociation mechanisms responsible for all observed vibrations are investigated. For example, the data shows that free CH_2 stretching vibrations increase in a sub-linear fashion with increasing duty cycle. Approximately 44% of the CH_2 density is due to free daughter species at the largest (90%) duty cycle. This indicates that reaction kinetics are changing from cleavage of primarily the π bond of the C=C bond at lower duty cycles to cleavage of both π and σ (complete dissociation) at duty cycles approaching continuous wave biasing. This data will be tied to film growth.

FPT2 19 Asymptotic Expressions for the Parameters Describing Low Pressure Electronegative Plasmas RAOUL FRANKLIN, *The Open University* Experimentalists working in plasma processing need relatively simple expressions characterizing their plasmas. To that end we have revisited the Tables given by Franklin and Snell (1992) to obtain asymptotic i.e. algebraic expressions for the values of potential, ion speed and densities at the 'plasma edge' and the eigenvalue in terms of the parameters $\varepsilon = Te/Tn$ and $\alpha = nn_0/ne_0$, for the case where a single negative ion species is dominant. Given the geometry of most plasma processing systems, there is more interest in plane geometry, and so we have concentrated on that, but we have found analogous expressions for cylindrical geometry. Over almost all of the parameter space, we have obtained values that approximate well to the accurate computed solutions. Franklin, R. N. and Snell, J. (1992) *J. Phys. D: Appl Phys* 25, 435-7.

FPT2 20 Ion-ion Plasmas production and investigation GARY LERAY, PASCAL CHABERT, NICOLAS PLIHON, JEAN-LUC RAIMBAULT, *LPTP CNRS Ecole Polytechnique* A magnetized low-pressure electronegative discharge was used to produce ion-ion plasmas. We used both Ar/O_2 and Ar/SF_6 gas mixtures. The cylindrical plasma core is produced by an helicon wave, generated by a Boswell-type antenna excited at 13.56 MHz. The magnetic field strength is such that electrons are magnetized while ions are not, resulting in an electron-free plasma at the edge of the cylinder. The negative ion fraction was measured as a function of the radius by electrostatic probes and laser-induced fluorescence. The electrons represent less than one percent of the negative charge at the edge which allowed measuring the ion energy distribution function for both positive and negative ions. Finally, the criterion for sheath formation in electron-free plasmas was investigated.

FPT2 21 How many particles must a two-dimensional dusty plasma have to appear infinite? T.E. SHERIDAN, *Ohio Northern University* A complex (dusty) plasma disk (CPD) is a two-dimensional system of n particles interacting through a shielded Coulomb potential with Debye length λ and confined in an isotropic parabolic well. The emergence of macroscopic behavior in a CPD is studied by considering the dependence of the breathing frequency ω_{br} on n , λ , the disk radius R_0 , and the nearest neighbor distance a . An approximate analytical expression for ω_{br} is derived for $R_0 \gg \lambda$ with a/λ finite. In the plasma regime $a < \lambda$, so that each particle interacts with many other particles, $\omega_{br}^2 \approx 4$ independent of n . In the "condensed-matter" regime $a > \lambda$, nearest-neighbor interactions dominate and $\omega_{br}^2 \sim a/\lambda$. Exact solutions for $n = 100$ to 3200 particles approach the unbounded-plasma limit as n increases. Solutions with $n = 3200$ and a/λ between 0.25 and 0.5 are found to provide the best approximation to an infinite plasma.

FPT2 22 Breathing oscillation of elliptical Debye cluster K.D. WELLS, M.J. GAREE, A.C. HERRICK, T.E. SHERIDAN, *Ohio Northern University* An elliptical Debye cluster is a system of n identical particles confined in a two-dimensional anisotropic potential well and interacting through a shielded Coulomb potential. A model for this system has been developed which has three parameters: the number of particles, the well ellipticity, and the Debye shielding parameter. From numerical solutions of the model, we find as the ellipticity increases from circular to highly elliptical that the breathing mode persists and that the breathing frequency increases. For highly elliptical clusters, the breathing mode consists of particle motions predominantly in the direction of the minor axis of the ellipse. An elliptical cluster with $n = 49$ monodisperse microspheres was studied in the Dusty O.N.U. experiment (D.ONU.T). The anisotropic parabolic well was created using a rectangular aperture (17.5 mm \times 30.2 mm) placed on the lower electrode of an rf discharge. Plasma was created using ≈ 11 W of rf power for 18 mtorr of argon. The well ellipticity was determined by measuring the center-of-mass frequencies along the major and minor axes of the resulting elliptical cluster using both driven and thermally-excited oscillations. These two methods give results that are in good agreement. Cluster parameters were determined by measuring the frequency of the breathing mode and comparing with numerical eigenmode solutions of the model. The measured Debye shielding parameter was ≈ 2 . The measured cluster temperature was 400 K.

FPT2 23 HIGH PRESSURE PLASMAS AND LIGHTING

FPT2 24 Local field approximation and runaway electron generation in streamer tip conditions W.J.M. BROK, *Eindhoven University of Technology, The Netherlands* CHAO LI, *Centre of Mathematics and Informatics (CWI) Amsterdam, The Netherlands* J.J.A.M. VAN DER MULLEN, *Eindhoven University of Technology, The Netherlands* U. EBERT, *Centre of Mathematics and Informatics (CWI) Amsterdam and Eindhoven University of Technology, The Netherlands* Recent advances in lightning and streamer physics indicate that the kinetic behaviour of particles plays a role: the detection of x-rays emanating from lightning events indicates that processes occur in which individual particles have higher energies than can be accounted for in the models that have been used in the past. In order to investigate the influence of microscopic processes such as individual electron avalanches in front of a streamer tip, we are in the process of developing a hybrid fluid – particle model. As a step towards this goal, to study the manner in which the coupling between a fluid and Monte Carlo model can be established, we developed a Particle In Cell Monte Carlo simulation of a planar front. By means of this model the electrons kinetics in the tip of the front are studied and common fluid models assumptions such as the local field approximation are re-evaluated. Enhancement of the electric field, due to space charges in the front, is shown to augment the probability of runaway electron generation in the conditions typical for negative streamers.

FPT2 25 Density and lifetime evaluation of weakly ionized plasma for laser-triggered lightning by means of laser absorption MICHITERU YAMAURA, *Institute for Laser technology* The potential ability of lasers to control lightning can be improved by using a train of pulses with sub-millisecond separations [1-2]. Laser-triggered experiments in a small-scale (10 mm gap) atmospheric discharge facility show that the triggering is dramatically enhanced when a five-pulse train of sub-Joule energy is used instead of a single pulse. This effect increases rapidly as the pulse interval is reduced. In order to evaluate the trigger effect quantitatively, the plasma density produced by a pulsed KrF excimer laser with high repetition rate of kHz order was measured by means of laser absorption [3-4]. It appears that at a sub-millisecond pulse interval, sufficient positive and negative ions survive in subsequent pulses, thus enabling easy deionization. Hence, significant plasma build-up occurs from one pulse to the next. However, this persistence of ions would appear to imply that the rate of recombination (effectively a charge transfer between ions) is considerably lower than previously believed. [1] M. Yamaura, et al., *J. Appl. Phys.* **95**, 6007 (2004). [2] M. Yamaura, et al., *Appl. Phys. Lett.* **86**, 131502 (2005). [3] M. Yamaura, *J. Appl. Phys.* **98**, 043101 (2005) [4] M. Yamaura, et al., *Appl. Phys. Lett.* **88**, to appear in June (2006).

FPT2 26 Dependence of the Current on the Hollow Cathode Dimensions and Seed Electron Properties in a Pseudospark Discharge Initiation* SELMA CETINER, PETER STOLTZ, PETER MESSMER, *Tech-X Corporation* Hollow cathode discharges can be triggered by different mechanisms, including laser irradiation on the front or back wall of the cathode or beam triggering from another hollow cathode source, resulting in different developments of the discharge. The two-dimensional kinetic plasma simulation code OOPIC Pro and the two and three-dimensional

code VORPAL are used to study the properties of both standard and compact hollow cathode devices. This investigation studies variations in the peak initiation current with the hollow cathode dimensions and the location and energy of the seed electrons. The relative importance of secondary electrons due to both ion and electron impact is also studied. It is demonstrated that the magnitude of the peak current has a dependency on all these factors combined and trends cannot be established by varying a parameter in isolation.

*This work supported by the Office of the Secretary of Defense, SBIR grant #FA8650-04-C-2511 and performed in collaboration with J.-L. Cambier of AFRL/PRSA, Edwards AFB.

FPT2 27 Apoptosis in vascular cells induced by cold atmospheric plasma treatment RAYMOND SLADEK, EVA STOFFELS, *Eindhoven University of Technology* Apoptosis is a natural mechanism of cellular self-destruction. It can be triggered by moderate, yet irreversible damage. Apoptosis plays a major role in tissue renewal. Artificial apoptosis induction will become a novel therapy that meets all requirements for tissue-saving surgery. Diseased tissues can disappear without inflammation and scarring. This is particularly important in treatment of blockages in body tracts (e.g. cardiovascular diseases). Artificial induction of apoptosis can be achieved by means of cold plasma treatment. In this work an atmospheric micro-plasma operated in helium/air has been used to induce apoptosis in vascular cells. Parametric studies of apoptosis induction have been conducted; the efficiency is almost 100%. The apoptotic factors are ROS/RNS (reactive oxygen and nitrogen species). Their densities in the plasma have been measured by mass spectrometry. For apoptosis induction, RNS seem to be more important than ROS, because of their relative abundance. Moreover, addition of a ROS scavenger (ascorbic acid) to the cell culture medium does not reduce the occurrence of apoptosis. Cold plasma is a very efficient tool for fundamental studies of apoptosis, and later, for controlled tissue removal in vivo.

FPT2 28 The Plasma Pencil: A Novel Pulsed Plasma Source* TAMER AKAN, XINPEI LU, MOUNIR LAROUCSI, *Old Dominion University* One of the attractive characteristics of nonequilibrium plasmas is their enhanced plasma chemistry without the need for elevated gas temperatures. Using nanoseconds high voltage pulses the electron energy distribution function can be controlled in a way to shift it towards the high-energy tail. Higher electrons energies lead to enhanced gas phase chemistry. This is advantageous in material processing applications where advanced chemical processes under low temperature conditions are desirable. In this paper, we report on a novel pulsed cold plasma source, the "plasma pencil" [1], and its unique characteristics. The plasma pencil is capable of generating a cold plasma plume several centimeters in length. It exhibits low power requirements and by using helium as a carrier gas the gas temperature remains low for extended periods of operation. The plasma plume emitted by the plasma pencil can be applied to bare skin without causing any heating or painful sensation. In this paper, the characteristics of the plasma pencil will be discussed. These include the current-voltage characteristics, plume temperature, emission spectra, and the time and spatial evolution of the plasma plume. *Work supported by the Air Force Office of Scientific Research (AFOSR). [1] M. Laroussi and X. Lu, "Room Temperature Atmospheric Pressure Plasma Plume for Biomedical Applications," *Applied Physics Letters*, Vol. 87, 2005.

FPT2 29 Model calculations of O₂(1D) production in microcathode sustained discharges in argon/oxygen mixtures E. MUNOZ-SERRANO, G. HAGELAAR, J.P. BOEUF, L.C. PITCHFORD, *CPAT, Toulouse, France* It is now well established that non-thermal, high-pressure plasmas can be initiated and sustained between a microhollow cathode discharge (MHCD) acting as a plasma cathode and a third electrode placed some distance away. To investigate the properties of the plasma created in such a microcathode sustained (MCS) discharge configuration, we have developed a 2D quasi-neutral model of a radially expanding "positive-column" in which the current crossing the exit plane of the MHCD is input as a boundary condition. We are particularly interested in determining operating conditions leading to high yields of singlet delta (metastable) oxygen molecules O₂(1D), and thus the model includes a kinetic scheme to describe the plasma chemistry in pure O₂ and in Ar/O₂ mixtures. For 10% O₂ in a 50 torr Ar/O₂ mixture, a discharge current of 1 mA, a 200 micron MHCD hole diameter and 0.6 cm gap spacing, we find that the reduced electric field, E/N, on-axis at the mid-plane is about 15 Td. The calculated O₂(1D) yield on-axis near the exit of the MHCD is 10%. For higher O₂ partial pressures, quenching of O₂(1D) in 3-body collisions with O₂ and O atoms leads to a decrease in the predicted yield, but the optimum pressure depends on the assumed values for the 3-body quenching rates. Details of the model and results of species density profiles for a range of conditions will be presented.

FPT2 30 On the Influence of the Dielectric Barriers on the Atmospheric Pressure Glows in Helium PENG ZHANG, NING ZHOU, *ESI-CFD, 6767 Old Madison Pike NW, Suite 600, Huntsville, AL 35806* UWE KORTSHAGEN, *Dept of Mechanical Engineering, University of Minnesota, 111 Church Street SE, Minneapolis, MN 55414* ESI-CFD TEAM UNIVERSITY OF MINNESOTA TEAM Based on a two-dimensional fluid model with a local field approximation, the atmospheric pressure glow discharges (APGs) with two dielectric barriers in helium with nitrogen impurities are studied. The model self-consistently solves the Poisson equation for the electric field and the continuity equations for the densities of all species. The momentum equations are simplified by the drift-diffusion flux. The electrons, helium atomic and molecular ions, helium metastables, and nitrogen molecular ions are included in the simulation. The model successfully predicts the formation of self-organized filaments in the discharge gap. The results showed that smaller number of filaments forms for dielectric material with lower permittivity. And a uniform Townsend-like discharge can be obtained by using of a material with lower permittivity. Based on the simulation model, the APG initiation process in the reactor with a single dielectric barrier is studied. And the influence of the thickness of the dielectric is also investigated.

FPT2 31 Diagnostics of an rf-excited micro atmospheric pressure plasma jet S. REUTER, K. NIEMI, *Department of Physics, University Duisburg-Essen, D-45141 Essen, Germany* V. SCHULZ-VON DER GATHEN, T. MUSSENBRÖCK, T. GANS, *Center for Plasma Science and Technology CPST, Ruhr University Bochum, D-44780 Bochum, Germany* The "standard" 13.56 MHz rf-excited plasma jet operates at ambient conditions. It generates a homogeneous plasma in helium or argon with small admixtures (about 1 vol.-%) of oxygen¹. Absolute concentrations

of atomic oxygen have been measured in the effluent of the plasma jet by two-photon laser-induced fluorescence (TALIF). Even at several centimeter distance from the nozzle still there is 1% of the initial atomic oxygen density of 10^{16} cm^{-3} present². Here we present a modified μ -APPJ version particularly designed for investigation of the discharge interior. First emission spectroscopic investigations and tests of applicability are presented. The wettability of polymer Petri dishes could be adjusted in a wide range (wetting angle from 60° to below 10°). ¹S. Wang, V. Schulz-von der Gathen, and H.F. Doebele, *Appl. Phys. Lett.* **83**, 3272 (2003). ²K. Niemi, S. Reuter, V. Schulz-von der Gathen, and H.F. Doebele, *Plasma Sources Sci. Technol.* **14**, 375 (2005).

FPT2 32 Nonlinear lumped circuit modeling of an atmospheric pressure rf discharge M. LAPKE, D. ZIEGLER, T. MUSSENBRÖCK, T. GANS, V. SCHULZ-VON DER GATHEN, *Center for Plasma Science and Technology CPST, Ruhr University Bochum, D-44780 Bochum, Germany* The subject of our modeling approach is a specifically modified version of the atmospheric pressure plasma jet (APPJ, originally proposed by Selwyn and coworkers¹) with reduced discharge volume, the *micro* atmospheric pressure plasma jet (μ -APPJ). The μ -APPJ is a homogeneous nonequilibrium discharge operated with Argon or Helium as the feedstock gas and a percentage volume admixture of a molecular gas (O₂, H₂, N₂). The efficiency of the discharge is mainly due to the dissociated and activated molecules in the effluent that can be selected depending on the application. A variety of applications in surface treatment have already been demonstrated, e.g., in semiconductor technology, restoration and bio-medicine. In this contribution we present and analyze a nonlinear lumped circuit model of the μ -APPJ. We apply a two-scale formalism. The bulk is modeled by a generalized Ohm's law, whereas the sheath is described on a considerably higher level of mathematical sophistication. The main focus lies on the spectrum of the discharge current in order to support the characterization of the discharge via model-based diagnostics, i.e., the estimation of the spatially averaged electron density from the frequency of certain self-excited collective resonance modes. J. Park et al., *Appl. Phys. Lett.* **76**, 288 (2000)

FPT2 33 Measurement of metastable Ar atom density in atmospheric-pressure microgap discharge using laser absorption spectroscopy AKIHIRO KONO, *Nagoya University* TOMOYUKI SHIBATA, MITSUTOSHI ARAMAKI Atmospheric-pressure Ar glow discharge in a microgap between two knife-edge electrodes (10-mm length, 100- μm gap separation) driven by 2.45-GHz microwave is being studied aiming at an application to VUV excimer light source. One of the knife-edge electrodes has a gas sink at its ridge, enabling introducing gas flow through the discharge plasma. The density of metastable Ar atoms, which are precursors of excimer molecules, is studied using laser absorption spectroscopy. The beam of a tunable diode laser at wavelengths around 696.5 nm is arranged to pass through the microgap obliquely to have an absorption path length of ~ 1 mm. At a microwave power of 10 W, the observed absorption at the line center was $\sim 10\%$ with a pressure broadened line width of ~ 13 GHz, giving metastable Ar atom density of $3 \times 10^{13} \text{ cm}^{-3}$. In a similar condition, the electron density measured using a laser Thomson scattering technique was $3 \times 10^{14} \text{ cm}^{-3}$. The behavior of metastable atom density for varying discharge conditions is under investigation. (Work supported by Grant-in-aid 15075205 from MEXT Japan.)

FPT2 34 Atmospheric Pressure non-thermal plasmas for surface treatment of polymer films HSIAO-FENG HUANG, CHUN-HSIANG WEN, *Material and Chemical Research Laboratories, Industrial Technology Research Institute, Hsinchu, 310, Taiwan, R.O.C.* HSIAO-KUAN WEI, CHWUNG-SHAN KOU, *Department of Physics, National Tsing Hua University Hsinchu, 310, Taiwan, R.O.C.* Interest has grown over the past few years in applying atmospheric pressure non-thermal plasmas to surface treatment. In this work, we used an asymmetric glow dielectric-barrier discharge (GDBD), at atmospheric pressure in nitrogen, to improve the surface hydrophilicity of three kinds of polymer films, biaxially oriented polypropylene (BOPP), polyimide (PI), and triacetyl cellulose (TAC). This set-up consists of two asymmetric electrodes covered by dielectrics. And to prevent the filamentary discharge occur, the frequency, gas flow rate and uniformity of gas flow distribution should be carefully controlled. The discharge performance is monitored through an oscilloscope, which is connected to a high voltage probe and a current monitor. The physical and chemical properties of polymer surfaces before and after GDBD treatment were analyzed via water contact angle (CA) measurements, atomic force microscopy (AFM), and X-ray photoelectron spectroscopy (XPS) techniques.

FPT2 35 Spatially Resolved Gas Temperature Measurements in an Atmospheric Pressure DC Glow Microdischarge with Raman Scattering S. BELOSTOTSKIY, Q. WANG, V. DONNELLY, D. ECONOMOU, N. SADEGHI, DEPT. OF CHEM. ENG., U. OF HOUSTON TEAM, U. FOURIER DE GRENOBLE TEAM Spatially resolved rotational Raman spectroscopy of ground state nitrogen $N_2(X^1\Sigma_g^+)$ was used to measure the gas temperature (T_g) in a nitrogen dc glow microdischarge (gap between electrodes $d \sim 500 \mu\text{m}$). An original backscattering, confocal optical system was developed for collecting Raman spectra. Stray laser light and Rayleigh scattering were blocked by using a triple grating monochromator and spatial filters, designed specifically for these experiments. The optical system provided a spatial resolution of $< 100 \mu\text{m}$. Gas temperatures were determined by matching experimental spectra to model spectra obtained by convolution of theoretical line intensities with the apparatus spectral resolution, with T_g as the adjustable parameter. T_g was determined as a function of pressure and discharge current density ($P = 400\text{--}760$ Torr, $j_d = 200\text{--}1000 \text{ mA/cm}^2$). Midway between the electrodes, T_g increased linearly with j_d , reaching 500 K at 1000 mA/cm^2 j_d for a pressure of 720 Torr. Spatially resolved gas temperature measurements will also be presented and discussed in combination with a mathematical model for gas heating in the microplasma. This work is supported by DoE/NSF.

FPT2 36 Experimental Study on Atmospheric Pressure RF Capacitive He/CF₄/O₂ Discharges TAKASHI KIMURA, TAKAMASA HANAI, *Nagoya Institute of Technology* Electrical and optical measurements of atmospheric pressure capacitive radio frequency (13.56 MHz) He/CF₄/O₂ discharges were carried out by changing the mixture compositions of CF₄ and oxygen at the fixed He content of 99%. Those discharges were produced between two planar electrodes of 40mm- ϕ at the gap length of 1.0 mm. The impedance of the discharge gradually decreased as oxygen was mixed to He/CF₄ discharges, and then reached the minimum around the oxygen content of 0.1%, beyond which it increased with increasing oxygen content. Optical emission spectroscopy has been used in order to observe the excited species generated in the capacitive He/CF₄/O₂ discharges. Optical emis-

sion spectra used in this study exhibit emission lines of excited Ar, O and F atoms. The intensity at 704 nm emitted from the excited atomic fluorine increased markedly as oxygen was mixed to CF₄ discharges, and then reached the maximum around the oxygen content of 0.2 - 0.3%, beyond which it decreased with increasing oxygen content. The intensity at 845 nm emitted from the excited atomic oxygen was also investigated in order to grasp the dependence of the atomic oxygen density on the oxygen content. The intensity at 845 nm was approximately proportional to O₂ content, resulting in the linear relationship between the atomic oxygen density and the O₂ content.

FPT2 37 The Influence of Polymer Films on an APGD in Helium DAMIAN DELLA CROCE, GAGIK NERSISYAN, WILLIAM GRAHAM, *Physics and Astronomy, Queens University Belfast, BT7 1NN, Northern Ireland* Electrical and optical diagnostic techniques have been used to study the influence of various polymers in the gap of a Helium APGD. A gated ICCD was used to record short exposure time images (2 μs) through the development of the discharge current pulse. The APGD was generated between two parallel, glass 4mm thick plates which cover copper mesh electrodes. The gap was 5mm. Typically a 4.4kV (peak to peak) sinusoidal voltage was applied to the powered electrode with a frequency of 30kHz. The other electrode was grounded. The system was housed in an evacuated chamber, previously evacuated to a base pressure of 10^{-4} Pa, before Helium was introduced to static atmospheric pressure. A spectrometer was used to record the emission spectra from the discharge. To date studies on polypropylene (PP) and polyester (PET) have been conducted and polyamide will follow. Interesting trends are evident when they are compared to those for the He APGD with no polymer present. Electrically the traces for PET are dramatically different to those for PP and no polymer, which are comparable. Imaging shows that PP yields a filamentary discharge. PET on the other hand produces a glow-type discharge. We are currently studying if the different results are intrinsic to the polymer or the anti-cling surface treatments that the polymer suppliers may be applying. DD is supported by EPSRC and Dow Corning Plasma Solutions.

FPT2 38 Diagnostics of an Electron Beam Integrated Thruster* TSITSI MADZIWA-NUSSINOV, MAX LIGHT, PAT COLESTOCK, RON KASHUBA, RICK FAEHL, *ISR-6, Los Alamos National Laboratory* Since the 1970s, Russian scientists have been utilizing Plasma cathode electron (PCE) sources for production of electron beams [1], [2]. We have utilized a PCE source in our Electron Beam Integrated Thruster (EBIT) experiment. Using an ECR source at 2.45GHz, we made our PCE source (described in detail in another presentation at this conference) by biasing a conducting plasma chamber to negative voltages up to -140V. We left a small aperture of 2cm in diameter through which an electron beam is extracted into a downstream Pyrex glass chamber with magnetic coils for plasma confinement. The plasma-electron beam system was diagnosed using three methods: a Langmuir probe (for electron temperatures, space potentials and electron densities), spectroscopy (for electron temperatures) and a retarded electron potential energy analyzer (for electron energies and space potentials). In this paper we will briefly describe our experiment, the PCE source, and give details of the diagnostics and our initial results on EBIT. [1] Yu. E. Kreindel, *Plasma Cathode Electron Sources*~Atomizdat, Moscow, 1977, p. 144. [2] E. M. Oks, *Plasma Sources Sci. Technol.* 1, 249 (1992).

*This work was funded by DARPA.

FPT2 39 Use of a Plasma Cathode Electron (PCE) source in an Electron Beam Integrated Thruster (EBIT)* MAX LIGHT, TSITSI MADZIWA-NUSSINOV, PAT COLESTOCK, RON KASHUBA, RICK FAEHL, *ISR-6, Los Alamos National Laboratory* The electron Beam Integrated Thruster (EBIT) plasma propulsion concept centers around the use of an electron beam to ionize a propellant; a more efficient ionization mechanism than conventional electric propulsion concepts. In this paper we outline the EBIT concept, in particular, the generation of the electron beam in a Plasma Cathode Electron (PCE) source. The PCE beam

source utilizes a plasma as an electron beam cathode, eliminating lifetime and heating issues associated with material cathodes. Our PCE source was created using 1.5kW of microwave power at 2.45GHz delivered in a static magnetic field of 875Gauss. We were able to drive electron beams of greater than 100A in our source with very high beam efficiencies by biasing the ECR source chamber to -120V.

*This work was funded by DARPA.

SESSION GW1: DIAGNOSTICS I: ELECTRICAL

Wednesday morning, 11 October 2006

Salon CD Holiday Inn at 8:00

Mark Sobolewski, National Institute of Standards and Technology, presiding

*Contributed Papers***8:00**

GW1 1 Detailed Time-resolved Plasma Diagnostics in a Pulsed DC Magnetron Discharge IAN SWINDELLS, *The University of Liverpool* PETER KELLY, *Manchester Metropolitan University* JAMES BRADLEY, *The University of Liverpool* Mid-frequency (5 - 350 kHz) pulsed DC magnetron plasmas provide a stable, arc free sputtering process for deposition of metal oxide films. A combination of Langmuir probe and optical emission spectroscopy plasma diagnostics provide detailed time-resolved measurements of plasma density, n_e , electron temperature, T_e , plasma potential, V_p , and plasma excitation. The bi-polar waveform of the power supply, in particular the fast transient periods, drives the evolution and energetics of the plasma. Using electrical probes we observe a short lived increase in n_e and T_e during the on to off and off to on phases. This is accompanied by a burst of light in the optical emission. The large overshoot in voltage during the target reversal on to off drives the plasma potential to values of over +150 V relative to ground. Sheath dynamics at the boundaries between the plasma and the target, for the switch to the 'on-phase', and between the plasma and the substrate or walls, during the overshoot period, provide an explanation for the observed peaks. The effect different boundary conditions have on the bursts during the overshoot period is investigated.

8:15

GW1 2 Investigation of total energy flux density at a floating substrate in pulsed DC unbalanced magnetron. MARTIN CADA, *University of Liverpool* GREG CLARKE, *Manchester Metropolitan University* JAMES BRADLEY, *University of Liverpool* The total energy flux density (TEFD) at a floating substrate in an asymmetric bipolar pulsed DC unbalanced magnetron system with titanium target has been investigated using a thermal probe (in substrate) and a time-resolved Langmuir probe. It was found that for various pulsing parameters: 1) the TEFD is approximately 70% higher in a pulsing plasma than for DC operation and 2) the total energy flux density increases linearly with pulse frequency and decreases with duty cycle (with maximal value at 60% duty). The EFD for the charged particles (electrons and ions) and neutrals were calculated. The neutral particle flux was determined from the deposition rate. The charged particle energy flux at the floating substrate was calculated from the measured electron mean energy, charged particle concentration, plasma and floating potentials. Finally, the total energy balance was calculated and compared to the TEFD measured by the thermal probe. Good agreement between the measured and calculated TEFD was found for DC and low pulse frequencies. For higher frequencies, the calculated TEFD was observed to be several times lower than measured. We attribute this to the inability of the Langmuir probe technique to measure the high energy electrons and ions generated during the pulse transients.

8:30

GW1 3 RF Impedance of a Spherical Probe at High and Low Gas Pressure* R.F. FERNSLER, D.N. WALKER, *SFA, Crofton, MD* D.D. BLACKWELL, W.E. AMATUCCI, *Plasma Physics Division, Naval Research Laboratory* S.J. MESSER, *NRL-NRC Postdoctoral Associate* The plasma electron density n_{e0} is most often determined using a Langmuir probe to measure the dc current as a function of the applied dc voltage V_{dc} . The dc impedance Z_{dc} varies strongly with V_{dc} , and models are needed to relate Z_{dc} to n_{e0} . Secondary electron emission, ion collisions, and other effects further complicate the analysis. Alternatively, a variable rf voltage can be applied while holding V_{dc} fixed. As long as the rf voltage is small, the rf impedance Z_{rf} varies with the frequency f but not the amplitude of the voltage, and for a fixed frequency, Z_{rf} depends only on $n_e(r)$ and the neutral gas density N . In this talk theoretical and experimental results for Z_{rf} are related to n_{e0} for a small spherical probe. At low N , Z_{rf} becomes resistive whenever f equals the local plasma frequency, and both the real and imaginary parts of Z_{rf} peak when f equals the bulk plasma frequency. The peaks make n_{e0} easy to determine, and the resistance at lower frequencies can be used to determine $n_e(r)$ within the sheath and presheath. At high N , the resistance depends mainly on n_{e0}/N , so n_{e0} is again easy to determine. Theoretical and experimental results for several spheres will be compared with Langmuir-probe data at high and low gas pressure.

*Work supported by ONR.

8:45

GW1 4 Extended plasma parameter extraction using in-line RF metrology for multi-frequency plasma reactors STEVEN SHANNON, DANIEL HOFFMAN, MATTHEW MILLER, *Applied Materials Etch Engineering Technology Group* In-line RF metrology combined with plasma discharge models is a convenient, non-intrusive means for obtaining plasma parameters in industrial processing discharges. [1] Typically, this analysis is performed at the fundamental RF drive frequency used to sustain the discharge, and provides two equations (real and imaginary discharge impedance) from which at least two plasma parameters can be independently determined. This necessitates approximation of other plasma parameters such as discharge asymmetry and electron - neutral collision frequency to obtain accurate outputs. Currently, many state-of-the-art plasma reactors used for semiconductor manufacturing use multiple frequencies for independent control of multiple plasma parameters. [2] The purpose of this work is to demonstrate the extended capabilities of this in-line RF diagnostic when multiple frequencies are used to drive a CCP discharge, with particular focus on the replacement of approximated plasma parameters with calculated plasma parameters using this multi-frequency approach, and the extension of real time parameter tracking in plasma processing that it can provide. [1] Bull. Am. Phys. Soc. 48 (5) [2] IEEE Conf. Rec. 05CH37537 - 2005 Int. Conf. Plasma Sci., Talk 10498.

9:00

GW1 5 Response of an Isolated Dust Particulate in a DC Glow Discharge Subjected to External Excitations J. MCFERRAN, J. WEST, V. SUBRAMANIAM, A. KAHRAMAN, *Ohio State University* Isolated spheres of borosilicate glass are suspended in a DC glow discharge in neon. The response of spheres 16 to 42 times heavier than in previous work is observed under heavily damped conditions when displaced laterally by applying a transient voltage. It is shown that lateral excitation of the isolated particulate cannot drive the motion to classical resonance as observed in pre-

vious work involving axial displacements in RF plasmas. The base excitation (BE) model, rather than the classical forced damped oscillator model, is found to exhibit good agreement with the present results. A new means of estimating charge from the frequency response of the particulate motion using the BE model is described. Sheath polarization and ion drag effects neglected in previous work are included here. Ion drag is found to be the dominant drag mechanism for the heavier particulates. Finally, the trajectory of an isolated sphere displaced by radiation pressure while under heavily damped conditions is observed and analyzed.

9:15

GW1 6 Collisionless nonlinear damping of dust acoustic waves due to dust charge fluctuations* JYOTIRMOY PRAMANIK, *Institute for Plasma Research, Bhat, Gandhinagar, India* A novel

technique to calculate the damping effects on dust acoustic waves due to dust charge fluctuations in a dusty (complex) plasma is reported. The perturbed distribution function of the dust charge has been obtained by solving the linearized Vlasov equation introducing charge fluctuation effects in the source term. To get the damping coefficient, we followed the Dawson's model for longitudinal plasma oscillations. The present calculations show that dust charge fluctuations and the so called charging frequency (η) enhance the damping of the dust acoustic waves and also modifying the electrostatic energy density decay rate of dust acoustic wave. The breakdown of the linear theory is also discussed.

*The author gratefully acknowledges Dr. R. Ganesh, Dr. R. Singh, Prof. A. Sen and Prof. P.K. Kaw of Institute for Plasma Research, India for useful discussions on the subject.

SESSION GW2: HIGH PRESSURE DISCHARGES I

Wednesday morning, 11 October 2006; Salon B Holiday Inn at 8:00; William Graham, Queens University Belfast, presiding

Invited Papers

8:00

GW2 1 Energy transport and instabilities in high pressure plasmas.*
JOACHIM HEBERLEIN, *University of Minnesota*

While electric arc plasmas can be considered to be in local thermal equilibrium, any interaction of the arc with its surroundings will result in a non-equilibrium boundary layer. Two such non-equilibrium boundary layers will be considered. One is the interaction of an arc with a solid surface, i.e. what happens to the energy and current transfer if you have extremely steep gradients, and when diffusion processes dominate. Contradictory evidence and theories exist for such a situation. Recent Langmuir probe and Thomson scattering measurements have provided some insight and support qualitatively some previous modeling predictions. However, it may be questioned if a continuum approach is still valid when temperature gradients of 10^5 K/mm exist. The other boundary layer is encountered when a high velocity plasma jet is surrounded by a cold gas. The steep gradients in density and viscosity between the plasma jet and its surroundings result in fluid dynamic instabilities, enhanced by upstream arc instabilities. These instabilities result in entrainment of cold surrounding gas in form of larger bubbles, requiring a description of a jet consisting of two immiscible fluids. Approaches will be described for controlling these instabilities for an application like plasma spraying where the residence time of the particles is in the same order of magnitude as the period of the instability.

*Acknowledgment: support by NSF CTS 0225962 and CTS 0317429.

8:30

GW2 2 Characterization of Atmospheric Pressure Dielectric Barrier Discharges for Environmental Applications.

KUNIHIDE TACHIBANA, *Kyoto University*

Two types of atmospheric pressure glow discharge (APGD) schemes, i.e., a conventional parallel-plate type and a microplasma-integrated type, are compared from viewpoints of those plasma parameters and other physicochemical characteristics. In the former type, the discharge tends to constrict showing filamentary appearance as the current density increases. The tendency becomes noticeable when electronegative gases such as O_2 and H_2O are included. Therefore, in the glow mode the electron density cannot exceed the order of 10^{11} cm^{-3} , as measured by a mm-wave transmission technique, even though an elaborate method to control the voltage waveform is performed. The mechanisms concerning with the filamentation will be argued based on the variation of the accumulated charge density on the dielectrics from the spatially resolved measurement by a Pockels-effect method. On the centrally, the latter type with such a structure composed of stacked metal-mesh covered with dielectrics has been proved to be promising for stable operation at higher plasma density in the order of 10^{12} to 10^{13} cm^{-3} even with admixtures of O_2 and H_2O . This is of much advantage for many environmental uses in the effective production of oxidizing precursors such as O, OH and O_3 . In order to effuse the plasma out of the mesh-electrode holes, the effect of gas flow has been studied, and the modified structure enabling higher flow velocity is going to be tested together with the optimization of the operating frequency and the voltage waveform. The results of laser spectroscopic diagnostics of those radicals and ions such as N_2^+ will be explained at the conference.

Contributed Papers

9:00

GW2 3 Plasma properties in microcathode sustained discharges in oxygen containing mixtures – comparisons of experiments and models G. BAUVILLE, J.F. LAGRANGE, L. MAGNE, V. PUECH, *LPGP, Orsay, France* E. MUNOZ-SERRANO, L.C. PITCHFORD, *CPAT, Toulouse* N. SADEGHI, *LSP, Grenoble* M. TOUZEAU, *LTM, Grenoble* In this communication, we will summarize results of a joint experimental/modeling project whose purpose is to evaluate the feasibility of generating high yields of singlet delta (1D) metastable oxygen molecules in a microcathode sustained discharge (MCSD), a discharge configuration in which a microhollow cathode discharge is used as a plasma cathode with a third electrode being placed 0.5-1 cm away. From electrical and optical measurements and from modeling (presented in more detail in companion posters at this conference), we deduce the gas temperature, the [O] density profile, the spatial distribution of O₂(singlet sigma), the spatial distribution of the O₃, and the yield of O₂(1D) as determined from IR emission at points downstream from the discharge. These quantities are compared with results from a 2D quasi-neutral model. The baseline conditions are 10% O₂ in Ar at a total pressure of 50 torr, discharge currents on the order of 1 mA, and for a 200 micron microhollow cathode discharge diameter. This communication will focus on the intercomparison of results from the different diagnostics and from the model.

9:15

GW2 4 Simulations of nitrogen glow discharge phenomena for high-speed flow control THOMAS DECONINCK, SHANKAR MAHADEVAN, LAXMINARAYAN RAJA, *University of Texas at Austin* Plasma actuators offer a promising opportunity for high-speed flow control applications. The forcing of the flow occurs through three primary mechanisms: electrohydrodynamic forcing or ion drag, dilatation effects related to gas heating, and magneto-hydrodynamic forcing in the presence of magnetic fields. In order to gain a physical understanding of these factors, we developed a detailed computational model for the plasma and bulk flow. The model is based on a two-dimensional, self-consistent, multi-species continuum description of the plasma. We use a two-temperature chemical kinetics model that includes the following species: e⁻, N₂⁺, N⁺, N, and N₂. In this work, a surface plasma actuator with two bare-electrodes on a single plane is considered. The imposed background flow-field simulates a boundary layer with an external velocity of 700 m/s. Results include maps of charge density, temperature and electric potential profiles. For a pressure of 5 Torr and an applied voltage of 2500 V, the sheath region in front of the cathode is about 5 mm thick. The peak electron number density reaches ~ 1e16 m⁻³ in the bulk plasma. The number density of N₂⁺ is found to be dominant in the discharge, about two orders of magnitude higher than that of N⁺. Relative contributions of the body forces will be explored for different operating conditions.

SESSION HW: ALLIS PRIZE LECTURE

Wednesday morning, 11 October 2006; Salon CD Holiday Inn at 10:00; Greg Hebner, Sandia National Laboratories, presiding

10:00

HW 1 Nanoelectronics and Plasma Processing—The Next 15 Years and Beyond.

MICHAEL A. LIEBERMAN, *University of California, Berkeley*

The number of transistors per chip has doubled every 2 years since 1959, and this doubling will continue over the next 15 years as transistor sizes shrink. There has been a 25 million-fold decrease in cost for the same performance, and in 15 years a desktop computer will be hundreds of times more powerful than one today. Transistors now have 37 nm (120 atoms) gate lengths and 1.5 nm (5 atoms) gate oxide thicknesses. The smallest working transistor has a 5 nm (17 atoms) gate length, close to the limiting gate length, from simulations, of about 4 nm. Plasma discharges are used to fabricate hundreds of billions of these nano-size transistors on a silicon wafer. These discharges have evolved from a first generation of "low density" reactors capacitively driven by a single source, to a second generation of "high density" reactors (inductive and electron cyclotron resonance) having two rf power sources, in order to control independently the ion flux and ion bombarding energy to the substrate. A third generation of "moderate density" reactors, driven capacitively by one high and one low frequency rf source, is now widely used. Recently, triple frequency and combined dc/dual frequency discharges have been investigated, to further control processing characteristics, such as ion energy distributions, uniformity, and plasma etch selectivities. There are many interesting physics issues associated with these discharges, including stochastic heating of discharge electrons by dual frequency sheaths, nonlinear frequency interactions, powers supplied by the multi-frequency sources, and electromagnetic effects such as standing waves and skin effects. Beyond the 4 nm transistor limit lies a decade of further performance improvements for conventional nanoelectronics, and beyond that, a dimly-seen future of spintronics, single-electron transistors, cross-bar latches, and molecular electronics.

SESSION JW: BUSINESS MEETING

Wednesday morning, 11 October 2006

Salon CD Holiday Inn at 11:00

Greg Hebner, Sandia National Laboratories, presiding

11:00**JW 1 Business Meeting****SESSION KW: GENERAL COMMITTEE MEETING**

Wednesday noon, 11 October 2006

Salon CD Holiday Inn at 12:00

Greg Hebner, Sandia National Laboratories, presiding

12:00**KW 1 General Committee Meeting****SESSION LW1: PLASMA AERODYNAMICS AND PROPULSION II**

Wednesday afternoon, 11 October 2006; Salon CD Holiday Inn at 13:30; Igor V. Adamovich, Ohio State University, presiding

*Invited Papers***13:30****LW1 1 Physics of the after-spark channel decay in dense gas.**MIKHAIL SHNEIDER, *Princeton University, MAE Department*

Considerable experimental data on the dynamics of cooling of a post-discharge channel formed by high-power spark discharges, pulsed arcs, and laser sparks have been accumulated. Cooling of the hot post-discharge channel is a problem of major practical importance. The cooling rate determines the dielectric strength recovery rate. There is a regime when the turbulent gas motion develops in a decaying post-discharge channel, dramatically enhancing heat transfer compared with molecular heat conduction. Such turbulent motion arising in the after-spark channel can substantially enhance the rate of fuel-gas mixing, which may control the mixing rate in ramjet or scramjet engines. A known experimental results and simple theoretical models for self-consistent calculations of the entire evolution of a spark discharge and the subsequent cooling of the post-discharge channel, taking into account the generation and dissipation of turbulent motion of the gas are presented. Classical cascade and non-cascade mechanisms of a turbulence dissipation are discussed. The stabilizing effect of the continuous residual electric current on the plasma cooling in the channel is analyzed. This effect cannot be explained merely by Joule heating but is largely governed by the fact that the turbulent heat transport is substantially suppressed. The results for computed rate of restoration of dielectric strength are compared with known experiments.

*Contributed Papers***14:00****LW1 2 Modeling of Thermionic Devices With Nonequilibrium****Inert Gas Plasmas** SERGEY MACHERET, MIKHAIL SHNEIDER, RICHARD MILES, *Princeton University*

Large temperature gradients occur between surfaces exposed to high temperatures associated with aircraft engines and external surfaces, and thermionic devices may offer a way of converting a significant portion of the heat flux into electricity. We theoretically study a possibility of operating thermionic devices with self-sustained or auxiliary nonequilibrium ionization in inert gas filled cells, without the conventionally used cesium vapor. Modeling of plasma kinetics shows that under certain conditions (low pressure, relatively high voltage and emitted current) the electric field-induced heating of plasma electrons can result in self-sustained ionization sufficient for the argon-filled device functioning without external ionization. The self-sustained nonequilibrium ionization regime is also characterized by oscillations of electron temperature and density, with the frequency determined by ion motion. At relatively

low voltages or emitted currents, the heating of plasma electrons is not sufficient to sustain the ionization, and repetitive short pulses are shown to be capable of sustaining the plasma in an argon-filled device, with only a small fraction of the generated power spent on the auxiliary ionization.

14:15**LW1 3 A Microwave-Excited Microplasma Thruster: Plasma Diagnostics, Performance Testing, and Numerical Analysis**YOSHINORI TAKAO, KOICHI ONO, KOJI ERIGUCHI, *Department of Aeronautics and Astronautics, Kyoto University, Kyoto, Japan*

Decreasing the scale of propulsion systems is of critical importance on the development of microspacecraft. This paper is concerned with an application of microplasmas to a microthruster, presenting some experimental and numerical results. The microthruster consists of a cylindrical microplasma source 10 mm in length and 1.5 mm in inner diameter and a conical micronozzle fabricated in a 1.0 mm thick quartz plate with a throat diameter of 0.2 mm. The microplasma source produces hot plasmas by 4-GHz microwaves in the pressure range from 5 to 50 kPa, and then the micronozzle converts such high thermal energy into directional kinetic energy as a supersonic jet. Plasma diagnostics and performance testing showed that the electron density, rotational

temperature, thrust, and specific impulse obtained were 10^{19} m^{-3} , 1000 K, 1.1 mN, and 73 s, respectively, at an Ar/N₂ gas flow rate of 50/0.5 sccm and an input power of 9 W. Comparison with a numerical analysis implies that the micronozzle has an adiabatic wall rather than an isothermal one.

14:30

LW1 4 Experimental Studies of a Direct-Current Microdischarge Plasma Thruster STEPHEN A. YELDELL,*LAXMI-NARAYAN L. RAJA,†PHILIP L. VARGHESE,‡ *The University of Texas at Austin* Recently we proposed a novel Microdischarge Plasma Thruster (MPT) using direct-current microdischarges. The MPT uses a dc-microdischarge to provide intense and controllable heating of a propellant gas stream, before it is expanded into vacuum through a sub-millimeter nozzle. This paper reports experimental results for an MPT operated with inert gas (He and Ar) propellants. Characteristic dimensions of the discharge and the nozzle are about 300 μm . We report electrical characteristics of the MPT under different geometric and operating conditions. We have also performed optical imaging and emission spectroscopy of the MPT plume expanding into a vacuum. Results indicate that a stable microdischarge can be established in the MPT configuration, with bulk gas flow, at breakdown voltages as low as 150 V for upstream reservoir (stagnation) pressures ranging from 100 to 500 Torr. Optical images show a well collimated luminous plume that extends a few centimeters from the nozzle exit plane. Emission spectroscopy was used to make line-integrated relative intensity measurements of several transitions in helium between 380 and 590nm immediately downstream of the nozzle exit plane in the plume. Boltzmann plots based on emission intensity suggest electronic excitation temperatures of $\sim 0.3 \text{ eV}$.

*Graduate Student

†Associate Professor

‡Professor

14:45

LW1 5 ECR Discharge Ion Engines and Their Space Experiences HITOSHI KUNINAKA, *ISAS/JAXA* TATSUYA NAKAI, *University of Tokyo* KAZUTAKA NISHIYAMA, *ISAS/JAXA* Ion engine $\mu 10$ has a long life and high reliability because of electrodeless ECR plasma generation in both the ion generator and the neutralizer using 4GHz microwave. Measurements on the electron energy distribution in the ion generator revealed the discharge mechanism to heat gradually a part of the thermal electron along magnetic track. The high-energy electrons generate ions in collision process and return to the thermal electrons. The recycling process of electrons results in the effective plasma generation in comparison with the DC discharge ion generator, in which the high-energy electrons are expendable. Four $\mu 10$, each generating a thrust of 8 mN, specific impulse of 3,200 seconds, and consuming 350 W of electric power, propel the "HAYABUSA" asteroid explorer launched on May 2003. After vacuum exposure and several runs of baking to reduce residual gas, the ion engine system established continuous acceleration. In 2005, HAYABUSA, using

solar electric propulsion, managed to successfully cover the distance between 0.86 AU and 1.7 AU in the solar system, as well as rendezvous with, land on, and lift off from the asteroid. During the 3-year flight, the ion engine system generated a delta-V of 1,400 m/s while consuming 22 kg of xenon propellant and operating for 25,900 hours.

15:00

LW1 6 Experimental and spectroscopic study of flow actuation phenomena using DC discharge at a Mach 3 flow. J. SHIN, V. NARAYANASWAMY, L. RAJA, N. CLEMENS A study of flow actuation phenomena of DC discharge will be presented. An array of pin-like electrodes is flush mounted on a co-planar ceramic actuator that is inserted in the test section. The different discharge structures – diffuse, constricted, and mixed mode – are observed in the presence of a flow. A discernable actuation, as visualized by schlieren imaging, is achieved by diffuse discharge, whereas the constricted discharge does not show detectable flow perturbation at the same current. The flow actuation in the form of an induced oblique shock occurs within one frame of laser schlieren imaging at 4.5 kHz. Rotational (gas) and vibrational temperatures are measured by fitting spectra of N₂ and N₂⁺ bands near 365-395 nm. Electronic temperatures are measured using Boltzmann plot of Fe (I) lines. Gas temperatures of diffuse discharges drop from $\sim 1500 \text{ K}$ to $\sim 500 \text{ K}$ in the presence of a flow while vibrational and electronic temperatures remain almost the same at $\sim 3000 \text{ K}$ and $\sim 1.25 \text{ eV}$, respectively. Gas temperatures of constricted discharge are found to be similar with diffuse discharge whereas only diffuse discharge shows an actuation. An examination of spatial extent of the plasma reveals that the diffuse discharge occupies a larger region of the flow than the constricted discharge. This indicates that the flow actuation is dependent on flow dilatation which is governed by temperature rise as well as the spatial extent over which the temperature rise is observed.

15:15

LW1 7 Electron-Beam Produced Air Plasma: Optical Measurement of Beam Current* ROBERT VIDMAR, *University of Nevada, Reno* KENNETH STALDER, *Stalder Technologies and Research* MEGAN SEELEY, *University of Nevada, Reno* Experiments to quantify the electron beam current and distribution of beam current in air plasma are discussed. The air plasma is produced by a 100-keV 10-mA electron beam source that traverses a transmission window into a chamber with air as a target gas. Air pressure is between 1 mTorr and 760 Torr. Strong optical emissions due to electron impact ionization are observed for the N₂ 2nd positive line at 337.1 nm and the N₂⁺ 1st negative line at 391.4 nm. Calibration of optical emissions using signals from the isolated transmission window and a Faraday plate are discussed. The calibrated optical system is then used to quantify the electron distribution in the air plasma.

*This work is supported by the Air Force Research Laboratory, under grant numbers FA9550-04-1-0015 and FA9550-04-1-0444; and State of Nevada matching funds.

SESSION LW2: ELECTRON IMPACT IONIZATION AND EXCITATION II

Wednesday afternoon, 11 October 2006; Salon B Holiday Inn at 13:30; Klaus Bartschat, Drake University, presiding

*Invited Papers***13:30****LW2 1 Kinematically Complete Experiments on Single Ionization in Simple Atomic Systems.***MICHAEL SCHULZ, *University of Missouri-Rolla*

Fully differential studies on atomic reaction dynamics are crucially important to advance our understanding of the few-body problem. In the case of electron impact, fully differential cross sections for single ionization have been measured for several decades. The vast majority of these studies were restricted to electrons ejected into specific planes. More importantly, for ion impact such experiments are much more challenging and fully differential cross sections (FDCS) became only available a few years ago. However, at the same time these measurements for ion impact also yielded the first complete three-dimensional images of the FDCS. The sobering conclusion of these studies was that our understanding of ionization processes in atomic collisions is much less complete than assumed previously. In this talk new unexpected results on three-dimensional FDCS will be presented for kinematic regimes for which so far no experimental FDCS have been obtained yet. These include collisions involving highly relativistic and highly charged ions as well as relatively slow p projectiles. In collaboration with Ahmad Hasan, Natasha Maydanyuk, Matt Foster, Brian Tooke and Don Madison, University of Missouri-Rolla.

*Supported by NSF.

14:00**LW2 2 Multiparameter Ionization and Excitation Measurements.***JULIAN LOWER, *Centre for Antimatter-Matter Studies, RSPHYSSE, Australian National University, Canberra ACT 0200*

Over recent years there has been a sustained and impressive development of technologies to aid the measurement of atomic and molecular collision processes. In particular, the application of multi-parameter coincidence techniques to atomic and molecular fragmentation processes has uncovered interesting new phenomena e.g. [1,2]. The underlying idea is to map measured arrival coordinate of particles (spatial and temporal) on to parameters of physical relevance through the action of time independent or dependent electric and/or magnetic fields [3,4]. The main challenge is in fashioning such fields to obtain greatest sensitivity for the parameters of greatest interest. In my talk I will review recent spectrometer developments discuss the potential for further improvements. The power of modern measurement techniques will be illustrated by selected examples of recent measurements by our group and others. Strengths and weaknesses of various experimental approaches will be discussed. In collaboration with: S. Bellm, AMPL, RSPHYSSE, Australian National University; D.H. Madison, Z. Stegen, University of Missouri - Rolla; K. Bartschat, Drake University; Colm T. Whelan, Old Dominion University. [1] T. Weber et al., *Nature* **431**, 437 (2004). [2] M. Schulz et al., *Nature* **422**, 48 (2003). [3] J. Ullrich et al, *Rep. Prog. Phys.* **66**, 1463 (2003). [4] C. Miron et al, *Rev. Sci. Instrum.* **68**, 3729 (1997).

*I gratefully acknowledge the assistance of the Australian Research Council under Grant No. DP0452553.

*Contributed Papers***14:15****LW2 3 Charge Dependent Effects in Double-Photo-Ionization of Helium-Like Ions** MATT FOSTER, JAMES COLGAN, *Theoretical Division, T-4 Los Alamos National Laboratory*

A study is made of triple differential cross sections (TDCS) for double-photo-ionization (DPI) of helium-like ions. The angular distribution between the equal energy outgoing electrons is examined as a function of the nuclear target charge. Time-dependent close-coupling theory (TDCC) will be used to solve the time-dependent Schrödinger equation for both outgoing electrons. The TDCC method treats the correlation between the electrons without approximation. Previous theoretical models that have calculated the TDCS for helium-like ions have only included the electron-

electron interaction through approximate perturbative methods. We will analyze the effects of the electron correlation and its dependence relative to the nuclear charge. We will compare our calculations with previous experimental and theoretical work, where available.

14:30**LW2 4 Coincidence studies of electron impact ionization over the full in-plane angular range.*** BIRGIT LOHMANN, MARK STEVENSON, ANTHONY KEEHN, *Centre for Antimatter-Matter Studies, Griffith University*

Electron impact ionization is a fundamental collision process which plays a significant role in plasma physics, discharge physics and radiobiology. For example, modelling the interaction of electrons with matter in biological systems requires reliable data on electron impact ionization cross sections. Detailed information on the energy and angular distributions of the emitted electrons produced in electron impact ionization processes is obtained from coincidence measurements of the outgoing species [1]. However, experiments using conventional

electron coincidence spectrometers usually are unable to measure the full angular distribution of ejected electrons, due to mechanical constraints. We present fully differential cross sections for electron impact ionization of argon which have been obtained using a magnetic-angle-changer [2] in a conventional coincidence spectrometer, which has enabled us to measure the full 360 degree ejected electron distribution in the scattering plane. [1] D. S. Milne-Brownlie, S. J. Cavanagh, Birgit Lohmann, C. Champion, P.-A. Hervieux and J. Hanssen, *Phys. Rev. A*, **69** (2004) 032701. [2] F. H. Read and J. M. Channing, *Rev. Sci. Instrum.* **67** (1996) 2372

*Financial support from the Australian Research Council for the ARC Centre of Excellence for Antimatter-Matter Studies is gratefully acknowledged.

14:45

LW2 5 Ionization dynamics for electron impact ionization of H₂O* JUNFANG GAO, DON MADISON, *Department of Physics, University of Missouri-Rolla, MO 65409 USA* MARTYN HUSSEY, ANDREW MURRAY, *Schuster Laboratory, School of Physics and Astronomy, The University of Manchester, Manchester M13 9PL, UK* DEPARTMENT OF PHYSICS, UNIVERSITY OF MISSOURI-ROLLA COLLABORATION, SCHUSTER LABORATORY, SCHOOL OF PHYSICS AND ASTRONOMY, THE UNIVERSITY OF MANCHESTER COLLABORATION Water is arguably the most important substance in the universe. Recently (e, 2e) spectroscopy has been used to study low to intermediate incident energy (e.g. below 107.6eV) fully differential cross sections for electron impact ionization of water. These low energy results are very sensitive to the collision dynamics, so accurate theories are in the needed to interpret the experimental data. The distorted wave impulse approximation (DWIA) and molecular three-body distorted wave (M3DW) approximation were recently introduced by our group. These approximations will be used to study the fully differential cross sections for low energy electron-impact ionization of H₂O molecules. The importance of the polarization potential will be examined. Our theoretical results will be compared with recent experimental measurements.

*The support of the NSF under Grant Number PHY-0456528 is gratefully acknowledged. The EPSRC is also acknowledged for providing support for the experimental program.

15:00

LW2 6 Near-Threshold Electron Impact Excitation of the Electronic states of N₂ D.S. NEWMAN, M. LANGE, J. MATSUMOTO, J.C. LOWER, S.J. BUCKMAN, *CAMS, Australian National University* Using a new position-sensitive, time-of-flight technique we have measured differential scattering cross sections for a number of electronically excited levels of N₂ at energies between 8.5 and 15 eV. This technique has the advantage of providing a uniform transmission for the scattered particles as a function of energy, and thus removes substantial uncertainty from the inelastic cross sections that are derived through a comparison with the elastic scattering intensity. The present results are compared with a number of recent measurements.

SESSION MW1: DIAGNOSTICS II: OPTICAL

Wednesday afternoon, 11 October 2006

Salon CD Holiday Inn at 16:00

Ed Barnat, Sandia National Laboratories, presiding

Contributed Papers

16:00

MW1 1 Gaussian expansion and annular analysis of ultracold Sr plasma SAMPAD LAHA, CLAYTON SIMIEN, PRIYA GUPTA, THOMAS KILLIAN, *Rice University* Expansion of plasma in vacuum is an important problem in astrophysics and when intense lasers ablate solid targets. In an ultracold neutral plasma, the details of a self-similar expansion of Gaussian density distribution can be seen by absorption images. The image of the plasma is divided into concentric annuli, which gives us the ability to probe the plasma properties spatially. This gives direct verification of the fact that the density maintains its Doppler profile over time. Thus, we can use existing theories of a self-similar gaussian expansion to calculate the initial electron temperature (T_e), which plays a critical role in the evolution of the plasma. For example, calculating T_e will tell us how many ions are we losing due to three-body recombination (TBR). The annular analysis of the plasma also allows us to probe other phenomena such as the dependence of ion temperature with position (which gives us the correlation energy) and ion density singularities at some points (shock waves).

16:15

MW1 2 Electric Field Measurement by Fluorescence-Dip Spectroscopy in Krypton* TOBIAS KAMPSCHULTE, DIRK LUGGENHOELSCHER, JULIAN SCHULZE, UWE CZARNETZKI, *Institute for Plasma and Atomic Physics, CPST, Ruhr-University Bochum, Germany* MARC BOWDEN, *Dept. of Physics and Astronomy, The Open University, Milton Keynes, UK* The electric field in the boundary sheath of discharges is a key parameter for understanding the structure and dynamics of both electrons and ions. Knowledge of the field allows the determination of e.g. voltages, charge densities and currents. Electric fields can be measured directly by Fluorescence-Dip Spectroscopy (FDS). This technique is a combination of two-photon laser induced fluorescence and absorption spectroscopy using the Stark effect of Rydberg-states. It is non-invasive and provides high field sensitivity combined with excellent temporal and spatial resolution. Here the technique is applied for the first time to krypton as a probe gas. Rydberg-states up to $n = 50$ can be excited. Calibration measurements with known electric fields are performed and fields as low as 50 V/cm can be measured. In addition, the Stark-splitting has been calculated ab initio. Experimental and theoretical results agree very well. First measurements in the sheath of a capacitively coupled discharge in pure krypton are presented.

*Funding by: SFB 591

16:30

MW1 3 A Laser-based Measurement System for Atmospheric Pressure Plasmas MARK BOWDEN, *Open University, UK* RONAN FAULKNER, MIKE HOPKINS, *Dublin City University, Ireland* Plasmas operated at atmospheric pressure are the subject of an increasing amount of basic and application-based research. Due to the small size of the discharge regions, in-situ measurement of plasma properties is difficult, and research often is based

on simulation studies or on relatively simple measurements such as emission spectroscopy. Laser-based methods have the potential to provide time- and space-resolved measurement of plasma properties but until now have rarely been applied. To increase the ease of laser-based measurements in atmospheric conditions, we have developed an instrument that significantly enhances the amount of signal that is detected during a laser scattering or a laser fluorescence measurement. An external cavity is used with the measurement laser so that the measurement volume is repeatedly probed with the same laser beam. In this paper, the instrument will be described together with data from test measurements.

16:45

MW1 4 Gas temperature and the degree of dissociation for different operating regimes of a nitrogen helicon plasma source COSTEL BILOIU, EARL SCIME, XUAN SUN, IOANA A. BILOIU, ROBERT HARDIN, ZANE HARVEY, *West Virginia University, Physics Department, Morgantown, WV 26506-6315* We report on the gas temperature and the degree of dissociation in E, H, and W operating regimes of nitrogen helicon plasma. The gas temperature was inferred from the fit of synthetically generated spectra to the recorded emission spectra of the 2-0, 1-0, and 0-0 bands of the first positive system of nitrogen. The dissociation degree was inferred from the relative population ratios of atomic to molecular nitrogen states determined experimentally from integrated emission intensities of atomic triplet lines ($3s^4P - 3p^4S^0$ at 742.36 nm, 744.23 nm, 746.83 nm) and the molecular band ($B^3\Pi_g, v'=4 \rightarrow A^3\Sigma_u^+, v''=2$ at 750.39 nm). The computation took into account available published values of the transition probabilities and electron impact excitation rate coefficients. Electron energy distribution functions were obtained experimentally from the second derivative of Langmuir probe I-V characteristics. It was found that both the gas temperature and the dissociation degree increase as the discharge transitions from capacitively coupled (E) to inductively coupled (H) and then to helicon mode (W) operational regimes.

17:00

MW1 5 Estimation of N atom density in a nitrogen radical source for GaN growth by optical emission spectroscopy-comparison with appearance mass spectrometry K. SASAKI, J. OSAKA, H. KANAI, T. ISHIJIMA, H. TOYODA, H. SUGAI, *Nagoya University, Japan* N. SADEGHI, *Université Joseph Fourier de Grenoble, France* We adopted optical emission spectroscopy (OES) for estimating N atom density in a nitrogen radical source, which was used for the growth of GaN film by molecular beam epitaxy. In addition, we compared the N atom density evaluated by OES with that evaluated by appearance mass spectrometry (AMS). We measured the intensities of optical emissions from N (747 nm) and N₂ (337 nm, the 2nd positive band) using a monochromator combined with an ICCD camera. The ratio of the N to N₂ densities ($[N]/[N_2]$) was obtained from the emission intensity ratio, by considering the rate coefficients for electron impact excitations. The absolute N atom density was estimated from the density ratio with the help of a thermodynamic equation of state $p = ([N] + [N_2])k_B T_g$, where the pressure p was measured using a capacitance manometer and the gas temperature T_g was evaluated from the rotational temperature of N₂ 2nd positive band. We found an excellent agreement between the N atom densities evaluated by OES and AMS, when we assumed an electron tem-

perature of 10 eV and an N₂ vibrational temperature of 5000 K. This work was supported by 21st Century COE (Center of Excellence) Program "Information Nano-Devices Based on Advanced Plasma Science" of Nagoya University.

17:15

MW1 6 Characteristics of in-situ chamber cleaning for DPS+ metal etcher by using optical emission spectroscopy YONGH-WAN RYU, WOJIN CHO, YONGWOO LEE, MINCHUL CHAE, SUNGUN KWON, JAESEUNG HWANG, *Samsung Electronics SAMSUNG ELECTRONICS PROCESS DEVELOPMENT TEAM** Plasma enhanced in-situ chamber cleaning (ICC) is generally used for plasma processes such as plasma etching system and plasma enhanced chemical vapor deposition (PECVD) system. It is generally believed that ICC makes a chamber condition to be constant and be able to extend wet cleaning period. We have studied ICC characteristics for DPS+ metal etcher by using the optical emission spectroscopy (OES) as a function of the source power, the chamber pressure and the composition and total flow rate of the gases used. We observe that the higher source power and the lower pressure are more efficient for the ICC and also investigate the effects of the additional gases. We have applied our ICC condition to the patterned wafers and concluded that the chamber condition is maintained in a stable way. However, ICC treatment to the chamber result in some process changes such as the profile of the metal line and the oxide recess and the etch selectivity of the metal line to the oxide hard mask.

*Process Development Team, Samsung Electronics, San#24 Nongseo-Dong, Giheung-Gu, Yongin city, Gyeonggi-Do, Korea, 449-711.

SESSION MW2: THERMAL PLASMAS, ARCS, AND BREAKDOWN

Wednesday afternoon, 11 October 2006

Salon B Holiday Inn at 16:00

Sergey O. Macheret, Lockheed Martin, presiding

Contributed Papers

16:00

MW2 1 Three - dimensional mapping of electron temperature and electron density in an arc - anode boundary layer GUANG YANG, JOACHIM HEBERLEIN, *University of Minnesota* A DC transferred argon arc system, which allows control of the anode boundary layer by introducing cold cross flow, has been setup in our lab to recreate the situation in the anode region of a typical plasma spray torch. In this study, a laser Thomson scattering system, which can probe a location as close as 50 micron from the anode surface, has been developed and has been used to obtain electron temperature and electron density maps at different planes in the anode boundary layer. The effects of different operating conditions with different cross flow gases (argon and nitrogen) are presented. Our results have shown that increasing argon cross flow rate changes the arc attachment from a diffuse mode to a transition mode with multiple unsteady attachment spots and then to a constricted mode. The electron temperature in the attachment increases from 9000K to 13000K and the electron density increases from $5 \times 10^{21} \text{m}^{-3}$ to $1 \times 10^{22} \text{m}^{-3}$ as the arc attachment changes from

a diffuse mode to a constricted mode. In a constricted mode, an extended non-equilibrium region with low electron density ($< 10^{21} \text{m}^{-3}$) and relatively high electron temperature ($\sim 5000\text{K}$) is also formed. With nitrogen, the arc is constricted already at low cross flow rates. The three dimensional results allow the qualitative determination of the current and heat flux distribution in the anode boundary layer.

16:15

MW2 2 3D Finite Element Modeling of Arc and Jet Dynamics in a DC Plasma Torch JUAN TRELLES, EMIL PFENDER, JOACHIM HEBERLEIN, *University of Minnesota* The unstable behavior of the plasma jet in direct current plasma torches has been well documented experimentally, but the nature of the instabilities is not well understood. This is in part due to our lack of understanding of the forcing effect on the plasma jet caused by the arc dynamics, mainly because the confinement of the arc inside the torch limits its direct observation. In this research, the dynamics of the electric arc and the plasma jet in a plasma torch are modeled using a 3D, time-dependent, LTE model. The fluid and electromagnetic equations are solved in a fully coupled manner by a variational multiscale finite element method, which implicitly accounts for the multiscale nature of the flow. Simulations of a commercial torch operating with Ar-He under typical operating conditions used for plasma spraying are presented. The simulation results reveal the highly unsteady and quasi-periodic behavior of the arc as well as the undulating nature of the plasma jet. Furthermore, our simulations indicate a clear correlation between the arc and jet dynamics, furthering our understanding of the interactions between thermal plasmas and cold gases, as typically found in plasma processing systems.

16:30

MW2 3 Numerical investigation of stability of current transfer to thermionic cathodes* MARIA JOSE FARIA, MIKHAIL BENILOV, *Departamento de Fisica, Universidade da Madeira, Largo do Municipio, 9000 Funchal, Portugal* Considerable advances have been achieved in recent years in theory and modelling of current transfer from high-pressure arc plasmas to thermionic cathodes. Solutions describing the diffuse mode and different spot modes have been obtained and analyzed. However, this information is not yet sufficient for engineering practice: one needs to know also which of the modes are stable in some or other particular conditions. Unfortunately, a self-consistent stability theory is absent; hypotheses and speculations available in the literature are insufficient to explain experimental findings. In this work, stability of various modes of current transfer to thermionic cathodes of high-pressure arcs is studied numerically. The model of nonlinear surface heating is used. Particular attention is paid to the case where the arc is powered by a current source. It is found that the diffuse mode is stable at currents exceeding that corresponding to the first bifurcation point and is unstable at lower currents. The first spot mode is unstable between the bifurcation point and the turning point and is stable beyond the turning point. The second and subsequent spot modes are always unstable.

*Work performed within activities of the project POCI/FIS/60526/2004.

16:45

MW2 4 Advanced Modeling of Thermal Plasmas for Industrial Applications VITTORIO COLOMBO, EMANUELE GHE-DINI, *C.I.R.A.M. and D.I.E.M., University of Bologna* Modeling results are presented for different industrial thermal plasma sources using a customized version of the commercial code FLU-ENT capable of 2D and 3D transient simulation with advanced CFD models that take into account turbulence effects using different approaches (Reynolds Stress Model and Large Eddy Simulation), transport of species and radiation (Discrete Ordinate Model with interaction between radiation and solid surfaces). Simulations results are presented in order to show the capabilities of this modeling tool, which is very useful for the design of a wide range of atmospheric pressure thermal plasmas devices and related assisted processes, such as: ICPTs with injection of powders for spheroidization, DC twin-torch transferred arc plasma systems for waste treatment, DC non-transferred arc torch for plasma spraying and DC transferred arc torch for high quality plasma cutting.

17:00

MW2 5 Electric field measurements in moving ionization fronts during plasma breakdown ERIK WAGENAARS, GERIT KROESEN, *Eindhoven University of Technology, The Netherlands* MARK BOWDEN, *The Open University, United Kingdom* We have performed time-resolved, direct measurements of electric field strengths in moving ionization fronts during the breakdown phase of a pulsed plasma. Plasma breakdown, or plasma ignition, is a highly transient process marking the transition from a gas to a plasma. Some aspects of plasma breakdown are reasonably well understood, but many details remain unknown, mainly because of a lack of direct measurements of plasma properties. Most of the important processes in breakdown, such as electron multiplication in avalanches and propagation of ionization fronts, are controlled by the electric field distribution in the discharge region. We have developed an experimental laser technique capable of measuring spatially and temporally resolved electric field distributions in both plasma and neutral gas. The technique is based on detecting the Stark shift and mixing of high-lying Rydberg levels of xenon atoms, using a 2+1 photon excitation scheme with fluorescence-dip detection. With this experimental arrangement, we measured absolute, time-resolved electric field strengths during the breakdown phase of a low-pressure plasma between parabolic electrodes. Characteristic features of breakdown, such as a moving ionization front with electric field enhancement and the formation of a plasma sheath, were observed.

17:15

MW2 6 Steady-State Model for Laser-Guided Lightning-Like Discharges* M. LAMPE, R. FERNSLER, S. SLINKER, D. GORDON, P. SPRANGLE, *Plasma Physics Division, Naval Research Laboratory* We have developed a reduced model for laser-guided discharges, which can be solved efficiently over the complete length and duration of the discharge, and also provides analytic insights. We assume the laser pre-pulse designates a long thin channel with given low conductivity, and that current flows entirely in this channel. Maxwell's equations can be reduced to a diffusion equation for $E_z(z,t)$, with a diffusion coefficient $D(z,t)$ proportional to the channel conductance, very small ahead of the discharge and rapidly increasing at the discharge head. By specifying that the discharge propagates at a constant speed u , the diffusion equation is further reduced to a first-order O.D.E. in $\tau \equiv t-z/u$, which must be solved self-consistently with rate equa-

tions that determine $D(\tau)$. The required driving voltage pulse $V(\tau)$ is an output of the calculation. Even in absence of deionization processes, we show the discharge propagates only if T_e is large enough throughout the channel to drive continuing ionization. If the channel is narrow enough, this can occur at sustainable levels of E_z due to saturation of the N_2 vibrational energy sink.

*Supported by NAVSEA.

17:30

MW2 7 Simulation of the Plasma Dynamics at the Ionization Front of High Pressure Discharges Using Monte Carlo Methods on an Adaptive Mesh* ANANTH N. BHOJ, *University of Illinois* MARK J. KUSHNER, *Iowa State University* During breakdown of high pressure discharges, such as coronas, a thin ionization front propagates across the gap. The ionization front has steep spatial gradients in the electric field and electron temperature which produce commensurate gradients in excitation rates. In spite of operating at high pressures where the electrons are highly collisional, these gradients may be severe enough that electron transport is non-local. To address these conditions, a new computational technique was developed that captures the non-local nature of the electron energy distribution (EED) at the ionization front. The basic computational platform is a 2-dimensional plasma hydrodynamics model based on unstructured meshes that addresses electrostatics and multi-fluid charged particle transport. The EED at the ionization front is captured using an electron Monte Carlo Simulation executed on an adaptive, rectilinear mesh. The location of the adaptive mesh is determined by sensors that select regions where non-local transport might occur. From the EEDs computed

in the non-local regions, electron transport coefficients and sources are obtained and transferred to the fluid modules. Results will be discussed for positive and negative corona discharges in air and the non-local character of the ionization front will be described.

*Work was supported by the National Science Foundation.

17:45

MW2 8 Measuring the electrical breakdown of air for very small electrode separations EMMANOUEL HOURDAKIS, GARNETT W. BRYANT, NEIL M. ZIMMERMAN, *National Institute of Standards and Technology* Understanding the basic principles of electrical breakdown in air for small electrode separations is becoming very important in the design and operation of microscale devices such as MEMS sensors and actuators. This work presents a new method [1] for measuring the value of breakdown voltage in air for electrode separations from 400 nm to 45 μm . The method consists of bringing 2 evaporated Au electrodes on sapphire together in a parallel plate geometry. Amongst the improvements of our method are the measurement of plate separation and the very small surface roughness (average of 6 nm). We demonstrate the ability to deduce the value of the separation of the plates by the value of the capacitance. We analyze the data for small separations, using the theory of standard field emission and field amplification on the surface of a conductor. We come to a prediction about the geometry and size of the electrode surface protrusions that would produce the observed emission. For the first time, we look for these predicted protrusions using an AFM. We find several reasons why the standard theory does not appear to explain our data. [1] *Rev. Sci. Instrum.* **77**, 034702 (2006).

SESSION PR1: PLASMA APPLICATIONS FOR NANOTECHNOLOGY

Thursday morning, 12 October 2006; Salon CD Holiday Inn at 8:00; Toshiake Makabe, Keio University, presiding

Invited Papers**8:00****PR1 1 Ultimate Top-down Etching Processes Using Advanced Neutral Beam for Future Nano-scale Devices.**SEIJI SAMUKAWA, *Tohoku University*

For the past 30 years, plasma etching technology has led efforts to shrink the pattern size of ultra-large-scale integrated (ULSI) devices. However, inherent problems in the plasma processes, such as charge build-up and UV photon radiation, limit the etching performance for nanoscale devices. To overcome these problems and fabricate sub-10-nm devices in practice, neutral beam etching has been proposed. In this invited talk, I introduce the ultimate etching processes in the neutral beam sources and discuss the fusion of top-down and bottom-up processing for future nanoscale devices. Neutral beams can perform atomically damage-free etching and surface modification of inorganic and organic materials. This technique is a promising candidate for a practical fabrication technology for future nano-devices.

Contributed Papers**8:30****PR1 2 Deposition of vertically oriented single-walled carbon nanotubes in highly collisional atmospheric pressure plasma**

KUMA OHNISHI, *Dept of Mechanical and Control Engineering, Tokyo Institute of Technology* TOMOHIRO NOZAKI, KEN OKAZAKI, JOACHIM HEBERLEIN, *Dept of Mechanical Engineering, The University of Minnesota* UWE KORTSHAGEN We succeeded synthesis of vertically aligned single-walled carbon nanotubes (SWNTs) in atmospheric pressure radio frequency discharge (APRFD). This is because ion bombardment to the substrate, which causes cohesion or diffusion of catalyst nanoparticles as well as growing SWNTs, can be minimized in highly collisional plasma sheath at atmospheric pressure. In this process (Carbon source; CH₄, Wafer temperature; 700°C), it is essential for growth of SWNTs to supply radicals produced by plasma. Higher power supply causes higher growth rate. However, maximum power input was limited to 80 W because of the stability of the plasma. The higher substrate temperature up to 700°C means better yield (G band / D band) of SWNTs, and causes faster growth rate. The catalyst particles maintained their activities at least 20 minutes and the initial growth rate of SWNTs was about 4.0 μ/min at the condition of 60 W. The catalysts lost their activities, not because of the damage caused by plasma but because of the thermal sintering which was caused by high temperature like 700°C.

8:45**PR1 3 Measurement of plasma density and electron energy distribution function in a filamented capacitively coupled silane-argon plasma***

AMEYA BAPAT, UWE KORTSHAGEN, *University of Minnesota* A capacitively coupled, filamented argon-silane plasma is studied. This discharge has been shown to produce highly monodisperse, faceted, cube shaped silicon nanocrystals which were previously successfully used in novel single nanoparticle vertical Schottky barrier transistors. The striated filament has a diameter of about 3 mm and rotates erratically in the 5 cm inner diameter discharge tube at a frequency of about 150 Hz. The plasma is run at a pressure of ~ 2 Torr in 5% silane diluted in helium and argon. RF power up to 200 W is applied at 13.56 MHz. A capacitive probe (Braithwaite et al., *Plasma Sources Sci. Technol.*, vol. 5, 677 (1996)) is used to measure the ion density within the filament and the background plasma. Emission and absorption

spectroscopy combined with a model based on a Boltzmann solver and a collisional-radiative model for argon-silane are used to determine the electron energy distribution function. We expect that a better understanding of the plasma process will help to understand the formation of silicon nanocrystals with the unique cubic shape.

*This work is supported by NSF grant CTS-0500332.

9:00**PR1 4 Application of microplasma to synthesis of silicon nanoparticles**

KENJI SASAKI, *Dept. of Mechanical and Control Engineering, Tokyo Institute of Technology* TOMOHISA OGINO, DAISUKE ASAHI, TOMOHIRO NOZAKI, KEN OKAZAKI We developed microplasma to synthesize nanocrystalline silicon particles (nc-Si). Gas residence time in micro plasma reactor is of the order of μs, while time required for particle nucleation by three-body collision? is about ms. Thus it is possible to separate crystal nucleation and growth in a single reactor. This process is very important for synthesis nc-Si. Microplasma was formed in a capillary tube of diameter 470 μm which is connected to the VHF power source. We used Ar/SiCl₄ mixtures for nc-Si source for safety. H₂ was added to convert exhausted Cl to HCl. Electron density of micro plasma (N_e) was estimated by Stark broadening of H_β, and found that N_e is 1-3*10¹⁵ cm⁻³. Rotation temperature was measured to be approximately 1500 K. Intensity ratio of Si(288 nm)/Ar(750 nm) increased linearly with increasing initial concentration of SiCl₄. If the residence time was 30 μs, particle nucleation seemed to start in the discharge region, and particles keep growing involving impurity elements such as N or Cl. On the other hand, when residence time was set to shorter than 10 μs, the amount of impurities can be minimized. Under this condition, Raman spectra showed crystalline silicon peak around 520 cm⁻¹. TEM image also indicated the size of synthesized nc-Si to be in the range of 4-20 nm.

9:15**PR1 5 Synthesis of highly monodisperse Ge crystals in a capacitively coupled flow through reactor for photovoltaic applications***

RYAN GRESBACK, UWE KORTSHAGEN, *University of Minnesota* Germanium nanocrystals are interesting candidates for quantum dot-based solar cells. While the band gap of bulk Ge is ~ 0.7 eV, the energy gap can be increased due to quantum confinement to ~ 2eV for Ge particles of ~ 3 nm in size. With a single material, Ge nanocrystals of sizes from 3 -15 nm

would thus allow to span the entire range of band gaps that is of interest for photovoltaic devices. Moreover, compared to many other quantum dot materials that are currently studied for photovoltaic applications, Ge is perceived as non-toxic and environmentally benign. Ge nanocrystals are synthesized in a tubular, capacitively coupled flow through reactor. Germanium tetrachloride is used as a precursor. It is introduced into the plasma by a flow of argon and hydrogen. At typical pressures of 2 Torr and 40 W of RF power at 13.56 MHz, Ge crystals are generated and reside in the plasma for several tens of milliseconds. The size of the nanocrystals can be controlled in a range from 3-20 nm through the residence time. Particles are highly monodisperse. Organically passivated Ge nanocrystals self-assemble into monolayers when cast from colloidal solutions.

*This work is supported by NSF under MRSEC grant DMR-0212302, and by the Initiative of Energy and the Environment under grant IREE LG-C5-2005.

SESSION PR2: COMPUTATIONAL METHODS AND MODELING FOR PLASMAS

Thursday morning, 12 October 2006

Salon B Holiday Inn at 8:00

Jong Won Shon, Jusang Engineering, presiding

Contributed Papers

8:00

PR2 1 Revisiting the anomalous skin layer IGOR KAGANOVICH, *Princeton Plasma Physics Laboratory* Radio frequency waves do not penetrate into a plasma and are damped within it. The electric field of the wave and plasma current are concentrated near the plasma boundary in a skin layer. Electrons can transport the plasma current away from the skin layer due to their thermal motion. As a result, the width of the skin layer increases when electron thermal velocity is taken into account. This phenomenon is called the anomalous skin effect. The anomalous penetration of the rf electromagnetic field occurs not only for the electric field parallel to the plasma boundary (inductively coupled plasmas) but also for the electric field normal to the plasma boundary (capacitively coupled plasmas) [1]. Recent advances in the nonlinear, nonlocal theory of the anomalous skin layer are reported. It is shown that separating the electric field profile into exponential and non-exponential parts yields an efficient qualitative and quantitative description of the anomalous rf field penetration in inductively coupled plasmas. [1] I. D. Kaganovich, O. V. Polomarov, and C. E. Theodosiou, "Revisiting the anomalous rf field penetration into a warm plasma," to be published in *IEEE Trans. Plasma Sci.* (2006).

8:15

PR2 2 Neutral gas depletion through high electron pressures in dense plasmas* DEBORAH O'CONNELL, TIMO GANS, DRAGOS CRINTEA, UWE CZARNETZKI, *Institute for Plasma and Atomic Physics, CPST, Ruhr-University Bochum, Germany* NADER SADEGHI, *Laboratoire de Spectrometrie Physique, University Joseph Fourier and CNRS, Grenoble, France* An inductively coupled radio-frequency (rf) magnetic neutral loop discharge (NLD) allows plasma operation at extremely low pressures,

down to 10^{-2} Pa. In this pressure regime ohmic heating is inefficient and collisionless heating mechanisms become dominant. Temporal signatures in the electron energy distribution function (EEDF) are investigated using phase resolved optical emission spectroscopy (PROES) and Thomson scattering. As expected from global model predictions, both the degree of ionisation and the 'electron pressure' strongly increase with decreasing pressure. An interesting feature arises where the electron pressure can exceed the neutral gas pressure resulting in localised depletion of the neutral gas, in particular in the plasma production region around the neutral loop (NL). This depletion of neutral particles is investigated using spatially resolved LIF measurements on argon metastables and TALIF experiments on ground state krypton atoms. Diode laser absorption spectroscopy on metastable argon atoms is used to measure metastable densities and gas temperatures. The ratio of the metastables densities and ground state densities has been found to reflect the electron temperature.

*Funding: DFG (SFB 591 & GK 1051)

8:30

PR2 3 A benchmark study of the global model approximation D.D. MONAHAN, M.M. TURNER, *Dublin City University* Global, or volume-averaged, plasma chemistry models have been widely used in low temperature plasma physics. The assumptions and simplifications typically associated with these models severely limits the parameter domain over which they may be applied. Well defined boundaries to these domains, however, do not appear to have been established. Often only minimal model validation is offered in the literature. The aim of this project is to critically evaluate the performance of an elementary global model over a range of parameters and gas compositions by comparing such a model to a set of benchmark particle-in-cell simulations in Ar/O₂ mixtures. These simulations cover a wide range of conditions in terms of collisionality, electronegativity, and negative ion destruction mechanism. It is found, as expected, that the most significant limitation of the model appears to be the oft-used assumption of a Maxwellian electron energy distribution. Adopting the modifications proposed in [1] is shown to be a significant improvement upon this assumption. It is also found that acceptable model-simulation agreement can be obtained without accounting for the complex spatial structures observed in these discharges. [1] Gudmundsson, J. T., *On the effect of the electron energy distribution on the plasma parameters of an argon discharge: a global (volume-averaged) model study*, *Plas. Sourc. Sci. Technol.*, **10** (2001), 76-81.

8:45

PR2 4 Simulation of Plasma Spectra Using PrismSPECT NICOLAS PEREYRA, JOSEPH MACFARLANE, PAMELA WOODRUFF, IGOR GOLOVKIN, PING WANG, *Prism Computational Sciences, Inc.* PrismSPECT is a collisional-radiative spectral analysis code designed to simulate the atomic and radiative properties of LTE and non-LTE plasmas spanning a wide range of conditions. For a grid of user-specified plasma conditions, PrismSPECT computes spectral properties (emission and absorption), ionization fractions, atomic level populations, atomic transition rates, and line intensities and ratios. In designing PrismSPECT, a strong emphasis has been placed on ease of use for setting up problems, monitoring the progress of simulations, and viewing results. The collisional-radiative modeling in PrismSPECT includes: collisional ionization, recombination, excitation, deexcitation, photoionization, stimulated recombination, photoexcitation,

stimulated emission, spontaneous decay, radiative recombination, dielectronic recombination, autoionization, and electron capture. Line profiles include Doppler, natural (incl. autoionization contributions), and Stark broadening. Energy levels, cross sections and rate coefficients are based on the ATBASE suite of codes, which incorporates NIST atomic level energies and oscillator strengths when available.

9:00

PR2 5 Cross-platform, multi-language libraries for ionization and surface interaction effects in plasmas* PETER STOLTZ, SCOTT SIDES, NATE SIZEMORE, SETH VEITZER, *Tech-X Corporation* MIGUEL FURMAN, JEAN-LUC VAY, *Lawrence Berkeley National Laboratory* We are developing a library of

numerical algorithms for modeling plasma effects such as ionization, secondary electron production, and ion-surface interaction. The goal is to make this library accessible to a large number of researchers by making it available on multiple computing platforms (Linux, Windows, Mac OS X) and available in multiple computing languages (Fortran, C, Python, Java). We discuss our use of the GNU autotools and the Babel utility to accomplish this cross-platform, multi-language interface. We then discuss application of this library within the WARP particle-in-cell code for modeling effects of ion-induced electrons in the High Current Experiment and within the VORPAL particle-in-cell code for modeling kinetic effects in hollow cathode discharges.

*Supported by Lawrence Berkeley National Laboratory and by Department of Energy Office of Fusion Energy Science SBIR grants DE-FG02-02ER83553 and DE-FG02-03ER83797.

SESSION QR1: HIGH PRESSURE DISCHARGES II

Thursday morning, 12 October 2006; Salon CD Holiday Inn at 10:00; Skip Williams, AFRL/WPAFB, presiding

Invited Papers

10:00

QR1 1 Micro Discharge Under Supercritical Conditions – Physics and Application to Materials Processing. KAZUO TERASHIMA, *University of Tokyo*

Recently, micro discharge or discharge microplasma have attracted much attention. Miniaturization of discharge or plasma allows us easy generation of discharge or discharge plasma under a high-pressure condition even up to supercritical fluid (SCF). Applying plasma to SCF processing may yield a high efficiency due to a combination of advantages of plasma and SCF. In addition, plasma generated in SCF is anticipated to contain radical and ion clusters, which may lead to novel physical/chemical phenomena and reactions, comparing to typical gas plasma. In our previous works, we succeeded in generating discharge or discharge plasma in high-pressure CO₂, H₂O, Xe up to supercritical conditions, and discovered novel phenomena, such as the drastic decrease in the breakdown voltages of 1 micrometer-gap electrodes near the critical point. Furthermore, we have applied SCF plasma to materials synthesis processings, and succeeded in fabricating carbon materials including carbon nanotubes (CNTs), under milder condition (31.1-70°C, 7.38-12 MPa) of scCO₂, as a processing media and starting raw material, with no catalyst [3], comparing to conventional thermal equilibrium processing. In this study, we generate stable low-temperature plasma using DBD (dielectric barrier discharge) in supercritical CO₂ and Xe conditions. In addition to its diagnosis by optical emission spectroscopy and Raman spectroscopy, application of it to film depositions of carbon nanomaterials and Cu will be discussed.

Contributed Papers

10:30

QR1 2 Time resolved laser absorption spectroscopy in a self-pulsed microplasma.* X. AUBERT, A. ROUSSEAU, *LPTP, Ecole Polytechnique, CNRS, Palaiseau, France* J.F. LAGRANGE, N. SADEGHI, *LSP, UJF, CNRS, Grenoble, France* It was recently shown that microplasmas of the microhollow cathode type geometry may operate in a self-pulsing regime for intermediate current (0.1-1 mA) [1]. At lower current (< 0.1 mA) the plasma is stable and located inside the hole; at higher current (> 1 mA), the plasma is also stable but expands outside the hole on the cathode backside region. The self pulsing was attributed to the breakdown of the gas, outside the micro-hole, on the cathode backside. However, the mechanisms of the plasma ignition on the cathode backside are not understood and metastable atoms may play a major role. In the present work, time resolved diode laser absorption measurements have been performed through the micro-hole in the self-pulsing regime; the plasma hole ranges is in the range of 100 μm and the gas pressure ranges from 50 to 300 Torr; the feed gas is argon and the transition studied is 772.376 nm (Paschen nota-

tion 1s5-2p7). The objective is i) to measure the time evolution of the 1s5 metastable density, ii) deduce the gas temperature and plasma density from the absorption line profile. Similar results are performed in 3 electrodes configuration [1] A. Rousseau and X. Aubert *J. Phys. D: Appl. Phys.* **39** (2006) 1619-1622.

*Work supported by the French National Research Agency (ANR).

10:45

QR1 3 Absolute Atomic Oxygen Density Measurements by Two-Photon Laser-induced Fluorescence (TALIF) in the Effluent of an Atmospheric Pressure Plasma Jet ST. REUTER, *University of Duisburg-Essen* K. NIEMI, V. SCHULZ-VON DER GATHEN, *Ruhr Uni Bochum* H.F. DOEBELE, *University of Duisburg-Essen* A 13.56 MHz RF-excited plasma jet¹ is diagnosed in this work. The jet operates at ambient conditions. It generates a homogeneous plasma in helium or argon² with admixtures (~ 1%) of molecular gases, here oxygen. The temperature of the effluent is well below 100[r]C. The jet has been set up in a planar and a concentric version; both were compared by means of

TALIF-measurements. Absolute atomic oxygen density profiles have been measured in the effluent of the plasma jet. The atomic oxygen density close to the nozzle amounts to 10^{16} cm^{-3} . Even at several centimeters from the nozzle there still is 1% of the initial oxygen density. Emission spectroscopy down to 110 nm has been carried out as a function of distance from the exit nozzle with the effluent hitting an MgF_2 window in front of the slit of a vacuum UV monochromator. These spectra exhibit strong emission lines e.g. of oxygen at 130 nm, even at a distance of several centimeters from the nozzle. This work was supported by the "Ministerium für Wissenschaft und Forschung NRW" ¹J. Y. Jeong, S. E. Babayan, V. J. Tu, J. Park, R. F. Hicks, and G. S. Selwyn, *PSST* 7, 282 (1998). ²S. Wang, V. Schulz-von der Gathen, H.F. Döbele, *Appl. Phys. Lett.* **83**, 3272 (2003).

11:00

QR1 4 Electrical and emission studies of a dielectric barrier APGD operating with flowing helium and a moving substrate*

WILLIAM GRAHAM, DAMIAN DELLA CROCE, *Physics and Astronomy, Queens University Belfast, BT7 1NN, Northern Ireland* ALAN HYNES, *Dow Corning Plasma Solutions, Midleton, Ireland* The electrical and emission characteristics of the APGD created in a Dow Corning Plasma Solutions LabLinetrade-mark system have been measured to study the behaviour of a relatively large scale APGD system with flowing gas and a moving film. The LabLinetrade-mark system creates a 340mm x 300mm electrode structure with an inter-electrode gap of 5mm. To create a discharge a sinusoidally-varying voltage of up to 16 kV p to p was applied to brine/glass electrodes at frequencies of around 20kHz. A PET film was suspended, parallel to the glass dielectrics. A Pearson probe measured the time dependence of the discharge current. The time resolved plasma emission was recorded using a gated ICCD. At operating powers of 900 W and with a helium flow rate of 20 l/min, a peak in the discharge current was observed twice per applied voltage period, typical of behaviour reported in other APGD systems. Imaging of emission both through the outer face of one glass/brine electrode and the inter-electrode gap indicated that during these current peaks a spatially uniform discharge is created between the film and electrode surface both when the film is static or moving at up to 1 m/min. The authors gratefully acknowledge the assistance of B Twomey, J Tynan and D Dowling (UC Dublin).

*Supported by EPSRC and Dow Corning Plasma Solutions.

11:15

QR1 5 Fitting of asymmetric spectral lines as diagnostics for HID-lamps* MARTIN WENDT, *Fr.-L.-Jahn Str. 19, 17489 Greifswald, Germany* SILKE PETERS, HARTMUT SCHNEIDENBACH, MANFRED KETTLITZ Fitting of optically

thick side-on spectra is a valuable alternative to the Bartels' method and the Abel inversion for the determination of partial pressures and radial temperature profiles in HID lamps. We investigate a standard 150 W type HID lamp filled with Hg and NaI during dimming from 150 to 60 W. The model includes LTE plasma chemistry, asymmetric line profiles according to Al-Saqabi and Peach [1]. Van der Waals and Stark broadening constants are determined from spectra of a pure Hg lamp. Broadening constants for the Na D lines are taken from literature. We use the spectra at several side-on positions in order to derive pressures and temperature profiles in the Hg/NaI lamp. The results from fitting show with decreasing electrical power a constriction of the radial temperature profile, a linear decrease of the total pressure and a rapid decrease of the sodium content. Temperatures and total pressures are in good agreement with the experiment. [1] Al-Saqabi B N I, Peach G (1984) *J. Phys. B: At. Mol. Phys.* **20** 1175-1191.

*This work is supported by the BMBF under FKZ 13N8604.

11:30

QR1 6 Dynamic of the plasma current amplitude in a barrier discharge: influence of a photocatalytic material O. GUAIT-ELLA, S. CELESTIN, A. ROUSSEAU, *LPTP, Ecole Polytechnique, CNRS, Palaiseau, France* A. BOURDON, *EM2C, Ecole Centrale, CNRS, Chatenay, France*

For a better understanding of the plasma/photocatalytic material interaction under plasma exposure, a study of the electrical properties of a cylindrical sinusoidal dielectric barrier discharge (DBD) is performed with and without porous material containing TiO_2 . The metallic inner electrode is in contact with the gas gap. The presence of porous material made of silica fibres coated with nanoparticles of TiO_2 leads to a strong increase of the injected energy for the same applied voltage. For the same injected energy the time evolution of the current amplitude distribution function (CADF) shows two different peak populations on the positive half period (when the metallic inner electrode is positive) [1]. Apart from numerous low intensity plasma filaments (around 1 mA amplitude), much larger ones exist (around 1 A). These large current amplitude peaks are responsible for 50 to 70% of the injected energy depending on the presence of the photocatalytic material. They are attributed to desorption of charges triggered by light emitted by a first filament. The influence of 900 ppm of C_2H_2 as well as external ultraviolet irradiation on the CADF is also reported. [1] O. Guaitella, F. Thevenet, C. Guillard, A. Rousseau, *J. Phys. D: Appl. Phys* (2006) accepted.

SESSION QR2: ELECTRON AND POSITRON COLLISIONS

Thursday morning, 12 October 2006; Salon B Holiday Inn at 10:00; Murtadha Khakoo, California State University, Fullerton, presiding

*Invited Papers***10:00****QR2 1 Electron Collisions with Large Molecules.***VINCENT MCKOY, *California Institute of Technology*

In recent years, interest in electron-molecule collisions has increasingly shifted to large molecules. Applications within the semiconductor industry, for example, require electron collision data for molecules such as perfluorocyclobutane, while almost all biological applications involve macromolecules such as DNA. A significant development in recent years has been the realization that slow electrons can directly damage DNA. This discovery has spurred studies of low-energy collisions with the constituents of DNA, including the bases, deoxyribose, the phosphate, and larger moieties assembled from them. In semiconductor applications, a key goal is development of electron cross section sets for plasma chemistry modeling, while biological studies are largely focused on understanding the role of localized resonances in inducing DNA strand breaks. Accurate calculations of low-energy electron collisions with polyatomic molecules are computationally demanding because of the low symmetry and inherent many-electron nature of the problem; moreover, the computational requirements scale rapidly with the size of the molecule. To pursue such studies, we have adapted our computational procedure, known as the Schwinger multichannel method, to run efficiently on highly parallel computers. In this talk, we will present some of our recent results for fluorocarbon etchants used in the semiconductor industry and for constituents of DNA and RNA. In collaboration with Carl Winstead, California Institute of Technology.

*Supported by Office of Basic Energy Sciences, DOE.

10:30**QR2 2 Electron Collisions with Atoms and Molecules Relevant to Industrial, Planetary and Astrophysical Plasmas.*.**PAUL JOHNSON, *Jet Propulsion Laboratory*

Collision processes involving electrons with neutral atoms and molecules are among the principal mechanisms for energy exchange in industrial and naturally occurring plasmas. In many of these plasmas, large populations of low energy, secondary electrons are generated. Such secondary electrons are very effective in many of the relevant collision processes because both the cross sections and the electron energy distributions peak at low energies. In this talk, a series of experiments involving electron collisions with atomic oxygen, vibrationally excited molecular hydrogen and molecular nitrogen will be presented. Electron collisions with these species are of particular importance in planetary plasmas as demonstrated by, for example, the auroral phenomena at Earth and Jupiter, the electroglow of Jupiter, Saturn and Uranus, and UV emission from Earth, Titan and Triton, respectively. Further, such interactions are important in plasma processing of textile materials, nitrogen gas lasers, and fusion plasmas. The experiments to be presented involve two main experimental techniques (1) electron energy loss spectroscopy and (2) electron impact induced emission spectroscopy.

*This work was performed at the Jet Propulsion Laboratory, California Institute of Technology, under a contract with NASA. Financial support through NASA's PATM and OPR programs is gratefully acknowledged.

11:00**QR2 3 Electron-atom collision theory and applications.***IGOR BRAY, *ARC Centre for Antimatter-Matter Studies, Murdoch University*

During the last decade computational methods for electron-atom collisions have undergone major advances. In developing the convergent close-coupling (CCC) method the fundamental goal has been to have a theory which was valid at all projectile energies and for all atomic transitions of interest. Currently the CCC method has been shown to be particularly successful in reproducing experimental data for atomic transitions that are dominated by one-electron processes. This is the case for the lighter atoms such as H, He, He⁺, Li, and Na. Much of our effort in recent years has gone towards generalising the possible targets to incorporate heavier and more complex atoms which are important in various applications. In particular, we have considered Zn, Ba, and Hg for the lighting industry. Currently we are extending the method to inert gases such as Ne and Ar. In the talk we will review the CCC method and its applications, and also discuss the possible future directions.

*In collaboration with Dmitry Fursa and Andris Stelbovics, ARC Centre for Antimatter-Matter Studies, Murdoch University, Perth, Western Australia.

Contributed Papers

11:30

QR2 4 Resonances in positron-molecule annihilation* J.A. YOUNG, C.M. SURKO, *Univ. of California, San Diego* The positron (antiparticle to the electron) has unique interactions with matter. In atoms and molecules, it is attracted to the electrons and can annihilate to form gamma radiation. Using monoenergetic positrons from a trap-based beam, we have measured the positron-molecule annihilation rates as a function of positron energy [1,2]. In many molecules, we observe greatly increased annihilation at a fixed energy below the vibrational mode energies. This enhancement is due to quasi-bound positron states populated via vibrational Feshbach resonances (VFR). The resonant annihilation peaks grow exponentially with molecular size. In this paper, we discuss the latest data on positron capture and annihilation in small molecules, and we present new data on the effect of molecular temperature on annihilation rates. Finally, we relate the data to models of VFR and discuss the role of intramolecular vibrational energy distribution in the annihilation process. [1] S. J. Gilbert, et al., *Phys. Rev. Lett.*, **88**, 043201 (2002). [2] L. D. Barnes, et al., *Phys. Rev. A* **67**, 032706 (2003).

*This work is supported by NSF.

11:45

QR2 5 Elastic Scattering of Electrons by Small and Large Molecules.* D.W. SPIEKER, JUNFANG GAO, J.L. PEACHER, D.H. MADISON, *University of Missouri-Rolla* Theoretical calculations for elastic electron-molecule collisions will be presented for incident electron energies in the intermediate to low energy range. There exists a fair amount of experimental data for which there are no theoretical calculations for comparison in the 10-500 eV energy range. We will present differential cross section results for molecular hydrogen (H_2), molecular nitrogen (N_2), and trifluoromethane (CHF_3). We have used the program called General Atomic and Molecular Structure System, or GAMESS, to generate molecular orbitals. We use these to determine a potential interaction energy for the electron-molecule system. The distorted wave Born approximation (DWBA) was used to calculate the differential cross sections. The theoretical differential cross section results will be compared with experimental results.

*Work Supported by NSF PHY-0456528

SESSION RR1: MATERIAL PROCESSING IN LOW PRESSURE PLASMAS

Thursday afternoon, 12 October 2006; Salon CD Holiday Inn at 13:30; Jean-Paul Booth, Ecole Polytechnic, presiding

Invited Papers

13:30

RR1 1 The Role of Plasma Science in Materials Processing.MICHAEL BARNES, *Intevac, Inc.*

Plasma science has repeatedly enabled fundamental advances in materials processing since the late 1960's when it found its first applications in the manufacture of semiconductor integrated circuits. There have been numerous industrial uses of glow discharge plasmas outside of the semiconductor industry (e.g., the manufacture of hard disk drives, textiles, and MEMS); however, this paper will only give attention to its relevance in the semiconductor industry. It will begin with a historical perspective on the relevance of glow discharge plasmas to etching and vapor (i.e., chemical and physical) deposition of thin films. This will include its first uses in the bipolar integrated circuit industry as well as its origins in more mainstream applications. Surprisingly, by 1985 there were already over twelve reactors being used for plasma etching. Next, this presentation will discuss the 1990's inception and misconceptions surrounding high density plasmas. Although many multi-frequency and multi-electrode (e.g., capacitive, inductive) plasma systems are commonly used today, only gap fill of dielectric thin films into small features currently utilizes a relatively high density plasma as typically defined by plasma science. The paper will conclude with a discussion of several current problems of great interest to the semiconductor equipment industry and discuss where limitations in plasma technology may impede Moore's law.

Contributed Papers

14:00

RR1 2 Spatial and temporal structure of a sheath formed in a 300 mm, dual-frequency capacitive argon discharge ED BARNAT, PAUL MILLER, GREG HEBNER, *Sandia National Laboratories* ALEX PATERSON, JOHN HOLLAND, *Applied Materials* The spatial and temporal distributions of the electric fields of a sheath formed by a dual-frequency driven capacitive argon discharge are measured as functions of relative mixing between a low frequency current (13.56 MHz) and high frequency current (67.8 MHz). This is the first time a Stark effect based technique has been employed to measure sheaths of this nature. We find that for a

given total input power, as the high frequency power increases, both the total voltage across the sheath and the thickness of the sheath decreases. We also find that the temporal evolution of the potential across the sheath as well as the sheath thickness contain both rf components and that the high frequency oscillations become more prominent with increased high frequency power. For insight, comparisons of the measured spatial and temporal profiles are made to computational models commonly employed in the literature. These models include the collisional rf sheath model of Lieberman and extended to dual frequencies by Robiche et al. Where possible, we compare our measured trends to those predicted by the models, which in general, show good agreement.

14:15

RR1 3 Study of Nano-Contact Etching Characteristics Using C6F6 Gas. JONG-WOO SUN, SUNG-CHAN PARK, CHUL HO SHIN, CHANG JIN KANG, HAN KU CHO, JOO TAE MOON, *Process Development Team, Semiconductor R&D Center, Samsung Electronics* As device feature size shrinks to sub-0.1 μ m, oxide contact etching has become difficult to satisfy the process requirements. Especially, the aspect ratio of device has become higher and the mask thickness thinner. In this paper, we chose C6F6 as one of the promising candidates of next generation HARC etching gas, and have studied plasma and etching characteristics. Compared to other common etching gas (such as C4F6, C4F8), C6F6 could make more polymer and it could resolve the selectivity and profile problem. To identify the difference between C6F6 and other gases, plasma and etching characteristics were compared by QMS, OES, XPS, and etching tests. C6F6 showed 1.7 times higher polymer deposition rate than C4F8, and lower C/F ratio in polymer than other gases. This C/F ratio in polymer affected selectivity and profile during etching. C6F6 cracked into relatively larger molecules than other gases and this fragment patterns also affect polymer condition and etching characteristics. From the experiments, we used C6F6 to etch sub-0.1 μ m HARC etching and compared other gases.

14:30

RR1 4 Etching of high- k HfO₂ films in high-density chlorine-containing plasmas without rf biasing KOUICHI ONO, KEISUKE NAKAMURA, DAISUKE HAMADA, KAZUSHI OSARI, KOJI ERIGUCHI, *Kyoto University* Plasma etching of high dielectric constant (k) films is indispensable for the fabrication of high- k gate stacks. This paper presents the etching of high- k materials of HfO₂ in high-density chlorine-containing plasmas excited by electron cyclotron resonance. Experiments were performed with BCl₃/Cl₂ mixtures at a pressure of 5 mTorr in the absence of rf biasing; under these conditions, the difference between the plasma and floating potentials was of the order of 10 V. In pure BCl₃ plasma, some deposition was found to occur on HfO₂ surfaces to inhibit etching. By adding Cl₂ to BCl₃, the deposition was suppressed to result in the etching of HfO₂. The HfO₂ etch rate increased with increasing Cl₂ concentration, giving the maximum HfO₂ etch rate of about 100 nm/min at 60% Cl₂. At lower Cl₂ concentrations of 25-50%, the HfO₂ etch rate was > 20 nm/min, while the Si etch rate remained almost zero, thus giving a high selectivity of > 50 over Si. Moreover, by adding a small amount of O₂ to BCl₃/60%-Cl₂ plasma, the HfO₂ etch rate was found to increase to about 150 nm/min at 5% O₂, while the Si etch rate was also increased to deteriorate the selectivity over Si down to 4. The addition of Cl₂ and/or O₂ to BCl₃ would increase the concentration of Cl and decrease that of inhibitors BCl_x in the plasma. These results were compared with plasma and surface diagnostics, to understand plasma-surface interactions responsible for.

14:45

RR1 5 Study on the characteristics of etching organic hard mask for patterning high aspect ratio contact holes HYUN-SIL HONG, SUNG-IL CHO, MI-NA CHOI, CHANG-JIN KANG, HAN-KU CHO, JOO-TAE MOON, *Samsung Electronics* A hard mask etch scheme for high aspect ratio contact holes has been developed to improve the low selectivity. The removable organic materials were investigated as possible candidates of mask. However, the organic materials showed the profile problem of crock shape due to isotropic etch effect in O₂ chemistry. In this paper,

we introduce HBr or Cl₂ to improve the profile. Infra red spectroscopy (IR) and X-ray photoelectron spectroscopy (XPS) analyses were used to understand the etching mechanism. HBr and Cl₂ control the mask CD (critical dimension) and the profile. Cl₂ is more effective for profile changes than HBr. After etching the mask using Cl₂ or HBr, the IR analyses showed the formation of C-Cl or C-Br bonds, while C=C, C≡C, and aromatic groups are disappearing. It was shown the Cl and Br component are appearing through the XPS analyses. Based on results, halogen gases react at the surface of organic materials and this layer prevents from reacting with O₂. Passivation effect is prominent in the sidewall because the ion sputtering is low. Therefore, this halogenized layer prevents from isotropic etching and results in the tapered profile.

15:00

RR1 6 Low-pressure Plasma Fluorination of Polypropylene* YANG YANG, *Iowa State University* MARK STROBEL, SETH KIRK, HYACINTH CABIBIL, *3M Company* MARK J. KUSHNER, *Iowa State University* The surface energy and adhesion properties of commodity polymers such as polypropylene (PP) can be controlled by functionalization of the surface layers in plasmas. Affixing oxygen to the surface of PP, typically by atmospheric pressure coronas, raises surface energy and decreases hydrophobicity. Affixing fluorine lowers surface energy and increases hydrophobicity. In this paper, low-pressure plasma fluorination of PP will be discussed with results from computational and experimental investigations. PP was treated in low pressure (< a few Torr) capacitively coupled plasmas sustained in gas mixtures containing F₂. Process parameters (e.g., power, pressure, flow rate, position of PP in discharge) were varied. The fractional coverage of surface resident groups (CH, CF, CF₂, CF₃) was measured using ESCA. Plasma and surface processes were simulated using a 2-dimensional plasma hydrodynamics and surface chemistry model. The surface reaction mechanism consists of a hierarchy of reactions beginning with H abstraction by F atoms and followed by passivation by F and F₂. Ion (sputtering, scission) and photon (H dissociation, scission) activated processes are included. Comparisons will be made between the model and experiments for surface coverages of CH and CF_n.

*Work supported by 3M Company and the National Science Foundation.

15:15

RR1 7 A modeling of inductively coupled plasma in SF₆/O₂ for deep reactive ion etching of silicon TOSHIKAZU SATO, TOSHIKI MAKABE, *Keio University* There is still a strong requirement for a deep reactive ion etching (RIE) of silicon in micrometer scale for the fabrications of through wafer interconnects of LSI chips and micro electro mechanical systems (MEMS). Especially high etch rate more than 10 μ m/min is desirable for mass production of those devices. Here, attention should be given to the fact that the plasma is locally influenced by the wafer geometry comparable to the sheath thickness, causing distorted ion trajectories through the sheath. The design of fast silicon etching process can't be accomplished without understanding of the internal plasma properties and the plasma-surface interactions. In this work, we numerically investigate the 2D plasma structure in inductively coupled plasma in SF₆/O₂ and we also calculate the plasma structure near a sub-mm hole on a wafer. Calculation

shows the thinner sheath as compared with that of electropositive gases. As a result, the sheath will be affected by smaller wafer geometry. The ion flux distributions at the position in a hole and the estimated etch rate will be discussed.

SESSION RR2: LIGHTING PLASMAS

Thursday afternoon, 12 October 2006

Salon B Holiday Inn at 13:30

James Lawler, University of Wisconsin, presiding

Contributed Papers

13:30

RR2 1 Low-pressure positive column discharges in zinc and zinc halides DAVID SMITH, *GE Global Research* Zn-containing discharges were investigated by means of spectroscopic measurements of a capacitively-coupled discharge. Under optimum conditions (2 Torr Ar, 10-40 mW cm⁻³), the Zn positive column converts electrical power into zinc atomic radiation with an efficiency of > 50%. This value is comparable to the efficiency of a Hg positive column discharge, and does not strongly depend on whether the Zn was introduced as pure metal, or as zinc iodine or zinc bromide, a somewhat surprising result given the additional non-radiative power deposition mechanisms that are available in a plasma that contains molecules. A novel diagnostic based on analysis of selected emission line ratios was used to estimate densities of the ground state and excited states of Zn as a function of lamp wall temperature, and to better understand the important processes in these molecular plasmas.

13:45

RR2 2 Influence of the cathode composition on the performance of high pressure short arc xenon lamps OLGA B. MINAYEVA, DOUGLAS A. DOUGHTY, *PerkinElmer Optoelectronics, Fremont, CA* Thoriated tungsten has been widely used as a cathode material in arc lamps. The addition of thorium reduces the work function of tungsten and allows the cathode to operate at a lower temperature. However, most of the studies on thoriated cathodes were done either for welding arcs or for metal halide lamps, where reactions with the ambient gas could contribute to the cathode erosion. In the case of completely inert, high-purity

xenon gas and highly collisional arc plasma, the differences in performance of thoriated and non-thoriated cathodes are mainly material-based. In this talk we will discuss how 2% ThO₂ addition to tungsten cathodes changes the lifetime, ignition performance, and stability of xenon lamps.

14:00

RR2 3 Infrared Continuum Radiation from Metal Halide HID Lamps T.M. HERD, J.E. LAWLER, *University of Wisconsin* Lighting consumes 25% of all electrical power. Improving the efficiency of the widely used MH-HID lamps would have a significant impact on power consumption. We are studying the near IR continuum from MH-HID lamps. Near IR radiation from typical MH-HID lamps includes a continuum (> 50%), atomic lines (< 50%), and very weak molecular features. Analysis of the near IR is complicated due to the de-mixing of additives. Additive densities are determined by a balance between de-mixing from radial and axial cataphoresis and mixing from free convection and diffusion. The Hg produces most of the arc density and pressure while the additives contribute most of the free electron (e⁻) density and much of the radiation. The line width of the resonance broadened Hg 1014 nm transition is used to find the arc core Hg density. Absolute radiance measurements on optically thin, near IR Hg lines are Abel inverted to find the temperature as a function of radius. The electron density is determined from Dy I and Dy II lines using a Saha analysis. Our absolute near IR continuum measurements are compared to radiation transport simulations using the measured Hg density, temperature data, and e⁻ density as inputs. Results to date indicate that the near IR of MH-HID lamps is primarily e⁻ + Hg atom Bremsstrahlung.

14:15

RR2 4 Color separation in metal halide lamps W.W. STOFFELS, T. NIMALASURIYA, A.J. FLIKWEERT, W.J.M. BROK, J.J.A.M. MULLEN, G.M.W. KROESEN, M. HAVERLAG, *Eindhoven University of Technology, P.O. Box 513 5600 MB Eindhoven, The Netherlands* Metal halide discharge lamps are efficient lighting sources. However their widespread application is hindered by several problems. One problem is color separation. This is caused by a non-homogeneous distribution of radiating species within the lamp. It is believed to be the result of a complex interplay between diffusion and convection processes. In this contribution convection in the lamp is varied by placing the lamp in a rotating centrifuge. The resulting centrifugal force of up to ten times the normal gravitational force enhances the convection within the lamp and allows studying its effect on the color separation.

Invited Papers

14:30

RR2 5 Efficient Low-Pressure Metal-Halide Discharge Plasma Radiation Sources.

TIMOTHY SOMMERER, *General Electric Research*

Several efficient low-pressure metal-halide discharge chemistries have been reported in the patent literature since the year 2000.¹ Examples are halides of indium, tin, zinc, and gallium; typical gas mixtures are 200 Pa of a rare-gas and 1 Pa of the metal-halide species. The power density is near 50 mW/cm³. The conversion efficiency from electric power to radiation in the positive column exceeds 50 percent in some cases, a value that approaches the efficiency of positive column discharges in mercury and sodium metal vapors. It is not obvious how low-pressure metal-halide plasmas can be so efficient, since the plasma contains not only rare-gas atoms and metal atoms, but also molecules and radicals, where there are many nonradiative loss channels such as attachment, vibration, and dissociation. This talk will focus on work to maximize the fraction of input power that appears as radiation, and at such conditions, identify and understand the important nonradiative power channels.

¹US6972521, US6731070, US6603267, WO2005117064, US20050242737, WO2005031794, US20060071602.

15:00

RR2 6 Plasma Breakdown at Low Pressure.*

MARK BOWDEN, *Open University, UK*

Plasma ignition, the process by which an insulating gaseous medium turns into a conducting plasma, is considered to be well-understood in simple circumstances, involving processes such as electron multiplication, secondary electron emission and ionisation waves. In many practical cases, however, complicated geometry, different material surfaces, different gas mixtures, complex voltage waveforms and varying initial conditions lead to ignition processes that are much less easily described. The aim of this research is to study plasma ignition in simple electrode geometries, in order to identify the main breakdown mechanisms. We use a combination of space- and time-resolved measurements of plasma properties and modelling and simulation tools to study the breakdown behaviour. Phenomena occurring during the pre-ignition and ignition phases will be described.

*In collaboration with Erik Wagenaars, Wouter Brok, and Gerrit Kroesen, Eindhoven University of Technology, Netherlands.

SESSION SRP1: POSTER SESSION IIA
Thursday afternoon, 12 October 2006
Salon A, 4:00pm - 5:30pm Holiday Inn at 16:00

SRP1 1 INDUCTIVELY COUPLED PLASMAS

SRP1 2 Real time closed loop control of an Ar and Ar/O₂ plasma in an ICP

R. FAULKNER, F. SOBERÓN, A. McCARTER, D. GAHAN, S. KARKARI, V. MILOSAVLJEVIC, C. HAYDEN, A. ISLYAIKIN, V.J. LAW, M.B. HOPKINS, *Dublin City University, Ireland* B. KEVILLE, P. IORDANOV, S. DOHERTY, J.V. RINGWOOD, *National University of Ireland, Maynooth* Real time closed loop control for plasma assisted semiconductor manufacturing has been the subject of academic research for over a decade. However, due to process complexity and the lack of suitable real time metrology, progress has been elusive and genuine real time, multi-input, multi-output (MIMO) control of a plasma assisted process has yet to be successfully implemented in an industrial setting. A plasma parameter control strategy T is required to be adopted whereby process recipes which are defined in terms of plasma properties such as critical species densities as opposed to input variables such as rf power and gas flow rates may be transferable between different chamber types. While PIC simulations and multidimensional fluid models have contributed considerably to the basic understanding of plasmas and the design of process equipment, such models require a large amount of processing time and are hence unsuitable for testing control algorithms. In contrast, linear dynamical empirical models, obtained through system identification techniques are ideal in some respects for control design since their computational requirements are comparatively small and their structure facilitates the application of classical control design techniques. However, such models provide little process insight and are specific to an operating point of a particular machine. An ideal first principles-based, control-oriented model would exhibit the simplicity and computational requirements of an empirical model and, in addition, despite sacrificing first principles detail, capture enough of the essential physics and chemistry of the process in order to provide reasonably accurate qualitative predictions. This paper will discuss the development of such a first-principles based, control-oriented model of a laboratory inductively coupled plasma chamber. The model consists of a global model of the chemical kinetics coupled to an analytical model of power deposition. Dynamics of actuators including mass flow controllers and exhaust throttle are included and

sensor characteristics are also modelled. The application of this control-oriented model to achieve multivariable closed loop control of specific species e.g. atomic Oxygen and ion density using the actuators rf power, Oxygen and Argon flow rates, and pressure/exhaust flow rate in an Ar/O₂ ICP plasma will be presented.

SRP1 3 Electrical and plasma parameters of side type ferromagnetic ICP

KYEONG HYO LEE, YOUNG KWANG LEE, SUNG WON CHO, CHIN WOOK CHUNG, *Department of Electrical Engineering, HanYang University* PLASMA RESEARCH LABORATORY COLLABORATION A new class of plasma source for uniform processing of large surfaces, ferromagnetic ICP is developed in this presentation as an alternative to existing plasmas. This source has eight half square quartz tubes at side wall and each tube has two toroidal ferromagnetic cores. Electrical parameters are measured by an MKS impedance probe and plasma parameters are obtained from single langmuir probe data. Operating pressure is in the range of 2 mtorr to 50 mtorr and input power driven at 400 kHz is delivered up to 2 kW. Antenna voltage and current are less than 800 V and 6 A with high power factor and plasma density profile over 300 mm wafer is uniform at various pressure.

SRP1 4 On the E to H and H to E transition mechanisms in inductively coupled plasmas

MINHYONG LEE, KYEONGHYO LEE, CHINWOOK CHUNG, *Dept. of Electrical Engineering, HanYang University* Inductively coupled plasmas (ICP) exhibit two mode operations of capacitive coupling (E mode) and inductive coupling (H mode), and the density jump and hysteresis have been reported during the transition between these modes. In this study, the total power transferred to the plasma by capacitive and inductive coupling is calculated from Maxwells equations and global model, and from this, conditions required for stable E and H mode operations are obtained. The E to H and the H to E transitions occur when the system reaches critical electron densities. Analytical criterion for stable H mode operation that the skin depth should be smaller than $\sqrt{\frac{2}{3}}R$ at low pressure, and $2/\sqrt{3}(\omega/\nu)R$ at high pressure is derived from the calculation. The dependence of transition electron densities and powers of E to H and H to E transitions on the pressure and discharge dimension is also discussed.

SRP1 5 On the multistep ionizations in argon inductively coupled plasmas MINHYONG LEE, SUNGHO JANG, CHINWOOK CHUNG, *Dept. of Electrical Engineering HANYANG UNIVERSITY TEAM* The effect of the multistep ionizations on the plasma parameters in the inductively coupled plasma (ICP) has been investigated by experiments and theory. To obtain electron density and electron temperature precisely at various powers and pressures in the ICP, the electron energy distribution functions (EEDFs) are measured. It is found that at high pressures, the electron temperature from the EEDFs decreases and the electron density increases rapidly with the absorbed power while, at low pressures, the electron temperature is hardly changed and the electron density is almost linearly proportional to the absorbed power. The comparison between the experiment and our model including the multistep ionizations [M. H. Lee and C. W. Chung, *Phys. Plasmas* 12, 73501 (2005)] was done and the experiment was in close agreement with the model. This shows that the changes in the electron density and the electron temperature in the ICP are mainly due to the multistep ionizations.

SRP1 6 Diagnostics for an inductively coupled plasma in highly Ar-diluted oxygen ZHANG YONG,*SATOSHI HIRAO, TAKESHI OHMORI, *Keio University* TAKESHI KITAJIMA, *National Defence Academy* TOSHIKI MAKABE, *Keio University* Oxygen plasma has been widely used in microelectronics fabrications. It is known that the growth rate of SiO₂ in Si-wafer is enhanced in Ar-diluted O₂ plasma. One of the key reactions in the surface is caused by the oxygen metastable atom O(¹D₂), which has the potential for the surface activation. The work [1] shows that Ar metastable Ar(1s₅) contributes greatly to the production of O(¹D₂) in a CCP in highly Ar-diluted oxygen. In this paper, we have studied the influence of the Ar metastables on the production of O(¹D₂) in an inductively coupled plasma (ICP) in O₂(0-20%)/Ar. ICP was sustained by a single turn current coil driven at 13.56 MHz. Space-resolved 3D density profiles of O(³P), Ar(2p₁), and Ar(2p₉) were observed by Radon inversion of the line integrated optical emissions. And Ar metastable density was measured by laser absorption spectroscopy. The experimental result would be useful for the understanding of the mechanism of the production of O(¹D₂). [1] T. Kitajima, T. Nakano, T. Makabe, *Appl. Phys. Lett.* 88, 091501 (2006).

*Also Xi'an Jiaotong University.

SRP1 7 Dynamics of an E-H transition in ICP in Ar SATOSHI HIRAO, YONG ZHANG,*TOSHIKI MAKABE, *Keio University* Inductively coupled plasma (ICP) has been widely used as a high density plasma source in various applications. ICP has two proper modes. One is a low density capacitively coupled mode sustained by the static electric field caused by the local potential difference of the induction coil (E-mode), and the other is a high-density inductively coupled mode sustained by the induced electromagnetic field (H-mode)[1]. There is a transition between both modes in ICP, and the space and time change between the modes will be still interesting for us. In the present study, we will investigate the spatiotemporal 2D-t change of the optical emission in ICP in Ar by using ICCD camera located on the top of the reactor. We mainly focus on the emission from Ar(2P₁) as a probe of high energy electrons, and discuss the dynamic characteristics of the E-H transition by way of ionization of high energy electrons. [1] Y. Miyoshi, T. Makabe *et al.*, *IEEE Trans. Plasma Sci.*, 30(1), 130 (2002), and 33(2), 360(2005).

*Also Xi'an Jiaotong University.

SRP1 8 Experimental Study on Radio Frequency Inductively Coupled Ar/NF₃ Discharges KATSUYUKI HANAKI, TAKASHI KIMURA, *Nagoya Institute of Technology* We investigated the plasma parameters in radio frequency inductive Ar/NF₃ plasmas with the probe method and optical emission spectroscopy combined with actinometry. Plasma was produced in the cylindrical stainless steel chamber with 160 mm in inner diameter and 100 mm in length, and the power injected into the plasma was kept at 120W. Experiment was performed at three total pressures of 8m, 15m and 30 mTorr, changing the NF₃ content from 0% to 30%. The structure of the measured electron energy probability functions (EEDFs) did not change at any NF₃ content, resulting in the same effective electron temperature. The measured EEDFs deviated from the Maxwellian distribution due to the large depletion of the electrons with the energy higher than 11-13 eV. On the other hand, the electron density markedly decreased even in small NF₃ addition lower than 5%. The atomic fluorine density estimated by actinometry was approximately proportional to the NF₃ content. We investigated the effect of O₂ addition on the plasma parameters as well. The atomic fluorine density in Ar/NF₃/O₂ discharges depended on only NF₃ content. This fact may indicate that the reaction rate to produce the atomic fluorine by the collisions between the atomic oxygen and NF_x (x=1,2) is much lower than that by the collisions between the atomic oxygen and CF_x (x=2,3). The atomic oxygen density was approximately proportional to O₂ content.

SRP1 9 Probe Measurements and Optical Emission Spectroscopy in RF Inductively Coupled Ar/SF₆ Discharges TAKASHI KIMURA, MICHIO MABUCHI, *Nagoya Institute of Technology* With the probe method and optical emission spectroscopy combined with actinometry, we investigated the dependence of the plasma parameters on the SF₆ content in radio frequency inductively coupled Ar/SF₆ discharges. Plasma was produced in the cylindrical stainless steel chamber with 160 mm in inner diameter and 75 mm in length, and the power injected into the plasma was kept at 140W. Experiment was performed in the total pressure range from 5 mTorr to 25 mTorr, changing the SF₆ content from 0% to 30%. Under our experimental condition, the electron density and its effective temperature were independent of the SF₆ content. The electron density was on the order of 10¹⁶ m⁻³ and its effective temperature was about 4 eV. The atomic fluorine density estimated by actinometry, which was on order of 10¹⁹ m⁻³, was approximately proportional to the SF₆ content. We investigated the effect of dilution gas addition (H₂ and O₂) on the plasma parameters as well. The measured electron energy probability functions (EEDFs) did not depend on the dilution gas content for the SF₆ content higher than 10%, resulting in the constant effective electron temperature and the constant electron density. The atomic fluorine density gradually increased with increasing O₂ content whereas it markedly decreased with increasing H₂ content.

SRP1 10 Studies of Mode Transitions in Inductively Coupled Plasma Reactors ANDRE DALTRINI, STANISLAV MOSHKALEV, *Universidade Estadual de Campinas, Unicamp, Center for Semiconductor Components, Campinas, SP, Brazil* THOMAS MORGAN, *Department of Physics, Wesleyan University, Middletown, CT 06457* USA WILLIAM GRAHAM, *Physics and Astronomy, Queens University Belfast, BT7 INN, Northern Ireland*

Optical emission spectroscopy and Langmuir probe measurements have been used to study mode transitions and hysteresis in a GEC Inductively Coupled Plasma reactor operating in both Ar and Ar/O₂ mixtures over a range of pressures. Ar emission line ratios have been used to monitor the variations of the electron temperature and the influence of the metastable Ar atoms in both discharge modes [1]. The first results show a smooth decrease of the electron temperature with power, followed by an abrupt transition when the plasma jumps to the H mode, with a clear reduction in electron temperature. Similar results are obtained with a Langmuir probe. Also, a strong variation of the metastable density with the transition was observed. Its influence on the transition and associated hysteresis will be discussed. [1] S. A. Moshkalyov, P. G. Steen, S. Gomez, and W. G. Graham, *Appl. Phys. Lett.*, **75**, 328 (1999).

SRP1 11 Measurements of Nonlocal Electron Energy Distribution Functions in the Afterglow of an RF ICP Discharge*

JON BLESSINGTON, *West Virginia University* CHARLES DE-JOSEPH, JR., *Air Force Research Laboratory* VLADIMIR DEMIDOV, MARK KOEPKE, JASON WYNNE, *West Virginia University* In previous work [1], it was shown that even a small number of nonlocal fast electron, which do not significantly affect the overall mean electron energy, can dramatically change the plasma and near-wall sheath properties. In this work, Langmuir probe measurements of electron density, temperature and energy distribution functions (EEDF) in the afterglow of low-pressure (30-50 mTorr) noble-gas rf ICP discharges have been carried out. The experimental setup is described in [2]. The primary focus of this work was the investigation of the high energy portion of the EEDF which shows peaks corresponding to electrons with energies 5-20 eV, depending on the gas mixture. These peaks arise from electrons produced in Penning ionization with metastable noble gas atoms. This fast component of the EEDF can be controlled independently on the slow electrons, a direct consequence of the nonlocality. [1] V. Demidov et al. *PRL* **95**, 215002 (2005). [2] W. Guo et al., *PSST* **10**, 43 (2002).

*This work was supported by The Air Force Office of Scientific Research.

SRP1 12 CAPACITIVELY COUPLED PLASMAS II

SRP1 13 Abstract withdrawn.

SRP1 14 Abstract withdrawn.

SRP1 15 Investigation of the Spatial Distributions of CF₂, F and H Radicals in Capacitive Coupled Single- and Dual-Frequency RF Plasmas in Ar/CF₄ and Ar/CHF₃ Mixtures by the Emission and Absorption Spectroscopy. S.G. BELOSTOTSKY, O.V. BRAGINSKY, A.S. KOVALEV, D.V. LOPAEV, T.V. RAKHIMOVA, A.N. VASILIEVA The emission and absorption spectroscopy was applied to study the spatial distributions of CF₂ radicals and F and H atoms in capacitive coupled single- and dual-frequency rf plasmas in Ar/CF₄ and Ar/CHF₃. The use of imaging spectrograph equipped ICCD camera and four lattices covered wide spectral range from UV to near IR allowed us to provide applicability of actinometric measurements to CF₂, H and F in the wide spectral range and to obtain the spatial profiles of mole fractions of the radicals. The UV absorption spectroscopy of CF₂ carried out enabled to measure directly CF₂ line-of-view den-

sities that together with actinometric measurements of the CF₂ mole fraction allowed obtaining axial profiles of CF₂ concentration. Besides it also provided measurements of axial distribution of gas temperature. It is shown that CF₂ density in Ar/CHF₃ plasma is greater more by the order than in Ar/CF₄ plasma, although H atom density is higher only slightly. The ratio [CF₂]/[F] in Ar/CHF₃ compared to Ar/CF₄ is higher over hundred times. The densities of all radical increase with increasing both high- and low-frequency powers, though it mainly governed by HF power. The axial profile of CF₂ mole fraction is always peaked near the discharge center with rather small gradients to the electrodes indicating wall losses of the radicals. The axial profile for H mole fraction becomes concave at high LH powers particularly in Ar/CF₄ plasma that indicates destruction of C_xF_yH_z polymeric film covering the electrodes.

SRP1 16 Investigation of the Spatial Distribution Evolution of Electron Temperature in Capacitive Coupled Single- and Dual-Frequency RF Plasmas in Ar/O₂ mixture over the RF Period.

S.G. BELOSTOTSKY, O.V. BRAGINSKY, A.S. KOVALEV, D.V. LOPAEV, T.V. RAKHIMOVA, A.N. VASILIEVA, *Univ. of Houston* The emission spectroscopy was applied for studying the temporal-spatial behavior of capacitive coupled single- and dual-frequency (1.76 MHz + 81 MHz) rf plasmas. As observed in the low-pressure (< 100 mTorr) rf discharges, the intensity oxygen atom emission line O(3p⁵P → 3p⁵S) 777 nm is fully determined by the dissociative excitation of O₂ molecules with the ratio of O line to line Ar(2p₁ - 1s₂) 750 nm being a linear function of electron temperature. It allowed us to investigate evolution of the axial distributions of electron temperature over the rf period by using the temporally and spatially resolved actinometry technique. It was experimentally realized by the ns-gated ICCD camera equipped objective with narrow-band interference filters and synchronized with the LF voltage. It is shown that the high-frequency (HF) rf discharge provides uniform spatial distribution of electron temperature in the inter-electrode gap. With adding LF power, the strong electron heating near the electrode sheaths occurs synchronously with the LF period. With increasing LF power the electron heating becomes stronger and penetrates more deeply inside the bulk of plasma. At r pressures ≤ 50 mTorr the electron temperature in the discharge center doesn't changes with applying LF power, but it isn't already so at the higher pressure that directly shows coupling two rf plasmas with increasing pressure.

SRP1 17 Capacitive Coupled Single- and Dual-Frequency RF Plasma in Argon

OLGA PROSHINA, OLEG BRAGINSKY, VLADIMIR IVANOV, ALEXANDER KOVALEV, DMITRY LOPAEV, TATYANA RAKHIMOVA, ANNA VASILIEVA, *Institute of Nuclear Physics, Moscow State University, Russia* Capacitively coupled radio-frequency Ar plasma operated both in the Single Frequency (SF) and Dual Frequency (DF) regimes at high specific input powers has been studied both experimentally and theoretically in a pressure range of 20 mTorr - 100 mTorr. In the SF regime the discharge was operated at 1.76, 13.56 and 81 MHz. In the DF regime two frequencies combinations were used: i 13.56 - 81 MHz; ii 1.76 - 81 MHz. The measurements of the plasma density and the electron temperature by a Langmuir probe in the center between the electrodes as a function of the dissipated RF power were carried out. It was revealed that the low frequency (LF) power affects the electron density in a pressure range of 45 - 100 mTorr. The decrease of the pressure to 20 mTorr results in an absence of the LF power influence on the electron density and

consequently leads to the frequency decoupling. The PIC MC simulation was carried out to analyze the experimental data. It was shown that in SF discharge at 1.76 and 13.56 MHz the role of the secondary electron emission (SEE) is significant. The HF discharge at 80 MHz is operated in α -mode at the same powers. The role of SEE on the DF discharge operation is significant at the studied conditions. The frequency decoupling takes place for the conditions when the sheaths are almost collisionless for γ -electrons.

SRP1 18 Experimental and Theoretical Study of Ion Energy Distribution in SF and DF CCP discharges OLGA PROSHINA, OLEG BRAGINSKY, ALEXANDER KOVALEV, DMITRY LOPAEV, YURY MANKELEVICH, MIKE OLEVANOV, TATYANA RAKHIMOVA, ANNA VASILIEVA, DMITRY VOLOSHIN, *Institute of Nuclear Physics, Moscow State University, Russia* The theoretical and experimental study of ion energy distribution function (IEDF) in single and dual frequency capacitive coupled RF discharge in Ar was carried out. Parameters of plasma source were taken in the widely used range for research purposes: single frequency discharge (SF) at 80 MHz and dual frequency (DF) discharge at 1.76/80 MHz, specific input powers of 0.02–2 W/cm², pressures of 20–100 mTorr. The ion energy analyzer was used to measure IEDF on the grounded electrode. It was shown that the applied low frequency voltage governs energy width in the dual frequency regime. IEDF in SF and DF discharges was studied analytically and using Monte-Carlo (MC) simulations. Analytical expressions for IEDF and IEDF peaks location were derived. In MC simulations, ions trajectories were traced in a given electric field (from the global model and parametric expressions). Elastic and charge exchange collisions were taken into account. The MC calculations provide explanation of IEDF peaks height ratio in DF collisionless discharge. Theoretical estimations of IEDF shape in SF and DF cases are in good agreement with experimental data.

SRP1 19 Optical emission CT of etching plasmas for an effect of the anode phase of LF-bias voltage in a 2f-CCP in Ar and CF₄/Ar MIKIO ISHIMARU, TAKESHI OHMORI, *Keio University* TAKESHI KITAJIMA, *National Defense Academy* TOSHIAKI MAKABE, *Keio University* It is essential to control and optimize 2-dimensional ion flux distribution modulated by strong sheath dynamics in front of an oxide wafer deeply biased by a low frequency source in a 2f-CCP etcher. In our previous work, we have estimated the effect of the secondary electron from the wafer at the cathodic phase of the low frequency bias voltage on the functional separation in the 2f-CCP. In the present work, we discuss a temporal profile of low energy electrons of the anodic phase of the bias by using 2D-t OES system. The profile of the net excitation rate of Ar(2p₉) is still observed in the sheath region at the anodic phase of the wafer, although the net rate of Ar(2p₁) as a probe of high energy electrons is very weak. These results may be supposed that the majority part of the signal of Ar(2p₉) will be caused by the reaction between the low energy electron and Ar metastable atom. We will perform a measurement of the absolute density of Ar metastables by using LAS to identify the effect of low energy electrons in the 2f-CCP. [1] T. Akaike, T. Ohmori, T. Makabe, et al, 58th-GEC (San Jose; 2005).

SRP1 20 Low-pressure gas breakdown in dual-frequency (27/2 MHz) RF electric fields in nitrogen VALERIY LISOVSKIY,* JEAN-PAUL BOOTH,† *Laboratoire de Physique et Technologie des Plasmas, Ecole Polytechnique, Palaiseau 91128, France* KARINE LANDRY, DAVID DOUAI, VALERICK CASSAGNE, *Unaxis Displays Division France SAS, 5, Rue Leon Blum, Palaiseau 91120, France* VLADIMIR YEGORENKOV, *Kharkov National University, Kharkov 61077, Ukraine* We present measured breakdown curves for dual-frequency (27.12 / 2 MHz) discharges in nitrogen. RF voltages at frequencies of 27.12 MHz (HF) and 2 MHz (LF) were fed to the same powered electrode whereas another one was grounded. The inter-electrode gap was 20.4 mm. The 27 MHz breakdown curve is shifted to higher voltages and gas pressures when a 2 MHz voltage (< 300 V) is added, due to the increased loss of electrons due to the drift in the LF field. At LF voltages above 300 V the LF field contributes to gas ionization. Positive ions oscillating in the enhanced LF field can collide with the electrode surface and produce secondary electrons. Therefore the HF breakdown voltage is decreased and approaches zero (a self-sustained LF discharge is ignited). Adding an HF voltage always leads to a decrease in the LF breakdown voltage because of the reduction of electron losses due to oscillations in the HF field.

*Kharkov National University, Kharkov 61077, Ukraine.

†Currently at Lam Research Corporation, 4650 Cushing Parkway, Fremont, CA 94538, USA.

SRP1 21 Optical Emission Measurements of Dual Frequency Capacitively Coupled Plasmas ERIC BENCK, KRISTEN STEFFENS, *National Institute of Standards and Technology* Dual frequency capacitively coupled plasma sources are becoming increasingly important in semiconductor manufacturing processes. An imaging spectrometer combined with a high speed intensified CCD camera was used to obtain spatially and temporally resolved measurements of the optical emission from dual frequency (2 MHz / 13.56 MHz or 2 MHz / 27.12 MHz) plasmas created in a Gaseous Electronics Conference (GEC) reference reactor. The vertical distribution of the argon 750.4 nm transition was measured at the radial center of the discharge. For a single powered electrode the temporal distributions of the Ar excitation rate were also calculated. Significant changes in the temporal and vertical optical emission distributions were observed with changing feed gas (Ar, CF₄, and O₂) and gas pressure (100 mTorr to 1000 mTorr). The temporal distributions were insensitive to the amplitude of the lower frequency bias voltage. Changing from a single powered electrode to two separate powered electrodes also had a significant impact on the time resolved optical emission.

SRP1 22 COLLISION PROCESSES IN DISCHARGES AND PLASMAS

SRP1 23 Excitation of the near-uv continuum of H₂ by fast H atoms A.V. PHELPS, *JILA, U. of Colorado and NIST* We model the production of the near-uv continuum of H₂ by collisions of fast atoms, fast ions, and electrons with H₂ in a uniform-electric-field drift tube.¹ Relative intensities versus position at 300 Td < E/N < 20 kTd (1 Td = 10⁻²¹ V m²), at 0.95 to 0.12 Torr, and 4 cm electrode separation are normalized to electron excitation

coefficients at low E/N . Electron and heavy-particle induced excitation are separated by their growth toward the anode or the cathode, respectively. The excitation attributed to heavy-particles increases approximately as the cube of the distance from the anode. This growth is consistent with a three-step reaction sequence starting with a roughly uniform density of H_2^+ produced by electrons. A multi-beam model for the electrons, H^+ , H_2^+ , H_3^+ , fast H_2 , and fast H confirms this dependence. The principal excitation step is fast $H + H_2 \rightarrow H_2(a^3\Sigma_g^+) + H$ with a cross section roughly twice that for $H\alpha$ excitation.

¹Z. Lj. Petrović and A. V. Phelps, Int'l. Seminar on Reactive Plasmas, Nagoya, June 17-19, (1991).

SRP1 24 Possible Mechanism of "Additional" Production of H^- in a Glow Discharge S. BELOSTOTSKIY, D. ECONOMOU, D. LOPAEV, T. RAKHIMOVA, NUCLEAR PHYS. INST., MSU TEAM, DEPT. OF CHEM. ENG., U. OF HOUSTON TEAM, Based on measurements of H^- and H densities a DC glow discharge in H_2 ($P=0.1-3$ Torr) the rate coefficient of H^- production as a function of E/N was determined. To analyze the mechanisms of H^- production, a simple model of H_2 vibrational excitation was developed. Estimations of vibrational level densities ($v=3-5$) obtained from VUV absorption measurements were in reasonable agreement with the calculated data. The analysis revealed that standard mechanisms of H^- production (dissociative attachment to vibrationally excited molecules $H_2(v)$ and molecules in Rydberg states $H_2(itRy)$) were not enough to explain the experimental results. In order to describe both the shape (vs E/N) and the magnitude of the measured H^- production rate coefficient, an "additional" source of H^- , having a strong resonant electron attachment CS in the range of $\sim 5-9$ eV, should be invoked. Although H_2 has no resonances in the 5-9 eV range, water is known to strongly dissociatively attach in this range. Thus, even small amounts (0.1-1%) of water vapor in the apparatus can explain the origin of the "additional" H^- production. This result is corroborated by the work of Cadez *et al.* in Proc. of XXVII ICPG, 2005. This work was supported by the RFBR (No.05-02-17649a), Scientific School - 171113.2003.2 and NATO Collaborative Linkage Grant (No.980097).

SRP1 25 Model calculations of the "flame" in flowing-afterglow plasmas* RAINER JOHNSEN, RICHARD ROSATI, MICHAEL GOLDE, *University of Pittsburgh* Our recent experience in analyzing optical emission from flowing-afterglow plasmas has led us to re-examine some of the simplifying assumptions that are often made in such experiments. One is often forced to carry out observations in the first few centimeters downstream from the reagent inlet, a region in which the reagent gas distribution is highly non-uniform. In this region, the "flame," i.e., optical emission that arise from reactions of active particles (ions, metastables etc) with reagent molecules, actually is hollow, roughly cone-shaped region, the center of which is essentially dark, while a cursory visual inspection gives the appearance of a solid luminous cone. This occurs for both ring-shaped and point-like gas inlets. If one were to measure the electron density immediately downstream from the reagent inlet, one would find a minimum on the flow tube axis, rather than a maximum. One would also find that a simple "bulk-flow" model seriously overestimates the rates at which some chemical reactions occur, because the

reactions are limited by diffusion rather than by the chemical rates. We will present the results of model calculations and compare them to experimental observations of emission flames produced either by electron-ion recombination or metastable excitation.

*Supported by NASA.

SRP1 26 Dissociation, recombination and detachment in oxygen discharges diluted with argon JON T. GUDMUNDSSON, EYTHOR G. THORSTEINSSON, *University of Iceland* We use a global (volume averaged) model to study the presence of negative ions and metastable species in low pressure high density O_2/Ar discharge. In particular the role of argon dilution in the dissociation of oxygen is investigated and the increase in the metastable $O(^2D)$ density with argon dilution. Furthermore, the electronegativity of the discharge is explored as a function of argon dilution. We find the negative oxygen ion O^- to be the dominant negative ion in the discharge in the pressure range of interest, 1 – 100 mTorr. Dissociative attachment of the oxygen molecule in the ground state $O_2(^3\Sigma_g^-)$ and the metastable oxygen molecule $O_2(a^1\Delta_g)$ are the dominating channels for creation of the negative oxygen ion O^- . At low pressure (< 5 mTorr) electron impact detachment dominates the loss of negative ions but recombination involving O^- and O^+ ions is an important loss channel. At higher pressure detachment on $O(^3P)$ becomes the main loss channel for the O^- ion.

SRP1 27 Pump/Probe measurement of V-V transfer in O_2 and H_2 TAI AHN, *Univ of California - Riverside* IGOR ADAMOVICH, WALTER LEMPERT, *Ohio State University* We present new sets of V-V rate coefficients for vibrational levels 0 – 5 in O_2 and H_2 at 300 K, using a stimulated Raman – spontaneous Raman pump/probe apparatus. For O_2 it is found that previously reported semi-classical trajectory calculations of Coleti and Billing underestimate the V-V rate coefficients by approximately one order of magnitude, in agreement with recent measurements by of Kalogerakis and the earlier observations of Diskin. For H_2 non-resonant processes, comparison with recalculated semi-classical predictions using the identical potential to that given by Cacciatori and Billing results in predicted rates which are too fast, by a factor of ~ 2.5 , consistent with the previously reported value of Kreutz. However for the "resonant" V-V process, $H_2(v=1) + H_2(v=1) \rightarrow H_2(v=2) + H_2(v=0)$, predictions are found to be too slow, by a factor of approximately two, consistent with previous reported data of Farrow and Chandler. This suggests that semi-classical calculation methods that treat the rotational motion classically may be unsuitable for H_2 , due to rotational energy level spacings which are comparable to $k_B T$.

SRP1 28 Alignment relaxation and disorientation of $Ne^*(2p_i)$ atoms induced by collisions with $He(1s^2)$ * CRISTIAN BAHIRIM, *Department of Chemistry and Physics* VAIBHAV KHADILKAR, *Department of Computer Science, Lamar University* In order to explain experimental results in discharge cells at temperatures (T) between 17K and 600K obtained at Kyoto University (Seo *et al.* Journal of Physics B **36**, 1885 (2003)), we report quantum calculations for the disalignment and the disorientation of $Ne^*(2p_i)$ atoms on the $2p^5 3p$ electronic configuration induced by collisions with $He(1s^2)$. The excellent agreement theory-experiment for $77K < T < 600K$ indicates that the electrostatic interaction between atoms is accurately described by our model potential at internuclear distances below $12 a_0$. However,

significant discrepancies are revealed for $17\text{K} < T < 77\text{K}$. The experiment predicts that both the disalignment and the disorientation cross sections vanish near zero collision energy, while our quantum calculations indicate a resonant structure in this region. Therefore, the long-range interaction between atoms is re-analyzed. This study requires an important computational effort for the calculation of the rate coefficients for disalignment and disorientation of the $\text{Ne}^*(2p_i)$ atoms in isotropic collisions, with the inclusion of the statistical distribution of atoms. Agreement between theory and experiment is found when a slightly more repulsive long-range potential for the $e(3p) + \text{He}$ interaction is included in our model.

*We acknowledge the Research Enhancement Grant at LU for assistance.

SRP1 29 The sensitivity of calculated ion transport coefficients for testing ion-neutral interaction potentials MARK HOGAN, *U. S. Merchant Marine Academy* Several commonly measured ion transport coefficients were investigated in order to determine their sensitivity when used for testing the accuracy of proposed ion-neutral interaction potentials. The level of sensitivity was taken to be the average percentage difference between values of an ion transport coefficient calculated from two interaction potentials. 93 sets of comparisons were carried out. A variety of positive ions, negative ions, neutrals and temperatures were included in the comparisons done in order to draw as general a conclusion as possible. The sensitivity was determined to be 5.2% for mobility, 10% for the ratio of the transverse diffusion coefficient to mobility, 16% for the ratio of the longitudinal diffusion coefficient to mobility, 17% for the transverse diffusion coefficient, and 23% for the longitudinal diffusion coefficient. In particular, it was found that the longitudinal diffusion coefficient is the most sensitive test and that the mobility is the least sensitive test.

SRP1 30 Mobility of O^+ in He, Ne and Ar and Interaction Potentials of HeO^+ , NeO^+ and ArO^+ DANIEL DANAILOV, *Chatham College, Science Division, Pittsburgh, PA 15232* LARRY VIEHLAND, *Chatham College, Science Division* RAINER JOHNSEN, *University of Pittsburgh, Department of Physics, Pittsburgh, PA 15260* TIMOTHY WRIGHT, *University of Nottingham, UK* EDMOND LEE, *University of Southampton, UK and Hong Kong Polytechnic University* New experimental measurements are reported for the mobility of O^+ ions in He, Ne and Ar gases at 300 K. The accuracy of these new values is estimated as $\pm 2.5\%$, which allows them to serve as a stringent test of new *ab initio* potentials that we have calculated using the RCCSD(T) method. We employed the aug-cc-pV5Z basis set with counterpoise corrections and took spin-orbit coupling into account. The present experimental values for O^+ in He lie below the calculated ones, but the difference becomes statistically significant only at moderate and high values of the ratio of the electric field strength to the gas number density; even there they are only marginally significant. For O^+ in Ne the experimental values lie clearly below the theoretical curve and for O^+ in Ar the ion mobility dependence has clear minima in addition to the maximum shown in the other rare gases.

SRP1 31 Temperature dependence of argon excimer emission from pulsed discharge excited argon clusters MARK MASTERS, HANS SUEDHOFF, MIKE DE ARMOND, CLINT REYNOLDS, *Indiana University-Purdue University, Fort Wayne* Argon second continuum excimer emission is observed from a pulsed discharge excited pulsed supersonic argon expansion. The

expansion nozzle consists of a temperature controlled, 15 cm long slit with a variable width ($35 \mu\text{m}$ to $250 \mu\text{m}$). The intensity of the argon excimer emission near 126 nm is investigated as a function of the width of the expansion nozzle slit, temperature of the expansion nozzle and position within the cathode-anode gap. The pressure within the nozzle has been measured as 2–4 bar and the excitation consists of a 50 ns negative current pulse of about 15kV and 700A. The observation of the emission depends directly on the size and quantity of clusters formed in the expansion. To determine the dependence of the emission upon clusters and the cluster size distribution, the mean cluster size is diminished by increasing the expansion nozzle and gas temperature. The temporal evolution of the second continuum emission and the observed spectra are presented as a function of nozzle temperature and slit width.

SRP1 32 Effects of Electron Exchange in Fully Differential Cross Sections for Charged Particle Ionization* A.L. HARRIS, M. FOSTER, J.L. PEACHER, D.H. MADISON, *University of Missouri-Rolla* H.P. SAHA, *University of Central Florida* K. BARTSCHAT, *Drake University* Three dimensional fully differential cross sections (FDCS) for charged particle impact ionization of helium are examined. Previously, for heavy particle impact, the Three Distorted Wave (3DW) model had yielded good agreement with experiment in the scattering plane, but poor agreement outside the scattering plane. In particular, 3DW calculations for the perpendicular plane predicted a small flux of electrons with almost no structure, while experiment showed a much higher flux of electrons with structure. To better treat the ejected electron, the 3DW-Hartree Fock (3DW-HF) and 3DW-R Matrix (3DW-RM) theories are introduced. The primary improvement of these two calculations over a standard distorted wave treatment is that exchange between the continuum and bound electrons is treated properly. Results for ionization of helium by impact of both electrons and C^{6+} ions will be presented.

*Work Supported by NSF.

SRP1 33 Low-Energy Electron Impact Ionization of Molecular Hydrogen J.G. CHILDERS, KELLY KUPER, MURTADHA A. KHAKOO, *California State University, Fullerton, CA 92834, USA* Relative doubly-differential cross sections for the electron impact ionization of molecular hydrogen have been measured at incident energies of 25 eV and 40 eV and scattering angles of 20° to 130° . The calibration of the electron analyzer during these measurements employed the recent doubly-differential cross section measurements of atomic hydrogen.¹ These measurements represent a new calibration standard useful in the determination of the transmission function of electron analyzers. This work is funded by the National Science Foundation under grant # NSF-RUI-PHY-9731890.

¹J.G.Childers, K. E. James, Jr., Igor Bray, M. Baertschy, and M.A. Khakoo, *Phys. Rev. A* **69**, 022709 (2004).

SRP1 34 Laser optogalvanic spectroscopy of neon and krypton in a discharge plasma NAVEED PIRACHA, KURT NESBETT, SOHALA MOTEN, PHIL MOELLER, *John Carroll University* We report studies on the temporal evolution of the optogalvanic signal in neon and krypton using commercial hollow cathode lamps in conjunction with Nd: YAG pumped dye laser system. Transitions resulting from the excitation of $3s[3/2]_2$ and $5s[3/2]_2$ metastable states have been selected to study the discharge mechanism.

SRP1 35 Importance of Relativistic effects and Exchange between Bound and Continuum Electrons on Electron Impact Ionization of Xenon.* Z. STEGEN, D.H. MADISON, *University of Missouri-Rolla* H.P. SAHA, *University of Central Florida* K. BARTSCHAT, *Drake University* S. BELLM, J. LOWER, R.P. McEACHRAN, E. WEIGOLD, *Australian National University* Exchange between bound and continuum electrons, known as exchange distortion, can have a significant effect in electron impact ionization, especially for the case of spin-polarized projectiles. A proper treatment of this effect can be done by using an R-matrix or Hartree-Fock calculation for the continuum electrons. Due to the computational demands of these methods, the Furness-McCarthy local potential approximation is often used. The validity of the Furness-McCarthy approximation will be determined by comparing individual partial waves from each approach. In addition to this, the importance of using relativistic wavefunctions and potentials will be examined. The theoretical results will be compared to experimental asymmetries and branching ratios from Australia National University.

*Work supported by the NSF.

SRP1 36 The role of chemi-ionization in fluorescent lamp discharges ABDUR RAHMAN, GRAEME LISTER, *Osrsm Sylvania* VALERY SHEVEREV, *Polytechnic University* Chemi-ionization processes resulting from the interaction of two excited Hg atoms have been widely used in numerical models of fluorescent lamp discharges. In particular, the Penning process $\text{Hg}(6p^3P_2) + \text{Hg}(6p^3P_2) \rightarrow \text{Hg}^+ + \text{Hg}(6p^3S_0)$ has been invoked as an important contribution to ionization and to the maintenance electric field. There is no experimental measurement of the cross section for this process and experiments to measure cross sections of other chemi-ionization reactions have been shown to be unreliable [1]. Numerical calculations of cross sections for these processes [2] indicate that they are much smaller than those previously assumed. We present a series of computations showing the influence of the calculated cross sections on the ionization balance over a range of discharge parameters. For discharge parameters appropriate to fluorescent lamps under standard operating conditions, it is necessary to invoke alternative ionization mechanisms, such as 'ladder like' ionization via higher Rydberg states, in order to reproduce the experimental results. [1] V.A. Sheverev, G.G. Lister and V. Stepaniuk, 2005, *Phys. Rev. E* **71**, 056404 [2] J.S. Cohen, R. L. Martin, and L. A. Collins, 2002, *Phys. Rev. A* **66**, 012717.

SESSION SRP2: POSTER SESSION IIB

Thursday afternoon, 12 October 2006

Buckeye, 4:00pm - 5:30pm Holiday Inn at 16:00

SRP2 1 PLASMA DIAGNOSTICS AND SURFACE INTERACTIONS

SRP2 2 A new scheme for laser-induced fluorescence measurements in Xe II plasmas* GREG SEVERN, *University of San Diego* DONGSOO LEE, NOAH HERSHKOWITZ, *University of Wisconsin-Madison* We report laser-induced fluorescence (LIF) measurements in Xe II plasmas which utilize the $5p^4(^3P_1)5d[3]_{7/2}$ metastable state. The wavelength of the excita-

tion transition is 680.574nm in air. To our knowledge, this scheme has never been used before for LIF measurements in plasmas. The complete scheme is $5p^4(^3P_1)5d[3]_{7/2} \rightarrow 5p^4(^3P_1)6p[2]_{5/2} \rightarrow 5p^4(^3P_1)6s[1]_{3/2}$, and the detectable photon has a $\lambda = 492.15\text{nm}$ in the rest frame, in air. The plasmas are created in a hot filament, DC discharge, with $kT_e \sim 1\text{eV}$, $P_o \sim 1\text{mTorr}$, and $n_e \sim 10^9\text{cm}^{-3}$. Preliminary measurements suggest that the metastable state is sufficiently populated to permit measurements of ion velocity distribution functions (ivdfs). We also report on LIF measurements in XeII plasmas using a scheme commonly¹ used in Hall-Thruster plasmas, with excitation at 834.96 nm (air), and we assess the relative merits of the schemes. We are interested in these LIF schemes for the purpose of testing the generalized Bohm Criterion in the vicinity of sheath edge for two-ion plasmas. Proving new XeII LIF schemes for these plasmas permit measurements of the ivdfs for both ions, something never before accomplished.

*Work supported by DOE grant DE-FG02-03ER54728.

¹Hargus, Jr., W.A.; Cappelli, M.A. *Appl. Phys. B* (2001), **72**, 961.

SRP2 3 Electric field distribution around a biased probe immersed in an electrical discharge* ED BARNAT, GREG HEBNER, *Sandia National Laboratories* Electric field distributions are measured around a biased probe immersed in an argon discharge. The distributions are measured as functions of probe bias, argon pressure, and distance of the probe from the 'boundary' placed on the plasma by a powered electrode. The electric fields are symmetrically distributed around the probe when the probe is placed sufficiently far from this boundary, but become asymmetric when the sheaths around both the probe and the powered electrode began to couple. For select cases, we discuss how the space charge is distributed around the probe. We also discuss perturbations in the excited $1s_4$ states that result due to the presence of the probe. In general, we note that while the measurable fields around the probe are contained in a region around the probe on the order of a Debye length ($\sim 1 \lambda_{Debye}$), these perturbations extend many Debye lengths ($\sim 10 \lambda_{Debye}$). We discuss the implication of these measurements both in terms of conventional Langmuir probes used to measure plasma parameters, as well as charged grains of dust that exhibit collective behavior leading to the formation of plasma crystals.

*This work was supported by the Division of Material Sciences, BES, Office of Science, U. S. Department of Energy and Sandia National Laboratories, a multiprogram laboratory operated by Sandia Corporation, a Lockheed Martin Company for the US-DOE.

SRP2 4 Time resolved measurement of NO destruction using Quantum Cascade Laser in the mid-infrared L. GATILOVA, A. ROUSSEAU, *LPTP, Ecole Polytechnique, Palaiseau, France* S. WELZEL, J. ROEPCKE, *INP, Greifswald, Germany* The recent development of commercially available quantum cascade laser (QCL) in the mid infrared region offers new possibility for dynamic measurements in pulsed plasmas. Such diodes work near room temperature in pulsed mode. In the present study, we use the Q-MACS system to perform in situ time resolved measurement in a pulsed DC discharge. During each diode laser pulse (80 ns), the laser frequency is scanned over the absorption line, which gives the actual time resolution. The plasma is generated in a 50 cm long cylindrical glass tube in $\text{Ar}/\text{N}_2/\text{NO} = 90/10/0.9$ at 133 Pa. The

pulse duration and current are 1 ms and 20 mA respectively. NO line (1894.15 cm⁻¹) is used. The detection limit is about 0.2% for a 80 ns single shot time resolution. Numerical computations of the NO kinetics are compared to experimental results. Work supported by German/French exchange program PROCOPE.

SRP2 5 Measurement of dust particle size and density by a laser light scattering and extinction method CHANGRAE SEON, KILBYOUNG CHAI, HOYONG PARK, KAIST YONGHYUN SHIN, KWANGHWA CHUNG, KRISSE WONHO CHOE, KAIST The measurement of dust particle density was performed using the laser light extinction method. Using two spherical mirrors, a multi-pass setup was used for lowering the measurement limit of the system. In parallel, the particle size was measured using the laser light scattering method. To self-consistently determine the time evolution of the particle size, in-situ polarization-sensitive laser light scattering was used. Polarization light intensities (incident and scattered light intensities with the same polarization) were measured at 71[r]. Before applying the method to the dusty plasmas, the measurement accuracy was confirmed using a distilled water solution of the size-known particles. In addition, the size-known particles were injected into the argon plasma, and the particles trapped inside the plasma were used for the accurate measurement of the light scattering angle. The measured size of the dust particles in a Ar+SiH₄ (5%) 13.56 MHz capacitively-coupled plasma (160 mTorr, 150 W, 10 s after plasma on) was about 118 nm, which was also confirmed by scanning electron microscope photographs. The time evolution of the particle size and its number density was studied by both methods.

SRP2 6 LIF Measurement of Argon in Ar-Xe Plasma Sheath Boundary with Tunable Diode Laser* DONGSOO LEE, NOAH HERSHKOWITZ, Dept. of Engineering Physics, University of Wisconsin-Madison GREG SEVERN, Dept. of Physics, University of San Diego The Bohm sheath criterion in single and two-species plasma is studied with Laser-Induced Fluorescence (LIF) using a diode laser. Xenon is added to a low pressure unmagnetized dc hot filament argon discharge confined by surface multipole magnetic fields. The Ar II transition sequence at 668.614 nm is adopted for optical pumping to detect the fluorescence from the plasma and to measure the Ar ion velocity distribution function as a function of position relative to a negatively biased boundary plate. The structures of the plasma sheath and presheath are measured by an emissive probe. The ion concentrations of the two-species in the bulk plasma are calculated from measured ion acoustic wave phase velocity. The measured phase velocity data combined with the argon LIF data is used to determine the Xe ion velocity. Results are also compared with previous experiments with Ar-He plasmas in which the Ar ions were the heavier ion species [1]. [1] G.D. Severn et al, Phys. Rev. Lett., 90, 145001 (2003).

*Work Supported by US DOE Grant No DE-FG02-97ER54437.

SRP2 7 Atomic oxygen and O₂(a¹Δ_g) density measurements in a Micro-Cathode Sustained Discharge in oxygen and rare gases/oxygen mixtures. L. MAGNE, G. BAUVILLE, P. JEANNEY, B. LACOUR, V. PUECH, Laboratoire de Physique des Gaz et des Plasmas, Université Paris 11, bât 210, 91405 Orsay cedex, France This work presents first experimental investigations of atomic oxygen density and O₂(a¹Δ_g) production in a Micro-Cathode Sustained Discharge (MCSD) in pure O₂ and in argon (or

helium)/O₂ mixtures for a total pressure up to 130 Torr. A micro-hollow cathode discharge (MHCD), 200 micron in diameter, is used as plasma cathode for a discharge between the MHCD and a third electrode placed 8 mm away. In pure oxygen, the absolute atom density was measured by Two-photon Absorption Laser Induced Fluorescence (TALIF). It will be shown that, for a current of 1 mA and a pressure of 50 Torr, an atomic density of 3 10¹⁵ cm⁻³ is obtained near the micro-hollow cathode, and it decreases to 5 10¹⁴ cm⁻³ near the third electrode. If the MCSD is switched off while the MHCD is still on, the atom density decreases by an order of magnitude. 2D cartography of the atom distributions will be presented for different operating conditions. The density of the O₂(a¹Δ_g) metastable state was evaluated from the intensity of the 1.27 μm transition measured with a calibrated InGaAs detector. It will be shown that O₂(a¹Δ_g) densities up to 10¹⁶ cm⁻³ have been obtained for 10% O₂ in an argon/oxygen mixture at 50 Torr. Work is in progress to determine conditions for generating higher O₂(a¹Δ_g) densities.

SRP2 8 A Novel Temperature Measurement Approach for a High Pressure Dielectric Barrier Discharge Using Diode Laser Absorption Spectroscopy ROBERT LEIWEKE, BISWA GANGULY, Air Force Research Laboratory Tunable Diode-Laser Absorption Spectroscopy (TDLAS) technique based upon peak frequency shifts, β, and collision-broadened full widths at half maximum, w_c, of argon metastable 1s₃ → 2p₂ and 1s₅ → 2p₇ transitions, separated by 22.5 GHz, was used to measure both the gas temperature and the gas density in a short-pulse excited (≈ 10 ns applied voltage rise time having ≈ 200 ns duration) argon DBD operating between 50-500 Torr, 1-4 kV total applied voltage, and 5 kHz repetition rate. TDLAS technique is well suited for high pressure environments having a small gas temperature rise (ΔT < 100 K) where the Doppler width component w_D < w_c. If there is no resonance between the absorber and the perturber and the absorbing transition terminates on a metastable state then, according to Lindholm-Foley theory, β and w_c scale as nT^{0.3} where n is number density. Using the perfect gas law, the proportionality parameters β_o (frequency shift/Torr) and Γ_o (collisional broadening width/Torr) permits self-consistent measurements of both gas temperature and density. Reproducibility and accuracy of the temperature measurements were determined through the simultaneous independent measurements of these four parameters. The effects of applied voltage rise time on the power deposition and also metastable production efficiency will be reported.

SRP2 9 Cavity enhanced spectroscopy on micro spheres levitated in a plasma* RALF BASNER, GABRIELE THIEME, JOERG EHLBECK, JUERGEN ROEPCKE, INP Greifswald, Germany HOLGER KERSTEN, University Kiel, Germany JONATHAN P. REID, University of Bristol, UK PAUL B. DAVIES, University of Cambridge, UK Cavity enhanced spectroscopy has been successfully used as a diagnostic for aerosol droplets. In the present experiments the feasibility of applying this technique to solid micron sized particles levitated in an rf-plasma has been studied. A pulsed laser is used to excite whispering gallery modes in individual micro spheres leading to enhanced Raman scattering at corresponding wavelengths. The investigation of particles coated with fluorescent dye demonstrates the surface sensitivity of cavity enhanced spectroscopy. This non-invasive method gives direct access to the size and also the chemical composition of the micro spheres, and is so a very interesting tool for

the characterisation of growing layers deposited onto micro-particles i.e. in molecular plasmas. For particle investigation, an asymmetric capacitively coupled rf-discharge containing two electrodes is used. The upper electrode is rf-driven. The lower adaptive electrode (AE) is divided into ca. 100 square segments which can be biased individually with a DC-voltage allowing a specific manipulation of the particle position.

*Work supported by DFG, SFB/TR24.

SRP2 10 Spread function of real Fabry-Perot interferometer in imaging spectroscopy of inhomogeneous plasma* ALEKSANDR KRAVCHENKO, LIDIA LUIZOVA, ALEKSEI SOLOVEV, *Petrozavodsk State University* Working in the field of imaging spectroscopy of inhomogeneous plasma by spectrum line profile, we had found what additional parameters of real Fabry-Perot interferometer (FPI) impacts on its spread function. These parameters are parallelism degree and quality of polishing of the mirrors. But it is very difficult to model impact of these parameters on ideal mathematical FPI, because discreet model can describe very well alteration of the interferometer base. But, if we will integrate over surface of the mirror in this model, we will find two extra effects: different reflection angles in different points of the mirrors, caused lack of parallelism of the mirrors and wave refraction, caused differences between optical densities of the mirror's material and of the air. It is very important to describe as minimum this three effects, impacts on spread function of the interferometer, because even 100 nanometers FPI base differences in opposite parts of the mirrors may make interferometer impossible for usage. In our last research we try to make a model of real FPI, when it uses in imaging spectroscopy equipment.

*The research described in this publication was made possible in part by Award No. PZ-013-02 of the U.S. Civilian Research & Development Foundation (CRDF), of Ministry of Education of Russian Federation and of Government of Republic of Karelia.

SRP2 11 A Spatial Heterodyne Spectrometer for Plasma Spectroscopy* J.E. LAWLER, Z. LABBY, F. L. ROESLER, *Univ. of Wisconsin, Madison, WI* J. HARLANDER, *St. Cloud State Univ., St. Cloud, MN* Spatial Heterodyne Spectrometer (SHS) designs will revolutionize interferometric spectroscopy in the VUV. Advantages of interferometric spectrometers include: (1) a very high spectral resolving power with a large etendue, (2) excellent absolute wavenumber accuracy, (3) extremely broad spectral coverage, and (4) high data collection rates. Interferograms from a conventional Fourier transform spectrometer (Michelson interferometer) are recorded as a function of time using a single channel detector while moving a mirror. Interferograms from an SHS are spread in space across a detector array. The lack of moving parts means that an SHS is compatible with low duty cycle, transient sources common in the VUV. Our SHS has a CaF₂ beamsplitter and a matched pair of very coarse (23.2 groove/mm) echelle gratings blazed for 63.5[r]. Key mechanical components have temperature compensated designs and many parts, including the entire optical bread board, are made of Invar for long term phase stability. The 96 mm wide gratings are compatible with a theoretical limit-of-resolution of 0.058 cm⁻¹ (inverse maximum path difference of 2 x 9.6 cm x sin 63.5[r]) using a symmetric interferogram. The quality of interferograms recorded with a low resolution test camera indicated that the optics and mountings is satisfactory. First results with the full resolution 4 Mega-pixel VUV compatible CCD camera will be reported.

*Supported by NASA.

SRP2 12 Determining Plasma Conditions from Experimental Spectral Data Using Pegasys NICOLAS PEREYRA, JOSEPH MACFARLANE, PAMELA WOODRUFF, IGOR GOLOVKIN, PING WANG, *Prism Computational Sciences, Inc.* PEGASYS is a software tool used in the analyses of experimental spectra. Operating on an imported experimental spectrum, PEGASYS supports continuum background subtraction, wavelength calibration, and fitting to spectral lines. In addition, PEGASYS computes the best fit of an experimental spectrum to PrismSPECT results, thereby finding temperatures and densities most representative of the plasma. PrismSPECT is a collisional-radiative spectral analysis code designed to simulate the atomic and radiative properties of LTE and non-LTE plasmas spanning a wide range of conditions. For a grid of user-specified plasma conditions, PrismSPECT computes spectral properties (emission and absorption), ionization fractions, atomic level populations, atomic transition rates, and line intensities and ratios. In designing PEGASYS and PrismSPECT, a strong emphasis has been placed on ease of use. It features a user-friendly, graphical interface for setting up problems, monitoring the progress of simulations, and viewing results. Recent enhancements to PEGASYS, including line identification and curve fitting, will be discussed.

SRP2 13 Electron-Beam Produced Air Plasma: Optical and Electrical Diagnostics* ROBERT VIDMAR, *University of Nevada, Reno* KENNETH STALDER, *Stalder Technologies and Research* MEGAN SEELEY, *University of Nevada, Reno* High energy electron impact excitation is used to stimulate optical emissions that quantify the measurement of electron beam current. A 100 keV 10-ma electron beam source is used to produce air plasma in a test cell at a pressure between 1 mTorr and 760 Torr. Optical emissions originating from the N₂ 2nd positive line at 337.1 nm and the N₂⁺ 1st negative line at 391.4 nm are observed. Details on calibration using signals from an isolated transmission window and a Faraday plate are discussed. Results using this technique and other electrical signal are presented.

*This work is supported by the Air Force Research Laboratory, under grant numbers FA9550-04-1-0015 and FA9550-04-1-0444; and State of Nevada funds.

SRP2 14 In-situ characterization of oxygen plasma surface etching/modification by Infrared-Visible Sum Frequency spectroscopy DARCIE FARROW, EDWARD BARNAT, PAUL MILLER, GREG HEBNER, *Sandia National Laboratory* Unlike many other techniques used to characterize surfaces under plasma exposure, Infrared-visible sum frequency (IVSF) generation is a surface specific probe molecular vibrations that can be carried in situ to follow molecular interactions and plasma initiated chemistry at the interface in quasi real time. We present an in-situ characterization of octadecyltrimethoxysilane monolayers and common industrial polymers (polypropylene, polyethylene, polystyrene) on Quartz in the presence of a DC oxygen plasma and an atmospheric pressure glow discharge using IVSF. Analysis is based on hydrocarbon lines in the IVSF spectra as a function of plasma exposure time, voltage and oxygen pressure. This test system will be used to demonstrate the unique advantages and limitations of IVSF as an in situ surface diagnostic in plasma systems. This work was supported by the Division of Material Sciences, BES, Office of Science, U. S. Department of Energy and Sandia

National Laboratories, a multiprogram laboratory operated by Sandia Corporation, a Lockheed Martin Company for the United States Department of Energy's National Nuclear Security Administration under contract DE-AC04-94AL85000.

SRP2 15 Space and phase resolved electron energy distribution functions in an industrial dual-frequency capacitively coupled radio-frequency discharge* JULIAN SCHULZE, TIMO GANS, DEBORAH O'CONNELL, UWE CZARNETZKI, *Institute for Plasma and Atomic Physics, CPST, Ruhr-University Bochum, Germany* BERT ELLINGBOE, MILES TURNER, *NCPST, Dublin City University, Ireland* The excitation dynamics in a confined dual-frequency plane parallel CCRF discharge (Exelan, Lam Research Inc.), operated at 1.94 MHz and 27.12 MHz is investigated by phase resolved optical emission spectroscopy. The emission from different rare gas lines in a He-O₂ plasma with small rare gas admixtures is measured during one low frequency RF-cycle resolving the dynamics within every high frequency cycle with one dimensional spatial resolution along the discharge axis. In a detailed analysis a time dependent model, based on rate equations, is developed, that describes the dynamics of the population density of excited levels. Electron impact excitation out of the ground state, quenching, reabsorption and cascades are taken into account. Based on this model and the comparison of the excitation of various rare gas states, with different excitation thresholds, time and space resolved electron temperature and propagation velocity of the high energetic, directed electrons, heated at the sheath edge, are determined. These parameters reveal the time and space resolved electron energy distribution function.

*Funding: Lam Research Inc., SFI, the EU (FP5), the DFG (SFB 591 & GK 1051).

SRP2 16 Comparison of excitation temperature and electron temperature in low pressure argon plasmas HOYONG PARK, JUNKYU RHEE, JUNGHEE KIM, JONGSUB LEE, SEONGHUN LEE, SHINJAE YOU, HONGYOUNG CHANG, WONHO CHOE, *KAIST* Compared to other active diagnostic methods, the optical emission spectroscopy (OES) method using an emission spectrum from the plasmas has a benefit of non-intrusive, in-situ monitoring of the plasmas. In this work, a study was performed to investigate the relation between the excitation temperature (obtained by OES) and the electron temperature (obtained by a Langmuir probe) in low pressure argon plasmas. In order to compare the two temperatures for various experimental conditions, argon pressure and input power were independently varied. The collection optics consisted of an optical fiber and a bi-convex lens was used for a comparison between the local values of the two temperatures. The results so far achieved in capacitively-coupled argon plasmas of which electron energy probability function was bi-Maxwellian showed that the excitation temperature had the same tendency with the high energy part of the electron temperature as the rf power and the pressure were increased. From the results, the measured excitation temperature can be used as an indicator of electron temperature variation, which may be applicable to the plasmas where non-intrusive diagnostic methods are required such as in large area plasmas for LCD plasma processes.

SRP2 17 Gas temperature measurements in a microcathode sustained discharge in oxygen V. PUECH, J.F. LAGRANGE, N. SADEGHI, M. TOUZEAU, G. BAUVILLE, B. LACOUR, *CNRS LSP (GRENOBLE) TEAM, LPGP (ORSAY) TEAM* Microcathode sustained discharges (MCSD) produced between a microhollow cathode discharge (MHCD) and a third electrode offer the

possibility to produce high density plasmas at low E/N values. Such discharges in oxygen could be attractive for efficient production of singlet O₂ if the gas temperature remains low. The temperature of a discharge in oxygen at 50 Torr and for currents up to 2 mA and E/N of 25 Td was measured through a spectroscopic investigation of the plasma emission. The spatial distribution of the O₂(b¹Σ) and O(5p) was measured. These species have a very different behaviour: O(5p) is mainly produced inside the hole of the 0.2 mm diameter MHCD and its density decreases by two orders of magnitude over a distance of 3 mm. On the other hand, the O₂(b¹Σ) production by the MHCD is very low, and this state is mainly produced in the MCSD, with a smooth density gradient in the interelectrode gap. The gas temperature was determined in the MCSD from the high resolution spectra of the atmospheric band at 760 nm, while the gas temperature inside the hole of the MHCD was measured through the rotational spectra of the 337 nm 2nd positive band of nitrogen, introduced at low concentration in the discharge. In our experimental conditions, the gas temperature in the MHCD is lower than 650 K and less than 400 K in the MCSD.

SRP2 18 Radical Production in a Short-Pulse Excited, Flowing Gas Atmospheric Pressure Dielectric Barrier Discharge J.M. WILLIAMSON, P. BLETZINGER, D.D. TRUMP, *Innovative Scientific Solutions, Inc* B.N. GANGULY, *Air Force Research Laboratory* The production of plasma-chemical radicals in a short-pulse excited atmospheric pressure Ar / H₂O or He / H₂O dielectric barrier discharge as a function of gas flow rate and H₂O concentration was investigated. The plasma emission of excited Ar, He, OH, and N₂⁺ at 750, 706, 308, and 391 nm, respectively, were recorded for various flow conditions and H₂O concentrations as well as applied voltage. The change in plasma emission with different conditions was measured either by temporally integrated dispersed emission with a spectrometer/CCD or temporally resolved, wavelength selected emission with a spectrometer/gated PMT. The OH radical production increased with applied voltage and also with small additions of water but the emission was greatly reduced with higher water concentrations. The temporally-resolved OH and N₂⁺ emission was delayed with respect to the excited Ar and He emission due to the heavy particle production of OH and N₂⁺. The radical production as function of applied voltage, gas flow rate, and gas mixture will be presented.

SRP2 19 Monte Carlo simulation of the profiles of Hα emission in hydrogen Townsend discharges at high E/N* ZORAN PETROVIC, VLADIMIR STOJANOVIC, *Institute of Physics, Belgrade* Our goal is to calculate Hα emission from Townsend discharge in pure hydrogen between two parallel electrodes. Monte Carlo simulation technique was used to follow electrons and heavy particles for the conditions of high electric field (E) to gas density (N) ratios E/N... We used simple cross section sets for heavy particles, as provided by A.V. Phelps, where fast H atoms were produced by charge transfer collisions of H⁺, H₂⁺, H₃⁺ with H₂ and with the surface. After collisions we followed trajectories of all reaction fragments until their neutralization or thermalization down to the Hα excitation energy... As a result, for the conditions of experiment, we obtained spatially resolved emission profiles and end on Doppler broadened profiles. Agreement of Monte Carlo with experimental results supported prediction that the main excitation channel of Hα emission proceeds via fast H atoms.

*The work presented here was performed under MNZZS project 141025 (formerly 1478).

SRP2 20 Decomposition of N-Isopropylacrylamide in low-pressure helium plasma* HORACIO MARTINEZ, YAMILET RODRIGUEZ-LAZCANO, *Universidad Nacional Autonoma de Mexico* Emission spectroscopy was applied to observe decomposed species of N-Isopropylacrylamide (N-iPAAM) exposed to He plasma, which was generated by AC discharge at the pressure of 3.0 Torr. In the diagnosis measurement, several emission peaks assigned to the H_{α} and H_{β} atomic lines, CH_3O , CN ($B^2\Sigma-X^2\Pi$), CH ($A^2\Delta-X^2\Pi$), and C_3H_5 , CN , CHO , CH_2O and $C_4H_2^+$ transitions were observed and measured at various discharge times. The present results shows the presence of C_4H_2 and $C_4H_2^+$ which is not present in great concentration in the simulation done by Herrebout et al (IEEE Transactions on Plasma Science 31 (2003) 659), who used a one-dimensional fluid model for an RF acetylene discharge. The time dependence of the emission intensities was also investigated. When the discharge time of He plasma was increased, the emission intensities of the observed transitions also increased and then gradually decreased.

*This research was partially sponsored by DGAPA IN-109103 and CONACyT 41072-F.

SRP2 21 HIGH PRESSURE, LIGHTING, AND CHEMISTRY

SRP2 22 Low-pressure indium-bromide discharges for sustainable lighting PETER VANKAN, *Philips Lighting, PO Box 80020, 5600 JM, Eindhoven, The Netherlands* PIET ANTONIS, ARIEL DE GRAAF, Lighting up today's world requires massive amounts of energy: 20% of the world's electricity consumption is used for lighting, which illustrates nicely that energy efficiency is a key issue in sustainable lighting. Of all light produced, roughly half comes from low-pressure mercury vapour lamps. These lamps are limited to around 110 lm/W due to the Stokes-losses in the phosphor conversion. Therefore, to make a more energy efficient lamp, the mercury has to be replaced by another filling. This contribution will present a discharge based on indium-bromide that emits mainly in the UVA and visible region instead of the UVC, which strongly reduces the Stokes-losses and therefore offers the potential of a high energy efficiency. On top of that, the indium-bromide discharges are mercury-free, which gives an extra impulse for sustainable lighting. In this contribution we will show the indium-bromide discharge efficiency as a function of filling pressure and type of starting gas, diameter and coldest spot temperature. A maximum discharge efficiency of around 50% has been reached in a capacitively coupled lamp.

SRP2 23 Modelling Metal-Halide Lamps with Plasimo* JAN VAN DIJK, BART HARTGERS, MARK BEKS, WOUTER BROK, JOOST VAN DER MULLEN, *Eindhoven University of Technology* After a general introduction of the plasma simulation model Plasimo, being developed at Eindhoven University of Technology, we will discuss its application to the modelling of metal-halide lamps. The underlying model is based on a quite complete description of the plasma. It involves non-equilibrium plasma chemistry, the barycentric flow field, the gas temperature, spectrally and spatially resolved radiation transport and the electromagnetic field. Special attention will be paid to the elemental

diffusion sub-model, a non-equilibrium description of the plasma composition that is able to reproduce the process of elemental de-mixing. This convection-driven phenomenon is responsible for axial inhomogeneities in light output. This effect has been studied under various gravity conditions both on earth and in the International Space Station (ISS). A comparison with these experiments will be made. Plasimo (including the source code) is in principle available for fellow researchers. Interested parties are invited to contact the author or visit the Plasimo website, <http://www.dischargemodelling.org>.

*This research is sponsored by the Dutch Science Foundation STW

SRP2 24 Characterization of a cascaded arc - an extremely bright light source DANIEL SCHRAM, R. ZIJLMANS, J. GOUDSMITS, R. ENGELN, *Technische Universiteit Eindhoven* The need for a high intensity light source in spectroscopic applications like cavity enhanced absorption spectroscopy and spectroscopic ellipsometry is obvious, because it potentially leads to more accurate measurements in terms of signal to noise ratio. In this contribution we present an intense and stable broadband light source, a cascaded arc, and a thorough characterization of its light output and modulation possibilities. The light output is spectrally characterized in terms of absolute spectral radiance, which is determined by calibrating the used spectrometers with a tungsten bandlamp, which exhibits a known spectral light output. Furthermore we show the use of an extremely fast, flexible and surprisingly accurate modelling scheme, called: Flexible Approximate Simulation of a Thermal plasma (F.A.S.T.), to investigate the optimal geometry of the arc channel. The agreement between calculated and measured continuum emission is excellent: they show both an appreciable improvement in brightness of the source when the source channel is profiled.

SRP2 25 Striations in a low pressure RF-driven argon plasma W.J.M. BROK, H.C.J. MULDER, W.W. STOFFELS, *Eindhoven University of Technology, The Netherlands* In experiments we observed spatially periodic modulations of the light emitted by an argon plasma in a tube of 30 cm length and 2.5 cm radius. The plasma is capacitively excited by RF electrodes positioned towards the ends of the tube. The argon pressure is approximately 2 Torr. We studied the space and phase dependence of the light emitted by the spheroidally shaped striations. Temporal phase-shifts within one striation were clearly visible. Furthermore, a simple model of the electric field modulation inside the tube was used in conjunction with a Monte Carlo model in order to study the electron kinetics in the tube. The excitation rates resulting from this model are compared with the measurements.

SRP2 26 Wall Effects on Electron Beam Generated Plasmas.* DARRIN LEONHARDT, SCOTT WALTON, RICHARD FERNSLER, *US Naval Research Laboratory, Plasma Physics Division* Electron beam generated plasmas have been shown to possess intriguing characteristics for plasma processing applications such as low electron temperatures, high plasma densities and the capability to ionize all gases uniformly and in proportion to their relative concentrations. In this work, we discuss the effects of large versus small ionization-to-chamber volume ratios; i.e. what happens to the steady-state plasma as the system volume is decreased around the electron beam? At first glance, the presence of walls appears inconsequential. However, even in a modulated sys-

tem, the walls affect the electron temperature as well as the magnitude and distribution of the plasma densities. Time resolved data from in situ diagnostics (electrostatic probes and mass spectrometry) and theoretical expressions will be compared for various configurations of the chamber volume with fixed ionization regions.

*This work is supported by the Office of Naval Research.

SRP2 27 Generation of Negative Ions in Pulsed Boron Trifluoride Glow Discharge LUDOVIC GODET, SVETLANA RADOVANOV, JAY SCHEUER, *Varian Semiconductor Equipment Associates* GILLES CARTRY, CHRISTOPH CARDINAUD, *University of Nantes* In earlier studies (1, 2) of boron trifluoride pulsed discharges significant dependence of the plasma parameters upon the negative ion formation was observed. In these plasmas negative ions can reach relatively high densities $2\text{--}5 \cdot 10^9 \text{ cm}^{-3}$ which are comparable to the electron density. We have measured the ion energy distributions of positive and negative ions under various discharge conditions. The influence of negative ions on transport properties of charged particles, plasma parameters and structure of the sheath will be discussed. The role of heavy molecular ions in the process of ion-ion recombination is evaluated. [1] S. Radovanov, et al., JAP, 98, 113307, 2005. [2] Ludovic Godet Thesis, 2006, University of Nantes, France.

SRP2 28 Cold Jet Plasma Studies by Cavity Ring Down Absorption Spectroscopy (CRDS) PATRICK DUPRE, *The Ohio State University* SHENGHAI WU, TERRY MILLER, Reactive intermediates are of crucial importance both for combustion and atmospheric chemistry. We have set up a cold radical plasma source based on a pulsed slit jet supersonic expansion (5 cm long) and a transverse DC discharge. This source is inserted inside a CRDS cavity running in the near and mid infra-red ranges (the high resolution laser source is described in the second paper). We will present results obtained in the rotational temperature range of 15 to 30 K on various species including the metastable nitrogen (transition: $B^3\Pi_g(v'=2) \leftarrow A^3\Sigma_u^+(v''=4)$), hydroxyl radical (first overtone), methyl radical (fundamental transition of the antisymmetric CH stretch mode) and preliminary results on the weak $\tilde{A} - \tilde{X}$ transition of methyl peroxy (CH_3O_2). Density number of certain of these unstable species can reach $\sim 4 \times 10^{14} / \text{cm}^3$ inside the throat.¹ Sensitivities better than 40 ppb/pass/ $\sqrt{\text{Hz}}$ have been reached.

¹S. Wu, P. Dupr and T.A. Miller, Phys. Chem. Chem. Phys. 2006, 8, 1682

SRP2 29 High efficiency for dioxin dehalogenation using an electron source with a carbon nanotube MICHITERU YAMAURA, *Inst. for Laser Tech.* SHIGEAKI UCHIDA, *Tokyo Inst. of Tech.* CHIYOE YAMANAKA, *Inst. for Laser Tech.* We propose the application of an electron source with a carbon nanotube (CNT) for the dehalogenation of dioxin [1]. The dioxin consists of some amount of chlorine. As the chlorine content is increased, a highly poisonous dioxin is produced. It is clarified that a lot of electrons supply around the chlorine is treated on dioxin by dehalogenation due to the electron affinity of chlorine is very strong. Moreover, the dehalogenation treats on the dioxin without producing toxic by-products. To date, it has been confirmed that o-chlorophenol further the procession materials of dioxin is dehalogenated by utilizing electrons generated around a non-

equilibrium plasma. However, a rate of approximately 50% is not expected to be found for the dehalogenation because the number of electrons supplied by the non-equilibrium plasma is low. It is well-known that the CNTs have a high aspect ratio, high mechanical strength, and good chemical stability. Hence, the rate of dehalogenation drastically increases due to the abundant supply of electrons when a CNT electron source is used. The dehalogenation of o-chlorophenol with high or low concentration using the CNT electron sources and the characterizations of the CNT will be discussed. *A part of this work is supported by a Grant-in Aid for Young Scientists (B) Research of the Ministry of Education, Science, Sport and Culture, Japan. [1] M. Yamaura, and S. Uchida Japanese patent pending to be submitted 1 June 2006.

SRP2 30 Decomposition of Volatile Organic Compounds under Low-Energy Pulsed-Electron Beam Irradiation* MASATO WATANABE, *Tokyo Institute of Technology* ASUNA FUKAMACHI, AKITOSHI OKINO, EIKI HOTTA, KWANG-CHEOL KO, *Hanyang University* Development of treatment system of gaseous pollutants including some toxic substances, such as nitrogen oxides (NO_x) and volatile organic compounds (VOCs), is one of the important technological research subjects. It is well known that the non-thermal plasma processes using electrical discharge or electron beam are effective for the environmental pollutant removal. Especially, the electron beam can efficiently remove pollutant, because a lot of radicals which are useful to remove pollutant can be easily produced by high-energy electrons. In present study, decomposition of VOCs under electron beam irradiation was experimentally investigated in order to examine the kinetics of the process and to characterize the reaction product distribution. The experiments were carried out using a compact 100 kV secondary emission electron gun (SEEG). SEEG is based on ion induced secondary emission phenomena, uses a thin tungsten wire pulsed glow discharge device as a wire ion plasma source. Benzene and toluene were selected as representative VOC compounds. The experimental results indicate better benzene and toluene removal efficiencies and the SEEG represents a promising technology for the treatment of VOCs.

*This research was partially supported by the Ministry of Education, Science, Sports and Culture, Grant-in-Aid for Scientific Research (B).

SRP2 31 Dynamics of ionization fronts during high-pressure gas breakdown. DMITRY NIKANDROV, LEV TSENDIN, *St.Petersburg State Politechnical University, St.Petersburg, Russia* ROBERT ARSLANBEKOV, VLADIMIR KOLOBOV, *CFD Research Corporation, Huntsville, AL, USA* Dynamics of gas breakdown is important for numerous high-pressure plasma applications. This paper presents an analytical theory and numerical simulations of the high-pressure gas breakdown. The problem of discharge evolution after applying an external voltage $U(t)$ is divided into two sub-problems. The first sub-problem deals with the itroforce anode front initiated by the electrons present in the gap before the voltage was applied. An analytical solution for the ionization front dynamics is obtained by neglecting electron diffusion and assuming small variation of the electric field compared to the density variation. Expressions for the electron and ion densities, drift velocities, and the electric field are obtained. At the evolution stage, when $U(t)$ is decreasing, the formation of an itantiforce cathode-directed ionization front is possible. The second problem treats the evolution of the itantiforce (cathode directed) ionization front, which is initiated by the electrons generated up-

stream with respect to the electron drift. The situation, in which these electrons are emitted from the cathode, is analyzed. When the field perturbation becomes significant, the plasma region is formed, and the plasma boundary moves towards the cathode. The numerical and analytical solutions are in good agreement.

SRP2 32 γ action of metastable atom in Ar micro gap SUSUMU SUZUKI, HARUO ITOH, *Chiba Institute of Technology* To separate γ process that consisted of γ_i , γ_m and γ_p , Monte Carlo simulation (MCS) was performed [1] for the preparation. Generated numbers of ion, metastable atom and photon were calculated, and the feedback effect of those particles was investigated. It was ensured that the ratio of the ion returned to the cathode occupies 71% among the sum of those particles. Therefore, it was considered that main action of γ was γ_i by the ion returning to the cathode. However, it is evident that the metastable Ar having the long lifetime and high potential energy higher than 10 eV occupies 11% among the three kinds of particle. Therefore it is necessary to consider about the attribution of metastable atom for γ action. Rate of metastable Ar that arrives to the cathode is calculated from the solution of the diffusion equation [2] that can take account of the reflection of metastable Ar on the surface of electrodes. The diffusion coefficient of metastable Ar [3] and the collisional quenching rate coefficient [3] of metastable Ar by Ar in ground state are used for the estimation. The reflection coefficient [2] of metastable Ar at the electrodes is calculated as 0 using a boundary condition of the third kind. Approximately 30% of the metastable Ar enters the cathode. Therefore, the influence on the current by the γ action of the metastable Ar is small, but it can not be neglected. [1] S. Suzuki and H. Itoh, submitted to Jpn. J. Appl. Phys. [2] S. Suzuki, H. Itoh, N. Ikuta and H. Sekizawa, J. Phys. D, **25** (1992) 1568-1573. [3] A. H. Futch and F. A. Grant, Phys. Rev. **104** (1956) 356-361.

SRP2 33 Study of a Filamentary Dielectric Barrier Discharge in Air at Atmospheric Pressure SEBASTIEN CELESTIN, *EM2C - Ecole Centrale Paris / LPTP - Ecole Polytechnique* BARBAR ZEGHONDY, *EM2C - Ecole Centrale Paris* OLIVIER GUAITELLA, *LPTP - Ecole Polytechnique* ANNE BOURDON, *EM2C - Ecole Centrale Paris* ANTOINE ROUSSEAU, *LPTP - Ecole Polytechnique* Dielectric Barrier Discharges (DBD) at atmospheric pressure have many applications, for instance ozone production, surface treatment, and waste gas treatment. Generally, such a discharge is filamentary but it can be diffuse under particular conditions. Understanding the formation of the filament, which is an ionization wave or so-called "streamer," is very hard theoretically, numerically, and experimentally. This is due, first, to the non-linearity of the equations concerned, and second, because of the scaling in space and time of this phenomenon: a streamer has a radius on the order of a few microns, and propagates through distances of several centimeters in a few nanoseconds. In this study we will present the results obtained in experiments and in simulations for a plane-to-plane DBD. We electrically characterized this device and have observed collective effects that are still poorly understood. A point-to-plane DBD has also been studied for producing a much more localized discharge. In parallel with the experimental study we have developed a numerical model based on the Immersed Boundary Method (IBM) to introduce an electrode having a complex geometry into a structured Cartesian mesh. The first results of the code will be discussed.

SRP2 34 Study of UV efficiency of a plasma display panel in Ne/Xe/He mixtures HOYUL BAEK, TAESANG LEE, YONGSEOK JHO, *Korea Advanced Institute of Science and Technology* CHOONGSEOCK CHANG, *Korea Advanced Institute of Science and Technology & New York University* Plasma display panel is a mature technology with a substantial market. In this work, there is considerable interest in improving UV efficiency in PDP by optimizing gas mixture. For this, we develop 2D particle-in-cell/monte-carlo collisions (PIC/MCC) code. Using 2D PIC/MCC code, we carry out simulations of UV efficiency of a PDP in Ne/Xe/He mixtures, and find a gas mixture for high UV efficiency. Also, we study about mechanism of the striations, which occurs on the dielectric surface of the anode at simulations using PIC code.

SRP2 35 Dynamics of Statistical Fluctuations in Low-Current Microdischarges. VLADIMIR KHUDIK, *University of Toledo* ALEX SHVYDKY, *University of Rochester* CONSTANTINE THEODOSIOU, *University of Toledo* According to the Paschen's similarity law, when the product of the gas pressure and the system dimension is kept constant, $pd = \text{const}$, discharges in small and large systems exhibit the similar behavior. However, the influence of fluctuations (as well as nonlinear processes such as, for example, stepwise ionization and radiation trapping) on the discharge dynamics in systems with different dimensions is different: Their level is higher in smaller systems, so that statistical fluctuations change dramatically the discharge behavior in microdischarges operating in Townsend regime. We present a simple model that incorporates all main processes which cause fluctuations and that allows to describe analytically their dynamics. Close analogy to an oscillator driven by a random force is revealed. In this analogy, the voltage across the discharge gap is related to a generalized coordinate, the number of ions in subsequent generations is related to a generalized momentum, and fluctuations in the number of ions (i.e. fluctuations in the generalized momentum) play, in essence, role of the random force. In the same manner as a random force, fluctuations pump "energy" in natural oscillations of the discharge current. Without dissipation they grow in time which eventually leads to disruption of the discharge. Dissipation suppresses fluctuations and limits them at some level.

SRP2 36 Double Electric Layer in Stationary Shock Structures of a Supersonic Flowing Afterglow D.J. DRAKE, J. UPADYAY, S. POPOVIC, L. VUSKOVIC, *Old Dominion University, Norfolk, VA 23529* Mutual interaction between an acoustic shock wave and weakly ionized gas produces many effects that have been studied in recent years [1]. This interaction is manifested as plasma-induced shock dispersion and acceleration, shock wave induced double electric layer, localized increase of electron temperature and density, or enhancement of optical emission. A comprehensive review of this research and its significance for high-speed aerodynamics is given in Ref. [2]. We have performed experiments in a microwave flowing afterglow system and observed the enhancement of optical radiation in the interaction of a stationary shock wave with weakly ionized argon at 100-600 Pa. The enhancement of optical radiation coincided with the calculated standoff distance of the detached shockwave. We studied the stationary shock structures, mainly using the 4p excited state populations of argon, which were measured using absolute emission spectroscopy. Oblique shock parameters were evaluated exactly for the given model geometry, which were usually spherical. We will present results at the conference. [1] S. Popovic, L. Vuškovic, Phys. Plasmas **6** (1999) 1448. [2] P. Bletzinger, B. N. Ganguly, D. Van Wie, A. Garscadden, J. Phys. D: App. Phys. **38** (2005) R33.

SRP2 37 O atom number density measurements in repetitively pulsed plasmas by two photon laser induced fluorescence MRUTHUNJAYA UDDI, NAIBO JIANG, KRAIG FREDERICKSON, YVETTE ZUZEEK, IGOR ADAMOVICH, WALTER LEMPET, *Ohio State University* We present measurements of atomic oxygen number density in high pressure, non-equilibrium plasmas created by a high repetition rate (50 kHz) – short (20 nsec) pulse duration discharge. Measurements are performed using two photon absorption laser induced fluorescence (TALIF). Atomic oxygen mole fractions are presented as a function of time after plasma initiation in oxygen/helium, air, and air/methane mixtures at pressures of approximately 60-100 torr. Two approaches will be described for absolute number density calibration, comparison with two photon xenon spectra, and chemical titration with NO₂. Diagnostic issues relevant to short pulse plasmas, in particular mitigation of electromagnetic interference, will be described in detail.

SRP2 38 Optimization of Dielectric Barrier Discharge Plasma Actuators at Atmospheric and Subatmospheric Pressures ALEXANDER LIKHANSKII, MIKHAIL SHNEIDER, SERGEY MACHERET, RICHARD MILES, *Princeton University* Asymmetric dielectric barrier discharge (DBD) plasma actuators are known to be effective in aerodynamic control. We describe a comprehensive kinetic model for asymmetric DBD actuators in air. Application of the model shows that charging of the dielectric surface plays a crucial role, acting as a harpoon. The tangential force on the gas is shown to be directed downstream in both cathode and anode half-cycles. Inefficiency of gas acceleration is due to the motion of positive ions toward the exposed electrode in the cathode half-cycle. A near-optimal voltage waveform is proposed, consisting in high repetition rate short pulses of negative voltage in combination with positive dc bias applied to the exposed electrode. Computations show that repetitive-pulse waveform can induce gas velocities similar to those in conventional sine-voltage DBD actuators at considerably lower voltages and smaller plasma sizes. Increasing the peak pulsed voltage should increase the wall jet velocity by an order of magnitude. However,

at some threshold voltage the reverse (backward-directed) breakdown occurs. A modified voltage waveform is proposed and studied that would prevent the reverse breakdown. Results of modeling for low-pressure operation are also presented.

SRP2 39 Plasma expansion and invasion in the shock measured by diode laser fluorescence D.C. SCHRAM, O. GABRIEL, P. COLSTERS, P. VANKAN, R. ENGELN, *Technische Universiteit Eindhoven* TECHNISCHE UNIVERSITEIT EINDHOVEN TEAM, Expansion from a remote thermal plasma source, for plasma processing, is first supersonic, with density and temperature dropping due to rarefaction and adiabatic cooling. The plasma then over-expands and forms a valley before it passes a stationary shock front, after which subsonic expansion occurs. If in the over-expanded region the plasma is rarefied it becomes possible that atoms or molecules from outside enter the valley, and gets scattered into the supersonic expansion, therewith effectively mixing gas from outside. This process of "invasion" has been analyzed in detail by LIF with a diode laser on argon 1s5 metastable, with measurements both parallel and perpendicular to the expansion. Acceleration, rarefaction and cooling in the first expansion are in agreement with predictions. In the valley two distributions are observed: the fast, cold supersonic and a slower hotter one coming from outside the barrel shock. This invasion is as strong as the original flux from the source. Also some measurements are shown on O metastable indicating invasion of O₂ molecules in the expansion of Ar plasma.

SESSION UR: BANQUET

Thursday evening, 12 October 2006

Salon BCD Holiday Inn at 18:00

Greg Hebner, Sandia National Laboratories, presiding

18:00

UR 1 Banquet

THURSDAY AFTERNOON | SRP2

SESSION VF1: PLASMA-SURFACE INTERACTIONS

Friday morning, 13 October 2006; Salon CD Holiday Inn at 8:00; Svetlana Radovanov, Varian Semiconductor Equipment, presiding

Invited Papers

8:00

VF1 1 Plasma-Surface Interactions on a Spinning Wall Probed by Mass Spectrometry and Auger Electron Spectroscopy.*

VINCENT M. DONNELLY, *University of Houston*

We have developed a new approach for studying plasma-surface interactions. A cylindrical substrate in the reactor wall is rotated at a variable frequency of 800 to 200,000 rpm, allowing the surface to be exposed to the plasma 40% of the time and then analyzed in differentially pumped chambers at variable times after plasma exposure. Desorption of products from the surface is detected by a chopped molecular beam mass spectrometer (MS), while adsorbates are observed by Auger electron spectroscopy (AES). We have studied oxygen and chlorine-containing plasma reactions on anodized Al. We observe desorption of Cl_2 in chlorine plasmas, O_2 in oxygen plasmas, and Cl_2 , O_2 , ClO , and ClO_2 products in Cl_2/O_2 plasmas, due to recombination reactions on the surface. Absolute desorption yields are computed from a calibration of the pressure rise in the differentially pumped MS or AES chamber. Chemisorbed Cl and O detected by AES have little if any dependence on substrate rotation frequency. From these combined results, it appears that most adsorbates are strongly bound and do not participate in recombination and desorption. Recombination of a small percentage of weakly bound species occurs with a range of rates on the rough and porous anodized Al surface. In collaboration with Joydeep Guha, University of Houston.

*Supported by ACS/PRF and the University of Houston.

Contributed Papers

8:30

VF1 2 Influence of Ion Flux, Ion Energy, Fluorine Availability, and Surface Temperatures on SiO_2 Etch Rates in FC Plasmas

CALEB NELSON, SANKET SANT, LAWRENCE OVERZET, MATTHEW GOECKNER, *University of Texas at Dallas* A long residence time (4.9 s) plasma was employed to examine plasma surface interactions. Gas and surface reactions were correlated for different F:C ratio feedgas. In situ measurements of CF_x densities and process rates were made using an FTIR multipass system and an ellipsometer, respectively. Absolute fluorine densities were measured using actinometry. It was observed that etch and deposition rates varied as a function of ion flux, ion energy, fluorine availability, and surface temperature. These parameters were varied by changing source to chuck gap, increasing chuck bias power, different feedgas, and plasma induced surface temperature changes, respectively. Etch rates were found to increase with ion flux in a limited regime. Increasing ion energy was correlated to an increase in the overall etch rate. At low bias powers, a fluorine rich environment (CF_4) produced high etch rates, while a fluorine deficient plasma (C_4F_8) transitioned to lower etch rates and deposition. Finally, increasing surface temperature was found to change the net surface mechanism from etch to deposition.

8:45

VF1 3 In-situ measurement of an accumulation and a reduction of bottom charging on a SiO_2 contact hole with a high aspect ratio in a pulsed 2f-CCP in Ar and in CF_4/Ar

TAKESHI OHMORI, TAKESHI K. GOTO, *Keio Univ.* TAKESHI KITAJIMA, NDA TOSHIKI MAKABE, *Keio Univ.* SEIJI SAMUKAWA, *Tohoku Univ.* IKUO KURACHI, *MIYAGI-OKI* It will be essential to develop in-situ diagnostics for charging damage of a surface exposed to plasma etching under close and complementary cooperation between optical and electric procedures in a top-

down nanoscale plasma etching. The charging damage to the lower level elements in semiconductor devices is a latent issue during plasma etching of a topologically patterned wafer. In our previous paper, we have experimentally demonstrated a reduction of charging potential on a SiO_2 contact hole at the aspect ratio of 5, by utilizing the acceleration of negative charges to a wafer in a pulsed 2f-CCP with a SPC operation of the bias voltage in CF_4/Ar , and temporal change of the charging potential was observed corresponding to the flux velocity distribution of positive and negative charges incident on the contact hole under the conditions of a reduction on the charging potential [1]. In this work, we focus on the bottom charging potential at the high aspect ratio of 10 in a 2f-CCP in Ar and CF_4/Ar . The charging potential is increased above 55 V at a self-bias of -220 V in Ar. The potential in CF_4/Ar is decreased as compared with that of Ar. [1] *Appl. Phys. Lett.* **83** (22), 4637-4639 (2003), *Jpn. J. Appl. Phys. Express Lett.* **44** (35), 1105-1108 (2005).

9:00

VF1 4 Production of hyperthermal neutrals on surfaces*

TATIANA BABKINA, TIMO GANS, UWE CZARNETZKI, *Institute for Plasma and Atomic Physics, CPST, Ruhr-University Bochum, Germany* D.A. KOVACS, *Institute for Applied Plasma Physics, CPST, Ruhr-University Bochum, Germany* DETLEF DIESING, *Institute of Physical and Theoretical Chemistry, University Duisburg-Essen, Germany* The production of hyperthermal neutrals through neutralisation of energetic ions impinging an electrode surface is investigated. Measurements and computer simulations are carried out for various species (H, D, He, Ar) on different surfaces (C, Al, Fe, Au, W) for energies up to a few hundred eV. All measured energy distribution functions of hyperthermal neutrals are in very good agreement with the simulation results. The fraction of reflected hyperthermal neutrals and the shape of their energy distribution function depend strongly on the mass ratio of the impinging ion and the surface material. A smaller

ratio results is: more reflected particles, a higher mean energy, and a smaller energy spread. The produced hyperthermal neutrals can be used as a tuneable beam source with controlled energy distributions. Kinetically induced electron emission from metal surfaces is investigated for hyperthermal hydrogen and deuterium projectiles. The obtained results are in agreement with computer simulations and are well described by a model for the energy dissipation into the electronic system of the metal.

*Funding: DFG (SFB 616), FZ Juelich (VI)

9:15

VF1 5 Molecule formation in plasma at surface D.C. SCHRAM, J.H. VAN HELDEN, R.A.B. ZIJLMANS, G. YAGCI, *Technische Universiteit Eindhoven* J. ROPCKE, S. WELZEL, *Institut für Niedertemperatur Plasmaphysik* O. GABRIEL, R. ENGELN, *Technische Universiteit Eindhoven* TU/E TEAM, INP TEAM With diode laser spectroscopy and mass spectrometry the

generation of new molecules is studied in two types of plasmas: an expanding thermal plasma at TU/e and a microwave discharge at INP. Molecules formed in argon plasmas with N, H, O and C containing molecules were measured in a two laboratory study. Flows, pressure and power were designed such that an appreciable portion of the admitted gases could be dissociated. The results are very similar: predominantly H₂, N₂, CO, H₂O and/or O₂ are formed and to a lesser extent, NO, HCN and NH₃, C_nH_m and CO₂. Also H₂CO is observed. Surface generation is concluded for most of the observed molecules. The surface is passivated with radicals from the plasma and the abundances of specific precursor adsorbants as H, N, OH, NH₂, NO, CH₃ etc. is apparently important for the production of new molecules. Observation of excited species as H₂(r,v), N₂* and NO₂ (shuttle glow) near to surfaces at high fluxes of radicals forms a further support for the surface production mechanism.

SESSION VF2: TRANSPORT THEORY AND ELECTRON DISTRIBUTION FUNCTIONS

Friday Morning, 13 October 2006; Salon B Holiday Inn at 8:00; Rainer Johnson, University of Pittsburgh, presiding

Invited Papers

8:00

VF2 1 Moment Theory of Ion Motion in Devices with Fields that Depend Upon Time and Space.*

LARRY VIEHLAND, *Chatham College*

Recent work has extended the momentum-transfer theory of drift tubes to ion traps and similar devices where the external fields vary with both position and time. Four such extensions will be discussed: two-temperature (2T) and multi-temperature (MT) theories for atomic ion-atom systems, and spherical basis and Cartesian basis theories for molecular systems. In first approximation, the various theories give sets of differential equations with collision frequencies that vary with the effective temperature(s) characterizing the relative kinetic energy of the ion-neutral collisions. Solutions of the sets of equations provide the ion number density, average velocities, average energies and average temperatures as functions of time and of position in the apparatus. Such solutions will be discussed for the Maxwell model, for rigid spheres, and for general ion-neutral interactions. Emphasis will be placed on two new predictions obtained by using the 2T and MT theories to consider non-ideal quadrupole ion traps.

*Based upon work supported by the National Science foundation under Grant No. CHE-0412411.

Contributed Papers

8:30

VF2 2 Non-isotropic non-Maxwellian Electron Velocity Distribution Functions in Low-pressure Plasmas IGOR D. KAGANOVICH, *Plasma Physics Laboratory, Princeton University* DMYTRO SYDORENKO, *University of Saskatchewan, Saskatoon, Canada* YEVGENY RAITSES, PPPL ANDREI SMOLYAKOV, *University of Saskatchewan* We show that at very low pressures, the Electron Velocity Distribution Functions (EVDF) can become non-isotropic and non-Maxwellian. Specifically, plasmas in Hall thrusters are studied. Such plasmas are sustained at low neutral gas pressure, where the electron mean free path is large compared with thruster dimensions and the electron motion is almost collisionless. Particle-in-cell simulations show that electrons tend to stratify into different groups depending on their origin and confinement condition (i.e. whether they are trapped or not by the plasma potential). These different electron groups have to be treated separately, as they have completely different properties and cannot be lumped together into one Maxwellian EVDF, which

is implicitly assumed by the fluid approach. Moreover, the EVDF is found to be strongly non-isotropic due to the large electric field directed parallel to the walls and high plasma losses to the wall, especially in presence of strong secondary electron emission pertaining to Hall thrusters. Typically, the temperature in the direction of the electric field is a factor of two larger than that in the direction towards the walls.

8:45

VF2 3 Townsend Discharge in Methane at Very High E/N* ZELJKA NIKITOVIC, *Assistant Research Professor* ALEKSANDRA STRINIC, *Assistant Research Professor* VLADIMIR STOJANOVIC, OLIVERA SASIC, GORDANA MALOVIC, ZORAN PETROVIC, *Research Professor* INSTITUTE OF PHYSICS TEAM, We show preliminary comparisons between experimental data and Monte Carlo simulations for the spatial profiles of excitation coefficients for the molecular band CH (A₂ - X₂) produced in dissociative excitation by electron swarms and fast neutrals in methane. Measurements were made in parallel plate drift tube for E/N values between 500 Td and 11000 Td (E- electric

field, N - gas density, $1 \text{ Td} = 10^{-21} \text{ Vm}^2$). The spatial profiles of emission reveal significant heavy particle excitation even at moderately high E/N . Calculated absolute profiles are in excellent agreement with the experimental results. The calculations were based on the heavy particle cross sections of Petrović and Phelps [1]. [1] Z. Lj. Petrović, A. V. Phelps (1992) unpublished.

*141025 MNSTR

9:00

VF2 4 Probe diagnostics in low pressure dc discharge. Does the Langmuir Paradox exist? VALERY GODYAK, BEN AL-EXANDROVICH, ABDUR RAHMAN, *Osram Sylvania* Maxwellian electron energy distributions in a highly non-equilibrium plasma of low pressure dc discharges is one the oldest and fascinating mysteries of gas discharge physics. There is extensive literature and many hypotheses attempting to explain this paradox,

but the problem still remains unsolved. In this report we present results on the EEDF measurement in the positive column of a dc discharge in mercury vapor with differently oriented probes placed along the positive column over a wide range of discharge current showed that: a) - the EEDF is not Maxwellian, b) - is essentially anisotropic, c) - is not in equilibrium with discharge current (i.e. EEDF changes along the positive column), d) - the electron temperature inferred from the measured EEDF and that determined by the slope of the probe characteristic in semi-log scale are essentially different, e) - the linearity of the probe characteristic in semi-log scale (the sign of a Maxwellian EEDF) may occur at essentially nonlinear dependence of the second derivative of the probe characteristic on the probe voltage in semi-log scale. The main conclusions of this study are: a) - the absence of Maxwellian EEDF in the low pressure dc discharge and b) - the Druyvesteyn method is not applicable for measurement of highly anisotropic EEDF typical for the Langmuir Paradox condition.

SESSION WF1: CAPACITIVELY COUPLED PLASMAS

Friday morning, 13 October 2006; Salon CD Holiday Inn at 10:00; Miles Turner, Dublin City University, Ireland, presiding

Invited Papers

10:00

WF1 1 Negative Ions in Dual-Frequency Capacitively Coupled Fluorocarbon Plasmas.*

JEAN-PAUL BOOTH,[†] *Ecole Polytechnique*

Dual-frequency capacitively coupled plasmas in fluorocarbon-based gases are widely used for etching SiO_2 -based dielectric films in integrated circuit manufacture. We have studied a customized 2 + 27 MHz industrial etch reactor, running in Ar/O_2 with $\text{c-C}_4\text{F}_8$ or CF_4 gas mixtures at pressures in the region of 50 mTorr (6.6 Pa). Negative ions could play an important role in this type of plasma. The presence of negative ions will modify the positive ion flux arriving at a surface, and may even reach the surface and participate in etching. We have measured the electron density using a microwave hairpin resonator [1] and the positive ion flux with an ion flux probe [2]: the ratio of these two quantities varies strongly with gas chemistry and gives evidence for the presence of negative ions [3]. For example, by varying the flow of $\text{c-C}_4\text{F}_8$ in an Ar/O_2 mixture this ratio shows evidence of high electronegativity for high $\text{c-C}_4\text{F}_8$ flowrates. We have also measured the negative fluorine ion, F^- , density directly by high-sensitivity cavity ring-down absorption spectroscopy [4] in the wavelength range 340 to 360 nm to determine the density of absorbing F^- ions from the known photo-detachment cross-section. The F^- densities were seen to reach values in the 10^{11} cm^{-3} range, giving electronegative fractions, $\alpha = n_-/n_e$, of up to ≈ 15 when used in conjunction with the hairpin probe measurements. We acknowledge financial assistance from Lam Research Corporation. [1] Piejak et al, *J. Appl. Phys.* **95** (2004), 3785-3791 [2] Braithwaite et al, *Plasma Sources Sci. Technol.*, **5** (1996), 677-684 [3] Chabert et al, *Plasma Sources Sci. Technol.*, **8** (1999), 561-566 [4] Booth et al, *Appl. Phys. Lett.*, **88** (2006), 151502.

*In collaboration with Garrett Curley, Dragana Maric, Cormac Corr (Currently at PRL, Canberra, Australia), and Jean Guillon, LPTP, Ecole Polytechnique, 91128 Palaiseau, France.

[†]Currently at Lam Research, Fremont, CA.

Contributed Papers

10:30

WF1 2 New insights into electron heating and ionisation mechanisms in CCP discharges at low pressures* DEBORAH O'CONNELL, TIMO GANS, UWE CZARNETZKI, *Institute for Plasma and Atomic Physics, CPST, Ruhr-University Bochum, Germany* DAVID VENDER, *Port Arthur, Tasmania, Australia* ROD BOSWELL, *SP3/RSPHysSE, ANU, Canberra, Australia* Details on plasma sustainment of capacitively coupled plasmas (CCPs), at relatively low pressures when regular ohmic heating is

not efficient, are an open question for decades. The main difficulty has been the extreme diagnostics challenge. Recent advances in phase resolved optical emission spectroscopy (PROES) has allowed detailed spatio-temporal investigations of the electron dynamics, on a nano-second time scale, within the RF cycle. PROES and particle-in-cell (PIC) simulation results show that at comparatively low pressures ($< 10 \text{ Pa}$) the main ionisation channel in CCPs is via a large amplitude electron beam plasma interaction powered by the electric field of the sheath expansion into the plasma. Following this interaction and its associated waves and plasma ionisation, a resonance at the sheath edge is observed in both the PIC simulation and PROES measurements.

*Funding: DFG (SFB 591 & GK 1051).

10:45

WF1 3 Electron heating mechanisms in dual frequency capacitive discharges M.M. TURNER, *Dublin City University, Ireland* P. CHABERT, *Ecole Polytechnique, France* We discuss electron heating mechanisms in the sheath regions of dual-frequency capacitive discharges, with the twin aims of identifying the dominant mechanisms and supplying closed-form expressions from which the heating power can be estimated. We show that the heating effect produced by either Ohmic or collisionless heating is much larger when the discharge is excited by a superposition of currents at two frequencies than if either current had acted alone. This coupling effect occurs because the lower frequency current, while not directly heating the electrons to any great extent, strongly affects the spatial structure of the discharge in the sheath regions.

11:00

WF1 4 Electron heating and ionisation mechanisms in dual-frequency capacitively coupled radio-frequency discharges* TIMO GANS, JULIAN SCHULZE, DEBORAH O'CONNELL, UWE CZARNETZKI, *Institute for Plasma and Atomic Physics, CPST, Ruhr-University Bochum, Germany* BERT ELLINGBOE, MILES TURNER, *NCPST, Dublin City University, Ireland* Despite its technological importance, the complexity of power coupling mechanisms in radio-frequency (rf) discharges is not yet fully understood. Insight into power dissipation requires temporal resolution on various time scales, in particular the dynamics within the rf cycle. Electron dynamics and ionisation mechanisms in dual-frequency capacitively coupled rf discharges is investigated using phase resolved optical emission spectroscopy (PROES), resolving both the high (27.12 MHz) and low (1.94 MHz) frequency rf cycles, and particle in cell (PIC) simulations. The electron dynamics exhibits a complex spatio-temporal structure. Excitation and ionisation, and, therefore, plasma sustainment is dominated through directed energetic electrons created through the dynamics of the plasma boundary sheath. These electrons propagate through the discharge volume with finite velocity, and are predominantly produced during contraction of the low frequency sheath - not during the sheath expansion when power dissipation is highest.

*Funding: Lam Research Inc., SFI, the EU (FP5), the DFG (SFB 591 & GK 1051)

11:15

WF1 5 Nonlinear electron resonance heating in dual frequency capacitive discharges D. ZIEGLER, T. MUSSENBROCK, R.P. BRINKMANN, *Institute for Theoretical Electrical Engineering, Ruhr University Bochum, D-44780 Bochum, Germany* Capacitively coupled plasmas (CCP's) play a major role in material processing. The drawback of conventional single frequency CCP's is that the ion bombardment energy and the ion flux to the substrate itself cannot be controlled independently. The problem can be remedied by the use of dual frequency CCP's. In such sources, the ratio of the applied frequencies is obviously an important control parameter. Rauf¹ found that at large ratios (e.g., 100 kHz/13.56 MHz) the spectrum of the discharge current was just the superposition of two single-frequency spectra. For more comparable frequencies (e.g., 6.78 MHz/13.56 MHz), however, quite surprising nonlinear effects were observed. It is exactly this nonlinear behavior and its influence on the total energy budget that is dis-

cussed in this contribution - we present and analyze a nonlinear global model for a dual frequency CCP. Based on an exact analytical solution of the underlying equations we discuss the behavior of the model for various voltage ratios, frequency ratios, and gas pressures. We investigate in particular the heating at the plasma series resonance, either by direct excitation or via the nonlinear electron resonance heating mechanism².¹S. Rauf and M.J. Kushner, *IEEE Trans Plasma Sci.* **27**, 1329 (1999).² T. Mussenbrock and R.P. Brinkmann, *Appl. Phys. Lett.* **88**, 151503 (2006).

11:30

WF1 6 Global model of a Dual frequency Capacitive Discharge PIERRE LEVIF, PASCAL CHABERT, *LPTP CNRS Ecole Polytechnique* MILES TURNER, *Dublin City University* A major attraction of dual-frequency excitation is that it promises independent control of the ion flux and the ion energy. The electron heating mechanisms occurring within the dual-frequency sheath region were recently investigated by Turner and Chabert (*Phys. Rev. Letters* (2006) **96**, 205001). It was shown that the heating produced by the superposition of the two frequencies is much larger than the sum of the two frequency contributions. In the present paper, we use the heating models developed to construct a global model of a dual-frequency capacitive discharge operated in argon. For this, we must also discuss the dynamics of the sheath to obtain the equivalent of a dual-frequency Child law which relates the applied rf voltage, the electron density and the sheath size. By coupling the power and particle balance to the Child law mentioned above, one can obtain a self-consistent solution for all the plasma parameters. A major result of this model is that ion flux and ion energy are not decoupled since the low-frequency significantly contributes to plasma heating.

11:45

WF1 7 Frequency dependent ion kinetics in a 300 mm dual-frequency capacitively coupled plasma reactor G.A. HEBNER, E.V. BARNAT, P.A. MILLER, *Sandia National Laboratories* A.M. PATERSON, J.P. HOLLAND, *Applied Materials* Argon ion kinetics were measured in a dual frequency, capacitively coupled 300 mm chamber. Laser induced fluorescence measurements of the argon ion metastable lineshape yield information on the ion temperature, density and drift velocity. The spatially-resolved LIF technique is a nonperturbative probe to investigate energy deposition mechanisms, ion energy distribution functions, charge exchange reactions, neutral heating, and plasma potential gradients within the plasma. This talk will discuss ion characteristics for a single rf frequency drive (13, 60 and 160 MHz), combinations of rf drive frequencies, as well as scaling with pressure (10 - 70 mTorr), rf power, and radial position. We find that the ion density increased linearly with rf power, as did the electron density, indicating the ion metastable state is formed from direct impact ionization. The ion temperature was on the order of 500 K. Radially resolved ion drift velocity measurements show the radial drift velocity can be lower at 60 MHz than 13 MHz. Additional details will be discussed. This work was supported by Applied Materials and Sandia National Laboratories, a multiprogram laboratory operated by Sandia Corporation, a Lockheed Martin Company for the United States Department of Energy's National Nuclear Security Administration under contract DE-AC04-94AL85000.

SESSION WF2: HEAVY PARTICLE COLLISIONS, ATTACHMENT, AND RECOMBINATION

Friday morning, 13 October 2006; Salon B Holiday Inn at 10:00; Zoran Petrovic, Institute of Physics, Belgrade, presiding

Invited Papers

10:00

WF2 1 Detailed Studies of Cold and Ultracold Ions in RF Traps.

DIETER GERLICH, *Technische Universität Chemnitz*

The physics and chemistry determining the composition of the interstellar medium is quite different from other chemical systems since low densities ($< 10^7 \text{ cm}^{-3}$) and low temperatures prevail. For example, modeling the early stages of protostellar collapse requires a detailed understanding of ultracold hydrogen plasmas. This contribution concentrates on recent results in the field of cold gas phase ion chemistry, producing, modifying or destroying $C_m H_n^+$ ions and their deuterated variants ($m \geq 0, n \geq 0$). All experimental activities with charged particles are based on inhomogeneous, time dependent electric fields, created with suitable electrode arrangements. Rather complex machines have been constructed by combining for example temperature variable multi-electrode ion traps (e.g. a 22-pole trap) with atomic or molecular beams. In addition analytical tools such as laser induced reactions are used in order to understand the low energy dynamics on a state specific level. It is emphasized that reactions (in the trap or in space) often do not reach thermodynamical equilibrium, especially if traces of ortho-hydrogen are present.

Contributed Papers

10:30

WF2 2 Kinetic Energy Dependence of Endothermic Charge Transfer (KEDECT) in Xenon Ion – Hydrocarbon Collisions

CHARLES JIAO, ISSI BISWA GANGULY, ALAN GARSCADDEN, *Air Force Research Lab* KEDECT has been studied by Fisher and Armentrout (ref 1) who showed clearly the strong influence of modest rare gas ion kinetic energy in opening up dissociative charge transfer channels in silane. Charge transfers of fast xenon ions with CH_4 , C_2H_4 and C_3H_8 are studied using xenon plasma expansion through a small nozzle into low-pressure hydrocarbon gas. Branching ratios and relative reaction rates creating the parent ion and smaller molecular ions are measured under selected power levels of an rf coupled discharge. Xe^+ reacts with CH_4 to produce CH_4^+ (I) and CH_3^+ (II) in the ratio 1: 0.56 and an estimated rate coefficient $2.6 \times 10^{-10} \text{ cm}^3/\text{s}$. The $\text{Xe}^+(^2P_{1/2})$ reaction I with CH_4 is exothermic by 0.83 eV while reaction II is endothermic by 0.88 eV. The $\text{Xe}^+(^2P_{3/2})$ reactions with CH_4 are endothermic by 0.48 and 2.19 eV respectively, however mass spectrometry of the interaction region shows that the reactions do occur. The xenon plasma expansion can add up to 3 KTe kinetic energy to the ion, permitting the reactions to occur. Results for the other collision partners C_2H_4 and C_3H_8 are discussed. [1] Ellen R. Fisher and P.B. Armentrout, *J. Chem. Phys.*, 93, 4858 (1990).

10:45

WF2 3 Identification of modes of vibration in a HeNe* temporary molecule and interference effects in slow He-Ne collisions*

CRISTIAN BAHRIM, JOSEPH HUNT, *Department of Chemistry and Physics, Lamar University* The model potential for electrostatic interaction between $\text{He}(1s^2)$ and $\text{Ne}^*(2p^5 3p)$ atoms developed by Bahrim et al. (*Physical Review A* 56, 1305 (1997)) leads to 36 adiabatic electronic potentials, which were successfully tested in calculations for experiments in atomic crossed beams and discharge cells. The existence of deep potential wells below $6 a_0$ suggests that modes of vibration could form within these wells during a He-Ne collision. We identify several modes of vibration by using a Morse potential which best fits the electronic potential wells. Further, a set of transitions between vibrational-electronic states is proposed. For experimental testing

of our results an IR laser spectroscopy technique is proposed. The abundance of $\text{Ne}^*(2p_i)$ atoms after collision and successful absorption of IR photons is discussed. Also, this paper explains the oscillations observed in quantum probabilities for intermultiplet transitions between $2p_i$ states of the $\text{Ne}^*(2p^5 3p)$ atoms induced by collisions with $\text{He}(1s^2)$ atoms, which were reported in *Physical Review A* 56, 1305 (1997). Our semi-classical model explains the formation of the quantum oscillations as being the result of the interference between matter waves associated to two collisional channels near the avoided crossing region between these channels.

*We acknowledge the Research Enhancement Grant at LU for assistance.

11:00

WF2 4 Study of Vibration-Vibration and Vibration-Electronic Energy Transfer in Nitric Oxide

ALLEN WHITE, *Rose-Hulman Institute of Technology* IGOR ADAMOVICH, J. WILLIAM RICH, *The Ohio State University* The $v=1$ vibrational level of nitric oxide is populated via resonant absorption of a single line carbon monoxide laser. Higher vibrational and electronic levels of nitric oxide are populated by v-v and v-e energy transfer mechanisms, respectively. Infrared overtone emission spectra are observed via time resolved step-scan Fourier transform infrared measurements and time resolved gamma band and beta band ultraviolet emissions are also measured. Additional measurements were taken to detect associative ionization in V-V pumped NO, as well as the electron production rate. The v-v energy transfer rates are inferred by comparing time-resolved experimental results to computational models. Results indicate that current NO kinetic rate models must be modified to describe experimentally observed population rise times presented here.

11:15

WF2 5 Dissociative Electron Attachment to Acetylene

ANN OREL, SLIM CHOUROU, *Applied Science Department, University of California, Davis* Experimental studies of electron impact on acetylene show the presence of a Π^* resonance at 2.6 eV which leads to $\text{C}_2\text{H}^- + \text{H}$. These fragments both have Σ symmetry ($\text{C}_2\text{H}^-, ^1\Sigma; \text{H}, ^1S$), therefore, there must exist a curve crossing at bent geometries to explain these fragments. We per-

formed electron scattering calculations using the complex Kohn variational method to determine the resonance parameters of this system. We discuss the mechanisms leading to dissociation into the product channels and report the computed cross sections. The results are then compared to available experimental findings. Work supported by NSF PHY-05-55401.

11:30

WF2 6 State-selected predissociation of H₃ VALERY NGAS-SAM, ANN E. OREL, *Department of Applied Science, University of California Davis* Experimental studies of the predissociation of well-defined Rydberg states of H₃ have produced a complex three-body fragmentation pattern that is highly dependent on the initial state and show dramatic isotope effects. We present results of theoretical investigations for the fragmentation of selected Rydberg states of H₃ into three ground state hydrogen atoms as well as two-body predissociation into H + H₂⁺(v,j). The non-adiabatic couplings and the surfaces are taken from previous studies. The dynamics are carried out using a wave packet propagation method in full-dimensionality including the effects of the Jahn-Teller interaction. Work supported by the NSF PHY-02-44911.

11:45

WF2 7 Yield of electronically excited CN molecules from the dissociative recombination of HNC⁺ ion with electrons* RAINER JOHNSEN, RICHARD ROSATI, *University of Pittsburgh* DAPHNE PAPPAS, *Army Research Lab* MICHAEL GOLDE, *University of Pittsburgh* We report flowing-afterglow measurements of the CN(B-X) and CN(A-X) emissions from the dissociative recombination (DR) of HNC⁺ ions. A separate drift-tube study showed that the reaction Ar⁺ + HCN, the precursor reaction used in the flow-tube experiment, produces mainly HNC⁺ rather than its HCN⁺ isomer. Recombining HNC⁺ afterglows showed emissions of CN(B-X) and CN(B-A) but some arise from excitation transfer of metastable argon, Ar* + HCN. By adding xenon, Ar* atoms were removed and the pure recombination spectrum was recovered. Models simulating the ion-chemical processes, diffusion and gas mixing, were fitted to observed position-dependent CN band intensities. Absolute yields of CN(B) and CN(A) were inferred by comparing band intensities to those of CO bands from DR of CO₂⁺ ions. We conclude that the 300 K recombination coefficient of HNC⁺ is close to 2×10^{-7} cm³/s, that CN(B) is formed with a yield of ~ 20% and CN(A) with a yield of ~ 12%. The rotational temperature of CN(B) is around 2500 K, and CN(B) and CN(A) are far more vibrationally excited than predicted by the "impulse model" of Bates. This finding suggests that the recombination may involve a multistep mechanism.

*Supported by NASA.

Author Index

A

Abu Shamaleh, T.A. **FPT1 13**
 Adamovich, Igor **CT1 1, CT1 5, CT1 6, DT1 5, ET2 5, SRP1 27, SRP2 37, WF2 4**
 Adams, S.F. **FPT1 2**
 Adamson, S. **ET1 1**
 Ahn, Tai **SRP1 27**
 Ajello, Joseph M. **FPT1 33**
 Akan, Tamer **FPT2 28**
 Al-Hagan, Ola **FPT1 24**
 Al-Kuzee, Jafar **FPT2 4**
 Alexandrovich, Ben **VF2 4**
 Allan, Michael **DT2 4**
 Allegraud, Katia **FPT2 13**
 Alvarez, R. **FPT1 20**
 Alves, L.L. **FPT1 20**
 Amatucci, W.E. **GW1 3**
 Ambrico, Paolo F. **FPT1 21**
 Anderson, L.W. **FPT1 25**
 Andersson, P. **FPT1 28**
 Antonis, Piet **SRP2 22**
 Arakoni, Ramesh **DT1 2, ET2 4**
 Aramaki, Mitsutoshi **FPT2 7, FPT2 14, FPT2 33**
 Arefiev, Alexey **ET1 3**
 Arslanbekov, Robert **BT1 6, SRP2 31**
 Asahi, Daisuke **PR1 4**
 Astapenko, V. **ET1 1**
 Atzmon, M. **FPT1 4**
 Aubert, X. **QR1 2**

B

Baalrud, Scott **BT2 1, BT2 2**
 Babaeva, Natalie Y. **ET2 4**
 Babaritskii, Alexander **FPT1 47**
 Babkina, Tatiana **VF1 4**
 Baede, Tom **FPT1 46**
 Baek, HoYul **FPT1 10, SRP2 34**
 Bahrim, Cristian **SRP1 28, WF2 3**
 Bao, Ainan **CT1 6**
 Bapat, Ameya **PR1 3**
 Barnat, Edward **RR1 2, SRP2 3, SRP2 14, WF1 7**
 Barnes, Michael **RR1 1**
 Bartschat, K. **DT2 4, FPT1 31, FPT1 36, SRP1 32, SRP1 35**

Basak, A.K. **FPT1 43**
 Basner, Ralf **FPT2 10, SRP2 9**
 Basu, Sreerupa **DT1 6**
 Bauville, G. **GW2 3, SRP2 7, SRP2 17**
 Beks, Mark **SRP2 23**
 Bellm, S. **SRP1 35**
 Belostotskiy, S. **FPT2 35, SRP1 24**
 Belostotsky, S.G. **SRP1 15, SRP1 16**
 Benck, Eric **SRP1 21**
 Bengtson, Roger **ET1 3**
 Benilov, Mikhail **BT2 3, MW2 3**
 Bernard, Chad **DT1 5**
 Bhoj, Ananth N. **DT1 2, MW2 7**
 Biloiu, Costel **MW1 4**
 Biloiu, Ioana A. **MW1 4**
 Blackwell, D.D. **GW1 3**
 Blessington, Jon **SRP1 11**
 Bletzinger, P. **SRP2 18**
 Boeuf, J.P. **FPT2 29**
 Boffard, John B. **FPT1 25, FPT1 26**
 Bogdanov, E.A. **FPT2 15**
 Bohlmark, Johan **ET1 4**
 Booth, Jean-Paul **FPT2 5, SRP1 20, WF1 1**
 Boswell, Rod **WF1 2**
 Bourdon, A. **QR1 6, SRP2 33**
 Bowden, Marc **MW1 2**
 Bowden, Mark **MW1 3, MW2 5, RR2 6**
 Bradley, J.W. **FPT2 6**
 Bradley, James **GW1 1, GW1 2**
 Braginsky, O.V. **SRP1 15, SRP1 16**
 Braginsky, Oleg **FPT1 7, SRP1 17, SRP1 18**
 Braithwaite, Nicholas **FPT2 4**
 Bray, I. **FPT1 36**
 Bray, Igor **QR2 3**
 Breizman, Boris **ET1 3**
 Brinkmann, Ralf-Peter **FPT1 11, WF1 5**
 Brok, W.J.M. **FPT2 24, RR2 4, SRP2 25**
 Brok, Wouter **SRP2 23**
 Brunger, Michael **CT2 1, FPT1 23**
 Bryant, Garnett W. **MW2 8**

Buckman, S.J. **CT2 4, FPT1 36, LW2 6**

C

Cabibil, Hyacinth **RR1 6**
 Cada, Martin **GW1 2**
 Campbell, L. **FPT1 23**
 Cardinaud, Christophe **BT2 6, SRP2 27**
 Carmichael, Justine **ET1 6**
 Carr, Jerry **ET1 6**
 Cartry, Gilles **BT2 6, SRP2 27**
 Cassagne, Valerick **SRP1 20**
 Celestin, S. **QR1 6, SRP2 33**
 Cetiner, Selma **FPT2 26**
 Chabert, Pascal **BT1 4, FPT2 5, FPT2 20, WF1 3, WF1 6**
 Chae, Minchul **MW1 6**
 Chai, Kilbyoung **SRP2 5**
 Chang, Choong-Seock **FPT1 10, FPT1 18, FPT1 19, SRP2 34**
 Chang, Hongyoung **SRP2 16**
 Chen, Guangye **ET1 3**
 Chernysheva, I. **ET1 1**
 Childers, J.G. **SRP1 33**
 Cho, Han-Ku **RR1 3, RR1 5**
 Cho, Sung Won **SRP1 3**
 Cho, Sung-II **RR1 5**
 Cho, Woojin **MW1 6**
 Choe, Wonho **SRP2 5, SRP2 16**
 Choi, Ikjin **FPT2 9**
 Choi, Mi-Na **RR1 5**
 Chourou, Slim **WF2 5**
 Chu, Hsuan-Yih **BT1 2**
 Chung, Chinwook **FPT2 9, SRP1 3, SRP1 4, SRP1 5**
 Chung, Kwanghwa **SRP2 5**
 Chung, Kyu-Sun **FPT1 39, FPT1 40**
 Clarke, Greg **GW1 2**
 Clemens, N. **LW1 6**
 Coats, R.S. **FPT2 2**
 Colestock, Pat **FPT2 38, FPT2 39**
 Colgan, James **LW2 3**
 Colombo, Vittorio **MW2 4**
 Colsters, P. **SRP2 39**
 Colyer, C. **CT2 4**
 Cotzas, G. **ET1 1**

Crintea, Dragos **PR2 2**
 Curley, Garrett **FPT2 5**
 Czarnetzki, Uwe **FPT1 11, MW1 2, PR2 2, SRP2 15, VF1 4, WF1 2, WF1 4**

D

Daltrini, Andre **SRP1 10**
 Danailov, Daniel **SRP1 30**
 Davies, Paul B. **SRP2 9**
 De Armond, Mike **SRP1 31**
 De Benedictis, Santolo **FPT1 21**
 de Graaf, Ariel **SRP2 22**
 Deconinck, Thomas **GW2 4**
 DeJoseph Jr., C.A. **FPT1 2, FPT2 15, SRP1 11**
 Della Croce, Damian **FPT2 37, QR1 4**
 Demidov, V.I. **FPT2 15**
 Demidov, Vladimir **SRP1 11**
 Deminsky, M. **ET1 1, FPT1 47**
 Demura, A. **ET1 1**
 Diakomichalis, N. **FPT1 23**
 Diesing, Detlef **VF1 4**
 Dilecce, Giorgio **FPT1 21**
 Doebele, H.F. **QR1 3**
 Doherty, S. **SRP1 2**
 Donnelly, V. **FPT2 35, VF1 1**
 Douai, David **SRP1 20**
 Doughty, Douglas A. **RR2 2**
 Drake, D.J. **SRP2 36**
 Dupré, Patrick **FPT1 45, SRP2 28**
 Dyatko, N. **ET1 1**

E

Ebert, U. **FPT2 24**
 Economou, D. **FPT2 35, SRP1 24**
 Eden, J.G. **FPT1 48, FPT1 49**
 Ehiasarian, Arutun P. **ET1 4**
 Ehlbeck, Joerg **SRP2 9**
 El-Astal, Ali **FPT1 41**
 Eletsii, A. **ET1 1**
 Ellingboe, A.R. **FPT1 8, FPT2 6, FPT2 12**
 Ellingboe, Bert **SRP2 15, WF1 4**

Engeln, R. SRP2 24,
SRP2 39, VF1 5
Eriguchi, Koji LW1 3,
RR1 4
Essenhigh, Katherine
DT1 5

F

Faehl, Rick FPT2 38,
FPT2 39
Faria, Maria Jose MW2 3
Farrow, Darcie SRP2 14
Faulkner, R. MW1 3,
SRP1 2
Fehske, Holger FPT2 10
Fernsler, R. MW2 6
Fernsler, R.F. BT1 1,
GW1 3, SRP2 26
Flikweert, A.J. RR2 4
Foster, Matt DT2 1,
LW2 3, SRP1 32
Franklin, Raoul FPT2 19
Frederickson, Kraig
FPT2 17, SRP2 37
Fukamachi, Asuna
SRP2 30
Fukui, Wataru DT1 3
Furman, Miguel PR2 5
Fursa, D. FPT1 36

G

Gabriel, O. SRP2 39,
VF1 5
Gahan, D. FPT1 9,
SRP1 2
Gallagher, Jeffrey ET2 6
Gaman, C. FPT1 8,
FPT2 6, FPT2 12
Ganguly, Biswa FPT2 3,
SRP2 8, SRP2 18,
WF2 2
Gans, Timo FPT2 31,
FPT2 32, PR2 2,
SRP2 15, VF1 4, WF1 2,
WF1 4
Gao, Junfang LW2 5,
QR2 5
Garee, M.J. FPT2 22
Garscadden, Alan WF2 2
Gatilova, L. FPT2 13,
SRP2 4
Gay, T.J. DT2 5
Gerlich, Dieter WF2 1
Ghedini, Emanuele MW2 4
Gibson, N.D. FPT1 28
Gilgenbach, R.M. FPT1 4
Godet, L. BT2 6, FPT1 3,
SRP2 27

Godyak, Valery ET1 5,
VF2 4
Goeckner, Matthew
FPT1 5, FPT2 18,
VF1 2
Golde, Michael SRP1 25,
WF2 7
Golovkin, Igor PR2 4,
SRP2 12
Gordon, D. MW2 6
Goto, Takeshi K. VF1 3
Goudsmits, J. SRP2 24
Goulding, Rick ET1 6
Graham, William FPT1 41,
FPT2 37, QR1 4,
SRP1 10
Gresback, Ryan PR1 5
Grubert, Gordon K.
FPT1 42
Guaitella, O. FPT2 13,
FPT2 16, QR1 6,
SRP2 33
Gudmundsson, Jon T.
ET1 4, SRP1 26
Guillard, C. FPT2 16
Guillaume, Auday FPT1 17
Guillon, Jean FPT2 5,
FPT2 13
Gupta, Priya MW1 1

H

Hagelaar, G. FPT2 29
Hamada, Daisuke RR1 4
Hamaoka, Fukutaro BT2 5
Hanai, Takamasa FPT2 36
Hanaki, Katsuyuki SRP1 8
Hardin, Robert MW1 4
Harlander, J. SRP2 11
Harris, A.L. SRP1 32
Hartgers, Bart FPT1 16,
SRP2 23
Harvey, Zane MW1 4
Haverlag, M. RR2 4
Hayden, C. SRP1 2
Heberlein, Joachim
GW2 1, MW2 1,
MW2 2, PR1 2
Hebner, Greg FPT2 2,
RR1 2, SRP2 3,
SRP2 14, WF1 7
Helmersson, Ulf ET1 4
Herd, T.M. RR2 3
Herrick, A.C. FPT2 22
Hershkowitz, Noah BT2 1,
BT2 2, FPT1 14,
SRP2 2, SRP2 6
Hicks, Adam ET2 5

Hirao, Satoshi SRP1 6,
SRP1 7
Hoffman, Daniel GW1 4
Hogan, Mark SRP1 29
Holland, J.P. FPT2 2,
RR1 2, WF1 7
Hong, Hyun-Sil RR1 5
Hopkins, M.B. FPT1 9,
MW1 3, SRP1 2
Hoshino, M. FPT1 23
Hotta, Eiki SRP2 30
Hourdakis, Emmanouel
MW2 8
Hua, L.Z. FPT1 49
Huang, Hsiao-Feng
FPT2 34
Hunt, Joseph WF2 3
Hussey, Martyn LW2 5
Hwang, Jaeseung MW1 6
Hwang, Kiho FPT2 9
Hynes, Alan QR1 4

I

Illenberger, Eugen CT2 2
Ionin, Andrey ET2 1,
ET2 2
Iordanov, P. SRP1 2
Ishijima, T. MW1 5
Ishimaru, Mikio SRP1 19
Islyaikin, A. FPT2 12,
SRP1 2
Itoh, Haruo SRP2 32
Ivanov, Vladimir SRP1 17

J

Janczak, C.M. FPT1 28
Jang, SungHo SRP1 5
Jeanney, P. SRP2 7
Jha, Alok FPT1 30
Jho, Yong-Seok FPT1 10,
FPT1 18, FPT1 19,
SRP2 34
Jiang, Naibo SRP2 37
Jiao, Charles WF2 2
Jindal, Ashish FPT2 18
Jivotov, Viktor FPT1 47
Johnsen, Rainer SRP1 25,
SRP1 30, WF2 7
Johnson, Paul FPT1 33,
FPT1 34, QR2 2
Johnson, W.A. FPT2 2
Jones, M.C. FPT1 4
Jordan, N.M. FPT1 4
Jorgenson, R.E. FPT2 2
Jung, R.O. FPT1 25

K

Kaganovich, Igor BT2 4,
PR2 1, VF2 2
Kahraman, A. GW1 5
Kampschulte, Tobias
MW1 2
Kanai, H. MW1 5
Kang, Chang-Jin RR1 3,
RR1 5
Kanik, Isik FPT1 33,
FPT1 34
Karkari, S.K. FPT1 8,
FPT2 6, SRP1 2
Kashuba, Ron FPT2 38,
FPT2 39
Kato, H. FPT1 23
Keehn, Anthony LW2 4
Kelly, Peter GW1 1
Kersten, Holger FPT2 10,
SRP2 9
Keshav, Saurabh CT1 6
Kettlitz, Manfred QR1 5
Keville, B. SRP1 2
Khadilkar, Vaibhav
SRP1 28
Khakoo, Murtadha A.
FPT1 33, FPT1 34,
SRP1 33
Khudik, Vladimir SRP2 35
Khun, Josef FPT1 44
Killian, Thomas MW1 1
Kim, Junghee SRP2 16
Kim, K.S. FPT1 49
Kim, SeongSik FPT1 19
Kim, T.L. FPT1 48
Kimura, Takashi FPT2 36,
SRP1 8, SRP1 9
Kirk, Seth RR1 6
Kitajima, Takeshi SRP1 6,
SRP1 19, VF1 3
Knizhnik, A. ET1 1
Ko, Kwang-Cheol SRP2 30
Kochetov, Igor CT1 4,
ET1 1, ET2 3
Koepke, Mark SRP1 11
Kolobov, Vladimir BT1 6,
SRP2 31
Kono, Akihiro FPT2 7,
FPT2 33
Kononov, Grigory
FPT1 47
Korobtsev, Sergey FPT1 47
Kortshagen, Uwe FPT2 30,
PR1 2, PR1 3, PR1 5
Kou, Chwung-Shan
FPT2 34
Kovacs, D.A. VF1 4

- Kovalev, A.S. SRP1 15, SRP1 16
 Kovalev, Alexander FPT1 7, SRP1 17, SRP1 18
 Krasnoperov, Lev DT1 4
 Kravchenko, Aleksandr SRP2 10
 Krishtopa, Larisa DT1 4
 Kroesen, Gerrit MW2 5, RR2 4
 Krotov, Mikhail FPT1 47
 Kudryavtsev, A.A. FPT2 15
 Kuninaka, Hitoshi LW1 5
 Kuper, Kelly SRP1 33
 Kurachi, Ikuo VF1 3
 Kushner, Mark J. DT1 2, ET2 4, MW2 7, RR1 6
 Kwon, Sungun MW1 6
- L**
 Labby, Z. SRP2 11
 Lacour, B. SRP2 7, SRP2 17
 Lagrange, J.F. GW2 3, QR1 2, SRP2 17
 Laha, Sampad MW1 1
 Lampe, M. MW2 6
 Landry, Karine SRP1 20
 Lange, M. FPT1 36, LW2 6
 Lapke, M. FPT2 32
 Laroussi, Mounir CT2 3, FPT2 28
 Lau, Y.Y. FPT1 4
 Laurent, Therese FPT1 17
 Law, V.J. SRP1 2
 Lawler, J.E. RR2 3, SRP2 11
 Laxminarayan, Raja ET1 3
 Lee, Charles ET1 3
 Lee, Dongsoo SRP2 2, SRP2 6
 Lee, Edmond SRP1 30
 Lee, Jongsub SRP2 16
 Lee, Kyeong Hyo SRP1 3, SRP1 4
 Lee, MinHyong SRP1 4, SRP1 5
 Lee, Sanggon FPT2 9
 Lee, Seonghun SRP2 16
 Lee, TaeSang FPT1 10, FPT1 18, FPT1 19, SRP2 34
 Lee, Yongwoo MW1 6
 Lee, Young Kwang SRP1 3
 Leiweke, Robert SRP2 8
- Lempert, Walter ET2 5, FPT2 17, SRP1 27, SRP2 37
 Leonhardt, D. BT1 1, SRP2 26
 Leonov, Sergey CT1 4
 Leray, Gary FPT2 20
 Levif, Pierre WF1 6
 Lho, Taihyeop FPT1 39
 Li, Chao FPT2 24
 Liard, Laurent BT1 4
 Lieberman, Michael A. HW 1
 Light, Max FPT2 38, FPT2 39
 Likhanskii, Alexander CT1 3, SRP2 38
 Lin, Chun C. FPT1 25, FPT1 26
 Lisovskiy, Valeriy SRP1 20
 Lister, Graeme SRP1 36
 Loffhagen, Detlef FPT1 42
 Lohmann, Birgit LW2 4
 Longmier, Ben BT2 2
 Lopaev, D.V. FPT1 7, SRP1 15, SRP1 16, SRP1 17, SRP1 18, SRP1 24
 Lower, J. SRP1 35
 Lower, J.C. FPT1 36, LW2 6
 Lower, Julian LW2 2
 Lu, Xinpei FPT2 28
 Luggenhoelscher, Dirk MW1 2
 Luizova, Lidia SRP2 10
- M**
 Mabuchi, Michio SRP1 9
 MacFarlane, Joseph PR2 4, SRP2 12
 Macheret, Sergey CT1 3, LW1 2, SRP2 38
 Madison, D.H. FPT1 24, LW2 5, QR2 5, SRP1 32, SRP1 35
 Madziwa-Nussinov, Tsitsi FPT2 38, FPT2 39
 Maeda, T. FPT2 14
 Magne, L. GW2 3, SRP2 7
 Maguire, Paule BT1 3
 Mahadevan, Shankar GW2 4
 Mahony, Charles BT1 3
 Makabe, Toshiaki BT2 5, RR1 7, SRP1 6, SRP1 7, SRP1 19, VF1 3
 Makochekanwa, C. FPT1 23
 Malone, Charles P. FPT1 33, FPT1 34
 Malovic, Gordana VF2 3
 Mankelevich, Yury FPT1 7, SRP1 18
 Maric, Dragana FPT2 5
 Martinez, Horacio FPT2 8, SRP2 20
 Maseberg, J.W. DT2 5
 Masters, Mark SRP1 31
 Matsumoto, J. FPT1 36, LW2 6
 McCarter, A. SRP1 2
 McConkey, J. William FPT1 33
 McEachran, R.P. FPT1 32, SRP1 35
 McFerran, J. GW1 5
 McKoy, Vincent FPT1 29, QR2 1
 Medvedev, Dmitrii FPT1 47
 Messer, S.J. GW1 3
 Messmer, Peter FPT2 26
 Midha, V. ET1 1
 Mikhael, D. ET1 1
 Miles, Richard CT1 3, LW1 2, SRP2 38
 Miller, Matthew GW1 4
 Miller, P.A. WF1 7
 Miller, Paul RR1 2, SRP2 14
 Miller, Terry FPT1 45, SRP2 28
 Milosavljevic, V. FPT2 12, SRP1 2
 Minayeva, Olga B. RR2 2
 Modenese, Camila DT1 4
 Moeller, Phil SRP1 34
 Mohan, Man FPT1 30
 Monahan, D.D. PR2 3
 Moon, Joo-Tae RR1 3, RR1 5
 Morgan, Thomas SRP1 10
 Morrow, Tom FPT1 41
 Moshkalev, Stanislav SRP1 10
 Moten, Sohala SRP1 34
 Mulders, H.C.J. SRP2 25
 Mullen, J.J.A.M. RR2 4
 Munoz-Serrano, E. FPT2 29, GW2 3
 Murray, Andrew LW2 5
 Murray, Syd ET1 6
- Mussenbrock, T. FPT1 11, FPT2 31, FPT2 32, WF1 5
- N**
 Nakai, Tatsuya LW1 5
 Nakamura, Keisuke RR1 4
 Napartovich, Anatoly CT1 4, ET1 1, ET2 3
 Narayanaswamy, V. LW1 6
 Nelson, Caleb VF1 2
 Nersisyan, Gagik FPT1 41, FPT2 37
 Nesbitt, Kurt SRP1 34
 Newman, D.S. LW2 6
 Ngassam, Valery WF2 6
 Niemi, K. FPT2 31, QR1 3
 Nikandrov, Dmitry SRP2 31
 Nikitovic, Zeljka VF2 3
 Nimalasuriya, T. RR2 4
 Nishihara, Munetake CT1 5
 Nishiyama, Kazutaka LW1 5
 Nozaki, Tomohiro DT1 3, PR1 2, PR1 4
- O**
 O'Connell, Deborah PR2 2, SRP2 15, WF1 2, WF1 4
 Ogawa, Daisuke FPT1 5
 Ogino, Tomohisa PR1 4
 Ohmori, Takeshi SRP1 6, SRP1 19, VF1 3
 Ohnishi, Kuma PR1 2
 Okazaki, Ken DT1 3, PR1 2, PR1 4
 Okino, Akitoshi SRP2 30
 Oksuz, Lutfi FPT1 14
 Olevanov, Mike SRP1 18
 Ono, Kouichi LW1 3, RR1 4
 Orel, Ann E. WF2 5, WF2 6
 Osaka, J. MW1 5
 Osari, Kazushi RR1 4
 Overzet, Lawrence FPT1 5, FPT2 18, VF1 2
- P**
 Pamfiloff, Eugene FPT1 37
 Pappas, Daphne WF2 7
 Park, Hoyong SRP2 5, SRP2 16
 Park, S.-J. FPT1 48, FPT1 49

- Park, Seung-hoon **FPT1 10, FPT1 18**
- Park, Sung-Chan **RR1 3**
- Paterson, A.M. **FPT2 2, WF1 7**
- Paterson, Alex **RR1 2**
- Patterson, Marlann **BT1 2**
- Peacher, J.L. **FPT1 24, QR2 5, SRP1 32**
- Pekarek, Stanislav **FPT1 44**
- Pereyra, Nicolas **PR2 4, SRP2 12**
- Perram, Glen **ET2 6**
- Peters, Silke **QR1 5**
- Petrovic, Zoran **BT1 3, FPT1 27, SRP2 19, WF2 3**
- Pfender, Emil **MW2 2**
- Phelps, A.V. **SRP1 23**
- Philippe, Belenguer **FPT1 17**
- Philippe, Guillot **FPT1 17**
- Piracha, Naveed **SRP1 34**
- Pitchford, L.C. **FPT2 29, GW2 3**
- Plihon, Nicolas **FPT2 20**
- Popovic, Svetozar **CT1 2, FPT1 3, SRP2 36**
- Potapkin, B. **ET1 1**
- Potapkin, Boris **FPT1 47**
- Pramanik, Jyotirmoy **GW1 6**
- Proshina, Olga **FPT1 7, SRP1 17, SRP1 18**
- Puech, V. **GW2 3, SRP2 7, SRP2 17**
- R**
- Radjenovic, Branislav **BT1 3**
- Radmilovic-Radjenovic, Marija **BT1 3**
- Radovanov, Svetlana **BT2 6, FPT1 3, SRP2 27**
- Rahman, Abdur **SRP1 36, VF2 4**
- Raimbault, Jean-Luc **BT1 4, FPT2 20**
- Raitses, Yevgeny **VF2 2**
- Raja, L. **GW2 4, LW1 4, LW1 6**
- Rakhimova, T.V. **SRP1 15, SRP1 16, SRP1 24**
- Rakhimova, Tatyana **FPT1 7, SRP1 17, SRP1 18**
- Raskovic, M. **FPT1 3**
- Readle, J.D. **FPT1 49**
- Reid, Jonathan P. **SRP2 9**
- Rescigno, T.N. **DT2 3**
- Reuter, S. **FPT2 31**
- Reuter, St. **QR1 3**
- Reynolds, Clint **SRP1 31**
- Rhee, Junkyu **SRP2 16**
- Rich, J. William **DT1 5, ET2 5, WF2 4**
- Ringwood, J.V. **SRP1 2**
- Rodriguez-Lazcano, Yamilet **SRP2 20**
- Roepcke, J. **FPT2 16, SRP2 4, SRP2 9**
- Roesler, F.L. **SRP2 11**
- Ropcke, J. **VF1 5**
- Rosati, Richard **SRP1 25, WF2 7**
- Rousseau, A. **FPT2 13, FPT2 16, QR1 2, QR1 6, SRP2 4, SRP2 33**
- Rykova, E. **ET1 1**
- Ryu, Yonghwan **MW1 6**
- S**
- Sadeghi, N. **FPT2 35, GW2 3, MW1 5, PR2 2, QR1 2, SRP2 17**
- Saha, B.C. **FPT1 43**
- Saha, H.P. **SRP1 32, SRP1 35**
- Samukawa, Seiji **PR1 1, VF1 3**
- Sanchez, Sam **FPT1 5**
- Sands, Brian **FPT2 3**
- Sant, Sanket **VF1 2**
- Sasaki, K. **FPT2 14, MW1 5, PR1 4**
- Sasic, Olivera **VF2 3**
- Sato, Toshikazu **RR1 7**
- Schappe, Scott **DT2 2**
- Scheuer, Jay **BT2 6, SRP2 27**
- Schmidt, Jiri **FPT1 44**
- Schneidenbach, Hartmut **QR1 5**
- Schram, D.C. **SRP2 24, SRP2 39, VF1 5**
- Schubert, Gerald **FPT2 10**
- Schulz, Michael **LW2 1**
- Schulz-von der Gathen, V. **FPT2 31, FPT2 32, QR1 3**
- Schulze, Julian **MW1 2, SRP2 15, WF1 4**
- Scime, Earl **MW1 4**
- Scofield, J.D. **FPT1 2**
- Seeley, Megan **LW1 7, SRP2 13**
- Seon, Changrae **SRP2 5**
- Seymour, Greg **SRP2 2, SRP2 6**
- Shannon, Steven **GW1 4**
- Sheridan, T.E. **FPT2 21, FPT2 22**
- Sheverev, Valery **SRP1 36**
- Shibagaki, K. **FPT2 14**
- Shibata, Tomoyuki **FPT2 33**
- Shin, Chul Ho **RR1 3**
- Shin, J. **LW1 6**
- Shin, Yonghyun **SRP2 5**
- Shneider, Mikhail **CT1 3, LW1 1, LW1 2, SRP2 38**
- Shvydky, Alex **SRP2 35**
- Sides, Scott **PR2 5**
- Siefert, Nicholas **FPT2 3**
- Sigeneger, Florian **FPT2 10**
- Simek, Milan **FPT1 21, FPT1 44**
- Simien, Clayton **MW1 1**
- Sizemore, Nate **PR2 5**
- Sladek, Raymond **CT2 5, FPT1 46, FPT2 27**
- Slinker, S. **MW2 6**
- Smirnov, Roman **FPT1 47**
- Smith, D. **ET1 1, RR2 1**
- Smolyakov, Andrei **VF2 2**
- Soberon, F. **FPT1 9, SRP1 2**
- Sobolewski, Mark **FPT2 11**
- Solovev, Aleksei **SRP2 10**
- Sommerer, T. **ET1 1, RR2 5**
- Spieker, D.W. **QR2 5**
- Spinka, T.M. **FPT1 49**
- Sprangle, P. **MW2 6**
- Stalder, Kenneth **LW1 7, SRP2 13**
- Stancu, G. **FPT2 16**
- Starr, K.A. **FPT1 28**
- Stauffer, A.D. **FPT1 32**
- Steffens, Kristen **SRP1 21**
- Stegen, Z. **SRP1 35**
- Sternberg, Natalia **ET1 5**
- Stevenson, Mark **LW2 4**
- Stockli, Martin **ET1 6**
- Stoffels, Eva **CT2 5, FPT1 46, FPT2 27**
- Stoffels, W.W. **RR2 4, SRP2 25**
- Stojanovic, Vladimir **FPT1 27, SRP2 19, VF2 3**
- Stoltz, Peter **ET1 2, FPT2 26, PR2 5**
- Strelkova, Marina **FPT1 47**
- Strinic, Aleksandra **VF2 3**
- Strobel, Mark **RR1 6**
- Stumpf, Bernhard **FPT1 35**
- Subramaniam, V. **GW1 5**
- Suedhoff, Hans **SRP1 31**
- Sugai, H. **MW1 5**
- Sullivan, J.P. **CT2 4**
- Sun, Jong-Woo **RR1 3**
- Sun, Xuan **MW1 4**
- Sung, S.-H. **FPT1 48**
- Surko, C.M. **QR2 4**
- Suzuki, Susumu **SRP2 32**
- Swindells, I. **FPT2 6, GW1 1**
- Sydorenko, Dmytro **VF2 2**
- T**
- Tachibana, Kunihide **GW2 2**
- Takada, N. **FPT2 14**
- Takao, Yoshinori **LW1 3**
- Tanaka, H. **FPT1 23**
- Tchertichian, P. **FPT1 48**
- Terashima, Kazuo **QR1 1**
- Teubner, P.J.O. **FPT1 23**
- Theodosiou, Constantine **SRP2 35**
- Thevenet, F. **FPT2 16**
- Thieme, Gabriele **FPT2 10, SRP2 9**
- Thierry, Calegari **FPT1 17**
- Thorn, Penny **FPT1 23**
- Thorsteinsson, Eythor G. **SRP1 26**
- Timmons, Richard **FPT1 5**
- Touzeau, M. **GW2 3, SRP2 17**
- Toyoda, H. **MW1 5**
- Trelles, Juan **MW2 2**
- Tristan, Beaudette **FPT1 17**
- Trump, D.D. **SRP2 18**
- Tsendin, Lev **SRP2 31**
- Tsukijihara, Hiroyuki **DT1 3**
- Turner, M.M. **FPT1 13, FPT1 15, PR2 3, SRP2 15, WF1 3, WF1 4, WF1 6**
- U**
- Uchida, Shigeaki **SRP2 29**
- Uddi, Mruthunjaya **SRP2 37**
- Umanskii, S. **ET1 1**
- Umbel, J.D. **FPT1 2**
- Upadyyay, J. **SRP2 36**

Utkin, Yurii CT1 6,
DT1 5, ET2 5

V

Vagin, Nikolay ET2 3
van der Mullen, J.J.A.M.
FPT2 24
van der Mullen, Joost
FPT1 16, SRP2 23
van Dijk, Jan FPT1 16,
SRP2 23
van Helden, J.H. VF1 5
Vankan, P. SRP2 39
Vankan, Peter SRP2 22
Varghese, Philip L. LW1 4
Vasekova, Eva FPT2 4
Vasilieva, A.N. SRP1 15,
SRP1 16
Vasilieva, Anna FPT1 7,
SRP1 17, SRP1 18
Vay, Jean-Luc PR2 5
Veitzer, Seth ET1 2,
PR2 5
Vender, David WF1 2
Verma, Nupur FPT1 30
Vidmar, Robert LW1 7,
SRP2 13

Viehland, Larry SRP1 30,
VF2 1
Vizcaino, V. CT2 4
Voloshin, Dmitry SRP1 18
von Keudell, Achim DT1 1
Vuskovic, L. FPT1 3,
SRP2 36

W

Wagenaars, Erik MW2 5
Walker, D.N. GW1 3
Walter, C.W. FPT1 28
Walton, S.G. BT1 1
Walton, Scott SRP2 26
Wang, L.M. FPT1 4
Wang, Ping PR2 4,
SRP2 12
Wang, Q. FPT2 35
Wang, Shiyang FPT1 34
Warne, L.K. FPT2 2
Watanabe, Masato
SRP2 30
Wei, Hsiao-Kuan FPT2 34
Weigold, E. SRP1 35
Wells, K.D. FPT2 22
Welton, Robert ET1 6
Welzel, S. SRP2 4, VF1 5

Wen, Chun-Hsiang
FPT2 34
Wendt, Amy BT1 2
Wendt, Martin QR1 5
West, J. GW1 5
White, Allen WF2 4
Williams, Skip ET2 6
Williamson, J.M. FPT1 2,
SRP2 18
Winstead, Carl FPT1 29
Woo, Hyun-Jong FPT1 39
Woodruff, Pamela PR2 4,
SRP2 12
Wright, Timothy SRP1 30
Wu, Shenghai SRP2 28
Wynne, Jason SRP1 11

Y

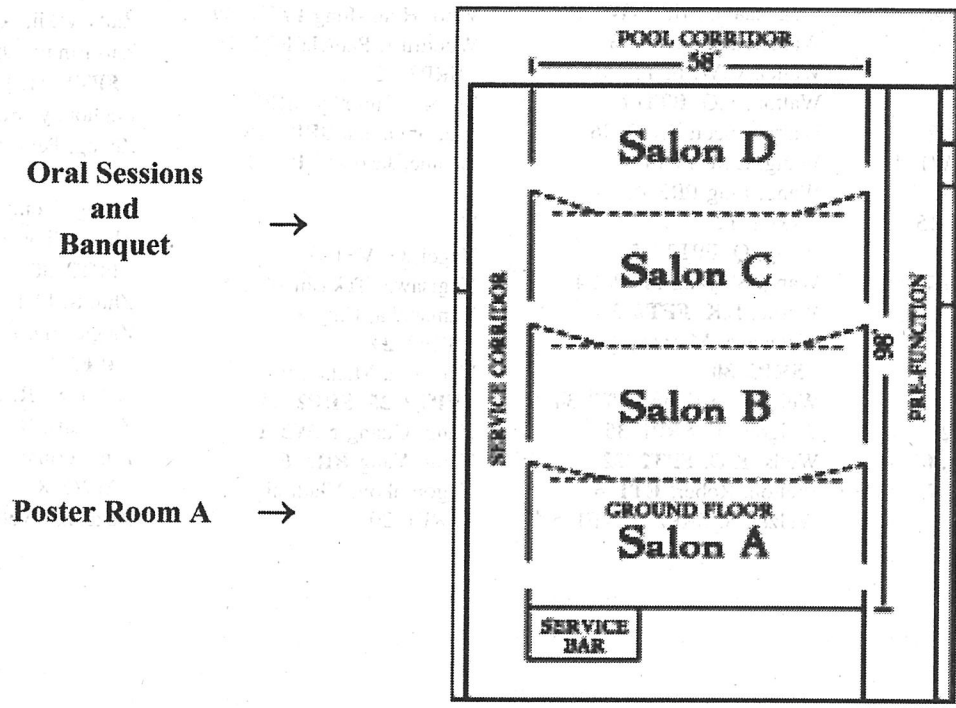
Yagci, G. VF1 5
Yagisawa, Takashi BT2 5
Yamanaka, Chiyoe
SRP2 29
Yamaura, Michiteru
FPT2 25, SRP2 29
Yang, Guang MW2 1
Yang, Yang RR1 6
Yegorenkov, Vladimir
SRP1 20

Yeldell, Stephen A. LW1 4
Yong, Zhang SRP1 6
You, Shinjae SRP2 16
Young, J.A. QR2 4
Yousif, Farook Bashir
FPT2 8
Yuryshv, Nikolay ET2 3

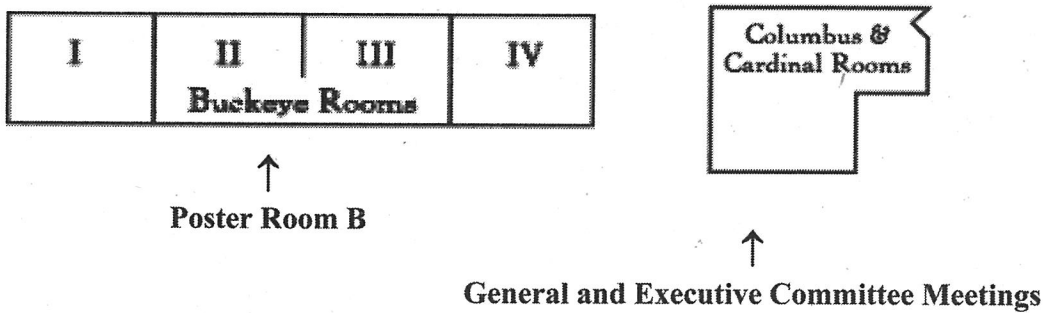
Z

Zaitsevskii, A. ET1 1
Zatsarinny, Oleg DT2 4,
FPT1 31, FPT1 36
Zeghondy, Barbar SRP2 33
Zhang, Peng BT1 5,
FPT2 30
Zhang, Yong SRP1 7
Zhou, Ning BT1 5,
FPT2 30
Zhu, S. FPT1 4
Ziegler, D. FPT2 32,
WF1 5
Zijlmans, R. SRP2 24
Zijlmans, R.A.B. VF1 5
Zimmerman, Neil M.
MW2 8
Zuzeek, Yvette SRP2 37

Holiday Inn - Main Ballroom - Ground Level



11th Floor Rooms



On the Cover: Photo of a Mach 3 ionized gas supersonic wind tunnel and blunt body test object illustrating characteristic bow shock. Plasma is produced in a high pressure, aerodynamically stabilized diffuse discharge plenum, examples of which have been operated at pressures as high as 6 bar in helium and 0.5 bar in nitrogen. Work performed at Ohio State University.

Epitome of the 59th Annual Gaseous Electronics Conference of the American Physical Society

18:00 MONDAY EVENING
9 OCTOBER 2006

AS **Reception**
Ohio State - Department of
Mechanical Engineering, Multi
Purpose

8:00 TUESDAY MORNING
10 OCTOBER 2006

BT1 **Plasma Sources I**
Salon CD, Holiday Inn

BT2 **Plasma Boundaries: Sheaths and Boundary
Layers**
Salon B, Holiday Inn

10:00 TUESDAY MORNING
10 OCTOBER 2006

CT1 **Plasma Aerodynamics and
Propulsion I**
Adamovich, Popovic
Salon CD, Holiday Inn

CT2 **Collision Processes with
Biological and Environmental Applications**
Brunger, Illenberger, Laroussi
Salon B, Holiday Inn

13:30 TUESDAY AFTERNOON
10 OCTOBER 2006

DT1 **Plasma Chemistry**
von Keudell
Salon CD, Holiday Inn

DT2 **Electron Impact Ionization and Excitation I**
Foster, Schappe, Rescigno
Salon B, Holiday Inn

16:00 TUESDAY AFTERNOON
10 OCTOBER 2006

ET1 **Plasma Sources II**
Salon CD, Holiday Inn

ET2 **Oxygen-Iodine Lasers**
Salon B, Holiday Inn

19:15 TUESDAY EVENING
10 OCTOBER 2006

FPT1 **Poster Session IA**
Salon A, Holiday Inn

FPT2 **Poster Session IB**
Buckeye, Holiday Inn

8:00 WEDNESDAY MORNING
11 OCTOBER 2006

GW1 **Diagnostics I: Electrical**
Salon CD, Holiday Inn

GW2 **High Pressure Discharges I**
Heberlein, Tachibana
Salon B, Holiday Inn

10:00 WEDNESDAY MORNING
11 OCTOBER 2006

HW **Allis Prize Lecture**
Lieberman
Salon CD, Holiday Inn

11:00 WEDNESDAY MORNING
11 OCTOBER 2006

JW **Business Meeting**
Salon CD, Holiday Inn

12:00 WEDNESDAY NOON
11 OCTOBER 2006

KW **General Committee Meeting**
Salon CD, Holiday Inn

13:30 WEDNESDAY AFTERNOON
11 OCTOBER 2006

LW1 **Plasma Aerodynamics and
Propulsion II**
Shneider
Salon CD, Holiday Inn

LW2 **Electron Impact Ionization and Excitation
II**
Schulz, Lower
Salon B, Holiday Inn

16:00 WEDNESDAY AFTERNOON
11 OCTOBER 2006

MW1 **Diagnostics II: Optical**
Salon CD, Holiday Inn

MW2 **Thermal Plasmas, Arcs, and Breakdown**
Salon B, Holiday Inn

8:00 THURSDAY MORNING
12 OCTOBER 2006

PR1 **Plasma Applications for
Nanotechnology**
Samukawa
Salon CD, Holiday Inn

PR2 **Computational Methods and Modeling for
Plasmas**
Salon B, Holiday Inn

10:00 THURSDAY MORNING
12 OCTOBER 2006

QR1 **High Pressure Discharges II**
Terashima
Salon CD, Holiday Inn

QR2 **Electron and Positron Collisions**
McKoy, Johnson, Bray
Salon B, Holiday Inn Chair

13:30 THURSDAY AFTERNOON
12 OCTOBER 2006

RR1 **Material Processing in Low
Pressure Plasmas**
Barnes
Salon CD, Holiday Inn

RR2 **Lighting Plasmas**
Sommerer, Bowden
Salon B, Holiday Inn

16:00 THURSDAY AFTERNOON
12 OCTOBER 2006

SRP1 **Poster Session IIA**
Salon A, Holiday Inn

SRP2 **Poster Session IIB**
Buckeye, Holiday Inn

18:00 THURSDAY EVENING
12 OCTOBER 2006

UR **Banquet**
Salon BCD, Holiday Inn

8:00 FRIDAY MORNING
13 OCTOBER 2006

VF1 **Plasma-Surface Interactions**
Donnelly
Salon CD, Holiday Inn

VF2 **Transport Theory and Electron Distribu-
tion Functions**
Viehland
Salon B, Holiday Inn

10:00 FRIDAY MORNING
13 OCTOBER 2006

WF1 **Capacitively Coupled Plasmas**
Booth
Salon CD, Holiday Inn

WF2 **Heavy Particle Collisions,
Attachment, and Recombination**
Gerlich
Salon B, Holiday Inn



0003-0503(200610)51:5;1-S